Molecular mechanisms of Streptococcus pyogenes tissue colonization and invasion

Antonin Weckel

Université Paris Descartes

Ecole doctorale BioSPC

Institut Cochin INSERM U1016 / Equipe Barrières et Pathogènes

Molecular mechanisms of *Streptococcus pyogenes* tissue colonization and invasion

By Antonin WECKEL

PhD Thesis in Microbiology

Directed by Agnès Fouet

Thesis defense: 30th of October 2018

Jury members:

Pr Anna NORRBY-TEGLUND	Reviewer
Dr Pascale SERROR	Reviewer
Pr François VANDENESCH	Examiner
Dr Philippe BOUSSO	Examiner
Dr Agnès FOUET	PhD supervisor

"We have to remember that what we observe is not nature herself,
but nature exposed to our method of questioning"

Werner Heisenberg

Physics and Philosophy: The Revolution in Modern Science (1958)

Acknowledgements

I would like to thank Pascale Serror, Anna Norrby-Teglund, François Vandenesch and Philippe Bousso for having kindly accepted to be part of my defense jury, in particular to Anna Norrby-Teglund who came from Sweden for my defense.

It has been 12 years now that I realized I want to work in life science research. Considering the beginning of my memories, this is more than half of my life having this idea stuck in my head. I want here to take the time to acknowledge all the people who contributed to this seed to grow into the doctor I'm about to become: the beauty of a flower resides less in the seed than in the quality of the environment it is exposed to during its growth. I consider that over the past years, I have been enlightened and watered by being surrounded by many wonderful people. While this dissertation and PhD are mine, this work belongs also to all of them.

Thanks to Agnès and Claire for accepting me in the team and project. Agnès was a wonderful supervisor, always here when I needed her. I learned so much with her; she was a very good GPS during my PhD, I never felt lost and her directions were always correct. A very kind, upright and mindful boss. Thanks to Claire for always being kind and frank with me.

Céline Méhats. Officially my "collaborator". We had such a friendly and productive collaboration. You put so much energy into this project that started from nothing. You are a wonderful researcher and I am so glad I had the chance to work with you.

Thanks to Thomas Guilbert. He gave me the knowledge, the curiosity, the will to work in microscopy. I never ever did microscopy before I met him and I still remember his first "lesson" on the microscope. He replied to several calls while I was such in a state in the L2 microscope during my night experiments. 9pm, 10pm. He was in bars, restaurants. He shouldn't have replied. But I am so glad he did!!

Thanks to Thierry Meylheuc for the SEM images. I will never forget the excitement of the first session with you, discovering the beautiful landscape of the infection at the nanometric level.

Thanks to Magalie for all the help and support at the beginning of my PhD. Thanks to Samuel for being my biochemistry mentor and such a friendly colleague. Thanks to Constantin, my last year roommate, labmate, late evening-mate, weekend-mate and dissertation-mate. I am glad we had the opportunity to do our last year together, working next to you made everything easier to go through.

Thanks to all past and current members of my team. Abdel, Asmaa, Anne-Sophie, Céline, Clara, Gerald, Julie and Lionel. A very nice environment and people to work in and with. Thanks to all the interns I had the chance or not to supervise. You learn a lot from your own mistakes, but also from those of others. Special thanks to Dorian, Quentin and Sandra.

Thanks to the Donnadieu team. I owe you a lot, I had so much help and so many advice from all of you. I would not have done a 100^{th} of what I did in microscopy without you. You always welcomed me and tried to help. Thanks to Elisa, Vincent, Emmanuel, Alain, Sarah, Chahrazade.

Thanks to my former teacher and supervisors (Mr Poisson, Marie-Claude Serre, David Ermert and Anna Blom). You trusted me, and gave me all the knowledge and tools to start my PhD in the most comfortable way possible.

Thanks to the people from the facilities I used during this PhD: Cybio, Proteomic facility and the Imag'IC facility. Thanks to Maryline Bajolle for her kindness and help. Thanks to Méchain building, Florian, Gaëlle, Christophe, Marina, Mickaël, Roy, Maxence, Ghina, Fanny, and all the people at the Institute I've been working for a couple of years .

Thanks to JeCCo and associates, Armelle, Stéphane, Marion, Gabrielle, Gabriel, Simon, Robin, Cyril, Mariangela, Rozenn, Anaïs, Vincent, Milica. Thanks for all this time releasing pressure from our day work and from the beer tap.

I always think of Coralie, Béatrice, Nicolas and David as a special category of friends. We did secondary school together. I know them for more than 10 years. Thanks for all the time spent together and for being friends I wish to keep all my life. Who could have guessed while taking our daily lunch in the Agora we would ever be here for my PhD!

ENS was a great opportunity on many aspects. Meeting Pierre, Aurélien, Noémie, Anne, Justine, Thomas, Valentine, Milena, Julia, Ralitza and Xavier was one of the best. So many parties, so many holidays and memories altogether. So much fun. Thank you all.

Thanks to Mickael and Alex. Thanks for making me speak English and drinking beer on a regular base. You are true friends that always helped me through time of doubts.

I have two brothers and a sister, Adrien, Amélie and Louis. I am so glad we had the opportunity to spend monthly time together for several years in Paris when we were reunited. Though we are no longer on the same continent, I know I have a wonderful family I can count on at any time in my life and this is invaluable. Thanks to all the members of my family, for their care and love, especially my godmother Corinne. Thanks to my grandfather for saying since I knew I wanted to do research: “A researcher who searches, it is easy to find, but a researcher who finds, we are still searching for them”. To which I used to reply in my innocent and naive youth and with a sense of humor: “I will not become a researcher, but a finder”.

My parents definitely played a critical role in my calling to science. Though none is a scientist, I have been nurtured on science very early in life, and I will never ever be able to thank them sufficiently for that. They gave me all I needed to develop my curiosity and to have the best education. They kindly supported all my life decisions. My prepa was a difficult time not only for me but also for them, they bore and tolerated things many parents would not have. It was a time none of us regret, but I don’t know if they realize that I would not have done it without them. They have always trusted me, more than I ever did, or ever will trust myself. The further I get from childhood, the further I am from their life, the harder it is for me to retain tears thinking of my own mother not sleeping for me to grow up in the most suitable environment. I don’t know if anything can be worth what they did for me, but I want to thank them and dedicate this PhD to them.

So far I described many “categories” of people that helped me over the past years. Coralie enters all categories: she has always been here for me and for a long time, she cared for me, she was here at any time of the day and night for my tears and my laughs, she helped me a lot to release the pressure from the lab. You tolerated my bad mood and accepted that I come and leave our sweet home in the middle of the night, and the following days when I was tired and unpleasant. Thank you. We did it, together, hand in hand.

Remerciements

J'aimerais remercier Pascale Serror, Anna Norrby-Teglund, François Vandenesch et Philippe Bousso d'avoir gentiment accepté de faire partie de mon jury de thèse. Merci en particulier à Anna Norrby-Teglund qui a fait le déplacement depuis la Suède.

Cela fait maintenant 12 ans que j'ai réalisé que j'aimerais travailler dans la recherche en biologie. En prenant compte de l'âge de mes premiers souvenirs, j'ai eu cette idée coincée dans ma tête durant plus de la moitié de ma vie. J'aimerais ici prendre le temps de remercier toutes les personnes qui ont contribué à faire de cette graine le docteur que je suis sur le point de devenir : la beauté d'une fleur réside moins dans la graine que dans l'environnement auquel elle est exposée durant sa croissance. Je considère que durant ces dernières années, j'ai été nourri des lumières et « arrosé » par la présence autour de moi de nombreuses personnes fabuleuses que j'aimerais remercier. Car si ces travaux et ce manuscrit sont miens, ils appartiennent aussi à toutes ces personnes.

Merci à Agnès et Claire pour m'avoir donné l'opportunité de rejoindre l'équipe. Agnès a été une excellente encadrante, toujours disponible pour moi. J'ai beaucoup appris à ses côtés, elle a été un très bon GPS pour me guider durant cette thèse, je ne me suis jamais senti perdu et ses indications ont toujours porté leur fruit. Une cheffe gentille et sincère. Merci à Claire pour son honnêteté et sa gentillesse envers moi.

Céline Méhats. Ma « collaboratrice ». On a eu une collaboration si fructueuse et sympa. Tu as mis une telle énergie dans ce projet qui ne partait de rien. Tu es une chercheuse incroyable et c'est une chance que j'ai eu d'avoir pu travailler avec toi.

Merci Thomas, il m'a transmis la curiosité et l'envie de faire de la microscopie. J'ai débuté grâce à lui, et je me souviens encore de son premier « cours ». Il a été décisif à des moments où j'étais dans un état de désespoir avancé au microscope au milieu de mes nuits de manips. 21h, 22h. Au bar, restaurant. Il n'aurait pas dû répondre mais je le remercie mille fois de l'avoir fait.

Merci à Thierry Meylheuc pour la microscopie électronique à balayage. Je ne pourrais jamais oublier l'excitation lors de notre premier voyage à l'échelle nanométrique dans le paysage des tissus infectés.

Merci à Magalie pour son aide et soutient en début de thèse. Merci à Samuel, mon mentor en biochimie et un collègue très sympa. Merci à ~~Antonin~~ Constantin, mon acolyte et compagnon de bureau, de labo, de fin de journée, de week-end et de thèse. Je suis ravi d'avoir partagé ma dernière année de thèse avec toi, travailler à tes côtés a permis de rendre tout plus facile à vivre.

Merci aux membres actuels et passés de mon équipe. Abdel, Asmaa, Anne-Sophie, Céline, Clara, Gerald, Julie et Lionel. Un environnement agréable et des personnes sympas avec qui travailler. Merci aux stagiaires que j'ai eu la chance ou non d'encadrer. On apprend de ces erreurs, mais aussi de celles des autres. Un merci en particulier pour Sandra, Quentin et Dorian.

Merci à l'équipe Donnadieu, je leur dois beaucoup. Je n'aurais guère fait qu'un centième du projet sans leurs conseils. Je vous ai surnommé ma « famille d'accueil » car je me suis toujours senti accueilli et bien reçu, avec de nombreux conseils et outils. Merci à Elisa, Vincent, Emmanuel, Alain, Sarah et Chahrazade.

Merci aux différents encadrants et professeurs (Mr Poisson, Marie-Claude-Serre, David Ermert et Anna Blom) qui m'ont donné envie de faire de la recherche, qui ont cru en moi et m'ont toujours poussé à me dépasser. Vous m'avez donné tous les outils et connaissances pour débuter ma thèse le mieux possible.

Merci aux membres des plateformes Cybio, Protéomique et Imag'IC. Merci à Maryline Bajolle, la clé de voûte de l'institut sans qui tout s'effondrerait. Merci au personnel de la laverie, Khemwantee et Romero. Merci à tous mes collègues de Méchain, Florian, Gaëlle, Christophe, Marina, Mickaël, Roy, Maxence, Ghina, Fanny. Merci aux autres membres de l'Institut avec qui j'ai travaillé pendant plusieurs années.

Merci aux Jecco et associés, Armelle, Stéphane, Marion, Gabrielle, Gabriel, Simon, Robin, Cyril, Mariangela, Rozenn, Anaïs, Vincent et Milica. Merci pour tous ces moments à relâcher la pression du travail et du fût de bière.

Coralie, Béatrice, Nicolas et David forment une catégorie d'amis à part. Nous avons été au lycée ensemble, je les connais depuis 10 ans. Merci pour tous ces moments passés ensemble. Qui aurait cru lors de nos déjeuners à l'Agora que nous nous retrouverions ici à ma thèse ?!

L'ENS a été une opportunité sur de multiples aspects. Rencontrer Pierre, Noémie, Anne, Justine, Thomas, Valentine, Milena, Julia, Ralitza et Xavier fut la plus grande. Merci pour tous ces souvenirs de soirée et de vacances ensemble. On s'est bien marré.

Merci à Mickael et Alex. Merci de m'avoir permis de régulièrement parler anglais et boire des bières. Vous avez toujours été présents à des moments de doutes, merci.

J'ai deux frères et une sœur ; Adrien, Amélie et Louis. Durant plusieurs années nous avons eu la chance de partager de nombreux moments en région parisienne où nous habitions tous. Bien que nous ne soyons plus sur le même continent, je sais désormais à quel point j'ai une famille formidable sur laquelle je peux compter à tout instant, et c'est inestimable. Merci à tous les autres membres de ma famille pour leurs attentions et leur amour, en particulier à ma marraine Corinne. Merci aussi à mon grand-père, lui qui ne rate pas une occasion depuis qu'il a su que je voulais faire de la recherche de me sortir : « Des chercheurs qui cherchent, on en trouve, mais des chercheurs qui trouvent, on en cherche ». J'aimais dans ma jeunesse innocente et avec une pointe d'humour répondre que je ne serai pas chercheur, mais trouveur.

Mes parents ont indubitablement joué un rôle dans ma vocation scientifique, bien qu'aucun ne soit scientifique. J'ai été nourri de science très tôt dans ma vie et je ne saurais jamais comment leur en remercier. Ils m'ont donné tout ce dont j'avais besoin pour satisfaire ma curiosité et pour avoir le meilleur enseignement. Ils ont gentiment accompagné, appuyé et aidé chacune des décisions importantes que j'ai prise dans ma vie. La classe préparatoire n'a pas été qu'un moment pénible pour moi, mais aussi pour eux, un moment où ils ont fait preuve de patience et tolérance comme certains parents n'auraient jamais pu. Un temps que nul ne regrette, mais je ne sais s'il réalise que je n'aurais pas réussi sans eux. Ils ont toujours eu et ont confiance en ma réussite plus que je n'en aurai jamais en moi. Plus je m'éloigne de mon enfance et adolescence, plus je m'éloigne d'eux et de leur vie, plus il m'est difficile de retenir des larmes en pensant à ma mère qui ne dort pas afin de me permettre d'évoluer dans un environnement le plus favorable possible. Aucun mot ni rien ne pourra compenser pour ce qu'ils ont fait pour moi, mais je tiens à les remercier infiniment et leur dédier cette thèse.

Jusqu'ici j'ai décrit plusieurs « catégories » de personnes. Coralie entre dans de nombreuses : elle a toujours été là pour moi et depuis longtemps, elle a pris soin de moi et a toujours été présente jour et nuit pour mes rires et mes larmes, elle m'a beaucoup aidé notamment à relâcher la pression du travail. Tu as toléré ma mauvaise humeur et que je rentre et reparte de l'appartement au milieu de la nuit, et mes lendemains où j'étais épuisé et désagréable. Merci. On a réussi (survécu ?), ensemble, main dans la main.

Abstract

Streptococcus pyogenes (Group A Streptococcus, GAS), is a Gram-positive pathogen responsible for a wide range of diseases, from superficial infections such as pharyngitis to invasive infections such as necrotizing fasciitis and endometritis. Endometritis was a huge social burden in the 19th century, killing one woman out of ten after delivery, and still corresponds to 27% of woman invasive infections in France. GAS strains are genetically diverse and harbor specific repertoires. *emm28* is the third most prevalent genotype in France and is associated with endometritis. By two complementary axes, we analyzed factors and mechanisms involved in GAS endometritis.

Using biochemical and cellular approaches, we characterized the interaction between *emm28*-specific surface protein, R28, and host cells. R28 N-terminal domain, $R28_{Nt}$, and its two subdomains promote the binding to endometrial, cervical and decidual cells. $R28_{Nt}$ and its two subdomains directly interact with the integrins α3β1, α6β1 and α6β4. $R28_{Nt}$ also promotes adhesion to pulmonary and skin epithelial cells. Our results suggest that $R28_{Nt}$-integrin interactions contribute not only to *emm28*-elicited endometritis, but also to the overall prevalence of the *emm28* strains.

To further characterize the initial events involved in the establishment of GAS endometritis, we developed a novel approach in which we infected *ex vivo* the human decidua, the mucosal uterine linen during pregnancy. We analyzed the outcome using state-of-the-art imaging set-up, image processing and analysis. GAS adheres to the tissue and grows at its surface; secreted host factors triggering this growth. GAS readily forms biofilm at the tissue surface, thread-like and inter-chains filaments ultra-structures composing these biofilms. GAS invades the tissue and this depends on the expression of the cysteine protease SpeB. GAS induces the cell death of 50% of cells within 4 h and this cytotoxicity depends on secreted factors, including the Streptolysin O (SLO). Finally, GAS restrains the tissue immune response at the transcriptional and protein levels, the latter depending on the expression of SLO and SpeB.

Résumé

Streptococcus pyogenes, également appelé Streptocoque du Goupe A (SGA), est un pathogène à l'origine d'une grande diversité d'infections, allant d'infections superficielles comme l'angine aux infections invasives, comme la fasciite nécrosante et les endométrites. Au 19ème siècle, une femme sur dix mourait après l'accouchement de fièvre puerpérale, notamment d'endométrite. En France, les infections gynéco-obstétricales correspondent encore de nos jours à 27 % des infections invasives à SGA chez les femmes. Les souches de SGA présentent une forte diversité génétique et de répertoire de facteurs de virulence. Le génotype *emm28* est le troisième génotype le plus prévalent en France et il est associé aux endométrites. Nous avons analysé par deux axes complémentaires les facteurs et mécanismes impliqués dans les endométrites à SGA.

Par des approches de biochimie et de biologie cellulaire, nous avons caractérisé l'interaction entre les cellules de l'hôte et R28, une protéine de surface spécifique du génotype *emm28*. Le domaine N-terminal de R28 ($R28_{Nt}$) et ses deux sous-domaines favorisent la fixation des bactéries à des cellules endométriales, cervicales et déciduales. Ils fixent de manière directe les intégrines α3β1, α6β1 et α6β4. Par ailleurs, $R28_{Nt}$ promeut aussi l'adhésion à des cellules épithéliales de la peau et des poumons. Ces résultats suggèrent que la fixation des intégrines par $R28_{Nt}$ concourt, non seulement, aux endométrites dues au génotype *emm28*, mais aussi, et de manière plus générale, à la prévalence de ce génotype.

Afin de mieux caractériser les étapes précoces essentielles au développement des endométrites à SGA, nous avons infecté *ex vivo* la décidue humaine, qui correspond à la membrane utérine durant la grossesse. Nous avons analysé les effets de l'infection de la décidue par des techniques de microscopie et d'analyse d'image de pointes. SGA adhère au tissu et se multiplie au contact de celui-ci grâce à des éléments sécrétés par le tissu. Sur ce tissu, SGA forme des biofilms composés d'ultrastructures ressemblant, pour certains, à des fils reliant deux coques d'une même chaine et, pour d'autres, à des filaments reliant plusieurs chaînettes ; certains s'organisent en réseau. GAS envahit en profondeur le tissu, ce qui dépend de l'expression de la cystéine protéase SpeB. SGA induit la mort de la moitié des cellules en moins de 4 h à travers la sécrétion de différents facteurs, dont la Streptolysine O (SLO). Enfin, GAS est capable de restreindre la réponse immunitaire du tissu à l'échelle transcriptomique et protéique, le contrôle protéique dépendant de l'expression de SLO et de SpeB.

Table of contents

List of principal abbreviations

C-ter: C-terminal

ECM: extracellular matrix

EPS: extracellular polymeric substance

Fg: fibrinogen

FH: factor H

FHL-1: factor-H-like protein 1

Fn: fibronectin

GAS: Group A Streptococcus

GBS: Group B Streptococcus

HVR: hypervariable region

LTA: lipotechoic acid

mRNA: messenger ribonucleic acid

NET: neutrophil extracellular traps

NF: necrotizing fasciitis

N-ter: N-terminal

Pg: plasminogen

Pm: plasmin

QS : quorum sensing

SA regulator : stand-alone regulator

SAgs: superantigens

SEM: scanning electron microscopy

sRNA: small ribonucleic acid

STSS: streptococcal toxic shock syndrome

TCS: two-component system

List of Figures of the introduction

List of Tables of the introduction

Foreword

Streptococcus pyogenes is a strictly human pathogen responsible for a wide range of diseases, from superficial infections, such as pharyngitis, to life-threatening invasive infections, such as necrotizing fasciitis and endometritis. *S. pyogenes* is also involved in post-infectious complications such as rheumatic fever. Strains are genetically highly diverse and classified through the sequencing of the *emm* gene, with more than 200 *emm*-types identified. *emm28* is the third most prevalent *emm*-type in France and is associated with gyneco-obstetrical infections. During the course of infections, numerous ubiquitous or strain-specific virulence factors are involved. However, there are few models that enable an integrative study of *S. pyogenes* early steps of infection which are involved in both superficial and invasive infections. The first part of this dissertation will be an introduction on *S. pyogenes* pathogenesis. The second part will present the main results of my thesis, composed of two complementary aspects addressing *S. pyogenes* and endometritis. The last part of my dissertation will discuss the results and conclude with some perspectives on this work. The introduction will review the most important features of *S. pyogenes* pathogenesis, focusing on the virulence factors, the mechanisms involved and the study models. In the result chapter, we will first present our results on the *emm28*-specific R28 protein involved in promoting adhesion to host cells and its receptors. In the second part, an original model of *ex vivo* infection of a human tissue will be presented, where bacterial colonization, biofilm formation, tissue invasion, induced cytotoxicity and modulation of the immune response are analyzed, with a focus on the role of the Streptolysin O (SLO) and the cysteine protease (SpeB) on several of these phenotypes.

Introduction

Introduction

In this introduction, we will first describe the main bacteriological and clinical characteristics of *S. pyogenes*, then the virulence factors and their regulations, the mechanisms involved in the pathogenesis and finally, the main experimental approaches to understand *S. pyogenes* pathogenesis.

1. *Streptococcus pyogenes* morphology, epidemiology and induced diseases

In this chapter, we briefly introduce the main morphological and microbiological characteristics of *S. pyogenes*, the strain classification, the different *S. pyogenes* induced diseases and their burden, genotypes prevalence and finally we focus on a specific association between *emm28* strains and gyneco-obstetrical diseases.

1.1. *Streptococcus pyogenes* history and morphology

1.1.1. The intimate relation between the history of *S. pyogenes* and puerperal fever

"Everything was in question; everything seemed inexplicable; everything was doubtful. Only the large number of deaths was an unquestionable reality." Ignaz Semmelweis was a young Hungarian physician in 1847 who worked in a Vienna hospital when he made this statement. The Vienna hospital had two clinics, and as shown in Figure 1, the mortality rate was strikingly higher in one than in the other (1). In the 19th century, up to one woman out of 10 died after delivery and this was not the case before (Figure 2). This had a huge societal impact and was a great society burden. It is during his investigation on the origin of the differences between the mortality rates in the clinics that he discovered that hand washing with specific solution (chlorinated lime) could strongly reduce maternal death rate (Figure 3). Semmelweis' train of thoughts that lead to his assumption that particles from cadavers were the cause of puerperal fever is summed up in Table 1.

Theodor Billroth is an Austrian surgeon thought to be the first to describe streptococcal infections, cases of erysipelas and wound infections. In 1874, he described "small organisms (Kettenkokken) as found in either isolated or arranged in pairs, sometimes in chains of four to twenty or more links" (2).Louis Pasteur became aware of these results as soon as 1875.

Table 1. Semmelweis' train of thoughts

Observation	Interpretation
• The maternal death rate in clinic 1 is higher than in clinic 2	• Endemic specificities of clinic 1 induce puerperal fever
• Student and professor only visit the clinic 1	• Students and professor could be the vector of the disease
• Professor Jakob Kolletschka, a forensic, died after a student hit him accidentally with a knife that touched the dead body. Autopsy of the professor revealed similar clinical manifestations as puerperal fever patients	• Something from the cadaver could explain both the professor and the maternal deaths
• Rotten fruit transmit putrefaction to living fruits	• "Disease" can be transmitted by contact
• The death rate was lower in December to April 1847, where the assistant professor went less to the morgue	• Physician, by coming from the morgue transfer the disease
• Women with high dilatation were most likely to die than others	• These women were "visited" several times, increasing the risk to get the disease
• There are more death in the 19th century than before	• Hospitals and the increase in knowledge in medicine correlates with the increase in maternal death rate

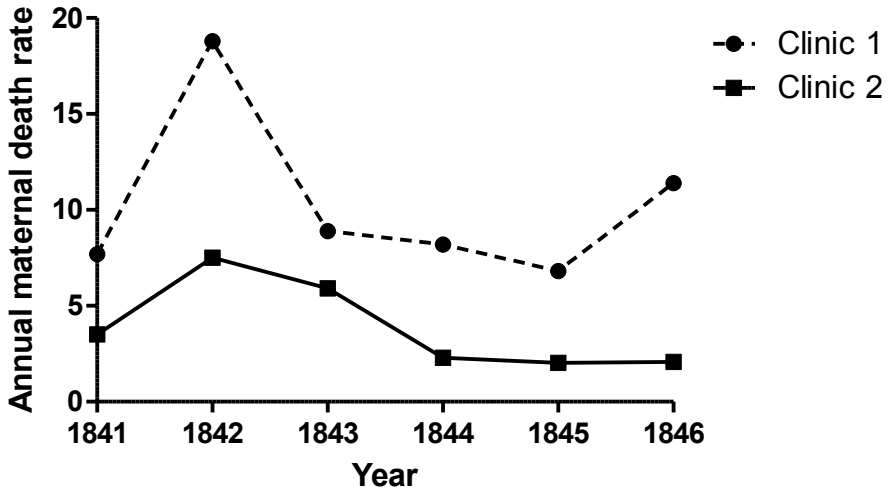

Figure 1. Maternal death rate in the two clinics
Clinic 1 was the normal clinic, where students and professors took care of pregnant women until delivery and after. In the Clinic 2, most women already had delivered and were taken care of by midwifes. Data from (1)

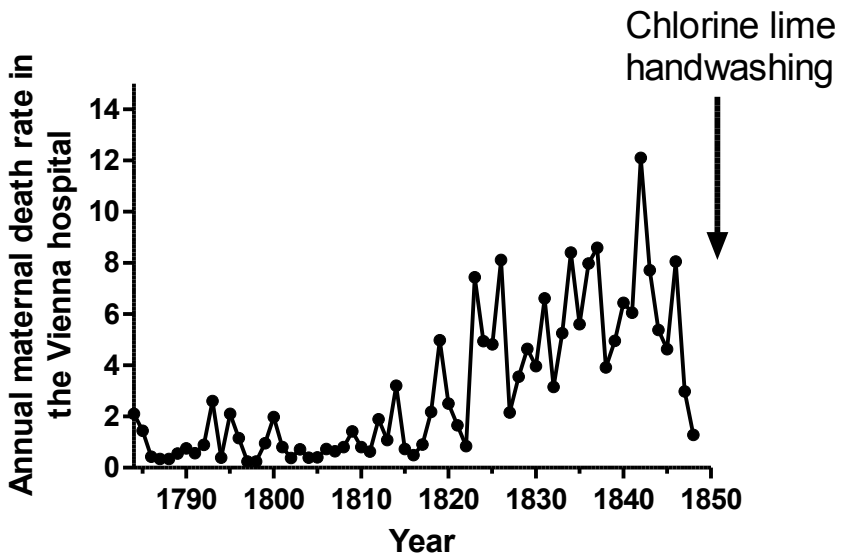

Figure 2. Evolution of the maternal death rate between 1784 and 1848
Before 1820, maternal death was low in the Vienna hospital (~1%), after 1820 and until handwashing was mandatory, the maternal death rate was around 6%. Data from (1).

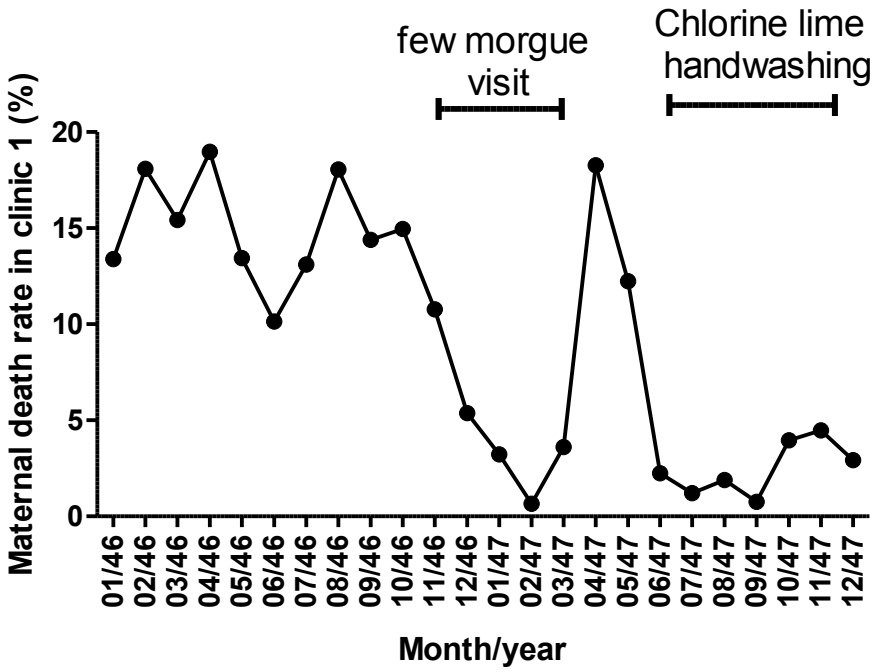

Figure 3. Monthly maternal rate between 1846 and 1847
There was a change in assistant professor in December 1846 until March 1847. In April 1847, Semmelweis became assistant professor and went every morning to the morgue before taking care of pregnant women. In May 1847, chlorine lie handwashing became mandatory. Data from (1)

On the 21st of January 1879, thirty years after Semmelweis' discovery, Maurice Perrin, a French physician declared: "How can we explain that in the countryside there is not even a case out of a 1000 of puerperal fever, perhaps even one out of 10 000, whereas in hospitals postpartum women suffer dreadful epidemy"[1] (3). In early 1879, Pasteur isolated microbes from a woman with puerperal fever, which looked exactly as the one described by Theodor Billroth. When Dr Hervieux, director of the Port-Royal maternity, claimed that a mysterious "miasma" was the explanation for puerperal fever and not a germ (called vibrion), he ended his speech by declaring: "I have an awful fear […]: it is to die before we ever find this vibrion"[2] (4). Pasteur at this point had not validated the Koch postulate for the puerperal fever. However, Pasteur replied on the same day to Hervieux's speech by stating "Let the Academy allow me to draw the dangerous microbe I believe is responsible for puerperal fever"[3], and he draw a microbe that Pasteur describes himself as "an organism made of grains in couples or chains"[4] (4). Later in 1879, Pasteur went to Hervieux's clinic and isolated from multiple women suffering puerperal fever the same organism as that isolated by Theodor Billroth, confirming his initial statement (4). The name *Streptococcus pyogenes* (streptus: chain, pyo: pus, genes: forming) was coined 5 years later in 1884 by Friedrich Julius Rosenbach (5).

Streptococci are classified through one of the very first serotyping methods, developed by Rebecca Lancefield in 1919. Lancefield identified several immunogens to distinguish streptococci, and most of them were carbohydrates. *S. pyogenes* belongs to the Lancefield Group A family of Streptococcus (GAS) (6).

1.1.2. GAS microbiological characteristics

GAS is a Gram positive bacterium, β-hemolytic, with a low G+C % DNA content. Cocci are assembled in chains of minimum two cocci (Figure 4). GAS is grown on blood or Todd Hewitt broth supplemented with 0.2% yeast extract agar plates and its multiplication is favored by CO_2 and anaerobia. GAS is auxotroph for 15 amino acids and its primary source of carbon is glucose [(7, 8), for review: (9)].

[1] «Comment se fait-il qu'à la campagne on ne compte pas un cas de fièvre puerpérale sur mille, peut-être sur dix mille accouchées, tandis que les hôpitaux de femmes en couches sont dévastés par d'effroyables épidémies?» p50
[2] « Mais, faut-il l'avouer, j'ai une peur terrible, une peur dont je ne puis me défendre, et que l'Académie comprendra : c'est celle de mourir avant qu'on n'ait découvert ce vibrion-là » p 256
[3] « Eh bien, que l'Académie me permette de dessiner sous ses yeux le dangereux microbe auquel je suis porté en ce moment à attribuer l'existence de cette fièvre » p 259
[4] […] organisme formé de couples de grains ou de chapelets de grains". p 272

GAS is a non-motile, extracellular and human specific pathogen. The size of the GAS genome varies from 1.75 to 1.9 megabases, harboring roughly 2000 genes. Eighty-five % of the coding genome is the core genome conserved between all strains. Moreover, 10 % of the metagenome corresponds to prophages, largely contributing to strain diversity (10).

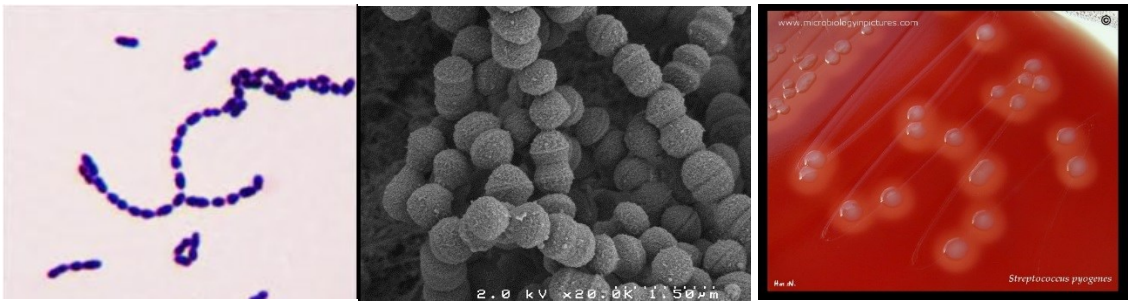

Figure 4. Morphology of GAS
Left: Gram-positive staining of GAS. Middle: Scanning electron microscopy of GAS. Right: GAS β-hemolysis on sheep blood agar plates.

1.2. GAS *emm*-typing

While identifying the carbohydrates involved in the Lancefield Group typing, Lancefield also isolated another major immunogen of GAS which is a protein, and she used this protein as a typing method for GAS strains. After discovering that a non-typable strain was less mucoid, she called this protein the M protein (11). She then set up the first collection and classification of GAS strains depending on the M protein expressed.

The main variations of the M protein are in the N-terminal domain, called the hypervariable region (HVR) (Figure 5) and the serotyping is based on antibodies directed against this region (12). This is an important functional domain, and antibodies against it highly decrease the strain virulence (13). The diversity of M proteins is explained by the immunological pressure and the critical importance of the M protein in virulence: people immunized for one M protein will no longer be affected by the strains presenting this M protein making it a major selective pressure. In addition to this, the more people are infected by a given strain, the smaller the pool of potentially neo-infected individuals is, reducing the strain prevalence. This immunological pressure implies a strong immunization against the M protein encountered, which occur to a lesser extent with antibiotic treatments which stop the infections before a strong immune response is established.

Today the classification no longer stands on serotyping but on genotyping, by sequencing the 5' of the *emm* gene, coding for the 50 first residues of the N-terminal domain of the M protein (14). The sequencing of an array of 1064 invasive strains identified 225 *emm*-types (15).

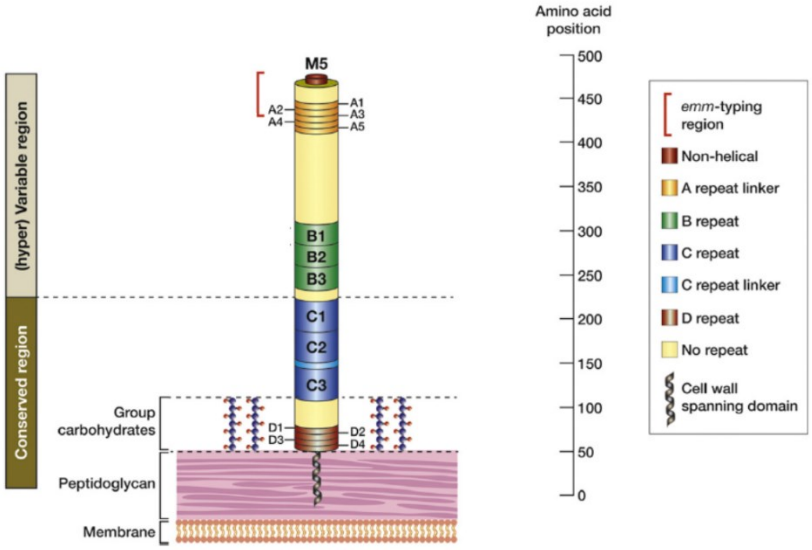

Figure 5. Structure of the M protein
Structure of the M5 protein to highlight the region used for serotyping (hypervariable region), and the 50 residues region now used for the *emm*-typing (in red). Adapted from (12).

1.3. GAS carriage and induced diseases

1.3.1. Asymptomatic colonization

GAS asymptomatic colonization or carriage is frequent in the throat: a meta-analysis showed that around 10% and 6% of children and 2.8% and 2% of adult are colonized in high-income and low-income countries, respectively (16). Some individuals are colonized for long periods of time (several years); the reasons for this persistent state are not well understood, but it appears that it has no role in post-infectious manifestations nor bacterial transmission (17, 18). Moreover, carrier children frequently switch *emm*-types throughout their lives (19).

1.3.2. Superficial infections

Pharyngitis and scarlet fever. Pharyngitis is a superficial infection of the oropharynx and GAS accounts for 4-10% pharyngitis cases in adults (20). GAS is annually involved in 616 million cases of pharyngitis in the world (21). Pharyngitis is more prevalent in OECD (National Organization for Economic Cooperation and Development) than non-OECD countries (16).

The complexity of GAS pharyngitis diagnostic is that most pharyngitis cases are not due to GAS and GAS is found asymptomatically in the throat. Consequently, a GAS positive swab does not systematically indicate a GAS-elicited pharyngitis. This could explain the dichotomy between GAS positive pharyngitis and serologically positive pharyngitis, with only around 50% of matches (16).

Impetigo and erysipelas without bacteremia. GAS is also involved in superficial skin infections, such as impetigo and erysipelas. In contrast to pharyngitis, impetigo is predominant in non-OECD countries, and there are an estimated 111 million cases of GAS-elicited impetigo per year (21).

1.3.3. Invasive infections

GAS invasive infections are infections during which GAS is found in normally sterile compartments or with Streptococcal Toxic Shock Syndrome (STSS). GAS invasive infections are responsible for 163 000 deaths per year (21) and, in France, their annual incidence is estimated to be 3.1/100 000, with a case-fatality ratio of 14% (22). Of note, the number of cases of invasive infections has been increasing in the world since 1990s (21), with an increase of 4% per year in France between 2007 and 2014, partly due to an increase in the number of invasive infections of people above 65 years of age (Figure 6).

Necrotizing fasciitis. Necrotizing fasciitis (NF) is the infection of the deeper layers of the skin, below the fascia, and is a rapidly progressing and life-threatening disease, with a mortality around 30% (23). In the United States of America, there are around 700 cases of NF per year and in France, in 2007, there has been 104 cases of GAS-elicited NF, of which 22 % were fatal (22, 24). NF risk factors are varicella, wound, burn and blunt trauma (25).

Bacteremia and septic shock. Bacteremia is the presence of bacteria in the blood and is associated with 60% of French invasive infections (https://cnr-strep.fr/). For some bacteremia, the origin of the bacterial translocation is unknown, and is called bacteremia without identified focus; this is the case for around 22% of French GAS invasive infections (22).

STSS. Bacterial toxins in the bloodstream or in a tissue can induce the hyperactivation of the immune system, further inducing a cytokine "storm" and shock followed by organ failures. This is called a septic shock and more specifically the STSS. STSS is the most life-threatening complication of GAS infections, with a mortality of up to 43% (22).

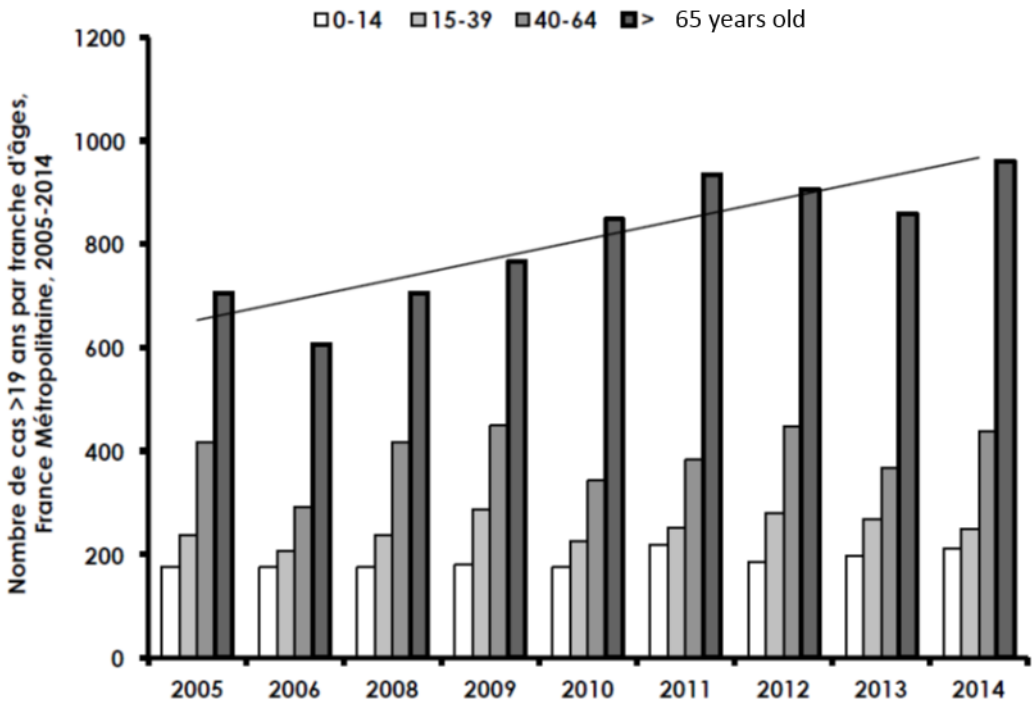

Figure 6. Number of invasive infections in adults in France
Number of cases of invasive infections in France depending on the age. There is an overall increase of the number of invasive infections in France, driven by an increase in the number of invasive infections in people aged above 65 years. From (https://cnr-strep.fr/).

Endometritis and Puerperal fever. Puerperal fever, or childbed fever, is the increase of temperature in the 24 h following delivery and is due to an infection, referred to as puerperal infection or post-partum infection. The majority of these infections are in the gyneco-obstetrical tract, including the endometrium. In this thesis, endometritis was studied as a model of GAS invasive infections.

While less frequent than in the 19th century, puerperal fever is still responsible for 75 000 maternal deaths annually in the world, affecting 5-10% of pregnant women (26). A recent analysis in the UK showed an incidence of post-partum endometritis of 109 cases per 100 000 persons/year (27), slightly higher with a US rate of 59 per 100 000 persons/year (28). A population based study in Sweden showed that 2% of women suffered endometritis following delivery (29). The post-partum is a favorable condition for infections with several pathogens: *Escherichia coli,* Group B Streptococcus (GBS), *Staphylococcus aureus*, anaerobic bacteria and *Listeria monocytogenes* (30), but GAS is involved in 50 % of maternal sepsis, making it the pathogen most frequently responsible for maternal infections; furthermore, it is the most aggressive one. In France, infections of the gyneco-obstetrical sphere still correspond to 26.8%

of women, all age groups considered, GAS invasive infections (https://cnr-strep.fr/) (Table 2), of which 15.9% are endometritis. Women have a 20-fold increased incidence of GAS invasive diseases compared with non-pregnant women (31). The postpartum, abortion, *in vitro* fertilization and intrauterine devices all are risk factors for endometritis and are involved in more than half of GAS-elicited endometritis France (Table 2).

Table 2. GAS gyneco-obstetrical invasive infections in France 2006-2015, risks factors and prevalence of the main *emm*-genotypes

GAS invasive infections	Women	Gyneco-obstetrical infections	Endometritis	Post-partum and risk factors*
All	2489	668/ *26.8%*	395/ *15.9 %*	201/ *8.1 %*
STSS	453/ *18.2%***	72/ *10.8 %*	27/ *6.8 %*	N.D.
Fatality case	283/ *11.4 %*	16/ *2.4 %*	5/ *1.3 %*	N.D.
emm28		168 /*25.1 %*	104/ *26.3 %*	54/ *26.9 %*
emm1		113/ *16.9 %*	66/ *16.7 %*	27/ *13.4 %*
emm89		123/ *18.4 %*	75/ *19 %*	40/ *19.9%*
others (30 genotypes)[a]		240/ *39.5 %*	150/ *38 %*	80/ *39.8 %*

*risk factors: abortion, intra uterine device, *in vitro* fertilization. [a] 30 other genotypes.
**First numbers correspond to the number of cases and strains, the second ones, in italic, to the percentages: first line percentage of all women invasive infections; STSS and fatality case: percentage of the STSS/deaths for each column. The percentage for the strain genotypes corresponds to the percentage of strains for each column. N.D.: not determined. From (https://cnr-strep.fr/).

1.3.4. Post-infectious complications

GAS infections are the indirect cause of several pathologies, such as glomuronephritis and rhumatic arthritis. They all are auto-immune diseases due to the cross-reaction between GAS epitopes and host epitopes (32). Overall, these complications are responsible for 354 000 deaths per year and the incidence is very important in developing countries, with for example 15 to 16 million people suffering from GAS induced rheumatic heart diseases and 282 000 new cases per year (21).

1.4. Epidemiology of the *emm*-types strains

The diversity of strains responsible for superficial and invasive infections is higher in developing countries than in high income countries, which could be explained by climatic differences, genetic susceptibility and social economic reasons (33, 34). The distribution of

strains responsible for invasive infections in France and in Europe is summarized in Figure 7 and Table 3, respectively.

Table 3. Main GAS *emm*-types involved in invasive infections in Europe from 1st January 2000 to 31st May 2017

Country	1st	2nd	3rd	4th
Czech Republic	*emm1*	*emm81*	*emm28*	
Denmark	*emm1*	*emm28*	*emm89*	
England/Wales	*emm3*	*emm1*		
Finland	*emm28*	*emm89*	*emm1*	
France	*emm1*	*emm28*	*emm89*	
Germany	*emm1*	*emm28*	*emm3*	
Greece	*emm1*	*emm12*		
Hungary	*emm1*			
Iceland	*emm1*	*emm89*	*emm28*	
Ireland	*emm1*	*emm12*	*emm28*	
Italy	*emm1*	*emm12*		
Norway	*emm89*	*emm28*	*emm3*	
Poland	*emm1*	*emm12*		
Portugal	*emm1*	*emm89*	*emm3*	
Romania	*emm1*			
Scotland	*emm1*			
Spain	*emm1*	*emm3*		
Sweden	*emm89*	*emm81*	*emm28*	*emm1*

emm-types involved in more than 10% of the invasive infections are represented in the order of prevalence from left to right. The countries are in the alphabetical order. The *emm28* genotype used in this thesis is underlined, the data do not include the most recent French epidemiological data (Figure 4), and *emm28* are no longer the second most prevalent strain in France since 2012. Adapted from (35).

emm1 strains are the most prevalent strains in high income countries, with a clone emerging in the 1980s that is more efficient in colonizing and that increased the *emm1* overall prevalence (36). Since 2008 in Europe, an *emm89* clone has been rapidly emerging (37). While there are more than 200 described *emm*-types, in 2016, 60% of GAS invasive strains in France are from four genotypes: *emm1*, *emm89, emm28* and *emm12* (Figure 7) (https://cnr-strep.fr/). In Europe, the main genotypes responsible for invasive infections are *emm1*, *emm28*, *emm89*, *emm3*, *emm12* and *emm81* (35).

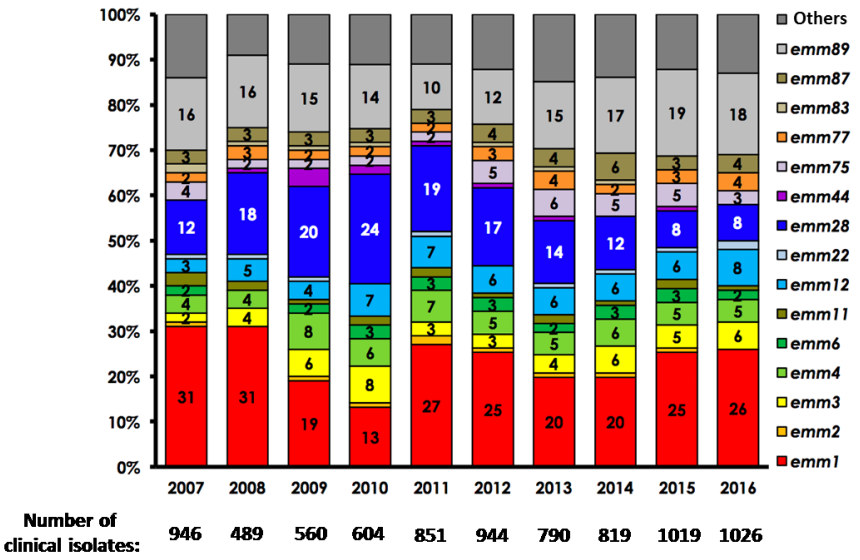

Figure 7. Distribution of GAS *emm*-types involved in invasive infections in France
(National Center for Streptococcus activity report, https://cnr-strep.fr/images/CNR-STREP/rapport/rapport_CNR-strep_2016.pdf).

1.4.1. Tissue tropism and *emm* patterns

GAS induces a wide range of diseases and there are few associations between diseases and genotypes (38). GAS strains can be classified with a sequence typing in five gene patterns, A to E, which is based on the analysis of the patterns of the *emm*, *emm*-like genes and *sof*/*sfbx* genes of numerous clinical strains (Figure 8) (39, 40).

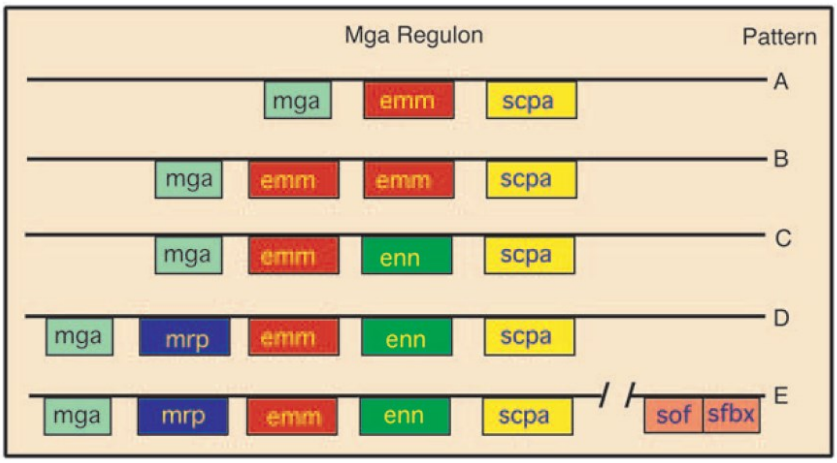

Figure 8. *emm* pattern classification
The organization of the Mga locus and the presence or not of *sof/sfbx* can discriminate GAS strains into 5 *emm* pattern, from A to E. From (41).

There is a clear association between specific *emm* patterns and skin/throat tropisms (40, 42). A-C strains represent ~47% of throat infections, but only 8% of impetigo isolates. In contrast, D

strains represent ~50% of impetigo strains, but only 2% of pharyngitis strain, and E pattern strains are equally represented in both infections, thus called ubiquitous (42).

1.4.2. The *emm28* association with gyneco-obstetrical sphere infections

The *emm28* genotype is one of the three main genotypes encountered in Europe (Figure 7, Table 2). It belongs to the E pattern and it is associated with gyneco-obstetrical infections, representing around 25% of these infections while being responsible for only 15% of all invasive infections (43). More specifically, the association between puerperal infections and the *emm28* was described in several countries (44–47). *emm28* strains are, together with *emm1*, associated with severe cases of puerperal infection (46). The R28 protein expressed by *emm28* strains has been implicated in the association of *emm28* strains with puerperal infection (48). The first sequence of an *emm28* genome identified two *emm28* specific genomic regions (RD1 and RD2) that could explain this association. RD2 is a 37.4 kb region with genes encoding several cell-wall anchored proteins, including AspA, also known as AgI/II (M28_Spy1325) and R28 (M28_Spy1336) (Figure 9).

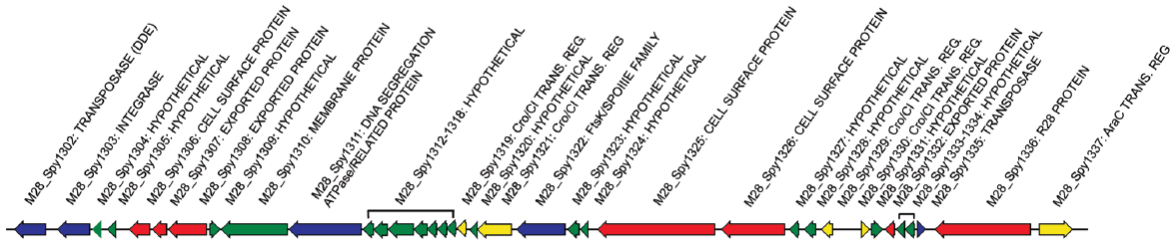

Figure 9. RD2 region of *emm28* strains.
In green are shown inferred hypothetical proteins of unknown function, in red, extracellular proteins, in yellow, putative gene regulators and in blue, putative mobility/transfer ORFs. From (45)

The integrative conjugative element RD2 contains several genes related to GBS genes and was most likely horizontally transferred from GBS (45, 49). Since GBS colonizes 10-30% of healthy women uro-vaginal tract (50), it was suggested that RD2 harbors genes involved in the *emm28* association with gyneco-obstetrical diseases.

2. GAS virulence factors and their regulation

2.1. GAS virulence factors

In this chapter, we will describe different factors whose implication in the GAS pathogenesis mechanisms will be discussed in chapter 3 and in the Results section. We will briefly discuss the concept of "virulence" factors in the light of GAS pathogenesis, and we will then describe the different virulence factors and then their regulation.

The virulence concept in the light of GAS pathogenesis

The concept of virulence and virulence factors, coined in the early 20th century aggressins and virulins by Rosenow, was based on the concept that some pathogenic elements could confer the pathogenic property to avirulent organisms (51). This was linked to the concept of intrinsic pathogenicity of a bacterium, in opposition to commensal and avirulent organisms, and to the intrinsic capacity of a factor to yield virulence. However, as described by Casadevall and Pirofski in 1999, virulence emerges from the intersection between the repertoires of factors of an organism and the host environment encountered (52). The pathogenicity of an organism is dependent on how much, where and when it expresses its factors. Moreover, many "virulence factors" expressed by highly pathogenic bacteria are also expressed by commensal bacterium, and the importance of factors in virulence depends on the genetic backgrounds (with the exception of certain toxins). Therefore, virulence properties and specificity of a factor are not intrinsic.

In the following paragraph, we will describe different factors which, in the host environment tested and the bacterial genetic background used, are implicated in the virulence of the tested strains. The virulence property of any factor cannot be extended to all GAS strains or diseases. The biochemical nature and main properties will be analyzed in this section, while the regulation is analyzed in section 2.2, and the role of these virulence factors in GAS infections is analyzed in section 3. Factors are discussed by their importance regarding my PhD work and in alphabetical order. A special focus is made on the R28 protein which is one of the main topics of this dissertation. The order of factors discussed and the focus on some factors/regulation pathways do not pretend to hierarchize them relatively to an importance in virulence.

2.1.1. Secreted factors

2.1.1.1. SLO, NADase, SLS, SpeB and Superantigens

SLO and NADase. Streptolysin O (SLO) is a pore-forming cholesterol-dependent cytotoxin (53), secreted as a 69 kDa protein. SLO forms pores through oligomerization of the protein after cholesterol and galactose binding at the cell surface (54, 55). At low multiplicity of infection, SLO pores induce in keratinocytes an endoplasmic reticulum (ER) stress through a cytoplasmic calcium increase (56). This ER stress induces the unfolded protein response in HeLa cells (cervical cells), which further increases asparagine secretion, used by GAS to multiply (57). Ultimately, these pores induce cell death in different cell types (reviewed in section 3.2). In response to the pores, different pathways were shown to restrain their effect: endocytosis and ectocytosis of the damaged membrane (Figure 10).

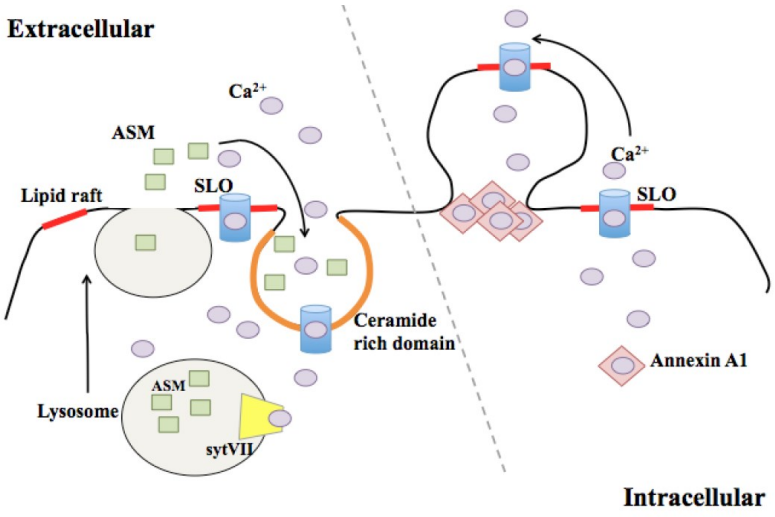

Figure 10. Membrane repair after SLO damages.
Left. Ca^{2+} increase in the cytoplasm is detected by Synaptotagmin VII (sytVII, yellow), which activates lysosome fusion at the membrane. This releases acid sphingomyelinase (ASM, green) in the extracellular compartment, which transforms sphingomyelin in ceramide rich domain, further triggering endocytosis of damaged membrane (58–61). **Right**. Ca^{2+} influx is sensed by annexin A1 which is recruited at the damaged membrane, which triggers ectocytosis of the pore, a mechanism described as "blebbing" (62, 63). From (64)

slo is cotranscribed with *nga*, coding for the streptococcal NAD-glycohydrase (NADase, Nga or SPN), and *if* coding for NADase inhibitor (IF). NADase is a SLO cofactor and is composed of two domains, one involved in the SLO mediated translocation and the second one is a domain wit β-NAD+ glycohydrolase activity (65, 66). In the bacterium, the NAD-glycohydrase activity of NADase is restrained through IF action (67–69). NADase is translocated into cells via a 70 amino acid domain of SLO but the pore formation is not required for NADase translocation

(66, 70). NADase binding to an unknown receptor forms a pore independently of the SLO mediated pores (54, 55). Intracellularly, NADase induces the depletion of NAD, which induces cell-death (67, 71). However, a NADase variant without the β-NAD+ glycohydrolase activity still triggers programmed cell death (72). Extracellular NADase reduces the release of IL-1β by macrophages, and this inhibition is independent from its translocation by SLO (73).

SLS. Streptolysin S, SLS, is a member of the thiazole/oxazole-modified microcins and the pro-SLS peptide is coded by the gene *sagA*. *sagA* is co-transcribed in an operon composed of nine genes (*sagA* to *sagI*) which encodes proteins that profoundly modify the initial 2.7 kDa peptide into the mature SLS (74). It is an oxygen stable cytotoxin that forms hydrophilic pores in multiple cell types, including immune cells, and it is, for example, responsible for GAS β-hemolysis. SLS cytotoxic activity is sevenfold higher when bacteria are in contact with cells than when they are not (75, 76), and its activity is stabilized by host high-density lipoprotein (HDL) or albumin (74, 77, 78). Recently, the mechanism of SLS red blood cells lysis was unraveled: SLS interaction with band 3 protein, also known as Anion exchanger 1 (AE1), induces Cl^- influx and subsequent osmotic shock (79).

SpeB. Streptococcal pyrogenic erythrogenic toxin B (SpeB) or streptopain or SPC (80), is commonly known as the streptococcal cysteine protease. It is produced as a zymogen of 40 kDa that is converted into a 28 kDa mature active protein after multiple intramolecular autocatalytic cleavages and reduction of the cysteine residue (81–84)**.**All clinical strains express SpeB (85) and *in vitro,* SpeB is predominantly produced during the stationary phase of growth. Structurally SpeB presents a papain fold and is active form is the dimer (86, 87). SpeB protease activity requires a three amino acid motif which makes it a broad-spectrum protease. Consequently, SpeB can degrade *in vitro* a very large number of host proteins (Table 4). SpeB also degrades several bacterial surface proteins (protein M and M-like, protein F1, Fba, C5a peptidase, protein H). Of note, SpeB capacity to degrade IgG was recently questioned (88), as SpeB only cleaves reduced IgGs, and reductive conditions might not be present *in vivo* (89).
In addition to its soluble form, SpeB can be retained at the bacterial surface by the alpha2-M-binding protein bound to the bacterial surface G-related alpha2-M-binding protein (GRAB) (90) and it remains active against several ligands. Noteworthy, surface bound SpeB degrades the anti-microbial peptide LL-37 (91). SpeB can also act as an adhesin; it binds laminin (92) and a variant of SpeB with a RGD motif present in 20 % of the tested strains directly binds to the integrins $\alpha V\beta_3$ and $\alpha_{IIb}\beta_3$ (93).

Table 4. SpeB interactions with host components

Protein	Activity	Reference
IgG	C	(94–97)
IgA,IgM, IgD, IgE	D	(97)
C3b	C/D	(98, 99)
Properdin	D	(100)
Chemokines	D	(101)
IL-1β	A	(102)
H-kininogen	Bradykinin release	(103)
Fibrinogen	D	(104, 105)
Plasminogen	D	(106)
Vitronectin	D	(107)
Fibronectin	D	(107)
Urokinase receptor	C	(108)
MMPs	A	(109, 110)
Decorin	D	(111)
Integrins	B	(93)
Laminin	B	(92)
A1AT	B	(112)
A2M	C	(91)

C= cleavage, A= activation, D= degradation, B= binding. Adapted from (89)

Superantigens. Superantigens (SAgs) are highly potent mitogens of the immune system: they induce hyper-activation and subsequent proliferation of human and some other mammalian T-lymphocytes. In conventional activation, peptides bind to the major histocompatibility class II (MHC) molecules expressed by antigen presenting cells (macrophage, B-lymphocytes and dendritic cells), and the recognition of the peptide/MHC complex by an antigen specific T-cell receptor (TCR) activates the specific T cells. The range of lymphocytes activated is limited by the epitope specificity of the TCR. In contrast, SAgs are able to induce activation of cells by binding non-specifically both the MHC and the TCR molecules (Figure 11).

SAgs are produced by a minority of organisms: some bacteria, among the most common bacterial geniuses, Group A, C and G *Streptococcus* and *Staphylococcus*, and viruses (113). Eleven SAgs have been described in GAS (114) and the overall SAg repertoires are conserved within *emm*-types. However, some strains within an *emm*-type express a specific repertoire of SAgs. The first GAS SAg, later termed SpeA, was identified in 1924 and called the "scarlet fever toxin". SpeC was discovered in 1960 (115). Because SpeA, SpeB and SpeC are able to induce fever when injected into rabbits (pyrogenicity), Kim and collaborators renamed these toxins streptococcal pyrogenic exotoxin (Spe) A, B and C (116). The SpeB was later shown not to be a SAg but the cysteine protease SpeB (80).

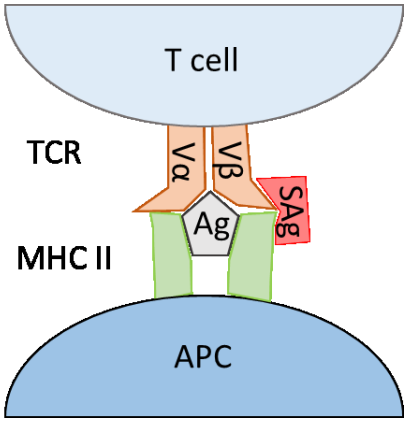

Figure 11. Mechanism of action of superantigens
APC: antigen presenting cell. MHC II: major histocompatibility complex class II. T cell: T lymphocyte. Ag = antigen. SAg = superantigen. TcR = T-cell receptor.

The amino acid sequence of the streptococcal superantigen SSA is very similar to staphylococcal SAgs (117). The streptococcal mitogenic exotoxin Z (SMEZ) is expressed by 94% of invasive strains in France (https://cnr-strep.fr/). Genetic analysis of a sequenced strain identified seven other gene coding for SAgs: *speG, speH, speI* and *speJ*, *speK*, *speL* and *speM* (118–122). The genes are associated with bacteriophages, except for *speG, speJ* and *smeZ* which are chromosomally encoded. Genes encoding GAS SAgs are not highly polymorph. Few alleles exist with minor diversity, except for the *smeZ* gene with so far 50 alleles identified, some of them containing nonsense mutations (123, 124)**.** The distribution of SAgs genes in GAS isolates are summed up in Table 5 (125). The strain used in this PhD was sequenced and its genome contains 5 genes coding superantigens: *smeZ, speG, speJ, speC* and *speK* (126).

SAgs bind the variable β chains (Vβ) of the TCR and the human T cell Vβ repertoire is composed of 50 different Vβ chains. Each SAg can bind more than one Vβ chain, and one SAg can activate up to 25% of the T cell repertoire. This is to be compared with the ability of a conventional peptide to activate only one subset of naïve T cells from the pool of $10^5 – 10^6$ cells. In addition to Vβ chains and MHC class II molecules, SAgs bind CD28 (127), a co-stimulatory receptor expressed by T cells, and SAgs interact with B7 (CD80/CD86) molecules present on antigen presenting cells. The binding of TCR to MHC molecule is a prerequisite for activation of T cells, but the interaction between B7 molecules of APC and CD28 of T cells is also necessary for T cell activation and the induction of pro-inflammatory cytokine genes (127).

Table 5. Repartition of the SAgs gene

	smeZ	*speG*	*speJ*	*speC*	*ssa*	*speA*	*speK*	*speH*	*speI*	*speL/M*
% of GAS strains	96	86.9	32.7	51.5	35.4	32.1	24.6	17.1	15.2	9.2

480 nonduplicate GAS isolates from Portugal between 2000-2005 were tested by PCR. Adapted from (125).

Binding of superantigens to T cells induces rapid release of TNF-α, TNF-β followed by IL-2, IL-6, IL-1 and IFNγ. In addition to Vβ specificities, each SAg induces responses of different intensities, as shown by the ability of SMEZ to induce ten times more cytokines than SpeA (128).

2.1.1.2. Other secreted virulence factors

DNases. DNases are enzymes that cleave DNA and play a potentially crucial role in defense against neutrophil extracellular traps (NETs) (129, 130). Eight types of DNases are expressed by GAS: *sda1, sda2, spd1, spd3*, *spd4* and *sdn*; *spn1* and *sdaB* are the only core genome encoded DNase genes in GAS, and they are present in all GAS strains (131, 132).

Sda1: the strain M1T1 acquired the DNase Sda1 *via* a bacteriophage and is the most important DNase for virulence of this clone (36, 130, 133). The importance of Sda1 in the emergence of the M1T1 strain and in its virulence is questioned (134–136).

Spd1 and Spd3 are bacteriophage encoded DNases (137, 138). Spd1 is reported to have an RNase activity but its role in virulence is unknown (137).

The EndoS family. Endo-beta-N-acetylglucosaminidase of *S. pyogenes* (EndoS) is a 108 kDa protein that removes carbohydrates from IgG in a specific manner, reducing Fc affinity for its receptors and diminishing the opsonophagocytosis of bacteria (95, 97).

$EndoS_2$. A variant of EndoS was described in serotype M49, named EndoS2 (139). EndoS2 activity differs from that of EndoS in the hydrolysis of N-linked glycans on native IgG chains and biantennary and sialylated glycans of the alpha1-acid glycoprotein (AGP).

IdeS. The immunoglobulin-degradin enzyme of *S. pyogenes* (IdeS), also known as Mac-1or MspA is a secreted cysteine protease that specifically cleaves the hinge region of IgG, but not the other immunoglobulins (140, 141). Mac-2 is a variant of IdeS that presents similar functions(142).

Sib35 is another anchorless immunoglobulin-binding protein. In contrast to IdeS or Mac-2, the 35 kDa Sib35 protein can bind IgA and IgM in addition to IgG. Sib35 is present in all GAS strains tested (143). Also, Sib35 binds to mouse B cells, enhances expression of MHC class II and B7-2 (CD86), induces the transition of cells to antibody producing plasma cells and

activates B cells proliferation. However, the overall importance of this phenomenon in GAS pathogenesis remains unexplored.

The Mac-1-like protein is a secreted protein and is a prokaryotic homolog of the human α-subunit of Mac-1, a leukocyte β2 integrin. This molecular mimicry enables GAS to bind CD16 at the neutrophil surface through the mac-1 like protein (144).

HylA. In GAS, three genes encode a hyaluronidase (HylA), also known as hyaluronate lyase: *hylA, hylP, hylp2*. *hylP* and *hylp2* are coded by bacteriophages and are thought to facilitate phage penetration in GAS. In contrast, *hylA* is coded in the core genome, but only ~25 % of GAS strains express detectable amount of functional HylA *in vitro* (145, 146). This is due to the presence of a point mutation in *hylA* that abolishes the enzymatic activity of the expressed HylA (147). Strains that express a functional HylA do not have the genes encoding the capsule biosynthetic pathway, the *hasABC* operon (148). There are homologs of the *hylA* gene in *Streptococcus pneumoniae*, GBS and *Staphylococcus aureus* (145), while there are no homologs to the *hasABC* operon (148). It is therefore hypothesized that the acquisition of the *hylA* gene is anterior to the acquisition of the capsule genes: a non-enzymatically active HylA was selected in strains that acquired the production of the capsule.

SIC and CRS. The streptococcal inhibitor of complement (SIC) is a 31 kDa protein whose gene is found in the genome of *emm1* strains and encoded on the same locus as the M protein, the Mga locus. SIC inhibits the formation of the membrane attack complex, avoiding complement mediated lysis of GAS (149). SIC also inhibits α-defensin, LL-37 and lysozyme, β-defensin, secretory leukocyte proteinase inhibitor, the chemokine MIG/CXCL0 (150–153). SIC can also inhibit the contact system; SIC is considered to be a major protein responsible for the increase of virulence of the M1T1 clone (136, 154, 155).

Of note, an *emm57* strain expresses a closely related to SIC protein (CRS), a SIC variant (156) and *emm12* and *emm55* strains express two distantly related SIC variants (157).

SP-SPT, SP-STK, SP-PTP. The eukaryote-type *S. pyogenes* serine/threonine phosphatase (SP-STP) and eukaryote-type *S. pyogenes* serine/threonine kinase (SP-STK) are secreted proteins involved in GAS virulence (158, 159). More specifically, SP-STP crosses cell and nucleus membranes and induces programmed cell death in pharyngeal cells (160). The *S. pyogenes* protein tyrosine phosphatase (SP-PTP) is responsible for Tyr-phosphorylation, even of eukaryotic components after infection. Its absence decreases bacterial growth, cell adhesion and cell internalization (161).

SpyA and SpyB. *S. pyogenes* ADP-ribosyltransferase (SpyA) is a C3 family ADP-ribosyltransferase whose gene is co-transcribed with the gene coding for SpyB (162). SpyA modifies the vimentin cytoskeleton in HeLa cells (162, 163). SpyA also induces the ADP-ribosylation of SpyB (164) which is a small heme binding protein (165). Finally, SpyA is an activator of the macrophage Nlrp3 inflammasome (166).

SpyCEP. *Streptococcus pyogenes* cell envelope protease (SpyCEP) is a serine protease that exists both as a secreted and a cell associated protein. It is secreted as an immature form of 170 kDa composed of two fragments, the N-terminal and C-terminal fragments which non-covalently binds to each other under non-denaturing conditions (167). In contrast to SpeB, it is expressed during the exponential phase. SpyCEP can cleave all chemokines that contain the ELR motif (CXCL-1,-3,-5,-6,-7,-8) (167); notably, SpyCEP is able to degrade IL-8 (168). Expression of SpyCEP decreases GAS adhesion to host cells and biofilm formation (169).

Sse. The role of the Streptococcal secreted esterase (Sse) is unknown, but its expression is upregulated in *covRS* mutants (170) and a *sse* null mutant presents a defect in growth in the laboratory rich medium THY (171). The null mutant is less virulent in mice model of necrotizing fasciitis (170) and there is a higher number of neutrophils at the site of infection compared to the wild-type strain (172). SSe hydrolyzes the platelet activation factor (173).

Ska. Plasminogen (Pg) is a single-chain glycoprotein that is part of the plasma and extracellular fluids. Pg is a key component of the fibrinolytic system. Upon binding to the serine proteases urokinase-type and tissue-type plasminogen activators, plasminogen is converted to the enzymatically active plasmin (Pm) that can cleave fibrin clots.

Streptokinase (Ska) is a single chain protein of 414 amino acid residues secreted not only by GAS, but also by group G and C streptococci. While achieving the same process as plasminogen activator, Ska does not harbor in itself a proteolytic activity. By specifically binding human Pg, Ska induces a conformational change in the Pg protein, which reveals an active site in the Ska-Pg complex. The enzymatically active complex can then cleave another Pg protein into Pm (“trigger cycle”). Since Pm has a higher affinity for free Ska than Pg, as soon as plasmin is present, another cycle takes place. Ska-Pm complexes are also enzymatically active and can convert a bound Pg into a bound Pm, creating the “bullet cycle” (Figure 12) (174–176).

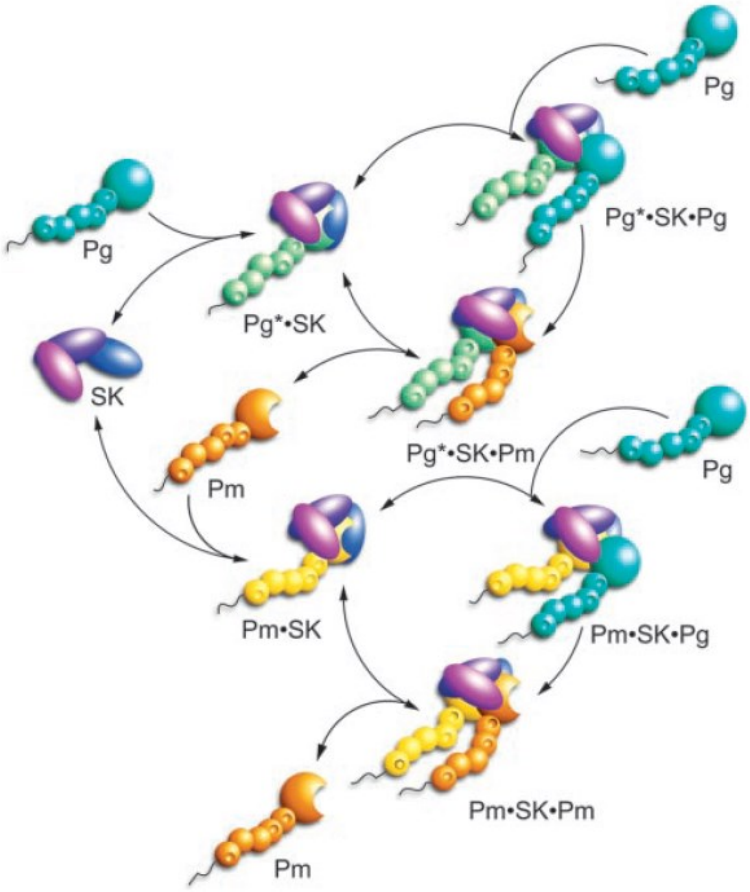

Figure 12. Mechanism of Ska transformation of plasminogen in plasmin.
Plasminogen: (Pg), SK: streptokinase, Pm: plasmin. From (177).

2.1.2. Surface-anchored virulence factors

2.1.2.1. Mga locus encoded proteins: M and M-like proteins, ScpA, SIC

M proteins and M-like proteins. The M protein was identified by Lancefield in 1928 (11). It is a major virulence determinant of GAS. It appears in electron microscopy as "tuftlike structures" (178). M proteins are cell-wall anchored protein, with a LPXTG motif close to the C-terminal end (179) and is composed of two chains. In proteins from the A-C genetic pattern (see 1.4.1), the M protein contains 4 repeat domains, A to D, that differ in size and amino acid sequence from one M protein to another. M proteins of strains of the *emm* pattern D do not present the A repeats, and E pattern strains M proteins present neither A nor B repeats (Figure 13). Therefore, E pattern M proteins are shorter than D pattern M proteins, themselves shorter than the A-C pattern M proteins.

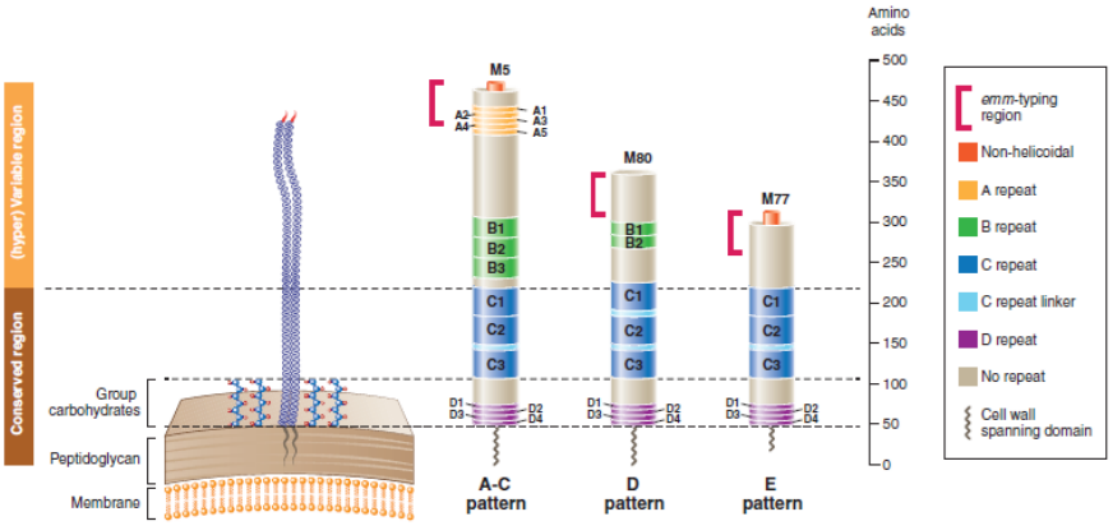

Figure 13. Structure of the M protein from the different *emm* patterns
The number and presence of the repeats A and B differ between the M proteins of the *emm* pattern strains. From (42).

Many strains express, in addition to the M protein, M-like proteins that are thought to come from a duplication of the *emm* gene with subsequent sequence divergence (Figure 8, Figure 14) (180). All strains of the C, D and E *emm* pattern express the Enn protein in addition to the M protein, and D-E strains also express the M-related protein (Mrp). Moreover 30% of M1 strains harbor the protein H, a M-like protein only found in this *emm*-type that belongs to the A-C pattern (181). The diverse host ligands bound by M protein are enumerated in Table 6.

M proteins have a non-ideal coiled-coiled structure (182); at 37°C, M protein dimers do not have stable coiled-coil structures (183). The C repeats, conserved among all M proteins, constitute the stable region of the coiled-coil structure of the M protein, whereas the B repeats contain several amino acid residues destabilizing this coiled-coil structure. Several explanations arose in the past to explain the potential role of this structural non-ideality in the M protein functions. First, these unstable coiled-coil structures could allow anti-parallel arrangement of the M proteins (183); second, the residues that destabilize the coiled-coil structure could increase the affinity for the ligands (184).

Interestingly, the coiled-coil destabilizing residues enable a "capture-and-collapse" model where the binding of fibrinogen brings sufficient energy to stabilize the coiled-coil structure (185, 186). Also the binding of IgG to the protein M dimers stabilizes the coiled-coil structure, enabling a higher C4BP-binding capacity and increasing the virulence (181).

M proteins bind at least one member of the family of inhibitors of the complement: Factor H, Factor H-like, C4BP and the cell surface complement inhibitor CD46 (187–190). M proteins can bind immunoglobulin G by the Fc domain (191). The C and D repeats are highly conserved among the M proteins and are responsible for the binding of factor H and serum albumin (192, 193). The B repeats are considered to be semi-variable and they contain, for most M proteins, the fibrinogen binding domain (194). The functional analysis of the M proteins highlight the clustering of M proteins, with ligand patterns conserved within given *emm* patterns but also M protein specificity within *emm* patterns (195). Strains of the *emm* pattern D cluster 4 represent 18% of the *emm* types and they express M proteins that can also bind plasminogen in the HVR region (194, 195). The M protein HVR is involved in the resistance to antimicrobial peptides and M1 protein inhibits antimicrobial peptides derived from β2 glycoprotein I (196, 197)

It is only in the beginning of the 1990s that M proteins were described as important adhesins (198, 199). Multiple features of M proteins are not conserved from one to another: for example, some M proteins bind fibronectin, others do not and similarly for the M protein/CD46 interaction (Table 6) (200–203). M proteins bind glycosaminoglycan and this property seems conserved among all M proteins tested (204).

M proteins are involved in bacterial aggregation, which is a critical feature of GAS virulence (205, 206)**.** Antibodies raised against the M proteins are a major source of the autoimmune diseases caused by GAS, since some M protein epitopes resemble host epitopes, and these similarities are called molecular mimicry (32, 207).

Two proteins that share structural similarities to M proteins were also identified. The plasminogen-binding group A streptococcal M-like protein (Prp) isolated from an invasive *emm98* strain is 66% similar to the Plasminogen-binding group A streptococcal M protein (PAM) isolated from a M53 strain. These proteins probably originate from a duplication of *emm* genes, but Prp and PAM coding genes have different phylogenic history (208). Both PAM and Prp bind plasminogen (208–210).

Table 6. M protein ligands

Emm Pattern	*Emm*-Type	Fn	Fg	Albumin	Ki	FH	FHL-1	C4BP	IgG	IgA	Pg	CD46	Ref
A-C	M1	■	■	■	■				■				(200, 211–214)
	M3	■	■	■									(200, 215)
	M5		■	■		■	■					■	(188, 190, 216–218)
	M6	■	■		■	■	■					■	(187, 188, 200, 213, 219–222)
	M12			■					■				(223)
	M24		■										(224)
	M46				■								(213)
	M55		■	■					■				(225)
	M18		■										(226)
	M23		■										(226)
D	M33										■		(194, 227)
	M41										■		(194, 227)
	M52										■		(194, 227)
	M53										■		(194, 210, 227)
	M56										■		(194, 227)
E	M2							■	■				(225, 228)
	M4							■	■	■			(228–233)
	M22							■	■	■		■	(216, 228, 229, 232, 234, 235)
	M28								■	■			(232)
	M49			■					■				(236)
	M50								■				(237)
	M60							■	■	■			(228, 233, 238, 239)

Fg=Fibrinogen, Fn= Fibronectin, Pg= Plasminogen, FHL-1= Factor H-like 1

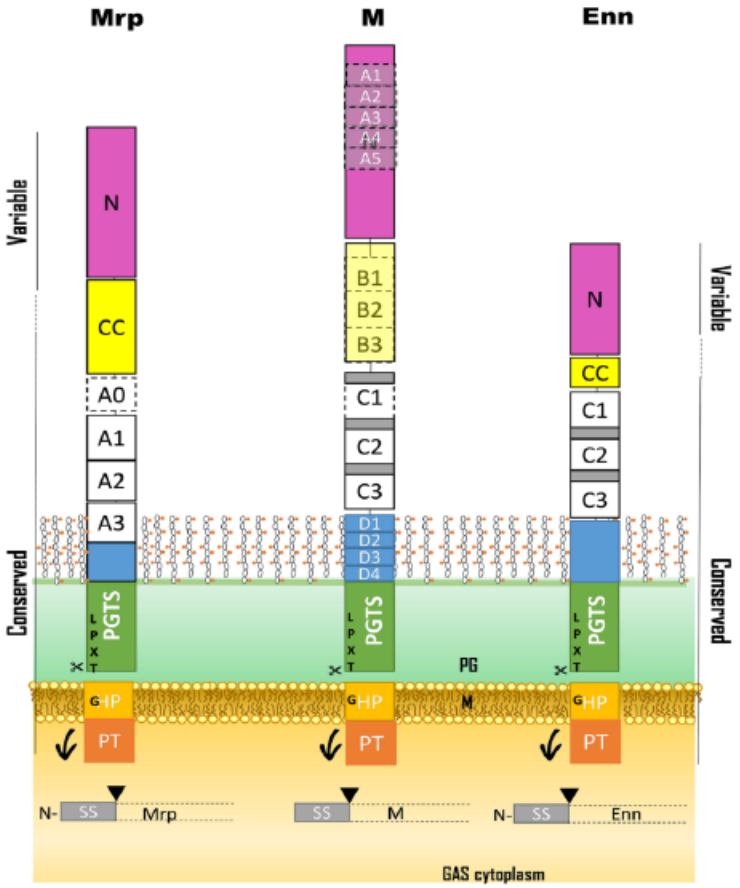

Figure 14. M and M-like proteins structure
Schematic representation of the predicted structure of the M-like proteins, Mrp and Enn, based on known and predicted structural features of the M protein. Following this is the N-terminal, the most variable portion of the proteins of all 3 families although considerably less variable in M-like proteins than in M proteins. The central core (CC) is an EQ rich portion in Mrp and M proteins, and an 18 aa residue motif in Enn proteins. The exposed C-terminal portion of Enn proteins contain C-repeats like those of M proteins, whereas Mrp proteins contain A repeats which differ in both sequence and predicted structure to the C repeats. The cell-wall associated portion is in Mrp proteins half as long as in the Enn proteins. Adapted from (240).

The vast majority of the studies were historically done with the GAS strains of the M1, M3 and M6 serotype. These strains are all of the A pattern that do not express the Mrp or Enn proteins, and they represent only 21 % of the *emm* types (42). Moreover, the M-like proteins, in addition or instead of the M proteins, are responsible for several binding to host proteins [reviewed in (240)] (Table 7). For example, the protein H is responsible for most of the binding of C4BP by M1-expressing strains (241); the Mrp4 is the major fibrinogen binding protein of the *emm4* strains (242); M18 binds Factor H/factor H-like-1 while Enn18 binds C4BP (243). Therefore, while our knowledge of the M protein structure and functions seems extensive, it

does not account for all the M protein patterns nor the M-like proteins. A lot is still to be learned from studies of these M-like proteins.

Table 7. Mrp and Enn host ligands

M-like	Fg	C4BP	IgG	IgA	Ref
Mrp2	■		■		(244)
Mrp4	■		■		(239, 242, 245, 246)
Mrp8	■		■		(247) (242)
Mrp9	■		■		(247)
Mrp13	■		■		(247)
Mrp15	■				(242)
Mrp22	■		■		(239, 242, 248)
Mrp28	■		■		(239)
Mrp49	■		■		(244)
Mrp60	■		■		(239)
Mrp76	■		■		(249–251)
Mrp95	■		■		(244, 252)
Enn2				■	(191, 244)
Enn4				■	(233)
Enn5			■		(253)
Enn18		■	■		(243) (253)
Enn49				■	(244)
Enn95			■		(244) (253)

ScpA. The C5a peptidase, ScpA, is a member of the subtilisin-like serine protease family and ScpA is anchored to the bacterial surface through a LPXTG motif (254). Its gene belongs the Mga locus, together with the genes of the *emm* family (Figure 8). ScpA is produced as a pre-peptide which is processed to the pro-peptide by autocatalytic cleavage (255). ScpA is common to several pathogenic streptococci (256) and is a highly specific endopeptidase which cleaves the C5a protein (255). C5a is an anaphylatoxin (a complement peptide) which plays a key role in the activation and recruitment of neutrophils to the site of infection, and ScpA accentuates GAS colonization in a murine model of infection (257–259). ScpA binds fibronectin (260) and has a role in the adhesion to the pulmonary A549 cells and endothelial HUVEC cells. Recombinant ScpA presents a higher binding to cells in the presence of serum than in its absence, potentially due to the presence of fibronectin (261). In contrast to the ScpA of GBS, ScpA of GAS does not seem to play a role in invasion. Interestingly, the ScpA is also able to cleave the C3a complement peptide, which influences C3 deposition at the bacterial surface. In a murine model of infection, ScpA peptidase activity is not involved in virulence (261).

2.1.2.2. FCT proteins

The fibronectin-binding, collagen-binding, T antigen (FCT) region is an operon including, among others, genes coding for the pilus, Nra, SfBI/PrtfI and the Protein F2.

Pili. GAS pili are encoded within the FCT region. There are nine FCT types, named FCT 1 to 9 (262). The pilus itself is encoded by three genes: the first one codes for the backbone protein (BP, also known as FctA) and the two others for the ancillary proteins AP1/Cpa and AP2/FctB. The FCT operon also encodes the polymerization machinery composed of the pilus-specific sortase enzymes, SrtB and SrtC2, and a putative chaperone protein/peptidase (SipA). The pilus is composed of multiple copies of the BP protein with one copy of an ancillary protein, and the assembly and export of the proteins is performed by the specific polymerization machinery. GAS strains express different variants of the pilus constituting proteins: 15, 16 and 5 variants of BP, AP1 and AP2 respectively (263). The pili are involved in biofilm formation, adhesion to pharyngeal cells, keratinocytes, primary tonsil cells and primary keratinocytes (264–266). Through its N-terminal domain, the AP1 subunit increases bacterial binding by forming a covalent thioester bond with different cell receptors (267). The AP1 subunit was also found to bind type I collagen and the pilus binds gp340, a salivary glycoprotein that induces bacterial aggregation (268, 269). Numerous functions were proposed for the pili, with the possibility that the functions vary from one FCT variant to another.

SfbI/Prtf1. SfbI is coded by a gene in the FCT operon, and is also known as PrtfI. It binds fibronectin through five repeats and an upstream binding region (270). It binds indirectly collagen and directly IgG (271, 272); it is involved in adhesion to pulmonary A549 cells and vaginal epithelial Hep2 cells in the presence of fetal calf serum and fibronectin (273). The internalization triggered by SfBI is dependent on a mechanism involving caveolae (274). In the absence of the M protein, SfbI confers resistance to phagocytosis and reduces complement deposition (275). Finally, SfbI covalently cross-links to fibrinogen with a thioester bond, and this interaction increases binding to cells (276).

Protein F2: FbaB and PFBP. *prtf2* is found in 60% of GAS strains and has two mutually exclusive variants: *pfbp* and *fbab* (277), coded in the FCT region. FbaB is a fibronectin binding surface protein (143). It is involved in adhesion and invasion of Hep-2 and primary endothelial cells (143, 278).

S. pyogenes fibronectin-binding protein (PFBP) is a 127 kDa protein that binds fibronectin (279).

2.1.2.3. *emm28* specific surface proteins

R28 protein. R28 is a cell-wall anchored protein encoded in RD2, an *emm28* specific region (Figure 9 and see section 1.4.2). It belongs to the Alp family of proteins that all share a common structure with a signal peptide, a similar N-terminal domain, multiple repeats identical at the level of single amino-acid residue within each protein and a LPXTG anchoring motif (280) (Figure 15).

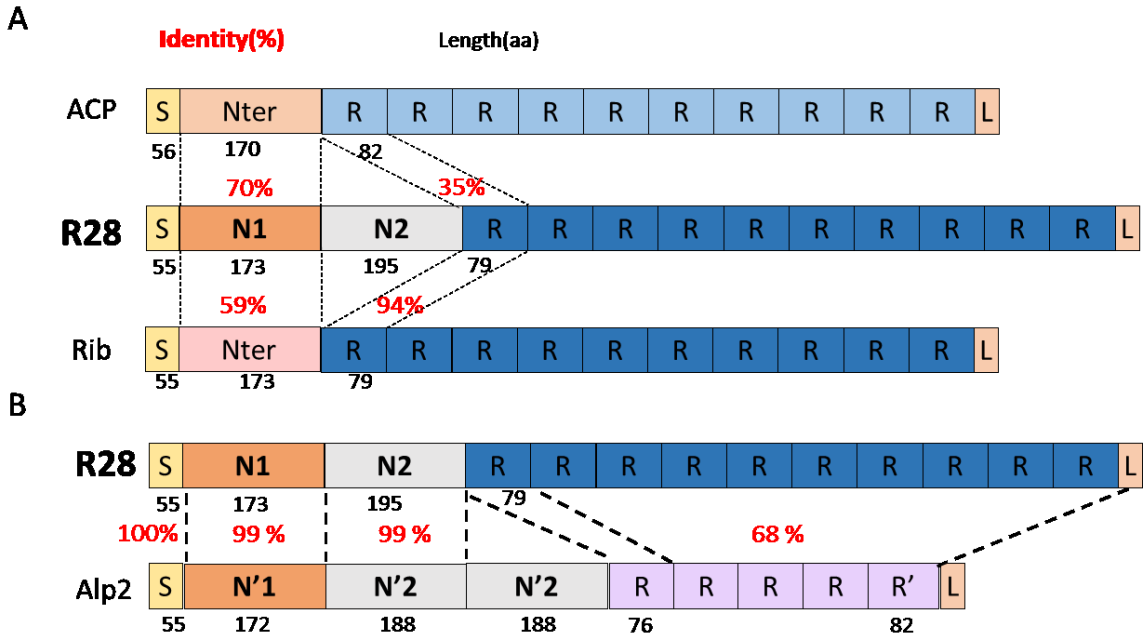

Figure 15. R28 and the structure of the Alp family proteins

S=signal peptide, R=repeats, L=LPXTG. Domain length is indicated in grey below as the number of amino acid residues. Identity between the different proteins and R28 is indicated in red. A. Comparison of the structures and sequences of Rib, R28 and ACP. B. Comparison of R28 and Alp2 proteins.

The Alp family is composed of four proteins expressed in GBS which are evolutionary related: alpha C protein (also known as ACP, or protein α), Rib, R28 (also known as Alp3 in GBS) and Alp2 (48, 280–282). R28 is composed of an N-terminal domain of 41.5 kDa followed by a variable (up to 15) number of repeats depending on the strain (48). R28 N-terminal domain can be divided into two subdomains N1 and N2, with N1 corresponding to the domain similar to all Alp proteins (Figure 15A). The N2 domain is partly similar to the β protein of GBS and presents an IgSF-fold (282). The repeats of R28 are 94% identical to Rib repeats and their structure is related to the Ig-like fold (283); R28 is thought to be a chimera between ACP, Rib and the unrelated β protein. Alp2 N-terminal domain is almost identical to R28 N-terminal domain, with a duplicated N2 domain (Figure 15B).

A R28 deficient *emm28* strain is non-adherent to the cervical cell line ME180, but nothing is known regarding the receptors involved (48). Rib is not involved in adhesion to cells (282) in contrast to ACP. ACP is the most studied member of the Alp family and the crystal structure of the N-terminal domain has been elucidated (284). It binds glycosaminoglycans in a region encompassing the end of the N-terminal domain and the repeats (285, 286), and the α1β1 integrin through a KTD motif localized in a β-sandwich subdomain at the N-terminal end of the N-terminal domain (287, 288). These interactions increase GBS internalization in ME180 cells (288).

Epf. The extracellular protein factor (Epf) is a 25 kDa surface protein encoded in the pathogenicity ERES island by M1, M4, M12, M28 and M49 strains. It has several C-terminal repeats, a unique N-terminal domain; Epf binds plasminogen (289, 290).

AspA. Antigen I/II (Ag I/II), also called AspA, is encoded in the *emm28* specific RD2 region (45) (Figure 9). The AgI/II is an adhesin that binds to gp340, a component of the human salivary (291). AspA is also involved in biofilm formation (292). AspA is necessary for GAS establishment in the nasopharynx of mice and a null mutant resist to phagocytosis to a lower extent (293).

2.1.2.4. Other surface virulence factors

DNase. SpnA is the only LPXTG bound DNase and it is involved in the escape of NETs (132, 294).

SOF and SfbX. The serum opacity factor is expressed by half of the GAS invasive strains of five states from the United States of America between 1995 and 1999 (295). SOF is both found at the bacterial surface and in the culture supernatants. The name arises from its activity of human serum opacification. The opacification domain avidly interacts with high-density lipoprotein (HDL) in host serum to form neo-HDL and insoluble cholesteryl-ester rich microemulsion (CERM), a property modulated by the interaction with apolipoprotein A-I, the major component of HDL (296). SOF binds to the C-terminal domains of fibronectin and fibrinogen (297–299). Proteins similar to SOF are found in fish and pig pathogenic Streptococci, which suggests an old evolutionary selected bacterial property (300). Apolipoprotein A-I has antimicrobial activity (301) and SOF interaction with it is thought to be a major virulence mechanism.

SfbX is only present in SOF positive strains and its gene is cotranscribed with *sof* (302). It is a fibronectin binding protein (279).

LTA. Lipoteichoic acid (LTA) is a polymer and a component of the cell wall of Gram positive bacteria. It is composed of 1,3-phosphodiester-linked glycerophosphate with a small lipid moiety (a diacylglycerol) which mediates the anchoring of the teichoic acid domains to the bacterial membrane (303). LTA has a dual localization: it is covalently bound to the membrane and it can form complexes with surface proteins of GAS, including M and M-like proteins (41, 304). When bound to surface proteins (and not when membrane bound), LTA readily exposes its lipid moiety, which makes LTA the major factor determining GAS surface hydrophobicity (41, 305) and it induces lymphocytes mitogenesis (306). It is involved in binding to phagocytes and to epithelial cells, and the glycolipid moiety binds to fibronectin (307–310). Since biofilm formation depends on hydrophobicity, the amount of bound LTA to the surface of GAS influences biofilm formation (41). Host apolipoproteins are thought to inhibit LTA effect on host cells, an effect that SOF could counteract.

Hyaluronic acid /Capsule. The capsule is composed of hyaluronic acid, a polymer of N-acetylglucosamine and glucuronic acid, structurally identical to the hyaluronic acid found in the extracellular matrix of humans (311). The capsule biosynthesis proteins are encoded by a 4.2 kb operon composed of the three *has* genes (*hasA, hasB, hasC*) (312–315). *emm4 , emm22* and *emm89* strains of the emergent clades do not harbor the *has* operon (37, 148, 316). Moreover, it was reported that *emm87* and *emm28* strains (including the strain used in this study) harbor a frameshift mutation in the *has* operon which induces the production of early truncated HasA protein, suggesting these strains are unlikely to produce a capsule (317). The capsule reduces adhesion to epithelial cells (318). Yet, the hyaluronic acid can act as an adhesin by binding CD44 at the cell surface. Moreover, GAS capsule is an anti-phagocytic factor (11, 319).

GAPDH. Streptococcal surface deshydrogenase SDH or glyceraldehyde-3-phosphate dehydrogenase (GAPDH), also independently named streptococcal plasmin receptor (Plr) is an enzyme expressed by numerous organisms, including yeast and mammalian cells. In the cytoplasm, it plays a major role in the glycolysis and GAPDH is also a surface bound protein, although it does not present any known anchoring signal. GAPDH has numerous roles at the bacterial surface and is considered as a major moonlighting virulence factor of GAS. GAPDH binds fibronectin, laminin, myosin, actin, lysozyme, plasmin, uPAR and it induces major

intracellular changes (320–322). It binds C5a which is necessary for C5a cleavage, and this cleavage impairs neutrophil recruitment (323). GAPDH is involved in adhesion to host pharyngeal cells and inhibition of phagocytosis (321). Surface bound GAPDH is involved in the properties and activities of SLO and SpeB among others factors important for virulence (324).

Lmb/Lbp. The laminin binding protein Lbp is a 34.1 kDa membrane bound protein, with a XXGC motif, and is highly conserved among the GAS strains (325, 326)**.** It is 98% similar to the GBS Lmb protein, a laminin- and zinc-binding protein. Lbp binds laminin through a zinc ion (326).

Scl1. Scl1 is a homodimeric protein with a variable domain in the N-terminal globular sequence, a collagen-like domain and a C-terminal anchoring domain (327, 328). Scl1 interacts with human collagen, binds integrins $\alpha 2\beta 1$ and $\alpha 11\beta 1$, promoting GAS internalization (329–331). Scl1 can also bind fibronectin, laminin, LDL, HDL, factor H and factor H-like I (332–336).

Shp and Shr. The Streptococcal heme receptor is a 145 kDa protein with a N-terminal domain and two heme-binding NEAT domains separated by a leucine-rich segment (337)**.** It is anchored into the membrane and crosses the cell-wall for exposure at the bacterial surface. Shr binds fibronectin and laminin *in vitro* (338). It is expressed by most strains tested and is necessary for blood survival through its capacity to transfer iron to the Streptococcal heme-binding protein (Shp) (339, 340).

CAMP factor. Christie Atkins Munch-Petersen (CAMP) factors are a family of conserved proteins that increase hemolysis of several Gram-positive bacteria, including GAS, with high sequence identity (341, 342). They attenuate the phagocytic activity of murine macrophages RAW 264.7 and promote adhesion and invasion to pharyngeal Detroit cells (342).

SEN. The Streptococcal surface enolase SEN is a 45 kDa plasminogen binding protein; the plasminogen binding site is mapped at the C-terminal domain (343, 344). It is a dimeric to octameric protein (345).

Fba. Fba is a 38 kDa cell wall anchored protein found in the M1, M2, M4, M22, M28 and M49 serotypes. It is highly similar to *S. aureus* FnBPA protein. It binds fibronectin, factor H, factor H-like 1, and is involved in invasion of the cervical Hep-2 cells and the binding to FHL-1

promotes intracellular invasion in pulmonary A549 cells (346–349). It is involved in phagocytosis resistance (348). Fba is shed from the surface by SpeB proteolytic activity (350).

SpyAD. SpyAD is a member of the GAS divisome machinery that binds to keratin and type VI collagen (351).

Beyond the bacterial proteome, the interactome

By binding many host proteins that bind numerous host ligands and by maintaining the host ligand binding capacity or functions, the repertoire of potential functions at the bacterial surface is increased. The binding of a host component can increase the bacterial repertoire of functions as an indirect effect: bound plasmin can degrade host clots, and bound C4BP inactivates the complement cascade, fibronectin can bind host receptors. These different examples highlight the importance of considering that virulence is not only achieved directly by the bacterial repertoire of virulence factors, but also by the whole interactome.

2.2. GAS regulation of virulence factors

Virulence is a means for bacterial multiplication and bacteria differentially express their proteins in response to bacterial resources: protein production has an energy cost, so specific proteins are expressed only when necessary, to optimize the energy used and save the remaining energy for bacterial multiplication (352). Proteins involved in resistance to host responses are also expressed only when necessary. This concept of optimization of protein expression was recently completed by studying *Escherichia coli*, where genes with no detectable benefit account for 31% of protein production *in vitro*, showing that bacteria not only produce essential proteins for their immediate fitness, but also produce at low levels potentially necessary proteins (353). Regulation is therefore the modulation of the intensity of protein production to optimize the fitness while probably maintaining “standby” production of other effectors.

More specifically, the diversity of GAS-induced diseases imply a tight regulation of GAS physiology to face the different hostile environments and nutrient availabilities: difference in the presence and abundance of sugar, proteins/amino acids, oxygen (CO_2), the pH and the osmolarity (9). This is achieved by intrabacterial and external sensing of numerous signals and subsequent physiological changes. Pathways regulating the bacterial metabolism intersect with the pathway regulating virulence: metabolism and virulence are coordinated, as described for other Gram positive bacteria, such as *S. aureus* (354) and as we will describe in the following chapter. Moreover, there are counterproductive effects of different factors during the course of

infections. For example, the capsule is an anti-phagocytic factor, but it also decreases bacterial colonization. SpeB is essential for colonization but is detrimental for blood survival (as explained latter). GAS therefore optimizes its protein production and modulates the expression of its virulence repertoire to adapt to each pathogenesis steps.

As for many pathogens, the "regulatory mesh" is highly complex in GAS, with many interlocked regulatory pathways. In contrast to many Gram positive and negative bacteria, GAS regulation does not depend on sigma factor for the response to stress or growth phase. We will describe in this section successively different levels of regulation in GAS: transcription, post transcription, translation and post translational regulation.

2.2.1. Regulation of gene transcription

We will describe two main systems that enable gene regulation in GAS: two component systems (TCS) and stand-alone activator/repressor.

2.2.1.1. Two-component system: CovR/S

GAS strains express 14 TCS, but not all are expressed by all *emm*-types. Two-component systems are composed of a sensor kinase protein (S) which after detecting a signal autophosphorylates, then phosphorylates a cognate intracellular receptor (R) which transduces the extracellular signal by binding to the regulatory regions of different genes. We will focus on the most studied two-component system, CovR/S.

The control of virulence (CovS/CovR), initially known as capsule synthesis regulator (CsrR/S), is the most characterized GAS TCS. The principal virulence genes and pathway under the control of the oligomerized phosphorylated CovR are listed in Figure 16 (355). CovR/S is involved in the regulation of up to 15% of GAS genes (271 genes), many of which are virulence factors and most of them are downregulated by CovR which therefore acts as a repressor of the expression of virulence genes (355, 356). Host selective pressure selects in the *emm1* and *emm3* genotypes for clones that do not express a functional CovRS system, which is thought to increase the expression of virulence genes involved in the resistance to the immune response, such as the capsule biosynthetic operon *has* (357). Moreover, *speB* is downregulated when CovS is inactive: since SpeB degrades bacterial surface proteins, this down regulation is thought to increase the amount of surface proteins present. However, this overexpression of virulence genes and the subsequent increased presence of the capsule has negative consequences on the colonization: a CovR/S mutant presents decreased biofilm formation, binding to fibronectin and

to keratinocytes (318). This suggests why "hypervirulent" strains are only found after intra-host selection: they present short term increased fitness and are therefore the result of "short sighted" evolution (358), and have long term decreased fitness by colonizing the host and disseminating between individuals with less efficiency.

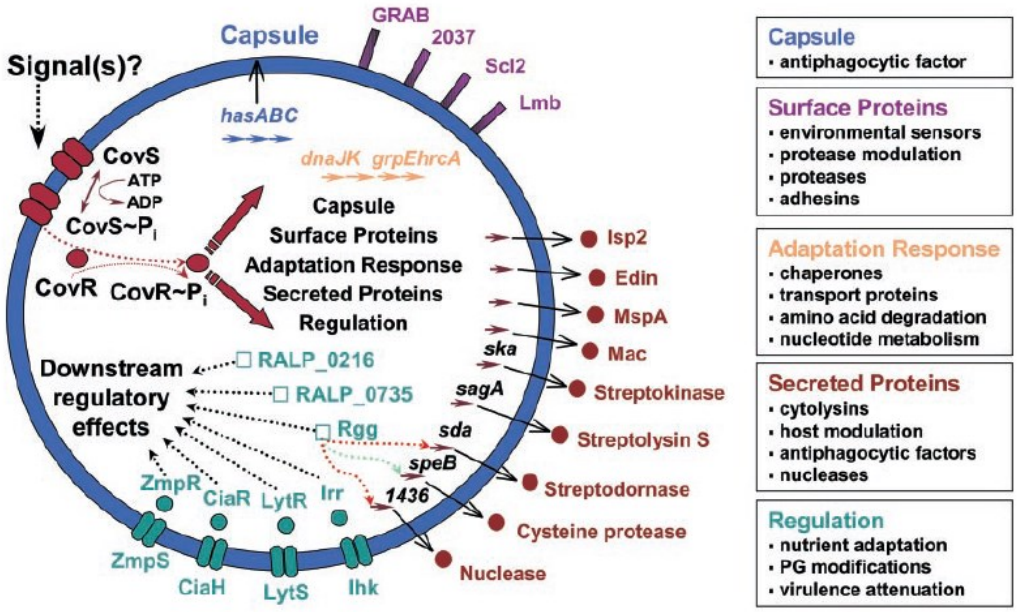

Figure 16. CovR/S system, genes regulated and pathways involved
The different pathways regulated by CovR/S are indicated, in addition to the genes ultimately regulated, and on the right is indicated the different regulated functions. From (355).

CovS phosphorylation depends on host extracellular signals such as Mg^{2+} and the host antimicrobial peptide LL-37: Mg^{2+} increases the repressive effect of CovR/S while LL-37 has an opposite effect, increasing virulence factors expression (359). The operon *cov* is under the repression of CovR itself: autoregulation is functionally explained by the subsequent amplification loop which results in very strong and fast decrease/increase of virulence factors expression. The *cov* operon can be activated by the RocA and Rgg (RopB) regulatory pathways and CovR represses the virulence related regulator RivR (360). Regulatory pathway intertwining results in signal integration from the different bacterial sensors.

2.2.1.2. Stand-Alone regulators: Mga, Rgg/RopB, RofA

GAS strains express 60 "stand-alone" regulators (SA), transcription regulators without determined external sensors. We will present the three most studied regulators: RofA, Mga and Rgg/RopB (Figure 17), and then we will describe briefly regulators important for mechanisms described in section 3.

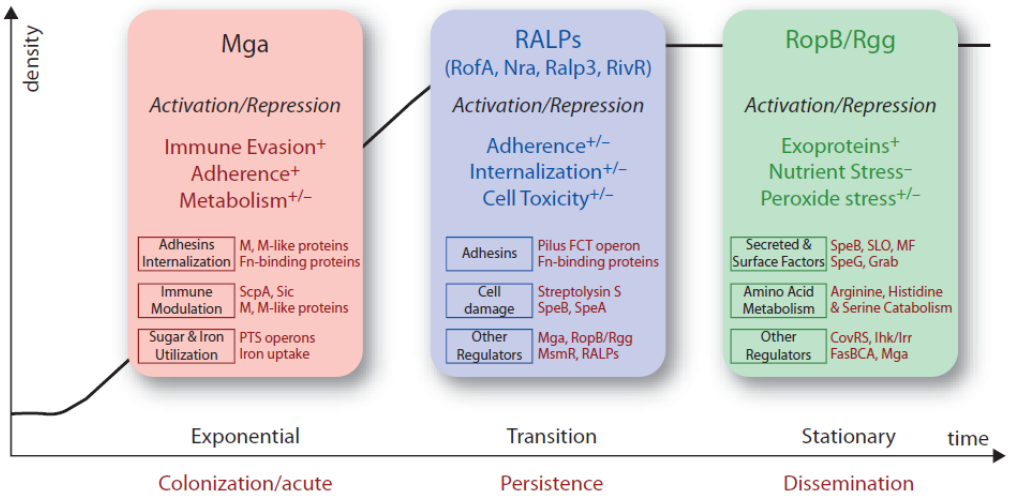

Figure 17. Stand-alone regulators

Growth, metabolism, and stand-alone response regulatory systems of GAS. An *in vitro* growth curve is shown in the background with growth phases indicated. Boxes representing each stand-alone network are placed at the growth phase during which they exhibit maximal expression and the relevant point during infection is given under the x axis. Whether functions are activated (+) or repressed (–) are shown as superscript. Overall processes and specific molecules regulated by each are shown. Adapted from (361).

Mga. Mga stands for multiple gene regulator of Group A Streptococcus (362) and is also known as VirR [for review (363)]. There are two main alleles of *mga*, *mga-1* is mainly found in SOF^- strains involved in throat infections, *mga-2* in SOF^+ strains, found in skin and generalist infections, which suggests an adaptative role for this divergence. *mga* is expressed at its highest level during exponential phase (Figure 17). *mga* is negatively regulated by RALP and Rgg/RopB (364, 365). *mga* expression corresponds to environments that support high bacterial multiplication and *mga* expression itself depends on various environmental cues, and no "sensor" has been identified, but Mga could play the role of sensor and repressor on its own. The phosphotransferase system (PTS) is a multiple protein system that couples the transport of sugars across the cytoplasmic membrane with their phosphorylation (366). Mga presents predicted PTS phosphorylation sites, which establishes a potential link between the carbohydrate metabolism and Mga regulation (Figure 17) (367–369). Either GAS multiplies symptomatically on the pharynx, or remains "silent" on the skin. Mga indirectly regulates many genes, up to 10% of GAS genome (Figure 18) (370): Mga controls the expression of genes coding for ScpA and M/M-like proteins, SIC in certain M1 strains and Fba in others (Figure 18). Mga regulates the synthesis of key virulence factors involved in adhesion and resistance to the immune system. During infection, plasma exudation enables the recruitment of immune

cells, but this also results in a flow of nutrients: favorable conditions are a signal of an hostile environment. Therefore, GAS expression of genes involved in resisting the immune system are increased, allowing to both take advantage of the nutrient flow (due to inflammation) and resist negative consequences of inflammation. Again, this exemplifies the intimate link between metabolism and virulence.

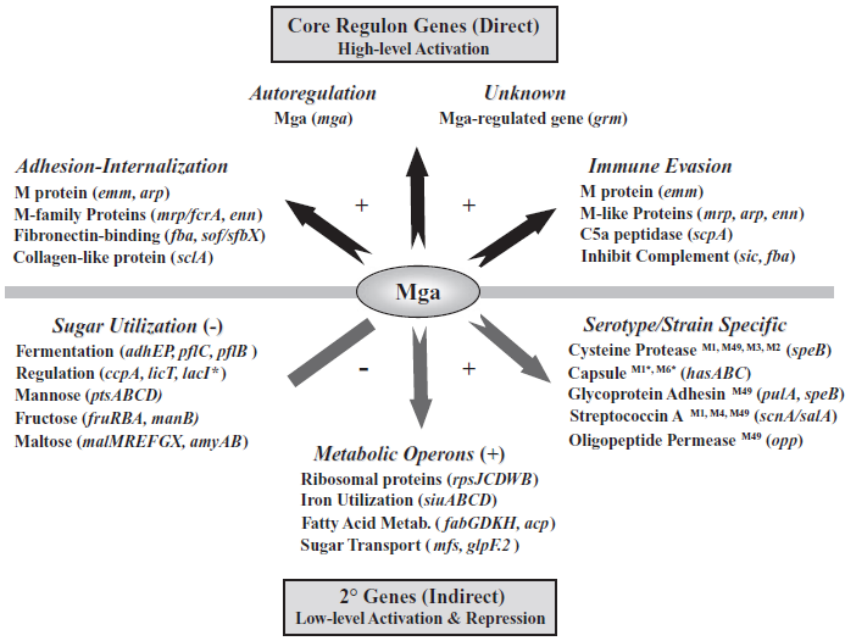

Figure 18. Main genes regulated by Mga
From (363)

RofA and the RofA-like protein type regulators (RALPs). There are four RALPs: RofA, Nra, Ralp3 and RivR (371); strains express either RofA or Nra, and some strains express in addition Ralp3 and/or RivR. The *rofA* gene belongs to the FCT locus and is adjacent to the *sfbI* gene (372); it is autoregulated. RofA upregulates the expression of the FCT region gene and it represses the genes coding SpeB, SpeA and SLS (365, 373).

Nra is expressed by FCT type 3 strains (374). Nra represses the expression of Mga regulated factors (SfbX, ScpA, Lsp, M protein, SpeA, SLO/NADase, AP1, Prtf2) and upregulates several metabolic pathways (375, 376). Nga represses Mga in the exponential phase, and during this phase Mga activates Nra expression. Hence, Nra may be involved in intracellular persistence. Nra also represses Rgg and other RALPs (375, 376).

Ralp3 is encoded in the region coding for the *eno-ralp3-epf-sagA* genes (ERES), and it controls the expression of *epf* and the *sag* operon (375). M1 Ralp3 strongly represses the capsule

biosynthetic operon and *speB* expressions, while the M49 Ralp3 has the opposite effect, which shows *emm*-type specificities (377).

RivR, also known as Ralp4, is a negative regulator of expression of virulence genes, such as the capsule operon and the gene coding for the GRAB protein (378).

The *in vivo* functions of RALPs are difficult to assess since the triggering signals are unknown, and each regulator controls at the same time genes encoding factors implicated in very distinct steps of infection. Moreover, as shown with Ralp3, the role may vary from one strain to another, making RALPs functions even more complex to assess.

Rgg/RopB. Rgg, also known as RopB, is a transcriptional regulator found in many low GC % Gram-positive bacteria. Rgg activates the expression of *speB* which is adjacent to *rgg*, but Rgg is not responsible for the growth-phase regulation of *speB*. Rgg regulates up to 30% of the genome in a given M49 strain but a much smaller set of genes in other M49 strains and other serotypes (379, 380). Rgg also represses the expression of several genes, encoding key virulence factor: SLO and NADase, DNAses, GRAB and SpeG [for review see (361)]. Aside from its regulation of virulence genes, Rgg also coordinates amino acid catabolism: the metabolism is switched to the use of amino acids as the primary source of energy. This corresponds to a situation of low nutrients, mimicked by the stationnary phase: Rgg/RopB expression is activated in response to stress (Figure 17).

CodY. CodY is a SA regulator found in several low GC gram-positive bacteria; intracellular branched amino acids (valine, isoleucine and leucine) binds to it, which increases CodY affinity for DNA (381). CodY is thus a metabolic sensor involved in the response to amino acid availability. CodY is principally a gene repressor and 17% of genes are differentially expressed in a *codY* deleted strain (382). CodY negatively autoregulates its transcription by directly binding its promoter (382) and an isogenic mutant strain expresses lower levels of genes *grab*, *sagA*, *sdaB/mf-1* and *speB* than the wild-type*;* and more *nga*, *prtS*, *scl*, *scpA*, *ska*, *slo* and *speH* than the wild-type strain. Moreover, CodY binds *in vitro* to the promoter of the dipeptide and oligopeptide permease genes *dpp* and *opp*.

LacD.1. LacD proteins belong to the family of tagatose bisphosphate aldolase which are metabolic enzymes involved in fructose, lactose and tagatose biphosphate cleavage (383). *lacD.1* originates from a *lacD.2* duplication, with LacD.1 deriving into a regulator and LacD.2 keeping the enzymatic role. There is functional divergence despite 82% similarity (384). After binding carbohydrates in a catabolic domain slightly different from that of LacD.2, LacD.1 is

able to regulate numerous genes: it is consequently a metabolic sensor and regulator. Notably, LacD.1 is a glucose responsive regulator of the expression of *speB* (385).

SRV. SRV is a regulator belonging to the Crp-Fnr transcription regulators family that share structural similarities (386). SRV upregulates *sic* expression and downregulates *speB* expression (382).

2.2.2. Small RNA regulation of virulence

Small regulatory RNAs (sRNAs) are involved in gene regulation through the stabilization or destabilization of mRNA, subsequently increasing or decreasing translation (387).

In GAS, FasX is a sRNA which stabilizes *ska* transcript, further increasing Ska production. FasX also represses the pilus operon translation, the FCT (388, 389). MarS is another sRNA involved in the stabilization of the *mga* transcript (390). *Pel* transcript is coded in the *sagA* operon, involved in SLS production and processing. *Pel* is involved in the transcriptional regulation of *emm*, *nga* and *sic*, and postranscriptional regulation of SpeB with a *pel* mutant readily producing SpeB, but not in its mature form (391). *rivX* affects the translation of *emm, scpA, mga*, and *speA* mRNAs (360). Interestingly, CovS negatively regulates *rivR* which controls *rivX* expression. Through a sRNA and different regulators, GAS strains integrate several signals to selectively modulate their virulence repertoire. Apart from these well characterized sRNAs, several bioinformatic analyses with or without Northern blot confirmation identified multiple putative sRNAs. The latest analysis identified 31 sRNAs, from which 15 were confirmed by Northern blot analysis, including 6 regulated by RNAses, suggesting a role for these enzymes in mRNA regulation (392). Of note, acting at translational levels, sRNA are thought to act faster than classical regulators of gene trancription, making them critical elements of bacterial plasticity.

2.2.3. GAS quorum sensing

While selection is at the individual level (one bacterium or another is killed) (393) evolution is at the population level [chapter 4 of (394)]. Quorum sensing (QS) is a process of bacteria sensing other bacteria and synchronizing their behaviors: cooperation between genetically linked bacteria and social behavior. One evolutionary advantage of bacterial social behavior is that group production increases the overall effect of an effector: for example, quorum sensing is a mechanism enabling a “All for one, one for all” mechanism (395). The other evolutionary advantage is kinship (also known as kin selection): the behavior of related individuals favors

the overall fitness of all individuals, even at the cost of individual's fitness, a classical example are sterile ants and bees. The fitness of a bacterial clone is linked to the amount of newly infected individuals, not the amount of individuals during one infection. Thus, for pathogens, synchronizing bacteria enable resource management, which optimizes the infectious process. In this light, QS is not only a means to increase effector production (lantibiotic production), but also a means to adjust behavior for the good of all linked genetically individuals (metabolic QS). QS often depends on the density (396): they are activated when there is a sufficient number of inducers, above a specific threshold, corresponding to the proximity of numerous genetically linked bacteria. While QS is often seen as a cooperation to optimize resources when the density is high, quorum sensing is also a way to ensure that secreted effectors will benefit only to bacteria in the vicinity that are genetically closely related: kin bacteria (397).

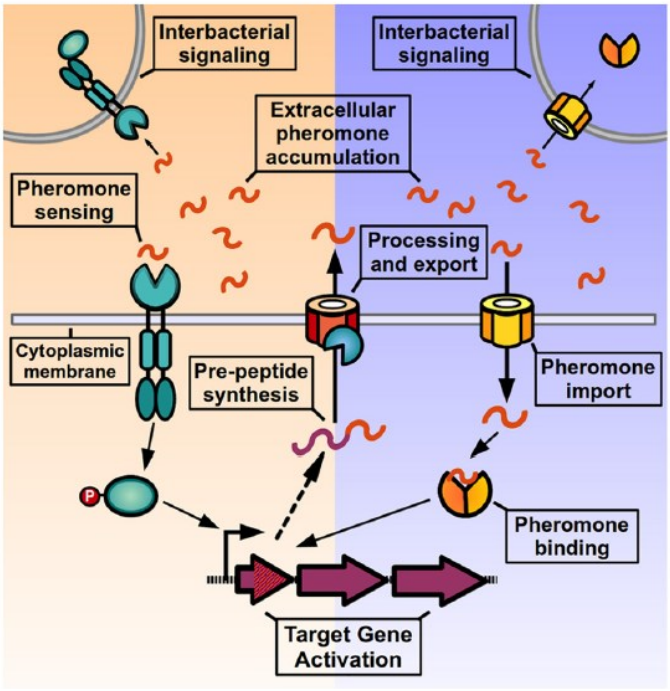

Figure 19. General pathway of quorum sensing

"Pheromone detection can either occur through two-component systems in the bacterial membrane (left side) or by direct binding by transcription factors after peptide import (right side)".From (398).

The general pathway of QS is as follows: one bacterium senses a signal, it will produce a propeptide which is matured into a peptide (called pheromone), which will trigger in other bacteria a switch of regulation, and the other bacteria will also secrete the propeptide, triggering an amplification loop (Figure 19).There are four main quorum sensing systems in GAS: Rgg, LuxS/AI-2, the lantibiotic system and Sil, the latest being only expressed and functional in 9 % of clinical isolates (399).

As an example, we will only describe the lantibiotic regulatory system. Several bacteria secrete anti-microbial peptides, from which they are protected by immunity proteins, which limits challengers' colonization. Such anti-microbial peptides are called bacteriocins. Class I bacteriocins are called lantibiotics; they are secreted by many Gram-positive bacteria (400). Lantibiotics act as a pheromone that will stimulate the secretion of the lantibiotics in siblings, further increasing the pool of lantibiotics and their effect on challengers.

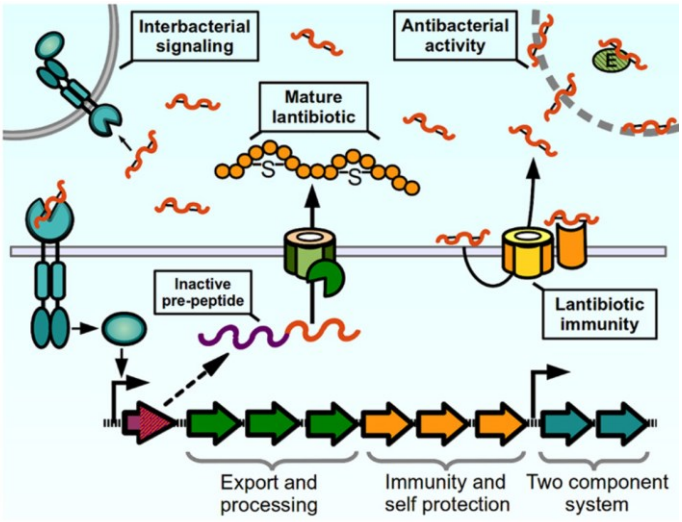

Figure 20. Lantibiotics mechanisms of regulation.
Small orange: pheromone. Left blue: two-component system. On the right, yellow: peptide import machinery. The pheromone either directly interacts with DNA after import, or binds to surface expose two-component systems, inducing a cascade that will ultimately lead to transcription activation. From (398).

2.2.4. Proteome regulation

Extracellular and surface bound GAS proteins are not protected from SpeB proteolytic activity, therefore SpeB produced by GAS influences the amount of GAS surface bound proteins, altering several phenotypes, such as internalization through PrtFI (401). Intra-host *de novo* mutation of CovR/S is thought to decrease the secretion of SpeB, further increasing the amount of surface bound anti-phagocytic proteins such as the M proteins (357). This idea is further supported by the observation that in M1 GAS, there is an inverse correlation between invasiveness and SpeB expression (402). In conclusion, virulence properties of bacteria are altered by the alteration of the surfacome, proteins expressed at the bacterial surface, which depends on the amount of SpeB expressed on top of genetic and transcriptomic regulations.

3. GAS virulence mechanisms

In this chapter, we will describe the different steps involved in GAS pathogenesis of superficial and invasive infections. Since both projects of this thesis focused on the early critical steps of GAS invasive infections, we will emphasize on these critical steps and we will not detail GAS resistance in the blood and dissemination in it, essential features of invasive infections.

3.1. Settling the infection and multiplication

3.1.1. Binding to the ECM

The mammalian extracellular matrix (ECM) is composed of collagen, fibronectin, laminin, proteoglycans and some tissue specific proteins such as keratin. It surrounds cells in conjunctive tissue and the binding of bacteria to ECM is a common critical step for bacterial colonization and invasion of host tissue. GAS strains harbor numerous surface proteins that are able to bind directly or indirectly the ECM components: 10 GAS proteins bind to fibronectin, 4 to laminin, 4 to collagen and one to keratin (Table 8). GAS can also bind to glycosaminoglycans, which could contribute both to adhesion to cells and to ECM (204).

Table 8. ECM components bound by GAS

	Virulence factor	Fibronectin	Laminin	Collagen	Keratin	Ref
All *emm* types	SpeB		■			(92)
	C5a peptidase	■				(260)
	LTA	■				(403)
	M protein and M-like	■				(200, 404)
	SfBI/PrtfI*	■		*Indirect*		(270, 271)
	Pilus			■		(268)
	Shr	■	■			(338)
	SclI	■	■			(333)
	SpyAD			■	■	(351)
	Lbp		■			(325)
***emm28* strains**	Fba	■				(349)
	Protein F2 (PFBP/FbaB)	■				(143, 277, 279)
	Epf			■		(289)
	SOF	■				(298)
	SfbX	■				(279)

* : SfBI/PrtFI binds collagen indirectly *via* bound fibronectin.

3.1.2. Biofilm formation

Biofilm are defined as aggregates of bacteria with self-produced extracellular polymeric substances (EPS). It is different from the planktonic stage of the bacteria and bacterial aggregates. Biofilm development is described as a four-step mechanism: stage 1, planktonic transient attachment to a surface; stage 2, formation of aggregates with secretion of EPS which increases the bacterial adherence; stages 3, maturation of the biofilm into a 3D-structure, and step 4, bacterial shedding from the biofilm (Figure 21). The composition of the GAS EPS is poorly described, but carbohydrates, proteins and extracellular DNA are implicated in the biofilm structure (405, 406).

The ability of bacteria to adhere to a surface or a substrate is critical for GAS biofilm formation: it initiates the first step of the biofilm formation (stage 1 and 2). Several matrix binding proteins and adhesins are involved in biofilm formation, such as Scl1, pili, AspA (264, 292, 407). AspA is involved in biofilm formation in the presence of its ligand gp340, but not when bacteria are seeded on polystyrene (292). Indeed, the amount of biofilm is the same in the presence or absence of AspA: on polysterene surface, bacteria are adsorbed to the surface without the need of adhesion. AspA therefore only plays a role in biofilm formation when it is required for adhesion.

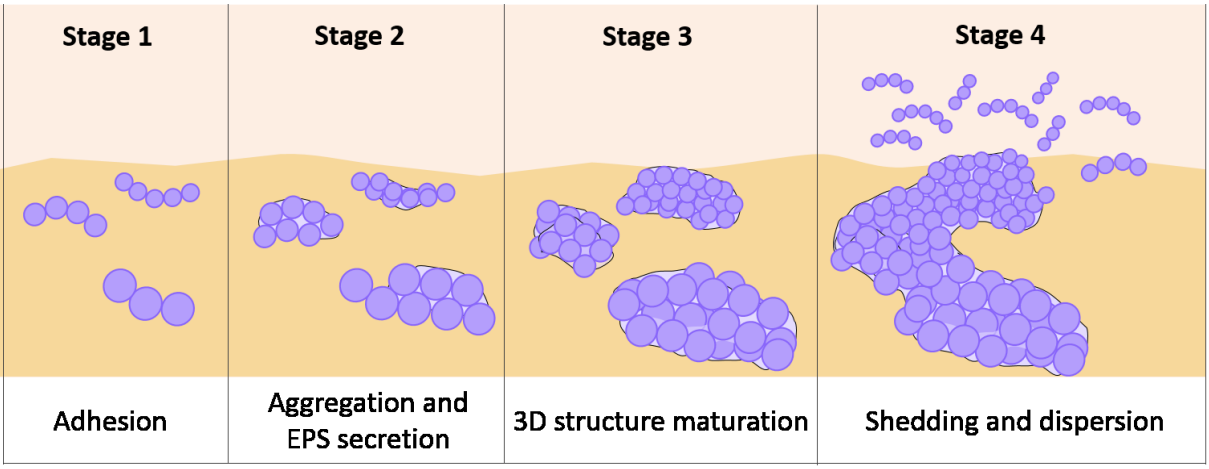

Figure 21. The four stages of GAS biofilm formation
In orange, the surface of a host tissue. In beige, the physiological liquid. In purple, GAS chains. In light purple: EPS.

GAS is a hyper-aggregative bacterium and aggregation in liquid medium is dependent on the homophilic interactions between M and the protein H in a M1 background (205). This aggregation in the absence of M protein could be mediated by other surface factors such as the pili (269). This aggregation step is crucial for GAS biofilm formation, as it initiates spontaneous microcolonies at host surfaces (Figure 21, stage 2). Aggregation contributes to biofilm formation, but does not systematically imply a capacity to form biofilm: a M49 strain readily forming aggregation in liquid culture is not able to form biofilm (408). GAS builds 3D structures without the need of EPS: microcolonies are not necessarily biofilms (408). This complexifies the study of GAS biofilm since EPS are hard to visualize, the only currently used technique is Scanning electron microscopy (SEM), while concanavalin A and wheat-germ agglutinin can be used to visualize lectins.

Multiple GAS surface proteins are involved in biofilm formation. There are striking differences between the different M-types and even between strains of a given M-type in the ability to form biofilms on different substrates (collagen, laminin, etc…) and there are also different biofilm morphologies (408). This indicates that the variation of surface protein repertoires from strain to strain has dramatic consequences on the biofilm formation. Nevertheless, studies point out a correlation between the FCT-type of strains and the capacity of strains to form biofilms (409).

The ability of strains to form biofilms not only depends on the surface protein repertoires and the substrate used, but also on the medium used (409). The presence of glucose stimulates biofilm formation (409); furthermore some strains produce biofilm in a pH-dependent manner (410, 411).

As a pleiotropic phenomenon, any environmental change that would affect the expression of surface proteins involved in the biofilm formation (such as Mga, CodY) and the production of SpeB which degrades surface proteins, will affect biofilm formation. Moreover, some environmental signals probably induce or repress biofilm formation, and it is difficult to distinguish regulators and environmental changes that affect the GAS surfactome, and therefore biofilm formation, from that affecting directly the production of EPS.

Nevertheless, several studies reveal the importance of regulators in biofilm formation. SRV is involved in the control of SpeB production which influences biofilm formation (405). Two other regulators/quorum sensing influence biofilm formation, SilC (408) and the SHP/Rgg pheromone signaling, but there is no clear indication regarding the molecular pathway involved (412).

On patient biopsies of GAS infections, bacteria are present as biofilms and 32% of 31 necrotizing fasciitis biopsies analyzed present biofilms (413). However, the ability of GAS to form biofilm *in vitro* does not reflect their ability to form it during human infection. This highlights that GAS biofilm formation is not an intrinsic properties of GAS: it is a specific program triggered by host signals and/or depending on the host (413).

In conclusion, biofilm formation is a very complex, multi-step process. Most studies were done *in vitro*, even one of the rare studies assessing bacterial formation of GAS on biotic surfaces (keratinocytes) used fixed cells to avoid cell death that would remove cells from plastic glass (414) but this also eliminates potentially host critical secreted factors that could be involved in inducing biofilm formation. While multiple factors are necessary for the first steps of biofilm formation (stage 1 and 2) in GAS, the host and bacterial factors triggering and altering biofilm formation *in vivo* are unknown.

GAS formation of biofilm in human tissue is a critical important virulence mechanism [for review (411)]. Penicillin does not efficiently eradicate GAS infections in up to 30% of pharyngitis despite the absence of penicillin resistance. Two main hypotheses explain antibiotic failure and GAS recurrent infections: bacterial internalization (section 3.1.3) and biofilm formation (415, 416). GAS biofilms are inherently tolerant to immune response and to antibiotic treatments, since they can suffer up to 500 mg/mL of gentamicin (414), by far exceeding clinical use of antibiotics. Moreover, biofilms increase the bacterial load in infected tissues and biofilm-positive biopsies are those with the highest bacterial burden (413).

3.1.3. Adhesion to host cells and internalization

GAS adhesion to host cells

In the battle to attach and remain at the host cell surface, GAS is thought to engage a two-step mechanism: first, the LTA by its lipid moiety overcomes the electrostatic repulsion of host membrane, establishing a labile binding, secondly, surface bacterial adhesins interact with host proteins to induce a high affinity binding (417).

During the initial steps of superficial infections, GAS strains bind to host cell surface. GAS strains express numerous adhesins (Table 9). Of note, not all these factors are expressed by each strain: *emm*-types have been selected to express different repertoires of adhesins during co-evolution. GAS attaches to cells either by directly binding to a host cell receptors, or by binding a host protein which binds to a cell-receptor, mechanism known as indirect binding or bridging. Known direct adhesins are the hyaluronic acid which binds CD44; M6, CD46; Scl1,

integrins α2β1 and α11β1 (201, 327, 329, 332). Other proteins mediate adhesion through cell bridging: SfbI/PrtfI, Prtf2, FBP and FbaB, through fibronectin; SEN through plasminogen; protein H through C4BP and SfBI through fibrinogen (143, 241, 276, 349, 418–421). The large majority of these adhesins were tested on Hep-2, initially described as pharyngeal cells and therefore a suitable model for the GAS interactions with host epithelium during pharyngitis, but later recognized as contaminants of HeLa cells, a carcinomal derived cervical cell line (422, 423). Every cell line expresses specific receptors, and the overexpression of certain receptors in Hep-2 cells could overestimate the role of a protein in adhesion. For example, the M protein has a role in adhesion to Hep-2 cells but not to pharyngeal or buccal cells (198). In contrast, several critical major receptors for adhesion to pharyngeal cells might not be expressed by HeLa cells, minimizing the potential importance of several GAS surface proteins.

Plasminogen, FHL-1, fibrinogen, C4BP and fibronectin are plasma proteins. Fibronectin and collagen are two bridging molecules found in the extracellular matrix, however these proteins are mainly found at the cell basal membrane (424). It is unclear if fibronectin is expressed and accessible by cells encountered during the early steps of GAS superficial infections. However, in the presence of a breach, blunt trauma and plasma exudation, where there is inflammation, all indirect interactions involving fibronectin and plasma components probably highly contribute to the bacterial ability to remain attached to cells. Since most invasive infections are subsequent to bacterial induced or already present inflammation, these bridging interactions are critical virulence determinants for GAS invasive infections (349, 425).

GAS internalization in non-phagocytic cells

GAS is an extracellular pathogen, but several reports indicate the presence of viable bacteria within non-phagocytic cells in biopsies and cultured cells (426). Different host and bacterial factors are involved in the invasion process (Table 9). GAS, GBS and *S. aureus* are three of the many Gram-positive extracellular pathogens that can occasionally be found viable inside epithelial cells (285, 427). In the following paragraphs, we will briefly discuss the entry mechanisms of GAS in non-phagocytic cells and we will specifically discuss its role in GAS pathogenesis of superficial and invasive infections.

Table 9. Factors involved in adhesion and invasion

		Cell-type							
	Virulence factor	Pulmonary	Endothelial	Pharyngeal	Hep-2	Keratinocytes	**Direct Receptor**	**Indirect receptor**	**Ref**
All *emm*-types	M and M-like				A/I(Fn)	A/I(Fn)	GAG, CD46	α5β1 integrin	(203, 204, 212, 428, 429)
	GAPDH			A					(321)
	ScpA	A	A						(261, 430)
	LTA				A	A			(198, 307–309, 431, 432)
	Hyaluronic acid				A		CD44		(432, 433)
	Pilus			A	A/I	A			(265)
	SfbI/PrtfI	A/I (Fn)			A/I(Fn)			α5β1 integrin	(418–420)
	SEN			A (Plg)					(421)
	Scl1		A		A/I		α2β1, α11β1 integrins		(327, 329–331, 434)
	Shr				A				(338)
	Lbp				A				(325)
	CAMP factors			A					(342)
***emm28* strains**	Prtf2 (FbaB)	A	A/I		A/I				(143, 278, 435)
	Epf					A/I			(289)
	Fba	I (FHL-1)			A/I (Fn)				(349, 436)
	SOF				A/I				(437, 438)

A(Fn): adhesion (in the presence of Fibronectin), A(Plg): adhesion (in the presence of plasminogen)
I(Fn): invasion (in the presence of Fibronectin)

Internalization could play different roles in the pathogenesis. Internalization induces cell apoptosis (section 3.2) and GAS internalization could enable transcytosis (section 3.2.1). Cytotoxicity and transcytosis through internalization could both contribute to GAS colonization and invasion of tissues (426).

GAS can be found in tonsils of patients with recurrent tonsillitis (439, 440). GAS intracellular bacteria resist to penicillin treatments (441). Strains from asymptomatic carriage and from patients with failure to antibiotic treatment have greater capacity to internalize than other strains (442, 443). This suggests strains with a great capacity to internalize are selected during antibiotic treatments. Strains that resist to erythromycin are also able to invade cells more than strains that are not resistant to erythromycin (444). Since Prtf1 increases bacterial internalization *in vitro*, the high capacity of erythromycin resistant strains to invade is potentially due to a higher presence of the *prtf1* gene in these strains compared to strains that do not resist to erythromycin (444–447). Either there is a genetic link between *prtf1* and erythromycin resistance genes, or more internalization enable *prtf1* expressing strains to survive β-lactam treatment, leading to a huge selective pressure for erythromycin resistance gene with macrolide treatments. GAS internalization is therefore clinically involved in recurrent pharyngitis, resistance to antibiotic treatments and asymptomatic carriage.

The most described internalization processes involves either SfBI/PrtfI or the M1 protein, through fibronectin binding (212, 448). M1 protein-mediated internalization in the presence of fibronectin involves the binding to β1 integrins and a zipper-like mechanism (212, 428). SfBI/PrtFI-mediated internalization in the presence of fibronectin depends on α5β1 integrins and involves caveolae (274, 445, 449). SclI-mediated internalization depends on SclI binding to α2β1 integrins (330). Direct or indirect binding to integrins containing the β1 subunit appear to be critical in several GAS internalization processes. β1-integrins and fibronectin interaction induces caveolae endocytosis of fibronectin for its turnover; also, even in the absence of fibronectin, integrins are recycled through caveolae recycling (450). Endocytosis of fibrin bound to αVβ3 enables clearance of fibrin deposition and vitronectin bound to αVβ5 induces endocytosis (451, 452). Therefore, endocytosis of integrin bound elements is a natural physiological pathway involved in many homeostasis processes. Consequently, integrin-mediated internalization of GAS could be seen as a consequence of GAS propensity to bind with high affinity cell surface integrins, activating outside-in signalization pathways involved in homeostatic recycling pathways.

This engulfment may even be an immune mechanism to restrict GAS infection through elimination of internalized GAS. GAS can be eliminated through the autophagy pathway, a phenomenon called xenophagy (453). Strains of serotypes M6, M49 and M3 are efficiently killed by epithelial cells (454–457). However, the highly virulent M1T1 clone can evade xenophagy and replicate in the cytosol of epithelial cells, in a SpeB dependent manner (458). SLO and NADase could also be involved in resistance to xenophagic killing (454), in a SpeB deficient strain. SLO/NADase induce cellular changes that prevent bacterial internalization in keratinocytes, potentially by inhibiting clathrin-dependent uptake of GAS (459, 460), further supporting internalization as a negative effect of GAS colonization.

3.1.4. Bacterial multiplication

Here we will mainly focus on the essential features of bacterial multiplication and its importance in pathogenesis.

Bacterial multiplication is an obvious and critical step in bacterial infection. As already discussed in section 2.2, from a bacterial point of view, infection in itself could be seen as means for the bacteria to acquire nutrients: virulence is a nutrient acquisition process, also termed “nutritional virulence” [for review: (461, 462)]. GAS induces diverse diseases (see section 1.3) and therefore faces various environments with very different nutrient accesses. Moreover, the overall ability of a bacterium to colonize a tissue is the result of bacterial multiplication and host-elicited killing. Many virulence factors have been studied for their involvement in resistance to host killing or increasing bacterial attachment, thus increasing colonization. However, this is assuming nutrient flow is not significantly limiting the colonization, and several reports highlight a direct role of virulence factors in the increase to nutrient access, which we describe in the following section

One central feature of the virulence-metabolic coordination is the SpeB protease. In laboratory medium, SpeB is maximally expressed during the stationary phase, considered as a stage where the amount of nutrients is limiting. Several metabolic regulators affect *speB* expression, such as LacD.1 and CodY, two metabolic sensors (section 2.2.1.2) [see (463) for a complete list of regulators of *speB*]. Opp and Dpp are polypeptide permeases: Opp imports tripeptides and Dpp imports hexapeptides and dipeptides. Inactivation of one or the other polypeptide permease decrease *speB* expression (464). The gene coding for SpeB is under the control of Rgg/RopB, which coordinates amino acid catabolism. It was proposed that the protease SpeB could play a similar role as the *Lactococcus lactis* protease PrtP: the combination

of protein degradation and import by a polypeptide permease is a mechanism of amino acid acquisition (465). This would give a rationale for the overexpression of *speB* in the stationary phase and its activation by Opp, Dpp, Rgg/RopB, LacD.1, CodY which are involved in amino acid catabolism, amino acid import and carbohydrate and branched chain amino acid sensing. By degrading proteins, SpeB would provide a source of amino acids and of energy from amino acid catabolism.

DNA was shown as a potential source of nutrients for different bacteria (466) and GAS strains express several DNAses. While less abundant than polypeptides/proteins, extracellular DNA or DNA released from dead cells could serve as a source of bacterial energy in addition to its role in gene acquisition (467).

Hyaluronidase was mainly studied for its ability to degrade GAS capsule and tissue hyaluronic acid, which increases bacterial invasion. However, hyaluronidase could increase the available source of carbohydrates, which would increase bacterial colonization (468).

GAS induction of cell death (see section 3.2) could also trigger nutrient release since the intracellular reservoir is rich in nutrients [reviewed in (469)] . Moreover, the unfolded protein response (UPR) triggered by SLO and SLS induces secretion of asparagine, which increases bacterial growth in a chemically defined medium devoid of asparagine (57, 470).

3.2. Tissue damage and invasion

Biopsies of GAS infected tissue clearly show that GAS not only colonizes the surface of a tissue, but can also penetrate deeper within the tissue, hereafter called tissue invasion. While breach and trauma are often associated with invasive infections, many invasive infections occur without apparent entry-port, suggesting the capacity of GAS on its own to invade tissues. Without any breach, GAS can cross an epithelium (translocation), and in the presence and absence of breach, GAS invades the extracellular matrix.

3.2.1. GAS crossing the epithelium

The different ways GAS can cross an epithelium are summed up in the Figure 22. To cross the epithelium, GAS can kill the cells that maintain the epithelium integrity (see 3.2). Another way to cross the epithelium is the transcellular route, where bacteria internalize inside cells and are released at the basal side of the cells (Figure 22).

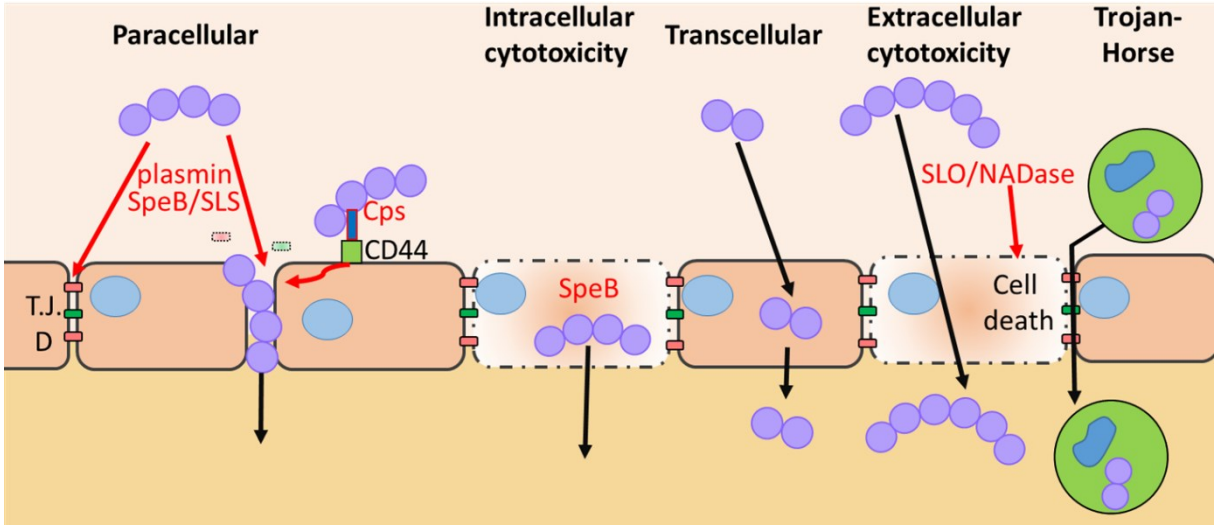

Figure 22. Different routes for GAS translocation across an epithelium

TJ-D: tight junctions- desmosome. Cps: capsule.

Bacteria can also be trapped and released by immune cells, known as the Trojan Horse strategy. This is discussed in the section 3.1.2. Finally, bacteria can cross epithelium in a paracellular mode, by altering intercellular junctions in several ways. First, GAS induces the degradation of the intercellular junctions, which promotes translocation, either through the LTA-CD44 binding or through the action of subcytotoxic dose of SLS (433, 471). GAS also degrades directly, through SpeB proteolytic activity (472), or indirectly through the SEN-plasmin binding (473), the intercellular junctions. Tricellulin is part of tight junctions between three cells and plasmin binding to tricellulin induces GAS to colocolize at these tricellular junctions, which triggers tricellulin degradation and bacterial translocation (421). SpeB can also directly degrade desmogleins, a component of the desmosome which is a type of intercellular junction (474).

3.2.2. Tissue degradation

After a breach or after crossing the epithelial barrier, GAS is in contact with the conjunctive tissue. Two ways to penetrate the conjunctive tissue are the Trojan-horse invasion and cell destruction. Another way consists in degradation of the ECM components (Figure 23). GAS broad spectrum cysteine protease SpeB is able to degrade the ECM components fibronectin and vitronectin (102).

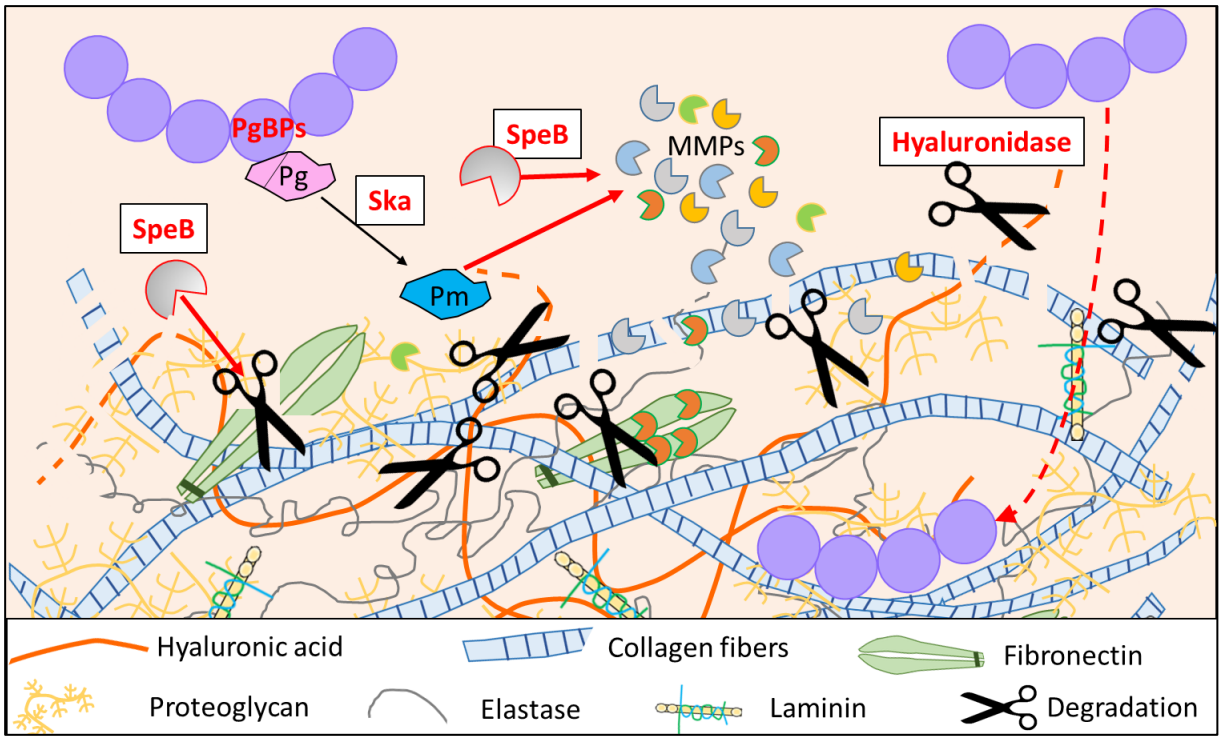

Figure 23 Extracellular matrix and its degradation by GAS

Representation of the ECM components and GAS mechanism of matrix degradation. PgBPs: plasminogen binding proteins. Ska: streptokinase. Pg: plasminogen, Pm: plasmin.

ECM degradation can also occur indirectly through host matrix metalloproteinases (MMPs) activated by SpeB (109, 110). Different GAS factors bind plasminogen (Table 10) which can be activated into plasmin by host effectors (uPA or tPA) or by GAS streptokinase. The bacterial surface-bound plasmin can activate MMPs (475, 476). Activated MMPs can degrade the components of the ECM, enabling bacterial dissemination within the tissue. Bacterial hyaluronidase can also degrade ECM hyaluronic acid, further promoting GAS invasion of the tissue and diffusion of secreted factors such as SpeB and SLO (468) (Figure 23).

3.2.3. Interaction with the fibrinolytic system

Plasma exudation is a source of nutrients for bacterial growth (see section 3.1.4), and the exudation depends on the vascular permeability. The binding of kininogen by the M protein and its subsequent activation in kinin by SpeB or by streptokinase/SpeB activated plasmin may create a local burst of kinin increasing vascular permeability (103, 175, 213). Moreover, as a host defense, the fibrinolytic system is critical to contain bacterial dissemination and is therefore an important defense mechanism against GAS (477). After activation of this system, thrombin cleaves fibrinogen in fibrin, which induces coagulation and bacterial trapping fibrin clots.

Plasmin is a host protease that can degrade these fibrin clots. Consequently, GAS can degrade fibrin clots either directly through SpeB or indirectly through the binding of plasminogen/plasmin at its surface (Table 10) (104–106, 476).

Table 10 Virulence factors interacting with plasma components

	Factor	Albumin	Ig	Fg	Plg/Plm	Complement	Other	Ref
All *emm*-types	M and M-like	B	B	B	B	C4BP, FH, FHL-1		(191, 193, 194, 478)
	SfbI/PrtfI		B	B				(272, 276)
	SEN				B			(343)
	GAPDH				B			(321)
	Ska				B/A			(174, 175)
	ScpA					D (C5a, C3a)		(255, 261)
	LTA	B						(403)
	Scl1					FH, FHL-1	LDL, HDL	(332, 334–336)
	SpeB		D	D	A	D (C3b)		(94, 98, 99, 104, 106)
	EndoS family		D					(95, 139–142)
emm28	Epf				B			(289)
	SOF			B				(479)
	Fba					FH, FHL-I		(346, 347)
Others	SIC					I (MAC)		(149)
	PAM/Prp				B			(208–210)

B: binds, A: activates, D: degrades
Ig: immunoglobulin, Plg: plasminogen, Fg: fibrinogen, Plg/Plm: plasminogen/plasmin. FHL-1: Factor H like I, FH: Factor H, LDL: low-density lipoprotein, HDL: high-density lipoprotein, MAC: membrane attack complex.

3.2.4. Cytotoxicity

GAS induces cell death in different contexts, to different cell types, and the mechanisms involved (necrosis, oncosis, apoptosis, pyroptosis) depend on the M-type, the virulence factors, the cell type and the experimental procedure. GAS can trigger extracellularly or intracellularly

cell death in lymphocytes, neutrophils, macrophages, keratinocytes, pulmonary cells, pharyngeal cells. This cytotoxicity depends on the independent or concomitant action of SLO, NADase, SLS, SpeB, SpyA, soluble M1 and SP-STP (Table 11). Cytotoxicity can also be induced indirectly: the activation of host matrix metalloproteinases by bacterial bound plasmin or by SpeB can also induce cell death (109, 110).

3.1. Control of the immune response

Host defends itself during the infection: antimicrobial peptides are secreted, pro-inflammatory cytokines are secreted to activate the immune responses, the complement system enable opsonization and bacterial clearance, phagocytic cells kill bacteria and a secondary immune response is induced. To establish infection, GAS expresses many virulence factors involved in countering and resisting the host defenses. In the following paragraphs we will review these different processes, with a special focus on the immunomodulation by GAS, since we analyzed the tissue responses to GAS infection during my thesis.

3.1.1. Resistance to anti-microbial peptides

At a basal level, immune and non-immune cells can secrete numerous anti-microbial peptides that restrain bacterial colonization and multiplication. SpeB releases dermatan sulphate from surface decorin, which inhibits α defensin (111). When SpeB is sequestered by GRAB, it degrades the cathelicidin LL-37 (91). Plasmin bound at the bacterial surface also degrades LL-37 (480). The N-terminal domain of the M1 protein sequesters LL-37, which inhibits the bactericidal effect, and the binding of the M protein to the hCAP-18, a LL-37 precursor, avoids LL-37 proteolytic activation (481). SIC is another critical virulence factor against anti-microbial peptides: SIC interferes with the bactericidal effect of the C3a, inactivates the α-defensin, LL-37 and lysozyme, the β-defensin, and the secretary leukocyte proteinase inhibitor (150–152, 154). The binding of albumin by LTA and M proteins, together with the SIC protein, inhibit chemokines such as CXCL9 that present antibacterial effects (153, 482). Finally, SOF degrades HDL which has an anti-microbial activity (300, 301).

Table 11. GAS-induced cytotoxicity and the factors involved

	Cell Type	M-Type	Cell-Death	Factor	Intra- or Extracellular	Ref
Immune cells	Murine macrophage J774/ THP1	M1	Caspase-1 dependent cell death	SpyA	E	(166)
	Murine macrophage J774/ THP1	M1	Apoptosis	SLO	E	(483)
	mouse peritoneal leukocytes	M5	unknown	SLS	E	(75)
	THP-1 macrophage	M1	Pyroptosis	Soluble M1	E	(484)
	Monocyte U937	M49	Apoptosis	SpeB	I	(485)
	Mouse neutrophil	M3	Apoptosis	SLS	E	(486)
	Mouse bone marrow derived macrophage	M49	Oncosis	SLO	E	(487)
	B and T lymphocyte	unknown	unknown	SLS	E	(488)
Epithelial cells	Keratinocytes OKP7	M1	Cell death with pyknosis	NADase	E	(489)
	Keratinocyte OKP7	M3	Apoptosis	SLO / NADase	E	(459)
	Keratinocytes HaCaT	M1	Programmed cell death	SLS	E	(76)
	Hep-2	M5	unknown	SLS	E	(75)
	Pharyngeal Detroit 562	M1	Apoptosis	SP-SPT	E	(160)
	Pulmonary A549, Pharyngeal Hep-2	M1, M49	Mostly apoptosis	SpeB	I	(490)
	HeLa	M6	Metabolic and programmed cell death	NADase*	E	(72)

*: NADase induces metabolic cell death, but a NADase natural variant without a NADase activity induces programmed cell death

3.1.2. Resistance to the complement system and phagocytosis

Macrophages recognize bacteria through their PRR (Pattern Recognition Receptor) or their opsonin (immunoglobulins and complement molecules) receptors such as the Fc and C1 receptors.

There are three pathways of complement activation, the classical, the lectin and the alternative pathway (see Figure 24). All lead to the secretion of peptides that recruit inflammatory cells (C5a, C3a, C4a), bind to complement receptor for phagocytosis (C3b) or form the membrane attack complex, MAC (C5b, C6, C7, C8, C9) that lyses bacteria (491). It is critical for bacteria to avoid the complement system activation, and three main strategies are developed to avoid it: 1) avoid recognition by initial peptides (C1q, MBL etc… see Figure 24), 2) degradation of the peptides or inhibition of the different proteases and 3) recruitment of one of the multiple complement inhibitor of the complement pathways: factor H and factor H-like 1 (alternative pathway), C4BP (classical), CD46 etc....

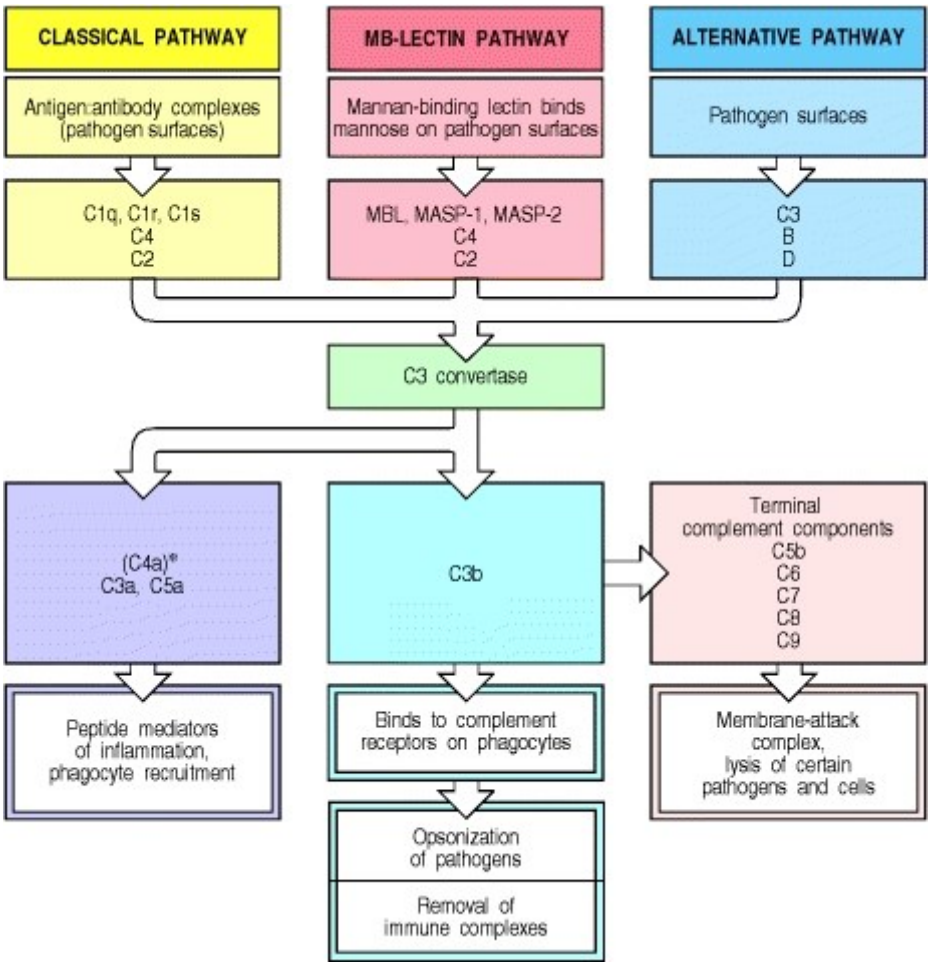

Figure 24. The complement pathway
Description of the main elements involved in the complement cascade. From (491).

3.1.2.1. Avoiding opsonization and inhibiting the complement cascade

There are two types of opsonization, the complement mediated opsonization and the antibody mediated opsonization. The antibody mediated opsonization is based on antibodies recognizing bacterial antigens by the Fab part of immunoglobulins. The available Fc domain can directly

serve as a ligand to trigger phagocytosis through the Fc receptor, or initiate the classical complement cascade though C1q binding to the Fc domain. GAS binds antibodies by their Fc domain through the M and M-like proteins and SfBI/PrtfI, rendering the Fc unavailable for the cellular Fc receptor (492).

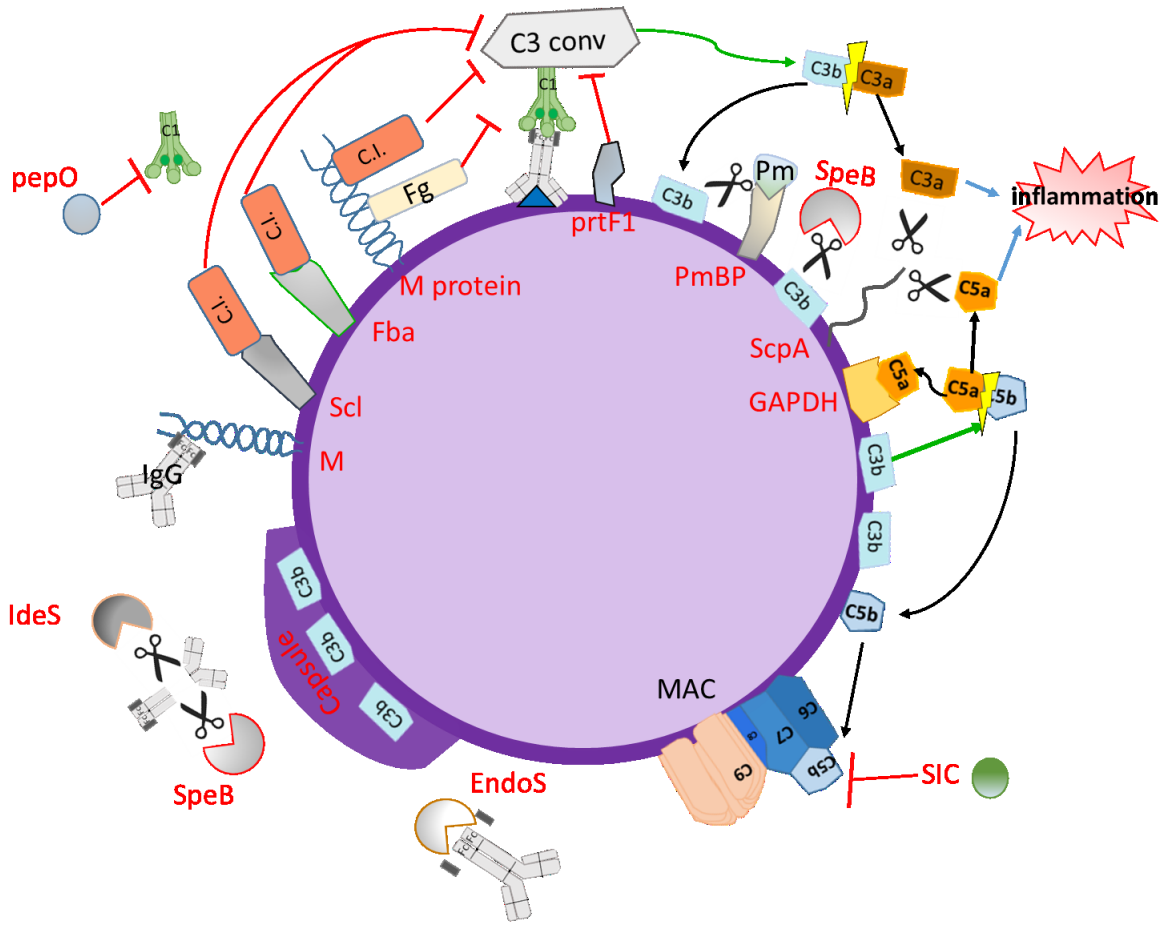

Figure 25. GAS resistance to the complement activation pathway
Schematic representation of the main mechanisms of GAS resistance to the complement cascade. C.I.: complement inhibitors, C3conv: C3 convertase, Fg= fibrinogen, PmBP: plasmin binding proteins, Pm: plasmin. Red arrow: inhibition. Black arrow: step of the pathway. Green arrow: cleavage. Scissors: degradation. Blue arrow: induction.

In addition, to remove the opsonic ability of antibodies, SpeB and IdeS can specifically cleave Fab bound antibodies, freeing the Fc activating domain from the bacterial surface and leaving the bacteria coated by a host-like coat (96, 493). However, SpeB ability to cleave IgG under the physiological, non-reducing, condition was questioned (88). EndoS and the M49 specific EndoS2 remove carbohydrates from IgG, which decreases the affinity of the Fc for the Fc-

receptor by 15-fold (94, 95). M and M-like proteins bind albumin, which plays an important role in determining the location of opsonic and nonopsonic epitopes (193).

Bacterial surface can also directly activate the deposition of C3b (alternative and lectin pathway). C3b can be degraded by SpeB and the plasmin bound at the surface of GAS (98, 99, 494). Moreover, bound plasmin can also degrade C5 (495). C3a is degraded by the C5a peptidase which also degrades C5a, the latter also being inactivated by its capture by GAPDH (261, 323). The alternative pathway is also inhibited by the degradation of properdin by SpeB (100). Recently, PepO, a secreted endopeptidase 68 % similar to *S. pneumoniae* PepO, has been involved in resistance to complement mediated bacteriolysis through the binding to C1q, which also decreases immunoglobulin mediated opsonization (496).

GAS strains can bind fibrinogen through several proteins (Table 10) and this binding inhibits the classical pathway of the complement by inhibiting the formation of C3 convertase through inhibition of the deposition of the C4b molecule (438, 497). In a similar way, Prtf1 on its own inhibits C3 deposition at the bacterial surface and SIC inhibits the MAC assembly, in a step prior to the C5b67 binding to the cell membrane (149, 275).

To inhibit complement activation, GAS can recruit the inhibitors of the alternative pathway factor H and factor H-like through the M and M-like proteins, the protein Fba and Scl1 (Table 10) (188, 192, 332, 334, 347, 348). C4BP binds to M and M-like proteins, and the M1 protein binds CD46, but its role in complement inhibition was not shown (201).

3.1.2.2. Inhibiting, limiting and surviving phagocytosis and NETS

GAS has developed several strategies to avoid recognition by immune cells. GAS covers its surface with host proteins, avoiding recognition by phagocytes: LDL and HDL are bound by Scl1, albumin by LTA and by the M protein/protein H (211, 335, 336, 403, 404).
By inhibiting opsonization (3.1.2.1), GAS avoids its recognition by phagocytic cells. Moreover, the capsule prevents the recognition of opsonins and antibodies at the bacterial surface (498, 499).

Some factors can also reduce phagocytosis. Intracellular SIC can interact with ezrin in PMN, which reduces bacterial phagocytosis and Mac-1-like protein can bind CD16 at the surface of neutrophils to reduce their phagocytic capacity (144, 500).

After being phagocytosed, GAS bacteria are able to survive and even replicate within the phagocyte (501, 502). More specifically, viable GAS are found mostly in macrophages, but

also in neutrophils (501). GAS avoids the fusion between the vacuole and the lysosome in a M1 dependent manner (502–504). The ability of M1 strains to inhibit the phagolysosome fusion in a M1 dependent manner was not reproduced with another M1 strain (505). The protein H has also been implicated in the intracellular survival, but the mutant lacking the protein H only was shown to express very low amounts of protein M1 (241, 503). These observations need to be confirmed with a non-M1 strain to see if intra-phagocytic cell survival is a M1-specific characteristic.

SLO and NADase are two factors involved in the prevention of the acidification of the vacuole, increasing bacterial survival in macrophages. At the single cell level, the ability of GAS to replicate in the cytosol of a viable human macrophage depends on SLO (506). Therefore, it is clear that GAS survives within macrophages (501), but the molecular mechanisms involved remain to be elicited.

In addition to the bacterial killing decrease, GAS survival in macrophages could allow for its transport from colonization sites to distant anatomical sites and tissue invasion (507).

Neutrophils not only phagocyte bacteria, they also trap bacteria within neutrophil extracellular traps (NETs) which are mostly composed of extracellular DNA. GAS secretes several DNAses (2.1.1.2) that are involved in the resistance to the NETs by freeing the bacteria from them (130, 133). Finally the M1 protein reduces NETs cytotoxic activity and SclI both reduces NET production and cytotoxicity (502, 508).

3.1.3. Modulation of the inflammation

GAS controls the immune response to increase its survival in tissues and in blood. Paradoxically, different virulence factors can induce anti-inflammatory responses while other, or the same, activate pro-inflammatory responses (Figure 26). SpyCEP is able to degrade IL-8 and other ELR containing cytokine, which decreases neutrophil migration across endothelial barriers (168) and Sse hydrolyzes the platelet activation factor which is a neutrophil chemoattractant (173). SpeB degrades a wide range of anti-inflammatory chemokines: CXCL1-7; CXCL10-14, CXCL16, CCL20 and CX3CL1 (101). The degradation of C5a and C3a by the C5a peptidase both contribute to a reduced inflammation.

However, SpeB and other virulence factors can induce pro-inflammatory responses. Protein sequestration and protein cleavage are classical pathways in inflammatory response activation. Since SpeB is a broad-spectrum protease, its proteolytic activity can affect multiple

proteins involved in inflammatory pathways, which further stimulates inflammation. SpeB releases the pro-inflammatory bradykinin from the protease inhibitor H-kininogen (103). IL-1β is a pro-inflammatory cytokine secreted as an inactive form which can be naturally cleaved to its active form by different host proteases during inflammation, or by caspase 1 during a specific cell death activation pathway. *In vitro*, SpeB cleaves the pro- IL-1β to its mature active form (509): any pathogen's protease which cleaves IL-1β will trigger a pro-inflammatory response, so IL-1β can be seen as a sensor of pathogen-associated proteolysis.

Moreover, SpeB, independently from its proteolytic activity, can trap the serine proteinase alpha1-antitrypsin and this could enhance the contact system activation, highly increasing the bactericidal activity of the plasma (112). SpeB production is strongly down-regulated in plasma (106), which could decrease this phenomenon and promote blood bacterial survival.

SpyA induces a pro-inflammatory cell death in murine macrophages (166). In a similar way, SLO induces caspase 1-dependent cell death in murine macrophages, which releases active IL-1β (510). After infection of murine macrophages, SLO and SLS synergistically induce the production of prostaglandin E_2, a proinflammatory molecule (511). However, in macrophages differentiated from peripheral blood mononuclear cells, a more relevant model, the production of IL-1β is induced in response to GAS, but independently of SLS or SLO (512). SLO activates human neutrophils by inducing the release of heparin-binding protein, a pro-inflammatory molecule (513).

Similarly to the IL-1β induction by SLO, data obtained using murine macrophages should be confirmed with human macrophages since it is becoming increasingly clear that murine macrophages differ significantly from human macrophages (514).

GAS strains secrete superantigens (SAgs) that are highly potent mitogens of the immune system (2.1.1.1). A similar effect was reported for LTA (306). SAgs are involved in psoriasis**,** acute rheumatic fever, Kawasaki disease, STSS and necrotizing fasciitis (119, 515, 516). The systemic hyperactivation of the immune responses are the principal characteristics of toxic shock syndrome, and GAS superantigens are directly involved in STSS [reviewed in (517)]. SAgs are also associated and implicated in different post-infectious complications, while the direct mechanisms involved remain to be established [reviewed in (518)]. The presence in both staphylococcal and streptococcal species of SAgs, the horizontally acquisition through bacteriophages, their dissemination within *emm*-types and the poor variability of the SAgs

genes, all suggest a critical role for these proteins in the setting up of infections. Activating the immune response could increase tissue inflammation which would increase nutrient availability through plasma exudation during the inflammation, however this would also activate a secondary immune response to which GAS cannot survive. The role of SAgs hyper-activation of the immune system within physiological tissue, such as the pharynx and the skin, and their evolutionary advantage remain unclear (519). One clue to the understanding of the role of SAgs in tissue colonization is that SAgs could be involved in anti-inflammatory responses. SAgs hyper-activation could trigger anergy of T cells or avoid a Th2 response which induces cytotoxic T cells proliferation (520). SAgs can induce the transition from CD4 T cells to CD4 T regulatory (Tregs) cells, which results in increased production of anti-inflammatory responses (521). Moreover, SAgs can also trigger CD8+ Tregs differentiation in human, decreasing CD4 T cell proliferation (522). Interestingly, the SAg doses required for IL-10 (anti-inflammatory) secretion by induced T cells are much lower than the doses for IFN-γ (pro-inflammatory). These results identify a novel crucial role of SAgs in the pathogenesis of GAS infections.

SAgs have a critical role in GAS colonization in a humanized MHC Class II mice; SpeA is essential in the colonization of mice nasopharynx (523, 524). The same SAg SpeA induces, through its binding of MHC class II molecules, a short term pro-inflammatory response followed by a long term hypo-inflammatory response with secretion of IL-10 and PD-L1, which contributes to T cell anergy by activating Tregs (525). The "hypervirulent" strains of the *emm1* genotypes express a natural variant of SpeA1, called SpeA2, which has a higher affinity for MHC class II molecules (526): this mutation is thought to contribute to the preferential dissemination of this clone, even more suggesting the importance of SAgs in GAS dissemination.

Human skin and pharynx harbor very specific immune resident cells with for example resident memory Tregs in the skin that are very different from systemic circulating cells (527). Resident specific cells probably play a significant role in the establishment of GAS colonization of these tissues and our understanding of SAgs importance for GAS virulence might arise from looking at the effect of SAgs on these different cell subtypes.

By degrading chemokines and pro-inflammatory peptides, GAS decreases the activation and recruitment of immune cells. The question remains: are pro-inflammatory reactions to GAS virulence factor side effects of their evolutionary selected functions (such as SpeB cleavage of IL-1β) or an evolutionary trait selected to promote the infection? As seen with SAgs, it is clear that bacterial effectors can induce systemic hyper-activation, which results in diseases such as

necrotizing fasciitis and STSS. However, the same systemic pro-inflammatory effectors could have anti-inflammatory effects in tissue. It is therefore important to increase our knowledge of the critical virulence factors responsible for GAS early innate immune response modulation. Targeting the mechanisms of GAS modulation of immunity at the barrier site could be key to the treatments of GAS infection, as shown by the reduction of GAS colonization in mice oro-pharynx when immunized against SpeA (523).

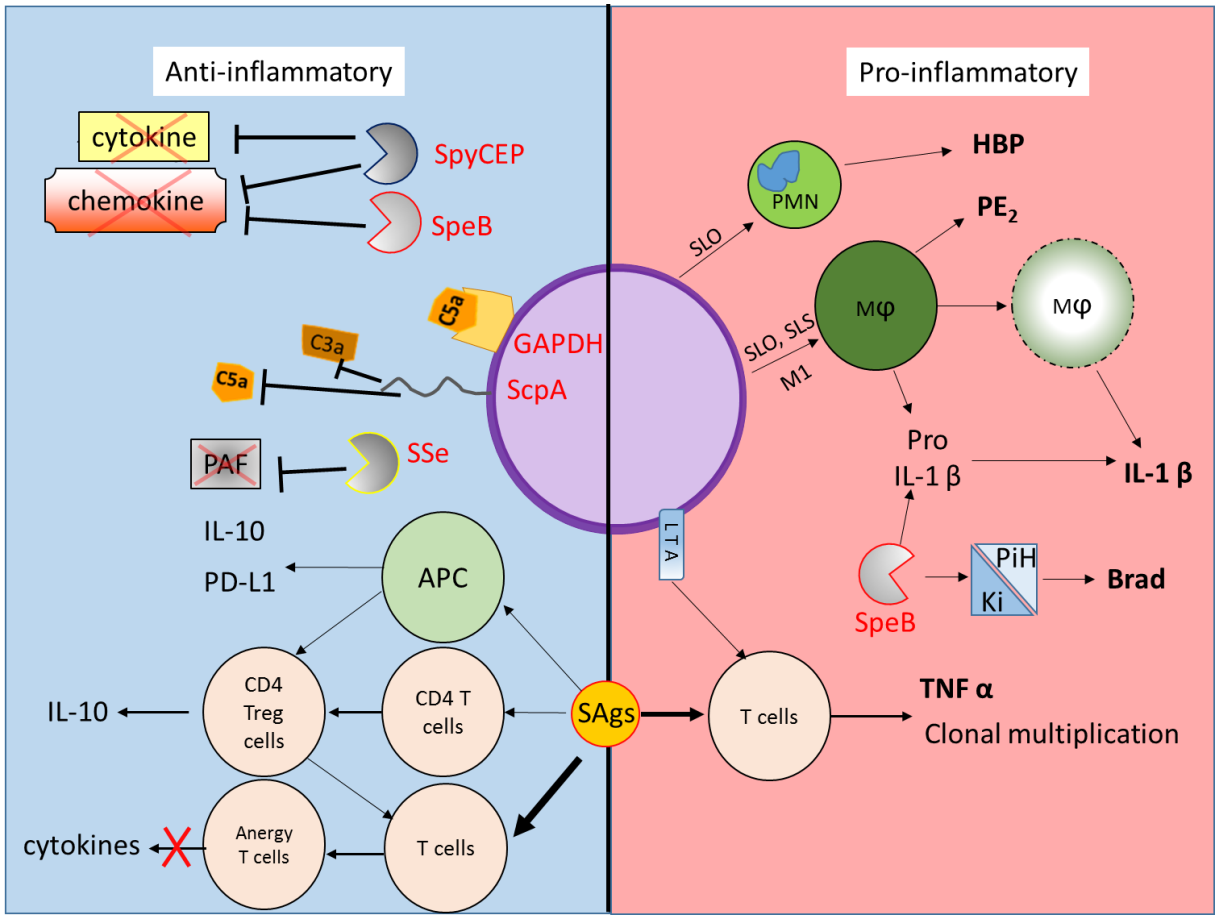

Figure 26. GAS: a "two-faced" modulator of the inflammation

Schematic representation of the different mechanisms of GAS modulation of the immune responses. APC: antigen presenting cells, Mφ: Macrophage, PMN= Polymorphonuclear, HBP= heparin binding protein, PiH= protease inhibitor H-kininogen, Ki= kininogen, Brad= bradykinin, PAF= platelet activation factor, PE_2= prostaglandin E_2.

4. Biopsies and experimental approaches to characterize GAS infections

GAS is responsible for a wide range of diseases that affect different tissues and there is a wide range of disease severity. In addition, GAS is genetically highly diverse and a strictly human pathogen. Finally, GAS ability to induce infections depends on the environmental context (for examples the presence of trauma, including blunt trauma, and the postpartum) and the host genetic background (528). Consequently, many independent different aspects of GAS infections can be studied.

One approach to understand GAS pathogenesis is to analyze disease characteristics in patient infected tissues (biopsies). Then different experimental approaches and models can be built up to mimic the pathogenesis, which enable to analyze the importance of specific factors in the pathogenesis. In the following paragraphs, I will shortly describe several models of infection. First, we will describe the insights from biopsies studies; then the different animal models but we will not discuss the invertebrate model of infection, because I consider it too remote from the questions treated during this thesis. We will also present the 3D organotypic approach and finally the study of human explants. Since in the Manuscript 2 we will present a new model of human explant, the decidua, we will conclude this section by presenting this tissue and its organization.

4.1. Biopsies

Since recurrent pharyngitis require tonsil removal and necrotizing fasciitis also necessitate the removal of infected tissue, researchers have had access to human biopsies since a long time to study the end point of GAS infections. Many parameters of bacterial infections were discovered through this approach, such as biofilm structure, intracellular cells status of GAS in immune and non-immune cells, antibiotic resistance (406, 413, 501, 529). Biopsies analyses are critical to describe phenotypes that models should try to recapitulate, to decrypt the mechanisms involved. One major challenge in biopsy studies is the number of host parameters that are not controlled and could explain the differences of morphologies between one patient and another (413). Biopsies studies unfortunately do not allow addressing all the critical parameters that played during the setup of patient infections.

4.2. Animal models

4.2.1. Rodent models

Mice, rats and chinchillas are three commonly used models for many bacterial infections, including GAS. Not all mouse strains can be used in the different mice models, and significant differences can be seen depending on the mouse genetic background (530). This makes the rodent model versatile, but the study of the genetic differences between mice strain already have unraveled host factors critical for infection (531).

To understand the pathogenesis of skin infections, a common model is injection of 10^6 to 10^8 bacterial in a subcutaneous or air sac model (532). However, this model does not recapitulate all human features of typical skin infections, such as impetigo, pyoderma, erysipelas, cellulitis or necrotizing fasciitis. The architecture of the murine skin might explain the phenotypic differences: murine epidermis is thinner, and the skin contains a lot more hair follicles than does the human skin, hair follicles that contain memory Tregs (533).

GAS is responsible for invasive infections in which bacteria are found in the blood (systemic infections). Several models try to recapitulate these infections: bacteria can be injected intravenously (IV), intraperitoneally (IP), intranasally (IN) or intratracheally (IT). These infection routes bypass all (IV) or most (IP, IN and IT) infectious step. IP is the less relevant, since the barrier to cross is one never encountered by GAS in humans (534). IN and IT systemic infections require the crossing of the lung epithelium (535). Many parameters can be monitored with these models, such as the bacteremia, the number of bacteria in different organs and the lethality. Many of these systemic models suffer from the poor viability of GAS strains in mouse blood compared to human blood. Lethality dose are still used as a marker of bacterial virulence, in spite of the virulence of bacteria in humans not correlating with mice virulence in systemic models (536).

One major feature of GAS is its ability to colonize the human oropharynx, especially the Waldeyer's ring which includes the tonsil: GAS is responsible for 700 million cases of pharyngitis per year (21), the analysis of GAS ability to colonize the oropharynx is therefore a clinical issue. Except for the mouse pathogenic strains B514/33 of the M type 50 (537) which expresses an atypical virulence repertoire (237), most human strains do not colonize on the long term the mouse or rat oropharynx, and to establish short term colonization, huge load of bacteria are instilled, not recapitulating the infection routes. Mice and rats are rodents so their nasopharyngeal organizations significantly differ from human oropharynx, for example there

is no equivalent for the Waldeyer's ring in the rodents. However, this model is informative for the understanding of active immunization: immunization with several virulence factors reduces the bacterial colonization. Another approach to model pharyngitis is the non-lymphoid associated tissue (NALT), which corresponds to the human tonsil. Some GAS strains briefly colonize these tissues but there are the same limitations as for the nasopharyngeal model.

To analyze long term mucosal colonization by GAS, a vaginal model was developed (538). In this model, mice are primed with estradiol and infected with GAS, which results in long term asymptomatic colonization. GAS poorly colonizes human vagina (0.03%) (539) and is responsible for puerperal sepsis in very specific contexts (see section 1.3.3). Mouse vagina recapitulates several human vaginal characteristics and is used to model other vaginal colonizers/ pathogens (GBS and *Candida albicans*). The vagina colonization model allows analysis of long term colonization of a mucosa. However, long term colonization also involves adaptation of bacteria to their environment, and in this case the mouse vagina is an environment very different from most human mucosa.

A rat model was also used to study post-infectious complications resulting from cross-reactivity of antibodies targeting bacterial antigens (autoimmunity). In this model, rats are immunized with GAS antigens and are monitored for their development of post-infectious sequelae such as rheumatic arthritis and endocarditis (540). The developed pathologies resemble those of humans and this model could help understanding the mechanisms involved in post-infectious autoimmune diseases.

GAS is responsible for approximatively 3% of ear infections (541). Biofilms are involved in GAS virulence but few models enable the study of biofilm on biotic surfaces. A model of chinchilla ear infections was set up to study biofilm formation and the pathogenesis of ear infections (542). The presence of three-dimensional GAS communities embedded in extracellular polymeric substance indicates that GAS readily forms biofilm in the chinchilla ear. Compared to *in vitro* studies, chinchilla ear infection mimics more closely the biofilm formation that occurs during human infection, and this model can lead to potential critical discoveries that could help fight against *in vivo* GAS biofilms.

Of mice and men: humanization of mice

There are two promising approaches for the study of strictly-human, or not, pathogens such as *Neisseria meningitidis*, *S. aureus* and GAS: humanization of mice and xenograft (543, 544).

Both approaches aim to reduce the inter-species barrier that limits the modeling of bacterial pathogenesis.

Mice transgenic humanization: what you miss, we will give it to you

A limitation of the murine models is the strict specificity of many GAS major virulence factors: GAS does not bind mouse C4BP and factor H, and is therefore intensely targeted by rodent complement cascade and eliminated; GAS binds mouse IgG with a very low affinity compared to human IgG; streptokinase does not target mouse plasminogen and superantigens do not affect murine immune cells (181, 241, 476, 517, 523). This list is not exhaustive and probably many GAS virulence factors are not functional in mice, greatly reducing our ability to understand the role of virulence factors without minimizing the effect of others that are at play in humans.

To solve this issue, mice expressing transgenically human factors in addition or instead of their native factors were generated: hu-plaminogen, hu-Factor H, hu-C4BP and hu-MHC class II (181, 476, 523, 545–548). The contribution to virulence can be assessed compared to the native mice, and these models take advantage of the human factor that functions as the native mouse factor: for example, human C4BP is able to inhibit the mouse complement cascade. With the possibility to generate multiple KO the number of factors tested and the specific contributions, synergy or complementarity, can be assessed (546). These humanized mice do not fully recapitulate the GAS pathogenesis but can yet be useful for specific questions. However, studies of the role of Factor H in virulence in C57BL transgenic mice and BalbC transgenic mice yielded contradictory results (546, 547). As with mouse models, understanding the differences in the genetic background of the mice could contribute to our understanding of critical host parameters in GAS infections.

Xenograft

Another approach is the xenograft: human pieces of skin are grafted onto immunodefficient mice. The tissues come from neonatal foreskin or plastic surgery. Compared to other pathogens, such as *N.meiningitidis*, xenografted mice are not commonly used for GAS studies. This approach was used to model impetigo and several features of human impetigo were reproduced (549, 550). Xenograft enables the study of the early steps of bacterial infection of tissues with relevant cells and extracellular matrix components. Immune responses and immune cell recruitment still correspond to the mouse systemic circulation that, furthermore, is immunosuppressed: this model does not allow the study of the humoral response to the infection.

4.2.1. Non-human primate models

Primate models were developed to overcome the species specificity of GAS and to test GAS pathogenesis in the presence of an immune system closer to the human one. GAS readily colonizes the oropharynx of different primates (baboon, rhesus monkey, chimpanzee, and the cynomolgus macaque) and in contrast to rodents, the animals suffer clinical manifestations resembling pharyngitis (551, 552). This colonization is long lasting and enables subsequent humoral immune responses, which could in a near future allow the study of rheumatic fever in this model. Primate is probably the best model to study GAS virulence factors involved in human pharyngitis, and already confirms the importance of the M proteins and the capsule in the colonization (553, 554). As said before, one limitation of mice models is the species-specificity of the superantigens (SAgs), which probably also explains our poor knowledge of SAgs role in GAS virulence. To better understand the pathogenesis of STSS, a model of primate sepsis was set up, which includes the intravenous injection of 10^{10} bacteria in baboons (555). Several human clinical manifestations (hypotension, organ failure) were observed, making primate models a promising model to understand the transition from bacteremia to STSS, and the virulence factors involved.

4.3. 3D organotypic skin model and *ex vivo* infections

4.3.1. 3D organotypic skin model

The 2D resolution, infection of epithelial cells *in vitro* is a good model to analyze GAS-host cells interactions: adhesion, internalization, epithelium crossing, cytotoxicity and cell responses to infection. However, it does not allow long-term study of GAS infections: cytotoxicity induces cell detachment and bacteria are released in the supernatant, not enabling CFU counts or fluorescence microscopy. Moreover, the absence of other cell-types than an epithelial cell line strongly simplifies the interactions that occur during GAS infections: the absence of matrix, immune cells and vertical penetration of a tissue decreases the extent to which epithelial cells can be used as an infection model. Tissue engineering is an old idea that started during world war II (556) and ended up in the setting up of 3D organic tissues with cells from many human organs. 3D skin explant is a tissue that contains epithelial cells seeded in a collagenous matrix. This is the simplest 3D skin explant engineered and it is a very good tool to assess biofilm formation or cytotoxicity of Streptococci strains (413, 557).

Moreover, tissue engineering is being more and more developed, with the generation of fibroblast and epithelial cells 3D tissue (558, 559); bioprinting is now extending the limit of

tissue engineering with 3D tissue incorporating dendritic cells (560–562). While still simpler than normal human skin, these models enable to have only one genetic background, they avoid versatility of human skin and avoid the use of animal models. It is without any doubt that these approaches will be more and more used to study GAS infections.

4.3.2. *Ex vivo* models of infection

To study the very early steps of infection, without grafting tissue to mice, models were developed where human tissue explants are infected *ex vivo* and the infection is monitored on the infected sample (563, 564). Human tonsil were infected *ex vivo* by GAS (265, 565) and human skin explants have been used to study GAS biofilm formation for the first time very recently (566). These models do not allow for long-term observation of the infection compared to the mice, with tissue viable for up to 24 hours. However, recent development of medium enables up to 7 days survival of this tissue (567). The advantage is that the tissue is infected extemporaneously, without the wound healing and possible adaptation that occurs during xenografting. *Ex vivo* models enable to study innate immune response and the limiting elements involved in the early host-pathogen interaction, but does not allow immune cell recruitment. In the second publication of this thesis, we will describe a new model of *ex vivo* infection of a human tissue, the decidua, and how it contributes understanding the critical early steps of GAS infections.

4.3.3. The decidua and maternal-fetal membranes

During the menstrual cycle, the endometrium, the mucosal lining of the uterus, undergoes differentiation in preparation to implantation of an embryo and to facilitate its development. In the second part of the menstrual cycle (after day 18), the differentiation of the endometrium is called decidualization from the Latin *decider*, to fall off or to detach. At the end of the human menstrual cycle, if the oocyte is not fertilized, the decidualized endometrial lining is eliminated during menstruation and the menstrual cycle begins again with a new series of endometrial differentiation.

During decidualization, endometrial stromal fibroblasts transform into specialized secretory cells. This transformation involves both the differentiation of fibroblasts and endometrial stromal cells into large polyploid (epithelioid-like) cells, called decidual stromal cells (DSC), the profound remodeling of the composition and organization of the endometrial extracellular matrix (ECM) and a massive influx of leukocytes, polynuclear cells, macrophages and NK cells.

The decidual extracellular matrix is mainly composed of diffused type I, III and VI collagens. In addition, type IV collagen and laminins are enriched around DSCs (569). The decidua is composed of 40 % of leukocytes and 60 % of DSCs. Circulating monocytes that infiltrate the decidua differentiate into decidual macrophages ($CD163^+$) which correspond to 20 % of leukocytes in the decidua (570). Seventy % of leukocytes are decidual NK cells that regulate embryo invasion and the remaining 10 % of leukocytes are T cells involved in the maternal-fetal tolerance (571).

The implantation of the embryo critically depends on the secretion of matrix metalloproteases by the decidua (572). After implantation, the embryo resides within the decidua and during its development, several embryonic cell subtypes associate with maternal cells (Figure 27a). After obliteration of the uterine cavity because of the enlargement of the amniotic cavity, around the fourth month of gestation, the maternal-fetal membranes present their definitive structures with the amnio-chorion membranes surrounding the amniotic cavity (fetal membranes) and the maternal decidua (Figure 27b). These membranes will slough off with the placenta after delivery.

The decidua prevents the embryo from being attacked by maternal immune cells, it supplies nutrition prior to placenta formation and protects both embryo and mother from infections. The large number of immune cells in the decidua is supposed to establish a balance between immune tolerance of the embryo and defense against infections (572). Twenty-four hours of infection with various pathogens (*Escherichia coli,* GBS, *Candida albicans* and *Gardnerella vaginalis*) induce the secretion by maternal-fetal membranes of the pro-inflammatory cytokines IL-6, CXCL8, TNF and the anti-inflammatory cytokine IL-10 (573–576). DSCs could play a role in the modulation of inflammation (572) and they express 4-6 types of TLR (577). Of note, *in vitro*, isolated DSCs produce TNF-alpha, IL-6 and CXCL8 after stimulation with Lipopolysaccharide (LPS) (577, 578). LPS, lipid A and LTA all increase secretion of IL-10 by isolated DSCs (579).

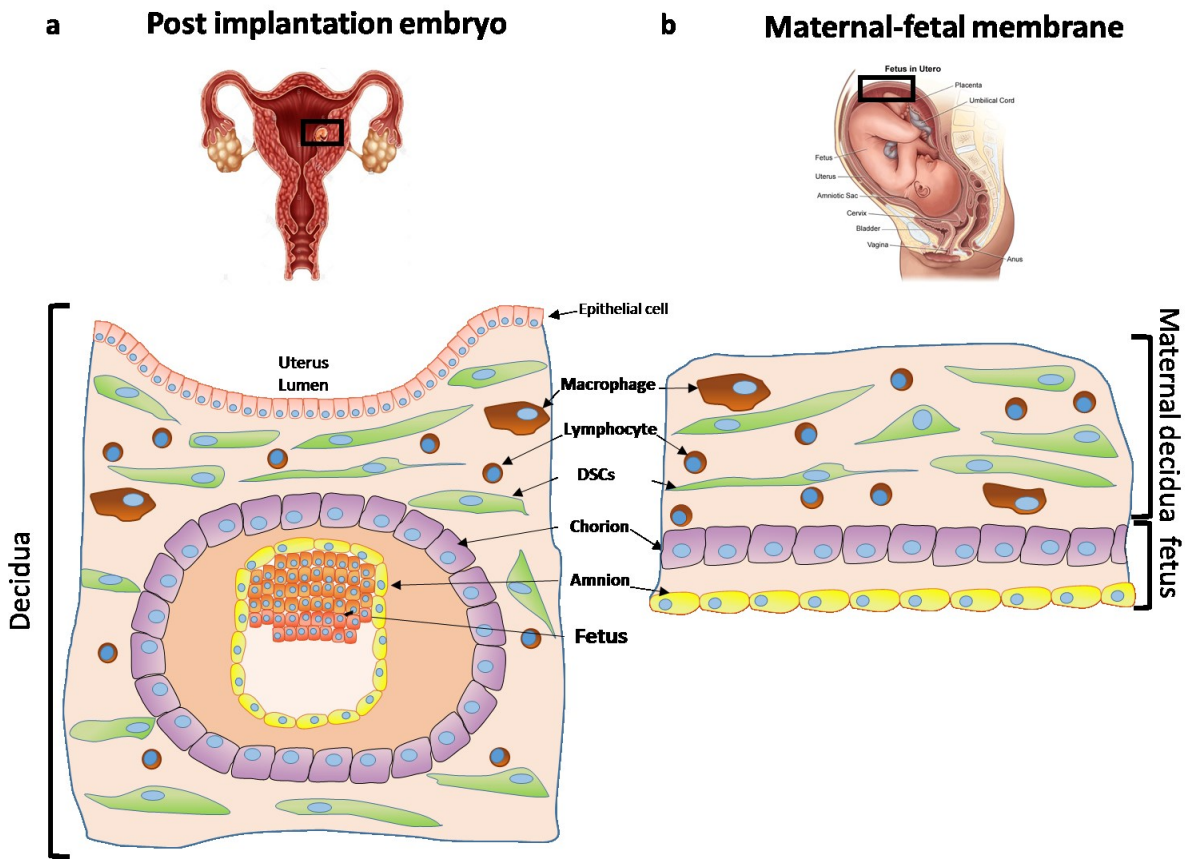

Figure 27. The development of the maternal-fetal membranes

In the top figures are represented the regions of interest (black rectangle) that are described in the schemes below as sections. **a**, the decidua post implantation of the embryo; **b**, a section of a maternal-fetal membrane at the end of pregnancy.

Research context

Research context

The main focus of the team is the deciphering of bacterial mechanisms involved in the crossing of host barriers. The bacteriology department of the Cochin Hospital of Paris hosts the National Reference Center for Streptococci since 2006. The team Barriers and Pathogens mainly focuses on GAS, involved in choc mild to severe infections, pharyngitis to necrotizing fasciitis and septic, and GBS, a pathogen which colonizes the vagina of 10-30 % of women. GAS is responsible for 517 000 deaths in the world, with 163 000 deaths due to invasive infections. These infections are a clinical concern for three reasons. GAS invasive infections are life-threatening and fast evolving diseases with a mortality rate of 25 %, there is a propensity for epidemical dissemination in health-care systems and finally, the number of invasive infections has been increasing in developed countries since the 1980s. The team preferentially analyzes how the mechanisms involved in the onset of GAS invasive infections.

The team is part of the "Département hospital-universitaire" (DHU) Risks in pregnancy, a consortium of obstetrical clinicians and researchers which aims at increasing the knowledge on pregnancy and peripartum diseases. GAS puerperal fevers were, in the nineteenth century, a significant burden, responsible for the death of one out of ten women after delivery. Prophylactic strategies have significantly decreased the number of cases, but endometritis still represents 26 % of women GAS invasive infections in France. In this context, the team studies GAS puerperal fever and endometritis as models of GAS elicited invasive infections. The team confirmed with French epidemiologic data the association between GAS *emm28* strains and gyneco-obstetrical diseases (43), and a representative *emm28* strain was selected on phenotypic and genotypic characteristics from a screening of 50 *emm28* strains involved in endometritis in France. This strain was fully sequenced and called M28PF1 (M28 GAS Puerperal Fever 1) (126). The main goals of this thesis were to characterize mechanisms involved in GAS *emm28*-elicited endometritis, and the role of different factors in these infections. We performed this analysis in two complementary parts: in the first one, we focused on the involvement of the R28 protein in the adhesion to host cells of the gyneco-obstetrical sphere; in the second one, we studied the establishment of GAS invasive infections on an original *ex vivo* model of human tissue infection, using the infection of the decidua as a model of endometritis.

In the first part, we aimed to identify specific *emm28* proteins involved in the association between these strains and gyneco-obstetrical diseases, which prompted us to study R28, an *emm28*-specific protein involved in adhesion to cervical cells. We assayed the role of R28 on

other cell lines potentially involved in gyneco-obstetrical diseases, identified the subdomains involved in promoting the adhesion and their cell receptors (Manuscript 1).

In the second part, we intended to better characterize the pathophysiological scenario of GAS endometritis. The endometrial linen of women after delivery is composed of decidua, a tissue derived from endometrial stromal cells and immune cells. The fetal membrane surrounding the fetus during pregnancy results from the association between maternal decidua and fetal cells. We therefore decided to infect *ex vivo* the decidua from maternal-fetal membranes acquired from healthy caesarians. To analyze the critical parameters involved in the poorly described window of establishment of invasive infections, we focused on the first hours of infection. More specifically, we studied the mechanisms involved in bacterial growth, biofilm formation, tissue penetration and in the modification of the host responses to the infection (Manuscript 2 and additional results).

Results

1. R28 protein and puerperal fever

"The N-terminal domain of the R28 protein promotes *emm28* Group A Streptococcus adhesion to host cells via direct binding to three integrins" (Manuscript 1)

(Manuscript accepted for publication in Journal of Biological Chemistry)

GAS *emm28* strains are associated with gyneco-obstetrical infections, including endometritis (44–47). This *emm*-type is the third most prevalent in France and one of the most prevalent in Europe (35, 43). R28 is a surface protein of GAS expressed nearly exclusively by *emm28* strains and is a member of the Alp family of GBS surface proteins. Noteworthy, GBS is a commensal bacterium of the vagina (50). A GAS *emm28* strain that does not express R28 adheres less to cervical cells than the wild-type strain (48). In this study, we assessed the potential implication of R28 is the association of *emm28* strain and gyneco-obstetrical infections. We dissected the potential role of R28 in the promotion of GAS adhesion on relevant clinical cells potentially involved during the pathogenesis of GAS endometritis.

First, we showed that an isogenic mutant for R28 presents decreased adhesion to primary decidual cells, cells that compose mucosal uterine-lining during pregnancy (Manuscript 1, Fig. 2). Then we show that the purified R28 N-terminal domain ($R28_{Nt}$) binds specifically to primary decidual cells, to endometrial epithelial cells (HEC-1-A) and to cervical cells (ME180). Beads coated with $R28_{Nt}$ also bind specifically to HEC-1-A. Finally, the exogenous expression of $R28_{Nt}$ increases the adhesion of *Lactococcus lactis* to HEC-1-A cells. Hence $R28_{Nt}$ promotes the adhesion of GAS *emm28* strains to clinical relevant cells possibly involved in endometritis.

We then investigated the subdomains involved in the adhesion to cells (Manuscript 1, Fig. 3). We subdivided the $R28_{Nt}$ in two halves, R28-N1 and R28-N2 domains (Manuscript 1, Fig. 1). N1 is the only domain conserved and similar to all N-terminal domains of proteins of the Alp family. R28-N1 and R28-N2 both contributed to adhesion to HEC-1-A cells as shown by experiments with purified proteins and coated beads. Moreover, R28-N1 and R28-N2 compete one with another suggesting they share common receptor(s).

The analysis of the capacity of $R28_{Nt}$ to bind cells after biochemical modifications of the cell surface showed that the receptors of $R28_{Nt}$ are membrane proteins (Manuscript 1, Fig.

4). A co-immunoprecipitation approach was set up to identify these receptors and a mass-spectrometry analysis identified several surface proteins as putative receptors, including the integrins α3β1, α6β1, α6β4 (Manuscript 1, Table 1). By ELISA, we demonstrated that $R28_{Nt}$, R28-N1 and R28-N2 all directly interact with α3β1, α6β1, α6β4 but not with α2β1, an integrin expressed by endometrial cells but that did not co-immunoprecipitate (Manuscript 1, Fig. 5, Fig. S3). We showed that these interactions did not require divalent cations in contrast to natural ligands; yet, these divalent cations altered the binding to α3β1 and α6β1 but not to α6β4.

Finally, since α3β1, α6β1 and α6β4 are expressed by numerous cell-types, we analyzed $R28_{Nt}$ ability to promote adhesion to other than endometrial cell-types (Manuscript 1, Fig. 6). $R28_{Nt}$ increased the binding of beads to pulmonary A549 cells, skin keratinocytes HaCaT and to a lesser extent to intestinal cells TC7, which express apically low amount of β1containing integrins.

In conclusion, our work indicates that R28 interacts directly to the three integrins α3β1, α6β1, α6β4 through its subdomains R28-N1 and R28-N2. These interactions contribute not only to adhesion to the endometrium, and consequently potentially to GAS endometritis, but also to the adhesion to other cell types and thus to the overall prevalence of the *emm28* strains.

Manuscript 1

The N-terminal domain of the R28 protein promotes *emm28* Group A Streptococcus adhesion to host cells via direct binding to three integrins

Antonin Weckel[1,2,3], Dorian Ahamada,[1,2,3], Samuel Bellais[1,2,3,†], Céline Méhats[1,2,3], Céline Plainvert[1,2,3,4,5], Magalie Longo[1,2,3], Claire Poyart[1,2,3,4,5], Agnès Fouet[1,2,3,4*]

From [1]INSERM U1016, Institut Cochin, [2]CNRS UMR 8104, [3]Université Paris Descartes (UMR-S1016) Paris France, [4]Centre Nationale de Référence des Streptocoques, [5]Hôpitaux Universitaires Paris Centre, Cochin, Assistance Publique Hôpitaux de Paris, France

Running title**:** GAS $R28_{Nt}$ interacts with integrins to promote adhesion

***** To whom correspondence should be addressed: Institut Cochin, 22 rue Méchain 75014 Paris, France; agnes.fouet@inserm.fr; Tel: + 33 1 40 51 64 50; Fax 33: + 1 40 51 64 54

† present address: Bioaster, 28 rue du Dr Roux, 75015 Paris

Keywords: host-pathogen interaction, *Streptococcus pyogenes* (S. pyogenes), infection, adhesion, integrin, protein-protein interaction

---

ABSTRACT

Group A Streptococcus (GAS) is a human-specific pathogen responsible for a wide range of diseases, ranging from superficial to life-threatening invasive infections, including endometritis ,and autoimmune sequelae. GAS strains express a vast repertoire of virulence factors that varies depending on the strain genotype, and many adhesin proteins that enable GAS to adhere to host cells are restricted to some genotypes. GAS *emm28* is the third most prevalent genotype in invasive infections in France and is associated with gyneco-obstetrical infections. *emm28* strains harbor R28, a cell wall-anchored surface protein that has previously been reported to promote adhesion to cervical epithelial cells. Here, using cellular and biochemical approaches, we sought to determine whether R28 supports adhesion also to other cells and to characterize its cognate receptor. We show that through its N-terminal domain, $R28_{Nt}$, R28 promotes bacterial adhesion to both endometrial–epithelial and –stromal cells. $R28_{Nt}$ was further subdivided into two domains, and we found that both are involved in cell binding. $R28_{Nt}$ and both subdomains interacted directly with the laminin-binding α3β1, α6β1 and α6β4 integrins; interestingly, these bindings events did not require divalent cat-ions. R28 is the first GAS adhesin reported to bind directly to integ-rins that are expressed in most epithelial cells. Finally, R28Nt also promoted binding to keratinocytes and pulmonary epithelial cells, suggesting that it may be involved in supporting the prevalence in invasive infections of the emm28 genotype

---

Streptococcus pyogenes, also known as Group A streptococcus (GAS), is a Gram-positive bacterium responsible for a wide range of diseases, from superficial infections such as pharyngitis and dermatitis, to severe invasive infections such as necrotizing fasciitis and endometritis (1–3). GAS infections are also responsible for post-infectious complications such as rheumatic arthritis and glomerulonephritis and, altogether, GAS infections are responsible for 517,000 deaths annually worldwide (4).

GAS strains are genetically diverse and are genotyped through sequencing of the 5' end of the *emm* gene (5) encoding the M protein, a major virulence factor; more than 250 *emm*-types have

been described (6). A link exists between genotype and tissue tropism, with throat- and skin-specialists and ubiquitous genotypes (7); a link between genotype of invasive strains and elicited disease exists for some but not all genotypes (our unpublished data, https://cnr-strep.fr/). Approximately 10 % of the GAS genome is composed of exogenous genetic elements encoding virulence factors, with substantial variation between different *emm*-types, which could account for the tropism (8). The first to third most prevalent genotype in Europe, *emm28*, is responsible for 8% of GAS invasive infections in France (9, 10, https://cnr-strep.fr/). It is associated to endometritis and for example, in France, 27% of GAS invasive infections in women occur in the gyneco-obstetrical sphere (10–13). *emm28* strains harbor an integrative conjugative element named RD2 that was likely horizontally transferred from *Streptococcus agalactiae*, also known as Group B Streptococcus (GBS) (13, 14). GBS colonizes 10-30% of healthy women's urogenital-tract (15) and it was suggested that the presence of this integrative conjugative element accounts for the *emm28* GAS gyneco-obstetrical tropism (13). This remarkable tissue association together with the high prevalence of *emm*28 strain invasive infections prompted us to study the role of R28, an RD2 encoded surface protein, in GAS *emm*28 infections.

Adhesion to host tissues is the initial step for all GAS infections. It is mediated by different factors, mainly surface proteins, that bind either extracellular matrix components, indirectly the cell surface through plasmatic or extracellular matrix components bridging, or directly to eukaryotic receptors [reviewed in (16) and (17)]. RD2 encodes four surface proteins including R28 and a R28-deficient *emm28* strain is non-adherent to the cervical cell line ME180 (18). R28 is a member of the Alp family composed of GBS proteins that share evolutionary and structural similarity and which includes the alpha C protein (also known as ACP or α), Rib, R28 (also known as Alp3 in GBS) and Alp2 (18–21) (Fig. 1A). These chimeric proteins are composed of a signal peptide, an N-terminal domain, repeats, and an LPXTG anchoring motif. The repeats number varies among clinical isolates and their structure is related to the Ig-like fold (22). The repeats are identical within one protein and the identity percentage between Alp members varies between 35 and 94, the latter being between Rib and R28 repeats. Repeats are considered to properly expose the N-terminal domain at the bacterial surface, potentially the functional domain (21). This domain is composed of one, for ACP and Rib, two, for R28, and three modules, for Alp2. The first modules of R28 and Alp2 share 99% identity and are 70 and 56% identical to the module of ACP and Rib, respectively. The second modules of R28 and Alp2 are 99% identical and is similar to the β protein, unrelated to the Alp family. Alp2 third module is a repeat of the second one (Fig. 1A) (21, 23, 24). Thus, R28 is a chimer of ACP and the β protein for its N-terminal domain and Rib for its repeats and it immunologically cross-reacts with both proteins (19, 25). ACP is the most studied member of the Alp family and the crystal structure of the N-terminal domain has been elucidated (24). It binds glycosaminoglycans in a region encompassing the end of the N-terminal domain and the repeats (26, 27), and the α1β1 integrin through a KTD motif localized in a β-sandwich subdomain at the N-terminal end of its N-terminal domain (24, 28, 29); this motif is absent from R28, Alp2 and Rib (Fig. 1A). These interactions increase GBS internalization in the cervical cell line ME180 (29).

In this study, we analyzed the capacity of R28 to promote adhesion to host cells and characterized the adhesion domain. We demonstrate that the N-terminal domain of R28 ($R28_{Nt}$) is sufficient to promote direct adhesion to different gyneco-obstetrical cell lines, and further identified two subdomains within $R28_{Nt}$ that are both involved in this adhesion process. We then characterized the chemical nature of the $R28_{Nt}$ receptor and isolated different ligands. We show that $R28_{Nt}$ interacts with the laminin-binding integrins α3β1, α6β1 and α6β4. Finally, we show that $R28_{Nt}$ increases adhesion also to skin and pulmonary cells, further extending the role of R28 as a GAS adhesin involved in GAS *emm28* prevalence.

Results

The N-terminal domain of R28 is sufficient to promote adhesion to human female genital tract cells

Association of GAS *emm28* strains with gyneco-obstetrical infections could be a consequence of its capacity to colonize the vaginal tract (10). A GAS R28-deleted mutant adheres less than the parental strain to cells from

the cervical ME180 lineage (18). To assay the role of R28 in a more physiological situation, we tested whether the phenotype could also be observed on human decidual stromal cells (hDSC) isolated from decidual biopsy of specimens obtained after caesarian delivery (Fig. 2A). The decidua is the lining of the uterine during pregnancy and consists of differentiated endometrial stromal fibroblasts and recruited leukocytes. It may be a direct target of GAS infection, a major cause of severe puerperal sepsis. The R28-deleted strain adhered significantly less (18%) to hDSC than the wild-type strain (Fig. 2A), confirming the role of R28 as an adhesin on physiologically relevant cells. We then sought to characterize the adhesion domain of the R28 protein using different cells from the female genital tract, hDSCs as well as two cell lineages, cervical cells (ME180), often used to study female genital tract infections, and endometrial epithelial cells (HEC-1-A). The six to 17 highly conserved 79-residue long repeats of R28 are considered to expose the 368 residue-long N-terminal domain at the bacterial surface, potentially the functional domain (Fig. 1A**)** (18, 29). Consequently, to analyze the ability of R28 to promote adhesion to various cells, we focused on the N-terminal domain of R28, $R28_{Nt}$, using biotinylated $R28_{Nt}$ (Fig. 2B-D). $R28_{Nt}$ displays higher binding capacity to hDSC, ME180 and HEC-1-A cells than soluble BSA (200, 10 and 10 times more binding at 10 µM, respectively). To confirm the capacity of $R28_{Nt}$ to promote adhesion, we tested whether $R28_{Nt}$-coated beads or a heterologous bacterium expressing $R28_{Nt}$ could bind more to HEC-1-A cells than the controls (Fig. 2E-I). $R28_{Nt}$-coated beads adhered three times more than the BSA-coated control beads ($p<0.05$) (Fig. 2E-G) and this binding was blocked by the addition of purified $R28_{Nt}$ antibodies ($p<0.05$) (Fig. 2H). Also, the *Lactococcus lactis* strain expressing $R28_{Nt}$ (Fig. S1A) adhered significantly more than the control strain harboring the empty vector (+35%, $p = 0.0066$) (Fig. 2H). The increased adherence may seem weak. However, in the absence of the repeats, $R28_{Nt}$ may be poorly exposed at the *L. lactis* cell surface or hidden by the protective polysaccharide pellicle (30) compared to the exposition of the complete R28 protein in GAS *emm*28 strains; this could lead to an underestimation of $R28_{Nt}$ capacity to promote adhesion. Thus, the N-terminal domain of R28 is sufficient to increase the adherence of a Gram-positive bacterium to endometrial cells.

Altogether these results demonstrate that $R28_{Nt}$ promotes bacterial adhesion to female genital tract cells.

Both N-terminal subdomains R28-N1 and R28-N2 are sufficient to promote adhesion to HEC-1-A cells.

The $R28_{Nt}$ domain is composed of two halves, from amino-acid residue 56 to 229 and from residue 230 to 424, which we termed R28-N1 and R28-N2, respectively (Fig. 1A and Fig. S1B (21). A BLAST alignment indicated that R28-N1 and R28-N2 share no similarity (E-value, 0.27). To test which sub-domain mediates adhesion, we produced and purified the corresponding peptides (Fig. S1B, S1C) and incubated them after biotinylation with ME180 and HEC-1-A cells (Fig. 3A-C). Both the R28-N1 and R28-N2 subdomains showed significant binding with both cell types compared to BSA ($p<0.001$ for both cell-types), with R28-N2 displaying an affinity two-to three-fold higher than that of R28-N1 (Fig. 3C). The R28-N1 and R28-N2 binding values indicate an additive contribution of R28-N1 and R28-N2 to the $R28_{Nt}$ binding on HEC-1-A cells and a synergetic one on ME180 cells (Fig. 3C).

To assess the binding of these subdomains in more physiological conditions, we tested whether R28-N1- and R28-N2-coated beads bound HEC-1-A cells (Fig. 3D). Twenty-seven % and 19% of R28-N1- and R28-N2-coated beads bound to HEC-1-A cells, respectively, a percentage significantly higher than BSA-coated beads (6.3%, $p<0.001$ and $p<0.05$ for R28-N1 and R28-N2 with HEC-1-A cells, respectively). We checked the binding specificity of the coated beads by incubating cells with an excess amount of soluble peptides (20 µM) and assessing the percentage of beads still bound to cells (Fig. 3D). Purified R28-N1 and R28-N2 peptides competed with their respective coated beads (6.3% and 4.5 % vs 27 % and 19%, for R28-N1 and R28-N2, respectively) confirming the binding specificity. Altogether, these data clearly indicate that both the R28-N1 and R28-N2 subdomains are sufficient to promote adhesion to HEC-1-A cells.

We then sought to determine if R28-N1 and R28-N2 have independent receptors. We performed competition assays in which we assessed the percentages of R28-N1- and R28-N2-coated beads bound to cells pre-incubated with excess amounts (20 µM) of soluble R28-N2 and R28-N1, respectively (Fig. 3D). These subdomains compete with one another ($p<0.005$),

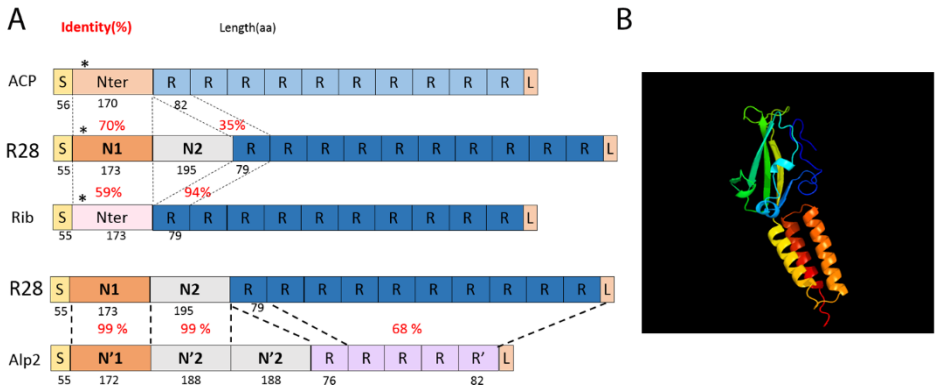

Figure 1. **Schematic representation of R28, Alp family members and R28-N1 predicted 3D structure.** *A,* Schematic representation of the Alp family members structure and similarity. Numbers in dark below the scheme indicate the length in amino-acid residues and in red the percentage of identify between two domains. S=Signal peptide, R= repeats, L= LPXTG. *= KTD in ACP, KAD in R28 and KPD in Rib. Modified with our sequence comparisons from (1–3). *B,* R28-N1 structure as predicted by Phyre. Green and yellow, the β-sandwich; yellow to red, the three-helix bundle

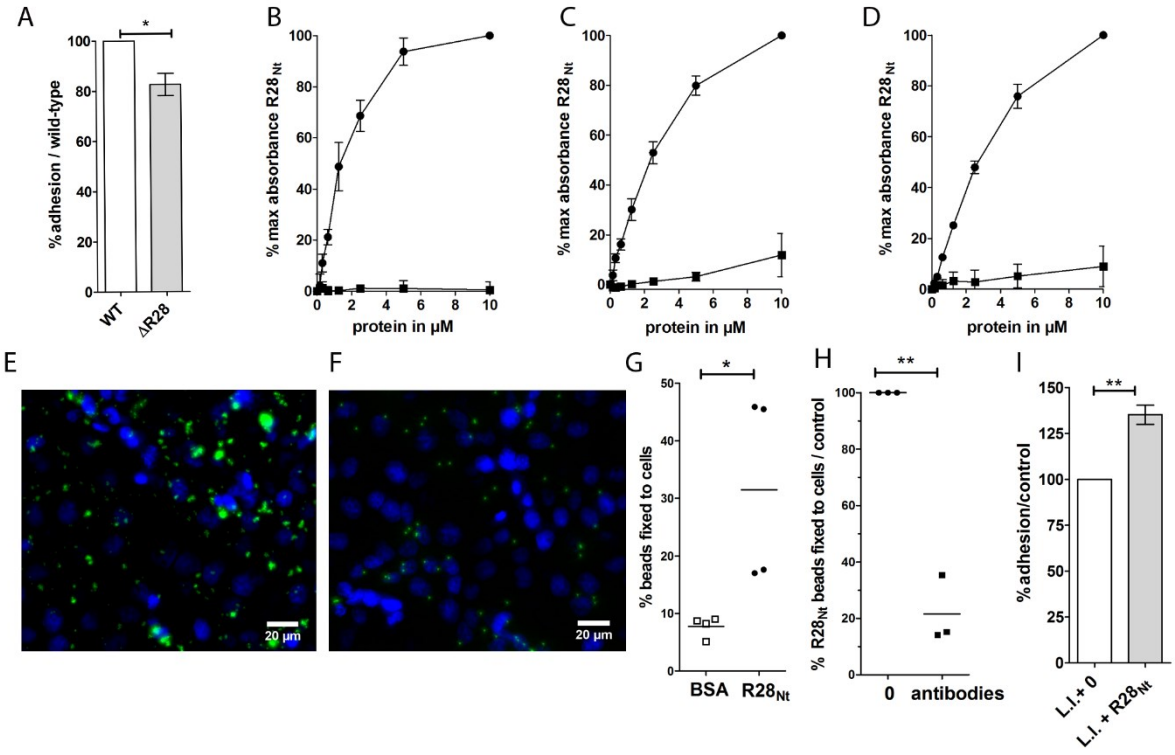

Figure 2. $R28_{Nt}$ is sufficient to promote adhesion to female genital tract cells. *A*, Binding of the ΔR28 strain to human decidual stromal cells (DSCs) is expressed as a percentage of that of the wild-type strain; Two-tailed t-test was performed on 6 independent experiments performed in triplicates. *B-D*, ELISA-based protein-cell interaction assay with biotinylated proteins, expressed as percentage of the maximum binding, on: *B,* secondary decidual cells (DSCs); *C,* ME180 cells and *D,* HEC-1-A cells. Circle, biotinylated $R28_{Nt}$; square, biotinylated BSA. Error bars correspond to SEM of four independent experiments. *E-F* representative immunofluorescence of coated fluorescent beads with *E,* $R28_{Nt}$ or *F,* BSA, on HEC-1-A cells. Coated beads in green and DAPI staining in blue. *G,* Binding of $R28_{Nt}$ or BSA coated fluorescent beads to HEC-1-A cells. One-tailed t-test. *H,* Binding of $R28_{Nt}$-coated fluorescent beads to HEC-1-A cells in the presence of purified anti-$R28_{Nt}$ antibodies, expressed as the percentage of that in the absence of anti-$R28_{Nt}$ antibodies. *I,* Adhesion of $R28_{Nt}$ expressing *L. lactis* (L.l + $R28_{Nt}$) to HEC-1-A cells, expressed as the percentage of that of the *L. lactis* empty vector strain (L.l. + 0). *H-I,* two-tailed t-test. *, $p<0.05$; **, $p<0.01$

suggesting that these subdomains share common receptor(s). Moreover, both displaced $R28_{Nt}$-coated beads lowering its binding level to unspecific binding level (BSA-coated beads, 6%), further supporting that R28-N1 and R28-N2 share a common receptor.

$R28_{Nt}$ adhesive properties are not conserved among all Alp family members

Among members of the Alp family, alpha C protein (ACP) binds, through its N-terminal domain, the α1β1 integrin (28) and, through a region encompassing the end of the N-terminal domain and the repeats, glycosaminoglycans (26, 27). In contrast, attempts to demonstrate that Rib is an adhesin have been unsuccessful (31). We focused on the shared N-terminal domains of these proteins, leaving out from ACP_{Nt} the region binding glycosaminoglycans. A BLAST alignment indicated that R28-N1 is 70% and 56% identical to the N-terminal domains of ACP and Rib respectively (Fig. 1A). Furthermore, a Phyre analysis predicted, with a confidence of 100%, that R28-N1 has the same structure as ACP, that is two domains, an N-terminal β-sandwich, sharing structural elements with the type III fibronectin fold, and a C-terminal three-helix bundle (Fig. 1B) (24). We thus wondered whether the adhesive properties of R28-N1 to cervical and endometrial cells are conserved among the ACP or Rib N-terminal domains. We tested the binding capacity of ACP_{Nt} and Rib_{Nt+2R} which contains, in addition to the N-terminal domain, two repeats which are 94% identity to the R28 repeats (Fig. 1A). We expressed and purified these peptides and analyzed their direct binding to ME180 and HEC-1-A cells (Fig. S1C, S1D; Fig. 3A, 3B). ACP_{Nt} binds to both cell-types, yet less than R28-N1 and consequently even less than R28-N2 or $R28_{Nt}$. Since ACP_{Nt} binds HEC-1-A, despite the absence of α1β1 integrin on its surface (32), we tested whether it shared a receptor with R28-N1 or R28-N2 by assaying, as for the R28-N1 and R28-N2 competitions, whether it can compete with R28-N1 and R28-N2 (Fig. 3D, 3E). ACP_{Nt} competes with itself and R28-N1 ($p<0.005$), suggesting that these subdomains share a common receptor, but not with R28-N2 (Fig. 3B). Moreover, we did not detect a competition between R28-N1 and ACP-bound beads (Fig. 3E). In contrast to ACP, Rib_{Nt+2R} does not bind to either ME180 or HEC-1-A cells, which indicates that this binding property is restricted to some Alp family members (Fig. 3 A, 3B). Moreover, because Rib_{Nt+2R} contains two R28-like repeats, its inability to bind ME180 and HEC-1-A cells suggests that R28 repeats do not mediate the adhesion on their own.

$R28_{Nt}$ receptor is a membrane protein

Our experiments were carried out in the absence of added extracellular or plasmatic protein; we consequently hypothesized that $R28_{Nt}$ binds directly to a cell surface receptor(s). To identify it, we first defined its chemical nature. As previously described (33), we applied to HEC-1-A cells different treatments that affect potential receptors depending on their chemical nature before incubating them with soluble $R28_{Nt}$ and quantifying bound $R28_{Nt}$ by flow cytometry (Fig. 4). Pronase and trypsin treatments significantly reduced, in a dose dependent manner, the percentage of positively labelled cells down to 10% and 29%, respectively. Also, neither heparinase I nor sodium periodate treatments affected $R28_{Nt}$ binding to cells (data not shown), excluding an interaction between $R28_{Nt}$ and glycosaminoglycans or carbohydrates which harbor vicinal hydroxyl groups. These results suggest that the $R28_{Nt}$ receptor is a cell-surface exposed protein. Similar results were obtained with R28-N1 and R28-N2 (Fig. S2A-S2B). Altogether, our data suggest that the $R28_{Nt}$, R28-N1 and R28-N2 receptor(s) is (are) a cell-surface exposed protein(s).

Identification of several putative receptors of $R28_{Nt}$

To identify R28 receptor(s), a co-immunoprecipitation experiment using HEC-1-A cells was set up followed by mass spectrometry analysis. Cross-linked $R28_{Nt}$ - cellular proteins complexes were resolved on acrylamide gels and Western blotting highlighted multiple high molecular, above 170 kDa, complexes (data not shown) absent in the co-immunoprecipitation without $R28_{Nt}$ incubation (control). The zones above 170 kDa of $R28_{Nt}$ and control immunoprecipitations were excised from gels and the protein contents were analyzed by mass spectrometry (Supplementary file). Hits enriched in the co-immunoprecipitation in the presence of the bait $R28_{Nt}$ in all three independent experiments were initially selected. From this list, and since the $R28_{Nt}$ receptors are cell-surface exposed proteins (Fig. 4), only such proteins were further selected (Table 1). Hence, through co-immunoprecipitation of $R28_{Nt}$ we identified several potential $R28_{Nt}$ receptors.

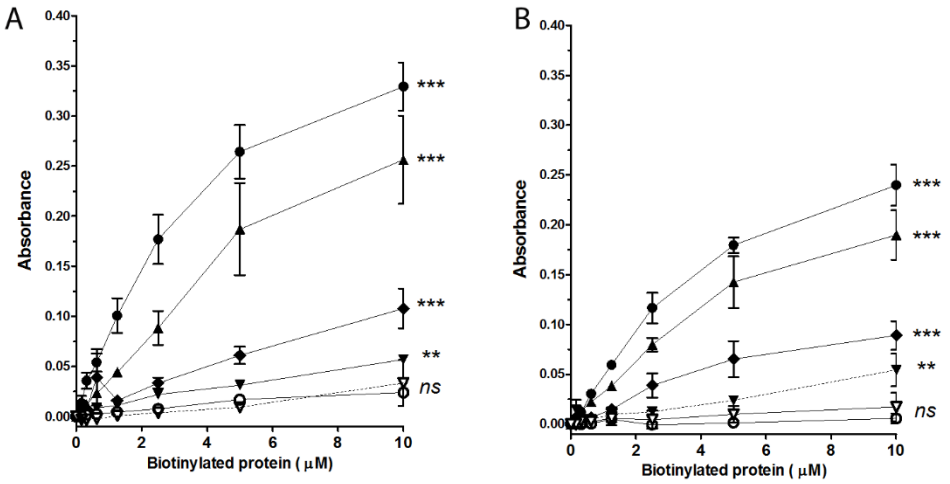

C

Cell type	HEC-1-A		ME180	
	B1	B2	B1	B2
R28-N1	0.0166	-0.0008	0.0156	-0.0005
R28-N2	0.0368	-0.0018	0.0440	-0.0018
$R28_{Nt}$	0.501	-0.0026	0.079	-0.0046
ACP_{Nt}	0.0038	-0.00002	0.0083	-0.0003

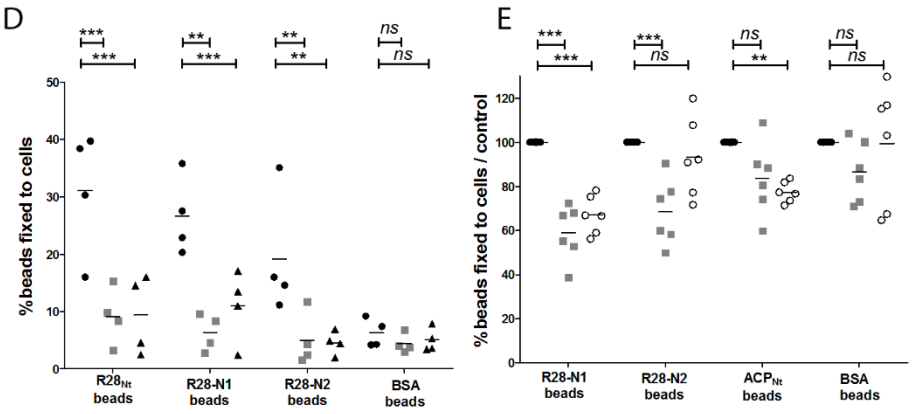

Figure 3. R28-N1, R28-N2 subdomains and ACP_{Nt} are sufficient to promote adhesion to HEC-1-A cells and compete differentially with each other binding. *A-B,* ELISA-based cell interaction assay with purified biotinylated $R28_{Nt}$ (●), the subdomains R28-N1 (◆) and R28-N2 (▲); ACP_{Nt} (▼), Rib_{Nt+2R} (○) and BSA (▽). Peptide solutions were incubated with *A,* ME180 cells or *B,* HEC-1-A cell, washed, fixed with paraformaldehyde and bound biotinylated proteins were detected as in an ELISA. The experimental data for biotinylated $R28_{Nt}$ and BSA are those used for Fig. 2*C* and 2*D*. The calculation for the absorbance is described in Experimental procedures. Error bars correspond to SEM of four independent experiments performed in duplicates. *C,* parameters of the non-linear fitting of figures *A* and *B*. *D-E*, Fluorescent (*D*) $R28_{Nt}$-, (*D, E*) R28-N1-, R28-N2-, (*E*) ACP_{Nt}- or (*D, E*) BSA-coated beads were incubated with HEC-1-A cells pre-incubated with 20 µM of recombinant R28-N1 (■); R28-N2, (▲), ACP_{Nt} (○) or not (●). **, $p<0.005$; ***, $p<0.001$; *ns*, not significant.

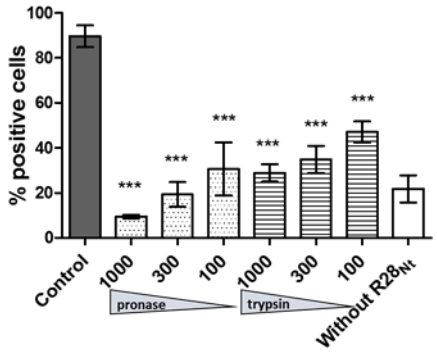

Figure 4. The $R28_{Nt}$ receptor is a cell surface protein. Analysis of $R28_{Nt}$ receptor chemical nature. Treatments were applied to HEC-1-A cells in suspension prior to incubation with purified $R28_{Nt}$; bound $R28_{Nt}$ is immunostained and cells were analyzed by flow cytometry. Dark columns: untreated cells; clear column: unspecific labeling of cells without incubation of peptide. Statistical analysis was performed against the untreated condition. Error bars correspond to SEM of three independent experiments. Two-Way ANOVA: ***, $p<0.001$.

Table 1. Main hits from mass spectrometry analysis of specifically co-immunoprecipitated $R28_{Nt}$ receptors

Common Name	Gene name	Relative raw intensity		
		Exp1	Exp2	Exp3
Basal cell adhesion molecule	*BCAM*	A	3.50	5.00
Cadherin-1;	*CDH1*	A	A	A
CD166 antigen	*ALCAM*	A	3.70	8.30
Desmoglein-2	*DSG2*	A	A	6.01
Ephrin type-A receptor 2	*EPHA2*	A	4.03	3.20
Integrin alpha-3	*ITGA3*	A	8.32	65.32
Integrin alpha-6	*ITGA6*	A	18.37	A
Integrin alpha-V	*ITGAV*	A	1.74	7.20
Integrin beta-1	*ITGB1*	A	3.50	6.55
Integrin beta-4	*ITGB4*	A	5.84	5.62
Prostaglandin F2 receptor negative regulator	*PTGFRN*	A	A	A
Transferrin receptor protein 1	*TFRC*	A	3.54	5.10

A, Absent from control condition.

$R28_{Nt}$, R28-N1 and R28-N2 interact directly with integrins

Of all the proteins identified as present in the complexes co-immunoprecipitated with $R28_{Nt}$, we decided to focus on integrins as possible $R28_{Nt}$ receptors. To test this, we assayed by immunofluorescence whether soluble $R28_{Nt}$ and highlighted integrin monomers are in close proximity at the surface of HEC-1-A cells (Fig. 5A-5C). At the cell surface, $R28_{Nt}$ indeed binds into clusters in close proximity to integrin α3, α6, and β1 clusters.

To confirm a direct interaction between $R28_{Nt}$ and integrins, we analyzed the binding of the extracellular domains of integrins to $R28_{Nt}$, R28-N1 and R28-N2 by ELISA (Fig. 5D-5F). Integrins α3β1, α6β1 and α6β4 all interact significantly more with $R28_{Nt}$, R28-N1 and R28-N2 than with BSA ($p<0.001$). To assess the binding specificity further, the same experiment was carried out with an integrin containing a subunit which, although it is expressed by HEC-1-A cells, had not been found in the mass spectroscopy analysis, namely α2β1 (Fig. S3) (32). In contrast to a natural ligand, type I collagen, neither $R28_{Nt}$ nor its two subdomains, R28-N1 and R28-N2, displayed interaction with α2β1, indicating that the integrins α3β1, α6β1 and α6β4 are true receptors of $R28_{Nt}$. The influence of divalent cations on the binding efficiency was assessed. As expected, binding of $R28_{Nt}$ to the different integrins in the presence of EDTA reflects that in PBS (Fig. 5G). Addition of the divalent ions Ca^{2+} significantly lowers binding of $R28_{Nt}$ to α3β1 and α6β1 (51% and 72% compared to in the presence of EDTA, respectively) and that of Mn^{2+} to α3β1 (45%). In contrast, binding to α6β4 was unchanged by the addition of divalent cations. Altogether, these data demonstrate the direct interaction between $R28_{Nt}$, R28-N1 and R28-N2 and the three integrins α3β1, α6β1 and α6β4.

$R28_{Nt}$ is sufficient to promote adhesion to different cell lines

So far, our study focused on the capacity of R28 to promote adhesion to endometritis-related cells; yet, *emm28* is the first to third most prevalent genotype for GAS invasive infections in Europe (9, 10, https://cnr-strep.fr/). Moreover, the R28-interacting integrins are expressed by numerous cell types, so we assayed whether R28 contributes to adhesion in other GAS-elicited invasive infections. We tested $R28_{Nt}$ ability to promote adhesion to other cell lines by testing the binding capacity of $R28_{Nt}$-coated beads to skin keratinocytes, HaCaT, pulmonary epithelial cell, A549, as well as the gut intestinal cells TC7, that do not display the integrins α3β1, α6β1 and α6β4 apically (Fig. 6) (35). $R28_{Nt}$-coated beads bind significantly and to a similar level (approximately 30%) A549, HaCaT and HEC-1-A cells (Fig. 2G and 6). In contrast, only 13% of $R28_{Nt}$-coated beads bind TC7 cells, not significantly different from the BSA-coated control beads. In conclusion, $R28_{Nt}$ is sufficient to promote adhesion to cell lines relevant not only for GAS endometritis but also for other GAS invasive infections.

Discussion

R28, a surface protein specifically expressed by *emm28* strains, which are associated with endometritis, promotes adhesion to cervical cells; its eukaryotic ligand was unknown (18). Currently in France, 50 % of GAS elicited endometritis are associated with puerperal fever, abortion, *in vitro* fertilization or spontaneous abortion (our unpublished data, https://cnr-strep.fr/), all situations where stromal decidual cells line the endometrium. Thus, GAS elicited endometritis may be favored by GAS adhering to decidual cells, in addition to epithelial cervical or endometrial cells. The R28 deleted strain was hampered in its capacity to adhere to human decidual stromal cells (hDSCs) (Fig. 2). That the mutant strain still adheres can be explained by the number of adhesins displayed by GAS strains (36–38), the deletion of a single one being insufficient for a total loss of adhesion capacity, as shown for example for Epf (39) and C5a peptidase (40). $R28_{Nt}$ binds to hDSCs, endometrial epithelial cells and cervical epithelial cells; it also promotes the adhesion of beads or heterologous bacteria to endometrial epithelial cells (Fig. 2). These data altogether confirm the role of R28 as an adhesin and extends its role to other cells potentially involved during endometritis.

R28 belongs to the Alp family of proteins, shared with GBS, which includes ACP, Rib and Alp2. The ACP N-terminal domain, but not that of Rib, also bound endometrial and cervical epithelial cells indicating that this property is not limited to R28 but not shared by all the members of the Alp family either (Fig. 3). Noteworthy, the ACP N-terminal domain shows a higher sequence identity to R28 N-terminal sequence than does Rib N-terminal domain, as well as a structural

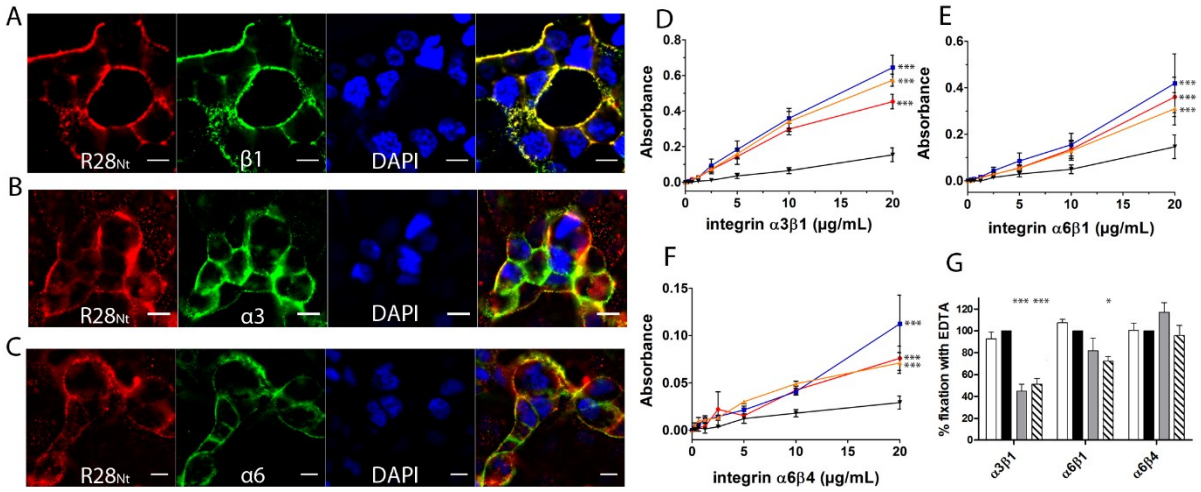

Figure 5. $R28_{Nt}$ and its subdomains interact with integrins α3β1, α6β1 and α6β4. *A-C* Immunostaining of $R28_{Nt}$ and different integrin monomers on HEC-1-A cells: *A*, β1; *B*, α3; *C*, α6. $R28_{Nt}$, red; the specified integrin monomer, green; DAPI, blue; the right-hand side image, merge. Scale bar corresponds to 5 µm. *D-F* Assessment of integrin binding: *D*, α3β1; *E*, α6β1; *F*, α6β4 binding to $R28_{Nt}$, red; R28-N1, blue; R28-N2, orange; BSA, black, by ELISA. Error bars correspond to SEM of three to five independent experiments. Two-way-ANOVA at 20 µg/mL with Bonferroni post-tests against BSA. *G,* role of divalent cations in the binding of integrins to $R28_{Nt}$, PBS, clear column; PBS + EDTA, dark column; PBS + Mn^{2+} , grey column; PBS + Ca^{2+}, hatched column. One-Way ANOVA of four independent experiments. *, $p<0.05$; ***, $p<0.001$.

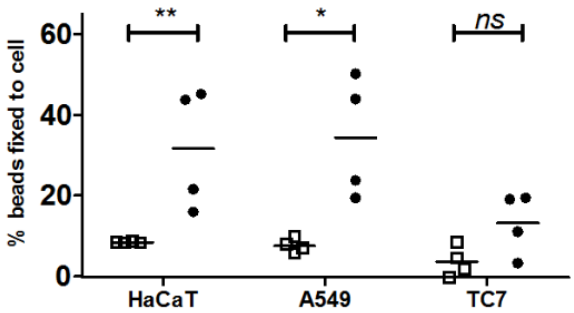

Figure 6. $R28_{Nt}$ increases binding to different cell lines. Binding of $R28_{Nt}$-, black circles; BSA-coated, empty squares, fluorescent beads to different epithelial cell types: HaCaT (keratinocytes), A549 (pulmonary) and TC7 (intestine). Four independent experiments performed in duplicates. Two-Way ANOVA. *, $p<0.05$ **; $p<0.005$; ns, not significant.

identity (18, 24); this could account for ACP but not Rib sharing the binding property. Furthermore, $R28_{Nt}$ and Alp2 N-terminal domain are near identical (20, 21), consequently this binding property could be extended to Alp2. Fifteen to 30% of women vaginal tract is colonized by GBS and all GBS strains present the gene encoding for one member of the Alp family (15, 41); most of these proteins are likely involved in GBS colonization.

The GBS proteins ACP and Alp3 (*i.e.* R28) bind glycosaminoglycan (26). Analysis using a set of constructions with different ACP domains suggested that a site beginning in the N-terminal region of ACP and extending into the repeat region is responsible for this binding (26, 27). Here, the $R28_{Nt}$ and ACP_{Nt} peptides we used were devoid of repeats region sequences, suggesting that the binding we observed was not that to glycosaminoglycan; this was confirmed by the absence of heparinase treatment effect on the $R28_{Nt}$ – HEC-1-A binding. This suggested that other receptors than glycosaminoglycan are involved in the R28-endometrial or -cervical cell binding.

In this study, pull-down experiments on whole cells indicate that $R28_{Nt}$ binds other integrins namely α3β1, α6β1 and α6β4 (Fig. 5). Furthermore, we demonstrate by protein-protein binding experiments that the binding is direct. Among already described GAS direct interactions, Scl1 interacts with integrins α11β1 and α2β1 (42, 43), SDH with urokinase plasminogen activator receptor (44), M6 and M1 with CD46 (45, 46) and hyaluronic acid capsule with CD44 (47). The direct binding of GAS to α3β1, α6β1 and α6β4 had never been described thus far. Cervical cells, endometrial epithelial cells and decidual cells all express, among others, the integrin subunits α3, α6, β1 and β4 (32, 48–50).The $R28_{Nt}$ interaction with integrins α3β1, α6β1 and α6β4 could therefore account for the binding of $R28_{Nt}$ to all these endometritis-related cells (Fig 2).

The α3β1, α6β1, and α6β4 may not be the sole $R28_{Nt}$ ligands. Indeed, we did not assay the direct interaction of $R28_{Nt}$ with all pulled-down proteins and the other candidates may interact indirectly, *via* the pulled-down integrins, or directly with $R28_{Nt}$. Other cell surface proteins could also interact with $R28_{Nt}$ and be missed in our screen since our co-immunoprecipitation experiments were carried out with HEC-1A cells; different cell types express different proteins, including different integrins. Further analyses may thus highlight other eukaryotic R28 receptors. Similarly, ACP binds α1β1 but may also bind other integrins (28) and among them α3β1, α6β1 or α6β4.

Our data suggesting that both R28-N1 and R28-N2 shared a receptor, we tested whether they both interacted directly with the three integrins, which they did (Fig. 5), supporting our competitive assay conclusion. To further characterize the interactions between $R28_{Nt}$ and integrins we assayed the influence of Mn^{2+} and Ca^{2+} on them. Our data suggested that at the molecular level the interactions between $R28_{Nt}$ and the various integrins are different and that cations induced conformational changes to α3β1 and α6β1, but not of α6β4, which interferes with $R28_{Nt}$ binding. Most integrin ligands require cations for their interactions, but, although not often described, cation independent interactions of integrins with proteins from pathogens have already been reported, for example between the αVβ5 integrin and the HIV Tat protein (51). Defining the R28 amino-acid residues involved in the interaction would provide clues regarding the molecular mechanism taking place. Establishing the structure of R28-N2 would shed light on the sequences potentially interacting with the various receptors and provide a framework for mutational analysis. ACP binds α1β1 through a KTD sequence located in a β-sandwich subdomain (24, 28); however, R28 harbors no KTD or related sequence and interacts with other integrins, it will be interesting to determine whether the same β-sandwich subdomain is nevertheless involved (Fig. 1A).

The absence of significant competition between ACP and R28-N2 could be related to the strong difference of affinity between R28-N2 and ACP for HEC-1-A binding. Also, the absence of competition between R28-N1 and ACP-bound beads could be a consequence of ACP and R28-N1 presenting distinct affinity for some receptors or ACP recognizing additional receptors.

R28 promotes direct binding to the cells. However, this is not the sole binding involved in the adhesion of GAS with hDSC as indicated by the fact that the mutant strain still adheres to the cells. GAS adhesion is a two-step process, a first more labile adhesion involving lipoteichoic acid followed by a second more specific and stronger adhesion involving adhesins (52). Many adhesins have been described and the interactions with epithelial cell surface receptors thoroughly

studied (reviewed 32, 47, 48). Most interactions are indirect, proteins of the extracellular matrix, such as fibronectin, form bridges with the host cells. GAS possesses numerous fibronectin-binding proteins, including the M protein that is variable among the *emm*-types and may not play always the exact same role. Also, M1 binds directly CD46 (46) and indirectly α5β1, *via* fibronectin. The dual interaction is required for efficient epithelial cell invasion (46). The interaction between R28 and integrins could potentiate other association(s) mediated by independent adhesins. More experimental support is needed to draw conclusions.

The involvement of R28 in the association between *emm28* and endometritis has been suggested (18) and our data support this suggestion. However, other factors may be involved in this association. They may be adhesins restricted to few genotypes, including *emm28*, such as Mrp28, M28, Enn28, FCT type 4 pilus proteins (Sfb1, Cpa) (53), Epf (39), and some RD2, a *emm28*-specific genomic region, encoded surface proteins (13). The unique conjunction of these in *emm28* strains may confer an advantage for binding to the endometrium. RD2 also encodes other proteins of unknown function as well as a regulator and they may be involved in diverse colonization or invasion steps of the endometrial or cervical tissue. The adhesion, colonization and invasion capacities of single or multiple mutant strains should be assessed.

R28 promotes adhesion to female genital tract cells including epithelial cells and it was suggested that it may contribute to GAS adhesion to different types of epithelial cells (18). We have shown that, indeed, it also promotes adhesion to endometrial epithelial cells and decidual cells, but also to pulmonary epithelial cells and to keratinocytes, natural targets for GAS invasive infections (Fig. 6). HaCaT and A549 both express α3, α6, β4 and β1 at their surface (54, 55) and that $R28_{Nt}$ interacts with the different corresponding dimers probably accounts for the increase of binding of $R28_{Nt}$ beads to these cell lines (Fig. 6). TC7 cells also express these integrins, but their localization is mainly basolateral (35); this could explain the lower binding of $R28_{Nt}$ to the apical side of TC7 cells compared to the other cell lines. This ability of $R28_{Nt}$ to promote adhesion to several cell lines, at least partially through integrins, suggests that expressing R28 is an advantage for *emm28* strains that is not limited to endometritis. This may represent a physiological explanation for the fact that *emm28* genotype is a prevalent genotype, being the first to third most encountered *emm*-type in invasive infections, in most European countries (9, 10, https://cnr-strep.fr/). Other *emm28* specific virulence factors could also participate in the prevalence and warrant further study.

In conclusion, through direct interaction with integrins, R28 supports *emm28* strains elicited endometritis and also contributes to the prevalence of this genotype.

Experimental procedure:

Bacterial strains and growth conditions

The strains used in this study are described in Table S1. The M28PF1 strain is a clinical isolate responsible for an endometritis (French National Reference Center (CNR) for Streptococci, https://cnr-strep.fr/) that was selected on phenotypic and genotypic bases from a collection of 50 *emm28* independent clinical isolates (56). GAS strains were grown under static condition at 37°C in Todd Hewitt medium supplemented with 0.2% Yeast Extract (THY) or on THY agar (THYA) plates. *L. lactis* strains were grown in Todd Hewitt (TH) medium, supplemented with 10 µg/mL erythromycin when necessary, at 30 °C without agitation or on TH agar (THA) plates. *Escherichia coli* strains were cultured in Tryptic Soy medium at 37 °C with agitation with, when necessary, added antibiotics at the following concentrations: erythromycin 150 µg/ml, ticarcillin, 100 µg/ml.

Genetic constructions and generation of the ΔR28 mutant

The DNA fragments encoding the proteins without signal peptide of $R28_{Nt}$, R28-N1, R28-N2, ACP and Rib_{Nt+2R} (nt 169-1272, nt 169-688, nt 688-1272, nt 154-681 and nt 171-1188, respectively) were amplified and cloned into pET2818 as described in (57). All fragments were amplified by PCR using genomic DNA from M28PF1, except for the fragments encoding ACP and Rib_{Nt+2R}, which were amplified from GBS strains A909 and BM110, respectively; the primers used are described in Table S2. The plasmid pOri_$R28_{Nt}$, contains the promoter of *hvgA* deleted of the *covR* consensus boxes, the signal peptide of the GBS BM110 surface protein HvgA, and the LPXTG anchor signal of HvgA subcloned from pAT28-covSP +SPA (57), with the addition of the sequence encoding $R28_{Nt}$ subcloned from pET2818_$R28_{Nt}$. The different

plasmids constructed and used during this study are described in Table S1.

The ΔR28 strain corresponds to an in-frame deletion mutant of the gene *Spy1336* encoding the R28 protein and was obtained by homologous recombination of the plasmid pG1-R28 following the same protocol as previously (57). The strain was entirely sequenced as described previously (56). No other significant mutation was found compared to the parent strain M28PF1 except for the gene deletion (56). The primers used for the generation of the plasmid pG1-R28 are described in Table S2. *L. lactis* strain was transformed by electroporation (58) with the empty vector (CCH2022) or pOri_R28$_{Nt}$ (CCH2023).

Protein production and purification

Peptide expressions were performed with the corresponding derived pET2818 plasmids (Table S1) and purification as described in (57), except for the gel filtration step which we did not perform. Peptides purity were confirmed using a 12% SDS-PAGE acrylamide gel and Coomassie Blue staining (Fig. S1C).

Antibodies

All animal experiments described in this study were conducted in accordance with guidelines of Paris Descartes University, in compliance with the European animal welfare regulation (http://ec.europa.eu/environment/chemicals/lab_animals/home_en.html) and were approved by the Institut Cochin University Paris Descartes animal care and use committee (n° 12–145). Mouse anti-R28$_{Nt}$ anti-serum was produced as follows. BalbC 6 weeks mice (Janvier laboratory) were subcutaneously injected with 100 µL of 50 µg/mL R28$_{Nt}$ solution in PBS+aluminium adjuvant. Two and four weeks after initial injection, mice were injected with 100 µL of a 25 µg/mL solution. The antibody purity and titer were determined a week after the last injection and assessed by western blot experiments. The purified R28-N1 or R28-N2 were injected into rabbits to produce polyclonal antibodies (Covalab). The following antibodies were used throughout the study: anti α3 integrin (P1B5; DSHB), rabbit anti α6 integrin (Novus) for ELISA, mouse anti α6 integrin (P5G10; DSHB) for immunofluorescence, mouse anti β1 integrin (P5D2; DSHB) and rat anti β1 integrin (AIIB2, DSHB).

Bacterial cell wall extracts

Overnight cultures of *L. lactis* were diluted 1/100 in 50 mL of TH broth and cultivated to DO = 0.5. Bacteria were centrifuged 10 min at 5000 rpm at 4°C and the pellet was washed once in wash buffer (Cold PBS 1X + EDTA 10 mM + PMSF 1 mM). Bacteria were centrifuged and the pellet was resuspended in 250 µL of mutanolysin buffer (Tri-HCL 20 mM pH 7.5 + Sucrose 1 M + EDTA 10 mM + PMSF 1 mM + protease inhibitor cocktail 1X (Roche) + mutanolysin 200 u/mL (Sigma)) and incubated for 90 minutes at 37°C. The protoplast suspension is then centrifuged 15 minutes at 10 000 rpm and 30 µL of the supernatant containing the cell wall extract is loaded on an acrylamide gel.

Cell culture

HEC-1-A (ATCC® HTB-112™) and ME-180 (ATCC® HTB-33™) cells were cultured as recommended, in McCoy's 5A medium (GibCo) supplemented with 10% fetal bovine serum (FBS) at 37 °C, 5% CO_2. A549 (ATCC® CCL-185™), HaCaT (AddexBio T0020001) and Caco/TC7 cells (CVCL_0233), were cultivated as recommended, in RPMI + 10 % FBS.

Isolation and culture of human decidual stromal cells (hDSC)

Decidual stromal cells were isolated from decidua parietalis, obtained from fetal membranes of non laboring women after a normal term (> 37 weeks of gestation) singleton-pregnancy delivered by elective caesarean section. The study of the human fetal membranes was approved by the local ethics committee (Comité de Protection des Personnes Ile de France XI, n° 11018, 03/03/2011) and informed consent was obtained from all donors. Furthermore, the study abides to the Declaration of Helsinki principles. Briefly, fetal membranes were dissected from placenta under sterile conditions and decidua attached to chorion leaf was peeled off amnion and placed in PBS. After the removal of blood clots, choriodecidua was cut in small pieces and digested with 0.2% collagenase B (Roche Diagnostics, Mannheim, Germany) in DMEM-F12 (Invitrogen, Cergy-Pontoise, France) at 37°C for 1h30. After the addition of DMEM-F12 containing 5% FCS and 100 µM EDTA, the cell suspension was filtered through a 100 µm nylon gauze and centrifuged at 400 g for 10 min. The cell pellet, resuspended in complete medium (DMEM-F12 containing 5% FCS, 100 IU/ml penicillin (Invitrogen), 100 µg/ml streptomycin

(Invitrogen)), were plated at a density of 10^5 cells/cm^2 and cultured in complete medium at 37°C in 5% CO_2 and 95% air in 75cm² flasks overnight. Medium was then renewed after several PBS washes. Cells were harvested with trypsin/EDTA when the cells were 90% confluent. The hDSCs were expanded further to passage 2 to 4 and thereafter, used in the experiments. hDSCs from at least two different women were used.

Adhesion of bacteria to cells

GAS strains M28PF1 (WT) and ΔR28 were diluted from an overnight culture, grown to the exponential phase at an OD = 0.5 and diluted in RPMI without glutamine to obtain a multiplicity of infection (MOI) of one. Confluent hDSCs in 24 well-plates were washed three times, bacterial solution was added and plates were centrifuged 5 min at 1000 rpm to synchronize bacterial adhesion. After 1 h of incubation at 4 °C, cells were washed three times with PBS and lysed with distilled water. Serial dilutions of cellular lysates were plated on THYA plates and the number of CFUs was determined after 24-48 hours growth at 37 ºC. Six independent experiments were performed in triplicates and ΔR28 values were normalized to WT adhesion for each independent experiment. Statistical analysis was performed using One-Sample T-test with Graph-Pad Prism 5.0.

For adhesion assay of *Lactococcus lactis* on HEC-1-A, cells were seeded 72 h prior to infection to reach confluence at 5-10 x 10^6 cells/well in 24-well plates. The protocols for the *L. lactis* CCH2022 and CCH2023 bacterial preparation and adhesion to cells was the same as above. For all experiments, three independent assays in triplicate were carried out for each infection. Paired T-test were performed with Graph-Pad Prism 5.0.

ELISA-based protein-cell interaction assay

The cell-protein binding assay protocol derives from Bolduc et *al.* 2007 (28). Briefly, cells are incubated with biotinylated proteins in PBS + BSA 1% for 1 hour at 4°C, then washed and bound proteins are revealed by streptavidin-HRP (GE Healthcare) and subsequent O-phenyldiamine (Sigma) revelation. Number of moles of biotin per mole of protein was evaluated using an HABA kit (Lifetechnologies): the ratio of biotin molecule per peptide molecule was around 5, except for Rib_{Nt+2R} for which it reached 9. Therefore, the fluorescence values obtained for Rib_{Nt+2R} were divided by 2 for comparison sake. Experiments were performed four times independently, except for Rib_{Nt+2R} performed three times. Statistical analysis was performed after non-linear fitting using a second order polynomial quadratic model and comparison of the extra sum of squares F-test of the best fit values using GraphPad Prism 5.0. Curves are fitted with an equation: Absorbance = B1 * concentration+ B2* (concentration)². Since this equation did not fit the BSA curve, statistical analysis to BSA were performed with Two-Way ANOVA with Bonferroni post-tests at maximum binding.

Beads fixation to cells

Fluosphere (Invitrogen, yellow green, 1 µm) were coupled with the different peptides following the manufacturer's recommendations. Correct coupling was confirmed by cytometric analysis with appropriate antisera. Indicated confluent cells in dark 96 well plates (Nunc, Lifetechnologies) were washed three times with cold PBS supplemented with 1 mM Ca^{2+} and 1 mM Mg^{2+} (PBS++). Beads were diluted to a concentration of 10^8 beads/mL in cold PBS++ and 150 µL of beads solution was added to cells and incubated 1 h at 4 °C. Cells were washed three times in PBS++, fixed 15 min at room temperature in paraformaldehyde 1%, quenched with 50 mM NH_4Cl. Fluorescence of the inoculum solutions, cells and cells incubated with beads were measured with a TECAN fluorescent plate reader with a GFP filter. Fluorescence of adherent beads corresponds to the fluorescence of the total well subtracted by the autofluoresence of a well containing cells only.

For competition assays, prior to beads adhesion, cells were incubated with 20 µM of specified peptide in PBS++ for 1 h at 4 °C; beads were then added and the experiments performed as described above. For antibody competition, beads were incubated with 10 µg/mL of purified anti-R28-N1 and anti-R28-N2 rabbit antibodies for 1 h at 4°C prior to incubation with cells. Experiments were performed at least three times in duplicates. Statistical analyses were performed with Two-Way ANOVA.

Flow cytometry analysis of protein binding to eukaryotic cells after different treatments

Confluent 72 h HEC-1-A cells were dissociated with cell dissociation buffer (Lifetechnologies) and treated with $NaIO_4$ (Sigma), pronase (Lifetechnologies), trypsin (Worthington Biochemical Corporation),

phospholipase A_2 (Sigma) or heparinase I (NEB) at the specified concentrations and as described by Gallotta et *al.* 2014 (33). Cells were then incubated with 20 µM soluble $R28_{Nt}$, R28-N1 or R28-N2 in PBS- BSA 0,5% and stained with mouse antiserum, and secondary anti-mouse PE coupled antibody. Fluorescence of cells was measured in an Accuri C6 BD cytometer. 100% staining was considered with cells untreated (Control). Unspecific labelling of cells by mouse antiserum and secondary antibodies was measured on untreated cells that were not incubated with the peptides, but underwent the same labeling protocol (without peptide condition). Experiments were performed at least three times independently. Two-Way ANOVA analysis was performed with GraphPad Prism 5.

Protein sequence comparison

These comparisons were carried out using the BlastP algorithm (https://blast.ncbi.nlm.nih.gov/Blast.cgi?PAGE=Proteins&PROGRAM=blastp&BLAST_PROGRAMS=blastp&PAGE_TYPE=BlastSearch&BLAST_SPEC=blast2seq&DATABASE=n/a&QUERY=&SUBJECTS=)

In silico *protein structure prediction*

Peptide structure was made using the Phyre software (http://www.sbg.bio.ic.ac.uk/phyre2/html/page.cgi?id=index).

Co-immunoprecipitation of cross-linked $R28_{Nt}$ receptors

HEC-1-A cells grown to confluence in T25 flask were washed three times with cold PBS++. A 6 mL solution of cold PBS++, 1% BSA, with or without (control) 20 µM $R28_{Nt}$ was added and incubation pursued for 1 h on ice. Cells were washed three times in cold PBS++ and 10 mL of 1 mM DTSSP (Thermofisher) was added for 2 h on ice. After one wash with PBS++, cross-linking was blocked with 10 mL of 50 mM Tris pH 7.5 for 10 min on ice. An equimolar mix of rabbit polyclonal anti R28-N1 and R28-N2 antibodies (1 mg/mL total, 1.7 mL per flask) was added to two freshly washed HEC-1-A T25 flask for 10 min to adsorb unspecific cell binding antibodies. Pre-adsorbed antibodies (1.5 mL) were added to each flask and incubated for 1 h at 4 °C. Unbound antibodies were removed by three washes with PBS++ and cells were lysed for 1 h at 4 °C with 1.5 mL of lysis buffer (PBS, protease inhibitor cocktail 1X (Thermofisher), phenylmethylsulfonyl fluoride 1 mM (Sigma), 1% SurfactAmp Triton X100 (Thermofisher)). Lysates were centrifuged at 15 000 g for 15 min at 4 °C and supernatants were incubated with 100 µL magnetic protein A beads (Pierce) for 1 h at 20 °C. Beads were then washed six times with 1.5 mL PBS, 500 mM NaCl, Triton 1% and complexes were eluted in Laemmli Buffer in disulfide-bonds preservation conditions (60mM Tris pH6.8, 1% SDS) at 95°C for 5 minutes. Gels were run in duplicate; one gel was used for western blotting with 15 % of the eluates, revealed with mouse anti-$R28_{Nt}$ antiserum to reveal cross-linked complexes and the other one for their identification by mass spectrometry. The western blotting indicated that $R28_{Nt}$ complexes were found above 170 kDa.

Short migration SDS-PAGE, protein trapping and peptide extraction

Eighty-five % of the eluate were loaded in the same condition as above for a two centimeters-migration, then stained with colloidal Coomassie blue (Quick Coomassie Stain from Clinisciences). Stained gels allowed visualization of protein abundance and molecular weight distribution. Protein-containing gel lanes from the two conditions (with the bait R28 and in its absence, control condition) were excised above the 170 kDa MW marker (Lifetechnologies Pageruler prestained protein ladder). The polyacrylamide gel constitutes a matrix where successive protein treatments were performed: salt, buffer and detergent removal by successive washes of 100 mM NH_4HCO_3 (or ABC)/Acetonitrile 50%, disulfide bonds removal by cystein reduction in ABC + 10 mM DTT at 56 °C for 30 minutes; free thiols protection by alkylation in ABC + 55 mM chloroacetamide for 30 minutes at room temperature and overnight digestion with trypsin. Peptides were then extracted using washes of 5% formic acid intercalated with gel shrinkages in 50% acetonitrile (ACN). All washes were pooled and evaporated before analysis.

C18 liquid nanochromatography and mass spectrometry

Mass spectrometry analyses were performed at the 3P5 proteomics facility of the University Paris Descartes using an U3000 RSLC nano-LC-system hyphenated to an Orbitrap-fusion mass spectrometer, all from Thermo Fisher Scientific. Peptides were solubilized in 7 µl of 0.1% TFA containing 10% ACN. They were loaded, concentrated and washed for 3 min on a

C18 reverse-phase precolumn (3 µm particle size, 100 Å pore size, 75 µm inner diameter, 2 cm length, Thermo Fischer Scientific). Peptides were separated on a C18 reverse-phase resin (2 µm particle size, 100 Å pore size, 75 µm inner diameter, 25 cm length from Thermofisher scientific) with a 35 minutes binary gradient starting from 99% of solvent A containing 0.1% formic acid in H_2O and ending in 40% of solvent B containing 80% acetonitrile, 0.085% formic acid in H_2O. The mass spectrometer acquired data throughout the elution process and operated in a data-dependent scheme with full MS scans acquired with the Orbitrap, followed by as many MS/MS ion trap CID spectra 5 seconds can fit (data-dependent acquisition with top speed mode: 5 seconds cycle) using the following settings: full MS automatic gain control (AGC): $2.10e^5$, maximum ion injection time (MIIT): 60 ms, resolution: $6.10e^4$, m/z range 350-1500 and for MS/MS; isolation width: 1.6 Th, minimum signal threshold: 5000, AGC $2.10e^4$, MIIT: 100 ms, peptides with undefined charge state or charge state of 1 were excluded from fragmentation, dynamic exclusion time: 30 s.

Identifications (protein hits) and quantifications were performed by comparison of experimental peak lists with a database of theoretical sequences using MaxQuant version 1.6.1.0. (59). The databases used were the human sequences from the curated Uniprot database (release june 2018) and a list of in-house contaminant sequences. Carbamidomethylation of cysteins was set as constant modification while acetylation of protein N-terminus and oxidation of methionines were set as variable modifications. False discovery rate (FDR) was kept below 1% on both peptides and proteins. The "match between runs" option was not allowed. For analysis, results from MaxQuant were imported into the Perseus software version 1.6.1.1. (60). Reverse and contaminant proteins (human keratins and non-human proteins) were excluded from analysis. Proteins of interest were selected based on reported intensity in 3 over 3 replicates for each group. All hits are presented in the supplementary file.

Selection of positive hits

The enrichment is defined as the ratio of raw intensity of the co-immunoprecipitation identified proteins in the $R28_{Nt}$ bait conditions compared to the control condition. Hits with a ratio above 1 and/or no peptide found in the control condition for all three independent experiments performed were considered as specifically enriched in the presence of R28. From this list, only surface exposed proteins are shown in Table 1.

Immunolabelling of bound $R28_{Nt}$ and coated fluospheres on HEC-1-A

Seventy-two hours after seeding on glass coverslips in 24 well plates, confluent HEC-1-A cells were washed three times in cold PBS++. A 10 µM solution of $R28_{Nt}$ in PBS++, 1% BSA was added to the cells for 1 h at 4 °C. Cells were washed three times in cold PBS++ and fixed 15 min at 20 °C with paraformaldehyde 1%. Cells were quenched with ammonium chloride 50 mM and blocked for 30 min with PBS-BSA 3%. Cells were incubated with primary antibodies for 1 h at 20 °C in PBS-BSA 1%. Cells were washed and incubated with secondary antibodies and DAPI at 1/5 000 for 1 h at 20 °C. Coverslips were mounted on slides with Mowiol, imaged on a Leica DMI6000 and images were analyzed with ImageJ. For the observation of bound coated fluospheres, 10^8 coated beads in PBS++ were added to the cells and treated as above. Beads did not require labelling since they are intrinsically fluorescent.

ELISA

To evaluate integrin binding to immobilized $R28_{Nt}$ or its sub-domains R28-N1 and R28-N2, ELISA were performed essentially as described in Six et *al.* 2015 (57). Proteins were coated at 5 µg/mL overnight. Fifty µL of integrins (human recombinant extracellular domain, tested for their ability to interact with known ligands, R&D) were incubated 2 h at 37 °C at the specified concentrations diluted in PBS-BSA 1%. Rat anti-β1 (AIIB2, DSHB) and rabbit anti-α6 (R&D) antibodies were used at a 1/200 dilution. Experiments were performed at least three times. Statistical analyses were performed as described above for the ELISA based protein-cell interaction assay.

The importance of divalent cations for the interaction between $R28_{Nt}$ and integrins was tested by ELISA with the same coating protocol as above with fifty µL at 10 µg/mL of integrins added to the wells. All solutions for the assay were made in PBS, PBS + 10 mM EDTA, PBS + 1 mM Mn^{2+} and PBS + 1 mM Ca^{2+}, as specified. Detection and revelation were performed as above. Values were normalized on the binding to the integrins in the presence of EDTA. One-Way ANOVA was performed to compare the four independent experiments.

Acknowledgements: We thank Wassim El Nemer, Julie Guignot, and Cecile Arrieumerlou for helpful discussions and Philippe Glaser for sequencing and providing the relevant contigs of the ΔR28 strain. We thank Cédric Broussard (LC-MS supervision and in-gel protein digestion), Evangeline Bennana (proteomics data collection, analysis and reporting), Marjorie Leduc (LIMS management), François Guillonneau, Philippe Chafey and Patrick Mayeux (proteomics expertise and experimental design) from the 3P5 proteomics facility of the Université Paris Descartes, Sorbonne Paris Cité and the Imag'IC facility, both at the Cochin Institute. We thank the Margottin-Pique team for access to the TECAN plate reader. This work was supported by Université Paris Descartes (AW contract n° KL2UD) the Département Hospitalo-Universitaire Risks in Pregnancy (PRIDE 2014, AF & CM), INSERM, CNRS, Université Paris Descartes. The Orbitrap Fusion mass spectrometer was acquired with funds from the FEDER through the "Operational Programme for Competitiveness Factors and employment 2007-2013" and from the "Canceropole Ile de France".

Conflict of interest: The authors declare none

References

1. Bisno, A. L., Brito, M. O., and Collins, C. M. (2003) Molecular basis of group A streptococcal virulence. Lancet Infect. Dis. 3, 191–200
2. Tart, A. H., Walker, M. J., and Musser, J. M. (2007) New understanding of the group A Streptococcus pathogenesis cycle. Trends Microbiol. 15, 318–25
3. Cunningham, M. W. (2000) Pathogenesis of group A streptococcal infections. Clin Microbiol Rev. 13, 470–511
4. Carapetis, J. R., Steer, A. C., Mulholland, E. K., and Weber, M. (2005) The global burden of group A streptococcal diseases. Lancet Infect. Dis. 5, 685–94
5. Beall, B., Facklam, R., and Thompson, T. (1995) Sequencing emm -specific polymerase chain reaction products for routine and accurate typing of group A Streptococci. J.Clin.Microbiol. 34, 953–958
6. Ferretti, J. J., Stevens, D. L., and Fischetti, V. A. (2016) Streptococcus pyogenes Basic Biology to Clinical Manifestations
7. Bessen, D. E. (2016) Tissue tropisms in group A Streptococcus: what virulence factors distinguish pharyngitis from impetigo strains? Curr. Opin. Infect. Dis. 29, 295–303
8. Beres, S. B., and Musser, J. M. (2007) Contribution of exogenous genetic elements to the group A Streptococcus metagenome. PLoS One. 10.1371/journal.pone.0000800
9. Gherardi, G., Vitali, L. A., and Creti, R. (2018) Prevalent emm Types among Invasive GAS in Europe and North America since Year 2000. Front. Public Heal. 6, 59
10. Plainvert, C., Doloy, A., Loubinoux, J., Lepoutre, A., Collobert, G., Touak, G., Trieu-Cuot, P., Bouvet, A., and Poyart, C. (2012) Invasive group A streptococcal infections in adults, France (2006-2010). Clin. Microbiol. Infect. 18, 702–10
11. Green, N. M., Beres, S. B., Graviss, E. A., Allison, J. E., McGeer, A. J., Vuopio-Varkila, J., LeFebvre, R. B., and Musser, J. M. (2005) Genetic diversity among type emm28 group A Streptococcus strains causing invasive infections and pharyngitis. J. Clin. Microbiol. 43, 4083–91
12. Colman, G., Tanna, A., Efstratiou, A., and Gaworzewska, E. T. (1993) The serotypes of Streptococcus pyogenes present in Britain during 1980-1990 and their association with disease. J. Med. Microbiol. 39, 165–178
13. Green, N. M., Zhang, S., Porcella, S. F., Nagiec, M. J., Barbian, K. D., Beres, S. B., LeFebvre, R. B., and Musser, J. M. (2005) Genome sequence of a serotype M28 strain of group a streptococcus: potential new insights into puerperal sepsis and bacterial disease specificity. J. Infect. Dis. 192, 760–70
14. Sitkiewicz, I., Green, N. M., Guo, N., Mereghetti, L., and Musser, J. M. (2011) Lateral gene transfer of streptococcal ICE element RD2 (region of difference 2) encoding secreted proteins. BMC Microbiol. 11, 65
15. Baker, C. J., Goroff, D. K., Alpert, S., Crockett, V. A., Zinner, S. H., Evrard, J. R., Rosner, B., and McCormack, W. M. (1977) Vaginal colonization with group B streptococcus: a study in college women. J. Infect. Dis. 135, 392–7
16. Nobbs, A. H., Lamont, R. J., and Jenkinson, H. F. (2009) Streptococcus adherence and colonization. Microbiol. Mol. Biol. Rev. 73, 407–50, Table of Contents
17. Courtney, H. S., Hasty, D. L., and Dale, J. B. (2002) Molecular mechanisms of adhesion, colonization, and invasion of group A streptococci. Ann. Med. 34, 77–87
18. Stålhammar-Carlemalm, M., Areschoug, T., Larsson, C., and Lindahl, G. (1999) The R28 protein of Streptococcus pyogenes is related to several group B streptococcal surface proteins, confers protective immunity and promotes binding to human epithelial cells. Mol. Microbiol. 33, 208–19
19. Wästfelt, M., Stålhammar-Carlemalm, M., Delisse, A. M., Cabezon, T., and Lindahl, G. (1996) Identification of a family of Streptococcal surface proteins with extremely repetitive structure. J. Biol. Chem. 271, 18892–18897
20. Lachenauer, C. S., Creti, R., Michel, J. L., and Madoff, L. C. (2000) Mosaicism in the alpha-like protein genes of group B streptococci. Proc. Natl. Acad. Sci. U. S. A. 97, 9630–9635
21. Lindahl, G., Stalhammer-Carlemalm, M., and Areschoug, T. (2005) Surface Proteins of Streptococcus agalactiae and Related Proteins in Other Bacterial Pathogens. Clin. Microbiol. Rev. 18, 102–127
22. Callebaut, I., Gilgès, D., Vigon, I., and Mornon, J. P. (2000) HYR, an extracellular module involved in cellular adhesion and related to the immunoglobulin-like fold. Protein Sci. 9, 1382–90
23. Glaser, P., Rusniok, C., Buchrieser, C., Chevalier, F., Frangeul, L., Msadek, T., Zouine, M., Couvé, E.,

Lalioui, L., Poyart, C., Trieu-Cuot, P., and Kunst, F. (2002) Genome sequence of Streptococcus agalactiae, a pathogen causing invasive neonatal disease. Mol. Microbiol. 45, 1499–1513
24. Aupérin, T. C., Bolduc, G. R., Baron, M. J., Heroux, A., Filman, D. J., Madoff, L. C., and Hogle, J. M. (2005) Crystal structure of the N-terminal domain of the group B streptococcus alpha C protein. J. Biol. Chem. 280, 18245–52
25. Stâlhammar-Carlemalm, M., Areschoug, T., Larsson, C., and Lindahl, G. (2000) Cross-protection between group A and group B streptococci due to cross-reacting surface proteins. J. Infect. Dis. 182, 142–149
26. Baron, M. J., Bolduc, G. R., Goldberg, M. B., Aupérin, T. C., and Madoff, L. C. (2004) Alpha C protein of group B Streptococcus binds host cell surface glycosaminoglycan and enters cells by an actin-dependent mechanism. J. Biol. Chem. 279, 24714–24723
27. Baron, M. J., Filman, D. J., Prophete, G. A., Hogle, J. M., and Madoff, L. C. (2007) Identification of a glycosaminoglycan binding region of the alpha C protein that mediates entry of group B Streptococci into host cells. J. Biol. Chem. 282, 10526–10536
28. Bolduc, G. R., and Madoff, L. C. (2007) The group B streptococcal alpha C protein binds α1β1-integrin through a novel KTD motif that promotes internalization of GBS within human epithelial cells. Microbiology. 153, 4039–4049
29. Bolduc, G. R., Baron, M. J., Gravekamp, C., Lachenauer, C. S., and Madoff, L. C. (2002) The alpha C protein mediates internalization of group B Streptococcus within human cervical epithelial cells. Cell Microbiol. 4, 751–758
30. Chapot-Chartier, M. P., Vinogradov, E., Sadovskaya, I., Andre, G., Mistou, M. Y., Trieu-Cuot, P., Furlan, S., Bidnenko, E., Courtin, P., Péchoux, C., Hols, P., Dufre, Y. F., and Kulakauskas, S. (2010) Cell surface of Lactococcus lactis is covered by a protective polysaccharide pellicle. J. Biol. Chem. 285, 10464–10471
31. Areschoug, T., Carlsson, F., Stålhammar-Carlemalm, M., and Lindahl, G. (2004) Host-pathogen interactions in Streptococcus pyogenes infections, with special reference to puerperal fever and a comment on vaccine development. Vaccine. 22 Suppl 1, S9–S14
32. Castelbaum, A. J., Ying, L. E. I., Somkuti, S. G., Sun, J., Ilesanmi, A. O., and Lessey, B. a (1997) Characterization of Integrin Expression in a Well Differentiated Endometrial Adenocarcinoma Cell Line (Ishikawa). J. Clin. Endocrinol. Metab. 82, 136–142
33. Gallotta, M., Gancitano, G., Pietrocola, G., Mora, M., Pezzicoli, A., Tuscano, G., Chiarot, E., Nardi-Dei, V., Taddei, A. R., Rindi, S., Speziale, P., Soriani, M., Grandi, G., Margarit, I., and Bensi, G. (2014) SpyAD, a moonlighting protein of group A Streptococcus contributing to bacterial division and host cell adhesion. Infect. Immun. 82, 2890–2901
34. Luca-Harari, B., Darenberg, J., Neal, S., Siljander, T., Strakova, L., Tanna, A., Creti, R., Ekelund, K., Koliou, M., Tassios, P. T., and Van Der Linden, M. (2009) Clinical and Microbiological Characteristics of Severe Streptococcus pyogenes Disease in Europe. J. Clin. Microbiol. 47, 1155–1165
35. Hamzaoui, N., Kernéis, S., Caliot, E., and Pringault, E. (2004) Expression and distribution of [beta]1 integrins in in vitro-induced M cells: Implications for Yersinia adhesion to Peyer's patch epithelium. Cell. Microbiol. 6, 817–828
36. Nobbs, A. H., Jenkinson, H. F., and Everett, D. B. (2015) Generic determinants of Streptococcus colonization and infection. Infect. Genet. Evol. 33, 361–370
37. Brouwer, S., Barnett, T. C., Rivera-Hernandez, T., Rohde, M., and Walker, M. J. (2016) Streptococcus pyogenes adhesion and colonization. FEBS Lett. 10.1002/1873-3468.12254
38. Rohde, M., and Cleary, P. P. (2016) Adhesion and invasion of Streptococcus pyogenes into host cells and clinical relevance of intracellular streptococci. in Streptococcus pyogenes: Basic Biology to Clinical Manifestations, pp. 1–39
39. Linke, C., Siemens, N., Oehmcke, S., Radjainia, M., Law, R. H. P., Whisstock, J. C., Baker, E. N., and Kreikemeyer, B. (2012) The extracellular protein factor epf from Streptococcus pyogenes is a cell surface adhesin that binds to cells through an n-terminal domain containing a carbohydrate-binding module. J. Biol. Chem. 287, 38178–38189
40. Lynskey, N. N., Reglinski, M., Calay, D., Siggins, M. K., Mason, J. C., Botto, M., and Sriskandan, S. (2017) Multi-functional mechanisms of immune evasion by the streptococcal complement inhibitor C5a peptidase. PLoS Pathog. 10.1371/journal.ppat.1006493
41. Kong, F., Gowan, S., Martin, D., James, G., and Gilbert, G. L. (2002) Molecular Profiles of Group B

Streptococcal Surface Protein Antigen Genes: Relationship to Molecular Serotypes. J. Clin. Microbiol. 40, 620–626
42. Humtsoe, J. O., Kim, J. K., Xu, Y., Keene, D. R., Höök, M., Lukomski, S., and Wary, K. K. (2005) A streptococcal collagen-like protein interacts with the α2β1 integrin and induces intracellular signaling. J. Biol. Chem. 280, 13848–13857
43. Caswell, C. C., Barczyk, M., Keene, D. R., Lukomska, E., Gullberg, D. E., and Lukomski, S. (2008) Identification of the first prokaryotic collagen sequence motif that mediates binding to human collagen receptors, integrins α 2β1 and α11β1. J. Biol. Chem. 283, 36168–36175
44. Jin, H., Song, Y. P., Boel, G., Kochar, J., and Pancholi, V. (2005) Group A streptococcal surface GAPDH, SDH, recognizes uPAR/CD87 as its receptor on the human pharyngeal cell and mediates bacterial adherence to host cells. J. Mol. Biol. 350, 27–41
45. Okada, N., Liszewski, M. K., Atkinson, J. P., and Caparon, M. (1995) Membrane cofactor protein (CD46) is a keratinocyte receptor for the M protein of the group A streptococcus. Proc. Natl. Acad. Sci. U. S. A. 92, 2489–93
46. Rezcallah, M. S., Hodges, K., Gill, D. B., Atkinson, J. P., Wang, B., and Cleary, P. P. (2005) Engagement of CD46 and alpha5beta1 integrin by group A streptococci is required for efficient invasion of epithelial cells. Cell. Microbiol. 7, 645–53
47. Cywes, C., Stamenkovic, I., and Wessels, M. R. (2000) CD44 as a receptor for colonization of the pharynx by group A Streptococcus. J. Clin. Invest. 106, 995–1002
48. Werner, J., Decarlo, C. A., Escott, N., Zehbe, I., and Ulanova, M. (2012) Expression of integrins and Toll-like receptors in cervical cancer: Effect of infectious agents. Innate Immun. 18, 55–69
49. Lessey, B. a, Castelbaum, a J., Buck, C. a, Lei, Y., Yowell, C. W., and Sun, J. (1994) Further characterization of endometrial integrins during the menstrual cycle and in pregnancy. Fertil. Steril. 62, 497–506
50. Wadehra, M., Forbes, A., Pushkarna, N., Goodglick, L., Gordon, L. K., Williams, C. J., and Braun, J. (2005) Epithelial membrane protein-2 regulates surface expression of αvβ3 integrin in the endometrium. Dev. Biol. 287, 336–345
51. Vogel, B. E., Lee, S.-J., Hilderbrand, A., Craig, W., Pierschbacher, M. D., Wong-Staal, F., and Ruoslahti, E. (1993) A novel integrin specifically exemplified by binding avb5 integrin to the basic domain of the HIV tat protein anmd vitronectin. J.Cell Biol. 121, 461–468
52. Hasty, D. L., Ofek, I., Courtney, H. S., and Doyle, R. J. (1992) Multiple adhesins of streptococci. Infect. Immun. 60, 2147–2152
53. Köller, T., Manetti, A. G. O., Kreikemeyer, B., Lembke, C., Margarit, I., Grandi, G., and Podbielski, A. (2010) Typing of the pilus-protein-encoding FCT region and biofilm formation as novel parameters in epidemiological investigations of Streptococcus pyogenes isolates from various infection sites. J. Med. Microbiol. 59, 442–52
54. Abban, C. Y., and Meneses, P. I. (2010) Usage of heparan sulfate, integrins, and FAK in HPV16 infection. Virology. 403, 1–16
55. Falcioni, R., Cimino, L., Gentileschi, M. P., D'Agnano, I., Zupi, G., Kennel, S. J., and Sacchi, A. (1994) Expression of [beta]1, [beta]3, [beta]4, and [beta]5 Integrins by Human Lung Carcinoma Cells of Different Histotypes. Exp. Cell Res. 210, 113–122
56. Longo, M., De Jode, M., Plainvert, C., Weckel, A., Huaa, A., Château, A., Glaser, P., Poyart, C., and Fouet, A. (2015) Complete Genome Sequence of Streptococcus pyogenes emm28 strain M28PF1, responsible of a puerperal fever. Genome Announc.
57. Six, A., Bellais, S., Bouaboud, A., Fouet, A., Gabriel, C., Tazi, A., Dramsi, S., Trieu-Cuot, P., and Poyart, C. (2015) Srr2, a multifaceted adhesin expressed by ST-17 hypervirulent Group B Streptococcus involved in binding to both fibrinogen and plasminogen. Mol. Microbiol. 97, 1209–1222
58. Caparon, M. G., and Scott, J. R. (1991) Genetic Manipulation of Pathogenic Streptococci. Methods Enzymol. 204, 556–586
59. Cox, J., Hein, M. Y., Luber, C. A., Paron, I., Nagaraj, N., and Mann, M. (2014) Accurate Proteome-wide Label-free Quantification by Delayed Normalization and Maximal Peptide Ratio Extraction, Termed MaxLFQ. Mol. Cell. Proteomics. 13, 2513–2526
60. Tyanova, S., Temu, T., Sinitcyn, P., Carlson, A., Hein, M. Y., Geiger, T., Mann, M., and Cox, J. (2016) The Perseus computational platform for comprehensive analysis of (prote)omics data. Nat. Methods. 13, 731–740

FOOTNOTES

This work was supported by Paris Descartes University (AW contract n° KL2UD) the Département Hospitalo-Universitaire Risks in Pregnancy (PRIDE 2014, AF & CM), INSERM, CNRS, Université Paris Descartes.

The abbreviations used are: GAS, Group A Streptococcus; GBS, Group B Streptococcus.

Supporting information

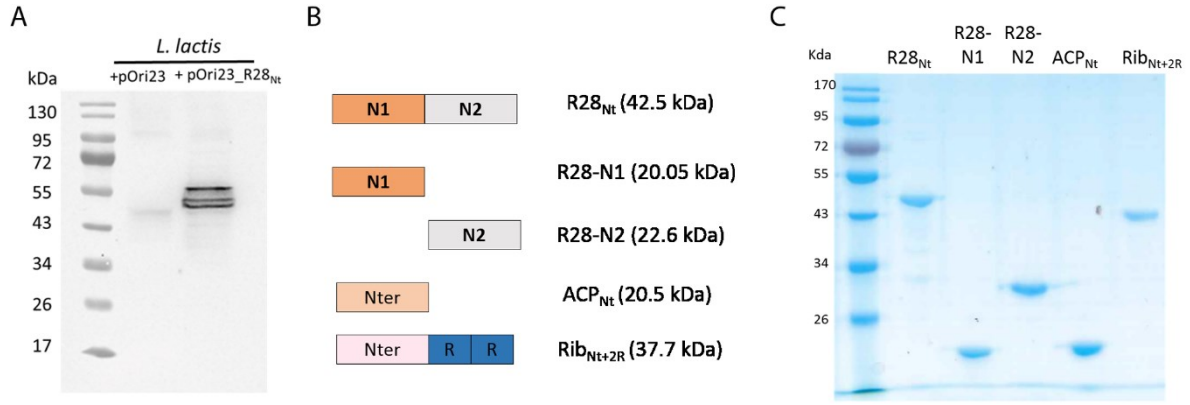

Figure S1. Schematic representation of constructed peptides used in this study, and their expression in *L. lactis* or *E. coli*. *A,* Western blot with anti-R28$_{Nt}$ antiserum of cell wall extracts of *L. lactis* expressing R28$_{Nt}$, + pOri_R28$_{Nt}$; or not, +pOri. *B,* schematic representation of the different peptides used in the study. Color code corresponds to Fig. 1*A*. *C,* Coomassie blue staining of an acrylamide gel with 1 µg of each peptide loaded.

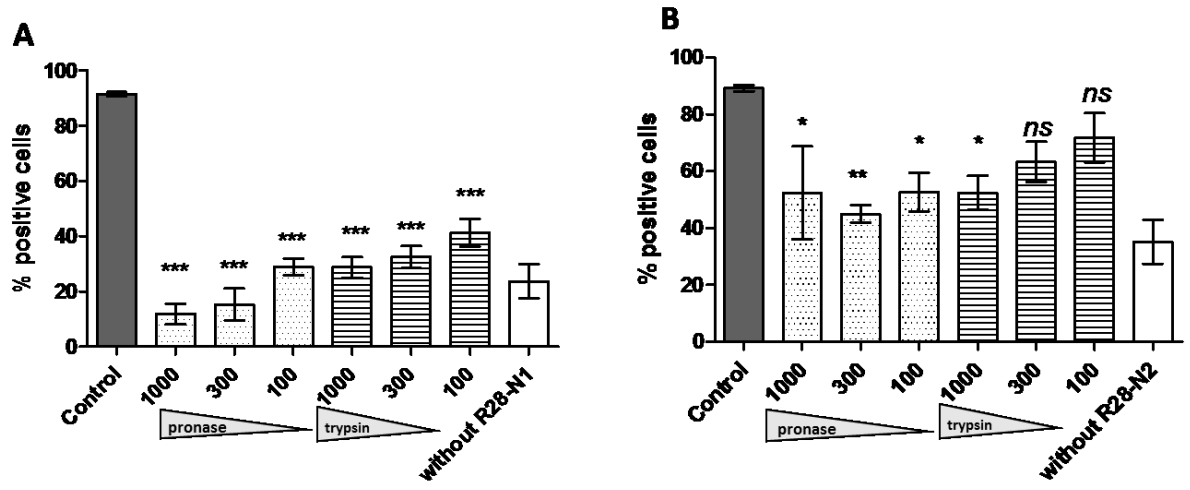

Figure S2. Effect of different treatments on the binding of *A*, R28-N1 and *B*, R28-N2 to HEC-1-A cells. Treatments were applied to HEC-1-A cells in suspension prior to incubation with purified R28-N1 and R28-N2; bound peptides were immunolabelled and cells were analyzed by flow cytometry. Statistical analysis was performed against the untreated condition Error bars correspond to SEM of three independent experiments. Two-Way ANOVA: *, $p<0.05$; **, $p<0.005$; ***, $p<0.001$; ns, not significant.

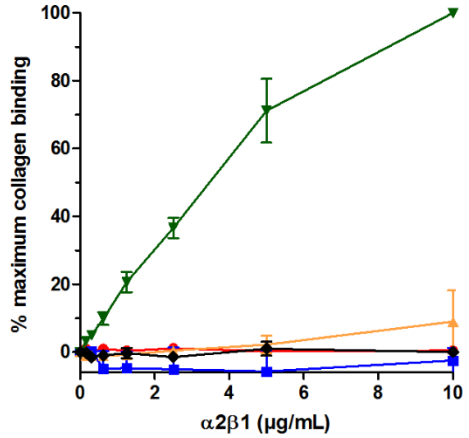

Figure S3. R28Nt, R28-N1 and R28-N2 do not bind the α2β1 integrin. Assessment of integrin α2β1 binding to $R28_{Nt}$, red; R28-N1, blue; R28-N2, orange; Type I collagen, green; BSA, black. The binding is expressed as percentage of that of the collagen at 10μg/mL integrin.

Table S1. Strains and plasmids used in this study

Strains or plasmid	Relevant properties	Source or reference
Escherichia coli		
BL21 λDE3	F^- *ompT gal (dcm) (lon) hsdSB (*rB^- mB^-) *endA1 hsdR17*(rK^-mK^+)	(1)
Streptococcus pyogenes		
M28PF1	*emm28* source of DNA for $R28_{Nt,}$ R28-N1, R28-N2 amplifications	(2)
ΔR28	M28PF1 lacking the *Spy1336* coding for R28	This study
Streptococcus agalactiae		
A909	serotype Ia, sequence type 7 , used for amplification of the gene of ACP	(3)
BM110	serotype III, sequence type 17, used for the amplification of the gene encoding Rib	(4)
Lactococcus lactis		
MG1363	Lac^- Prt^- ; NCDO 712 derivative	(5)
CCH2022	MG1363+ pOri23	This study
CCH2023	MG1363+ pOri23_$R28_{Nt}$	This study
Plasmids		
pG+host5	Erm; ColE1 replicon, thermosensitive derivative of pGK12; MCS pBluescript	(6)
pG1_R28	500 pb upstream (R28F1-R28R1) and 500 bp downstream (R28F2-R28R2) sequence of *Spy1336* cloned in pG+host5	This study
pET2818	Amp, oriR pBR322, T7 promoter, His-Tag coding sequence, pET28/16 derivative.	S. Mesnage (Pers. com.)
pET2818_$R28_{Nt}$	pET2818 with the sequence encoding the $R28_{Nt}$, without signal peptide. For the production of the peptide in *E. coli* with a His Tag	This study
pET2818_R28.N1	Ibidem with the sequence encoding R28-N1	This study
pET2818_R28.N2	Ibidem with the sequence encoding R28-N2	This study
pET2818_ACP	Ibidem with the sequence encoding ACP	This study
pOri23	Erm; *ermB,* ori ColE1, thermosensitive derivative of pIL253, P23 promoter of *L. lactis* MG1363	(7)
pOri23_$R28_{Nt}$	High level of expression of $R28_{Nt}$ at the cell wall of Gram-positive bacteria	This study

Table S2. Primers used in this study for cloning and protein purifications

Primer Name	Sequence*
R28-F1	CGACTCTAGA**GGATCC**GCCTGTGAGAGACGATCATA
R28-R1	ATCATTCTTATCGGCCCGTTGTTTCGTCTGTGAAG
R28-F2	GCCGATAAGAATGATCCAGC
R28-R2	CCATGATTAC**GAATTC**GCCTTAACTCGTATTCCTTT
R28_F	**CCATGG**CTACAATTCCAGGGAGTGC
R28_R	**GGATCC**ACCTTTTGGTTCGTTGCTATC
R28_N1_F	**CCATGG**GGTCTACAATTCC
R28_N1_R	**GGATCC**TGGTAGCGATACAACTAA
R28_N2_F	**CCATGG**ATAAAATTAAGTATTCGCC
R28_N2_R	**GGATCC**TTTTGGTTCGTTG
ACP_F	**CCATGG**GGTCAATAGTTGCTGCATCTACAAT
ACP_R	**GGATCC**TACTGACAATACTAACAATTTCTC

* restriction enzyme sites used for cloning are highlighted in bold

Supporting information file

The raw data of hits found by mass-spectrometry analysis of the co-immunoprecipitations are available in the supporting information file. In green and yellow are highlighted hits that are significantly enriched in the presence of $R28_{Nt}$ in all three independent experiments. In yellow are the surface exposed membrane proteins that correspond to Table 1 hits. In pink are highlighted the samples in which the given protein was not detected. CT-1, CT-2, CT-3 and R28-1, R28-2, R28-3, samples eluted from the control zones and $R28_{Nt}$ co-immunoprecipitated zones of experiments 1, 2, 3, respectively

Supplementary information references:

1. Studier, F. W., and Moffattf, B. A. (1986) Use of Bacteriophage T7 RNA Polymerase to Direct Selective High-level Expression of Cloned Genes. *J. MoZ. Biol*. **189**, 113–130
2. Longo, M., De Jode, M., Plainvert, C., Weckel, A., Hua, A., Château, A., Glaser, P., Poyart, C., and Fouet, A. (2015) Complete Genome Sequence of *Streptococcus pyogenes emm28* Clinical Isolate M28PF1, Responsible for a Puerperal Fever. *Genome Announc.* **3**, e00750-15
3. Michel, J. L., Madoff, L. C., Olson, K., Kling, D. E., Kasper, D. L., and Ausubel, F. M. (1992) Large, identical, tandem repeating units in the C protein alpha antigen gene, bca, of group B streptococci. *Proc. Natl. Acad. Sci. U. S. A.* **89**, 10060–10064
4. Six, A., Bellais, S., Bouaboud, A., Fouet, A., Gabriel, C., Tazi, A., Dramsi, S., Trieu-Cuot, P., and Poyart, C. (2015) Srr2, a multifaceted adhesin expressed by ST-17 hypervirulent Group B Streptococcus involved in binding to both fibrinogen and plasminogen. *Mol. Microbiol.* **97**, 1209–1222
5. Wegmann, U., O 'connell-Motherway, M., Zomer, A., Buist, G., Shearman, C., Canchaya, C.,

Ventura, M., Goesmann, A., Gasson, M. J., Kuipers, O. P., Van Sinderen, D., and Kok, J. (2007) Complete Genome Sequence of the Prototype Lactic Acid Bacterium Lactococcus lactis subsp. cremoris MG1363. *J. Bacteriol.* **189**, 3256–3270

6. Biswas, I., Gruss, A., Ehrlich, S. D., and Maguin, E. (1993) High-efficiency gene inactivation and replacement system for gram-positive bacteria. *J. Bacteriol.* **175**, 3628–35
7. Braun, L., Ghebrehiwet, B., and Cossart, P. (2000) gC1q-R/p32, a C1q-binding protein, is a receptor for the InlB invasion protein of Listeria monocytogenes. *EMBO J.* **19**, 1458–1466

2. GAS interaction with the decidua

"Group A Streptococcus efficiently colonizes and invades a human tissue and curtails its immune response during the early steps of infection" (Manuscript 2 and Additional results)

(Manuscript to be submitted to Nature Microbiology as a Letter)

To better understand the critical early steps of GAS endometritis, as a model of GAS invasive infections, we developed a model of *ex vivo* infection of a human tissue, the decidua. Maternal-fetal membrane surrounds the fetus during pregnancy and the maternal side, the decidua, derives from and is similar to the uterine linen in the post-partum.

These membranes obtained from healthy women with cesarean section were infected with a GFP-producing wild-type *emm28* GAS strain and the pathogenic mechanisms were analyzed and quantified by the use of customized imaging set-up and high-throughput image analysis. The different codes I wrote and used for this study are explained and available in the additional results p 98. The tissue surface is composed of fibronectin, and type IV collagen embedding decidual stromal cells and immune cells (Manuscript 2, Fig. 1). GAS efficiently colonizes the tissue and multiplies until it covers the whole surface; this multiplication is triggered by a tissue secreted element. Furthermore, element(s) secreted by decidual stromal cells are sufficient to trigger bacterial growth (Additional results, Fig. 1).

GAS forms microcolonies at the tissue surface and the bacterial layer is up to 16 µm thick (Manuscript 2, Fig. 1). We showed by scanning electron microscopy that this layer presents several extracellular polymeric substances, and thus corresponds to biofilms. These biofilms were characterized by distinct ultra-structures: thread-like structures, micrometric filaments and webs (Manuscript 2, Fig. 1 and S1). The kinetic of the formation of these structures depended on the donor and the presence of a flow accelerated the kinetic of the biofilm formation.

GAS bacteria, despite their absence of motility, are not restricted to the tissue surface during clinical infections. We therefore investigated the capacity of GAS to penetrate the decidua (Manuscript 2, Fig. 2 and S2). GAS invades actively the tissue, with twice more bacteria after 8 h than at 4 h of infection; furthermore, the invasion depends on the expression

of the cysteine protease SpeB. We showed in real-time *in situ* GAS internalization in phagocytic cells, and our results suggested that some GAS bacteria found deeper in the tissue correspond to end point of phagocytosis events. We further characterized bacteria within immune cells (Additional results, Fig. 2) and showed that GAS bacteria were not only phagocytosed by macrophage-like cells but also by neutrophil-like cells reaching the surface. We see at late time-points both phagocytic cells filled with GAS in CD45+ vesicles, with signs of immune cell death (Additional results, Fig. 2).

Then, we assessed the consequences of GAS infection on the tissue integrity (Manuscript 2, Fig. 3). GAS induced dramatic damages to cells, with abnormal nuclear morphology and cellular blebbing. We showed by TUNEL staining that more that 50 % of the cells are killed within 4 h and that all types of cell are affected. This cell-death is induced by secreted effectors, including the Streptolysin O (SLO).

Finally, we assessed the decidua immune responses to GAS infection (Manuscript 2, Fig. 4, S3 and S4). In the early time-points of infection, GAS induced the expression of 10 out of the 133 immunity-related genes tested, implying that GAS restrains the immune response at the transcription level. At the protein level, we confirmed a significant but limited accumulation of pro-inflammatory cytokines after infection with several cytokines that do not accumulate although their genes are overexpressed. SpeB and SLO mutants did not play a significant role in the expression of the pro-inflammatory cytokines genes. Yet, the SLO mutant induced lower accumulation of several tested cytokines at 4 h, and SpeB induced higher accumulation of some cytokines at 8 h. This indicates that SLO and SpeB are involved in the modulation of the immune response at the protein level. Altogether, these results demonstrate that GAS controls the inflammatory response by acting on the expression and the protein levels of inflammatory molecules.

Manuscript 2

Group A Streptococcus efficiently colonizes and invades a human tissue and limits its immune response during the early steps of infection

Antonin Weckel[1,2,3], Thomas Guilbert[1,2,3], Thierry Meylheuc[4,5], François Goffinet[6,7], Claire Poyart[1,2,3,8,9], Céline Méhats[1,2,3,10], Agnès Fouet[1,2,3,8,10,*]

[1]INSERM U1016, Institut Cochin, [2]CNRS UMR 8104, [3]Université Paris Descartes (UMR-S1016) Paris France, [4]MICALIS Institute, INRA, AgroParisTech, Université Paris-Saclay, Jouy-en-Josas, France [5]Plateforme MIMA2, Jouy-en-Josas, France, [6]Faculté de Médecine, Université Paris Descartes, Paris, France, [7]Service de Gynécologie Obstétrique I, Maternité Port Royal, Assistance Publique-Hôpitaux de Paris, Paris, France, [8]Centre National de Référence des Streptocoques, [9]Hôpitaux Universitaires Paris Centre, Cochin, Assistance Publique Hôpitaux de Paris, France, [10]These authors contributed equally. *e-mail: agnes.fouet@inserm.fr

Before the introduction of prophylactic measures, up to 10% childbirths were followed by the mother's death due to puerperal fever[1]. The vast majority of the cases were due to invasive infections elicited by *Streptococcus pyogenes,* also known as Group A Streptococcus (GAS). GAS is a Gram-positive human-specific pathogen also responsible for other invasive infections, such as necrotizing fasciitis and streptococcal toxic shock syndrome, causing 163,000 deaths per year in the world[2]. Little is known regarding the establishment of GAS invasive infections. The decidua is the port of entry of post-partum endometritis, leading to puerperal fever. To identify critical features of GAS early steps of infection, including the potential manipulation of the host response, we analyzed, after infecting *ex vivo* human decidua, the establishment of the infection with state-of-the-art customized tools. Here we show that GAS benefits from tissue secreted products to multiply at the tissue surface and forms biofilms. GAS invades the tissue; the cysteine protease SpeB[3,4] is involved in the invasion and the streptolysin O[5,6] in the cytotoxicity leading to the death of half the cells within the first two hours. Infection induces limited tissue immune response, with overexpression of less than 1/10th of the tested immunity-related genes. We demonstrate the remarkable capacity of GAS to infect a human tissue and restrain the immune response during the onset of invasive infections. Furthermore, mutant-infected tissues display weaken phenotypes paving the way to a prophylactic treatment against these life-threatening infections.

Most GAS studies focus on the acute phase of invasive infections to understand and improve the clinical treatments of these diseases. However, it is fundamental to unravel the mechanisms involved in the establishment of these infections which include multiple steps with, among others, adhesion to host tissue, nutrients acquisition and growth, invasion of the tissue and resistance to immune responses. The decidua is the mucosal uterine-lining during pregnancy and is made up of endometrial stromal cells and of 40% of leucocytes[7]. To characterize the steps involved in the first hours of GAS puerperal fever, we infected *ex vivo* the upper portion of the decidua that is sloughed off with the placenta[8]. GAS is genetically diverse; the *emm28* GAS strains are associated with obstetrical and gynecological infections[9–11]. We therefore used a wild-type (WT) *emm28* clinical strain isolated from a puerperal fever and its GFP and mutant derivatives[12].

Human decidual explants were infected with a GFP expressing wild-type strain (GFP-WT) derivative. GAS efficiently adheres to the tissue surface that is composed of a fibronectin layer covering cells embedded in an extracellular matrix containing type IV collagen (Fig. 1a). After 24 h of infection, GAS formed microcolonies of up to 16 µm thick (Fig. 1b) indicating the successful tissue surface colonization by GAS. We analyzed GAS multiplication at the tissue surface during the first hours of infection. In contact with the tissue, GAS multiplies until it covers the whole tissue surface (Fig. 1c,d, Supp video 1). Noteworthy, the kinetic was nearly identical on the tissues from the five subjects, out of six, on which growth occurred (Fig. 1d). We measured the growth parameters of initially scattered bacteria (Fig. 1e,f, Supp video 2). GAS grows exponentially at the tissue surface with a doubling time of 80 minutes, twice more that in THY, an optimized laboratory growth medium (Fig. 1f). We then quantified bacterial thickness increase (Fig. 1g,h). The mean thickness of the bacterial doubled in 4 hours reaching a mean value of 4.2 µm (Fig. 1h). For any given subject, the increase in thickness was locally highly heterogeneous with, after 6 h, hot-spots of more than 10 µm thick (Fig 1g). Yet, and similarly to the 2D-multiplication, the overall increase of the thickness was alike on all subjects considered (Fig. 1d,h). To analyze if diffusible host factors promote GAS growth *ex vivo*, we compared GAS growth in infection medium, RPMI, and in tissue-conditioned supernatants, which contain tissue-secreted products (Fig. 1i). GAS was able to multiply in conditioned supernatants from all subjects tested, whereas, in contrast to *Staphylococcus aureus* and Group B Streptococcus (GBS), other Gram-positive species responsible for endometritis[13,14], it is not able to multiply in RPMI (Fig. 1i and data not shown). This demonstrates that GAS benefits from tissue secreted products to multiply.

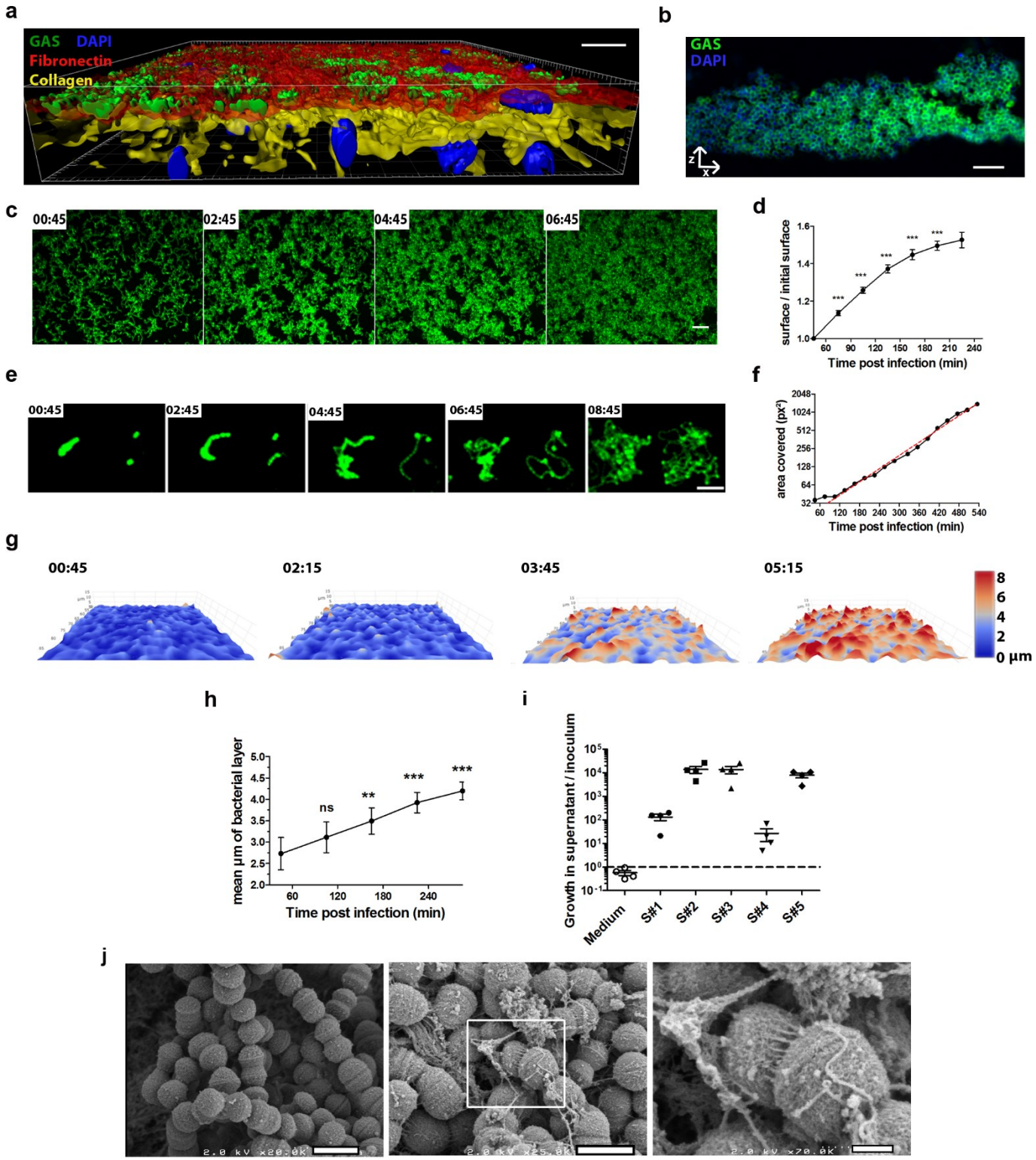
a
GAS DAPI
Fibronectin
Collagen
b
GAS
DAPI
c
00:45
02:45
04:45
06:45
d
surface / initial surface
Time post infection (min)
e
00:45
02:45
04:45
06:45
08:45
f
area covered (px²)
Time post infection (min)
g
00:45
02:15
03:45
05:15
8
6
4
2
0 µm
h
mean µm of bacterial layer
ns
**
***
***
Time post infection (min)
i
Growth in supernatant / inoculum
Medium
S#1
S#2
S#3
S#4
S#5
j

Fig. 1. Elements secreted by the tissue trigger GAS multiplication and formation of biofilm. a, Imaris 3D representation of a tissue infected under static conditions for 16 h. Fibronectin, red; type IV collagen, yellow; GFP-GAS, green; DAPI, blue. Scale bar: 20 µm. Magnification: 40X. **b**, Immuno-histofluorescence of a paraffin embedded tissue slice after 24 h of infection under static conditions. Anti-GAS, green; DAPI, blue. Scale bar: 10 µm. Magnification: 100X. **c** and **e**, z-max intensity projections of GFP signals from live acquisition images of GFP-WT at the tissue surface at the indicated time points, h:min. Scale bar: 10 µm (**c**) and 20 µm (**e**) Magnification: 25X. **d,** GFP signal area quantification of figure (**c**) and of the tissue of four other subjects: overtime ratio of the area covered by GFP-WT GAS compared to initial covered surface. The mean area of 3 to 11 fields for each time point for each tissue was used and the standard-error of the mean corresponds to the values of the 5 subjects. Two-Way ANOVA to the first time point. ***, $p<0.001$. **f,** Quantification of the surface covered by GFP GAS from image (**e**). An exponential curve was fitted (red dotted line) starting at time point 105 minutes. $R^2=0.9948$, $T_{1/2}= 82$ min. **g**, 3D surface heat-map of the thickness of the bacterial layer at different time points, observed by live imaging h:min. x, y and z are scaled. The color code is indicated on the right of the figure, in µm. **h,** Quantification of the mean thickness of the bacterial layer, the mean of 2 to 13 fields analyzed per time point per tissue from 5 independent subject was calculated and the standard-error of the mean corresponds to the values of these 5 independent tissues. **i,** Multiplication factor after incubation of GAS for 8 h in tissue-conditioned medium or RPMI. The ratio corresponds to the CFU after 8 h of growth compared to the inoculum. **j,** Left panel**.** Scanning electron microscopy (SEM) of S#6 tissue 1 h after infection, with no observable extracellular polymeric substance. Middle panel, SEM of tissue infected 1 h, washed and incubated for another 7 h under flow conditions. Right, higher magnification of the middle panel image. "Thread-like" structures ~20 nm thick can be observed connecting the cocci and ~200 nm long and filaments ~30 nm thick and up to several µm long are observed connecting streptococcal chains. Scale bars (in white), magnification: left (1 µm, 20 000 X), middle (1 µm, 25 000 X), right (250 nm, 70 000 X).

Biofilms are critical features of GAS invasive infections, involved in resistance to the immune system, to antibiotic and persistence at a tissue surface[15]. We analyzed whether GAS readily formed biofilm at the early time points of infection. At 4 and 8 h after decidua infection, different ultrastructures, not found one hour after infection, are present: intra-chains "thread-like" structures and inter-chains filaments (Fig. 1j, S1). The formation was time dependent, donor dependent and was accelerated by the presence of flow (Fig. S1). This shows that GAS already forms biofilms in the very first hours of infections. GAS therefore adheres to the tissue, uses secreted tissue factors to grow and forms biofilms.

On biopsies of GAS necrotizing fasciitis, GAS is observed deep within the tissue[16]; yet, the mechanisms involved in GAS tissue penetration are poorly characterized. While GAS is non-motile, bacteria were readily present at 4-5 micrometers below the tissue surface after 16 h of infection (Fig 2a, S2a). We then quantified at earlier time points the tissue invasion. An average of 600 invasion events per mm² were counted after 4 hours of static infection (Fig 2b); this corresponds to approximately two chains invading per 10^3 surface chains. Furthermore, there

are three times more intra-tissular bacteria at 8 h than at 4 h (Fig 2c); we hypothesized that it is partly due to tissue degradation, especially fibronectin degradation. We tested whether SpeB, a GAS major protease[4], is involved in tissue penetration. At 4 h the ΔSpeB strain invaded the tissue 2-fold less efficiently than the WT strain ($p=0.0428$) demonstrating that SpeB contributes to tissue invasion and supporting the involvement of matrix protein degradation (Fig 2c). Another potential source of bacterial invasion is internalization into host cells. We observed phagocytosis of GAS by immune cells 20 min after infections and bacteria remained inside immune cells 6 µm under the tissue surface up to at least 4 h after infection (Fig. 2d,e, S2b, Supp video 3). Our results suggest that GAS can actively invade host tissues during the onset of invasive infections, the invasion depending on SpeB and possibly relying partly on GAS survival in host phagocytic cells.

We then analyzed the consequences of infection on the state of the cells. As soon as 4 h after infection, we observed blebbing and dying immune cells (Fig. 3a, Supp video 4). After 16 h, we observed nuclei with altered morphology and DNA damages (Fig 3b). All types of cells, immune (CD45+) and non-immune (CD45-) cells, were damaged (TUNEL+) after 16 h of infection (Fig. 3c). Already at earlier time points, infection significantly induced cytotoxicity (Fig. 3d), with 27% and 57% TUNEL positive cells at 2 h and 8 h, respectively, compared to 7% and 11% without infection (Fig. 3e). To determine if cell death was induced by a GAS secreted factor, we measured cytotoxicity when bacteria were physically isolated from the tissue (Fig. 3f). In these conditions, GAS was still able to induce 21% and 37% of cell death at 2 h and 8 h, respectively, which demonstrates that GAS secreted factors induce cell death (Fig. 3e,f). SLO[5,6] being a pore-forming toxin described to induce cell death, we tested to which extent this protein was involved in GAS cytotoxicity on the whole tissue at early time points. At 2 and 4 h, the ΔSLO strain is twice less cytotoxic than the WT strain (25 and 33% versus 43 and 60 %, respectively) (Fig. 3g). However, even in the absence of SLO, GAS induces a significant cytotoxicity (Fig. 3g). In conclusion, GAS dramatically damages the cells within a few hours and SLO and other secreted factors are involved in the cytotoxicity.

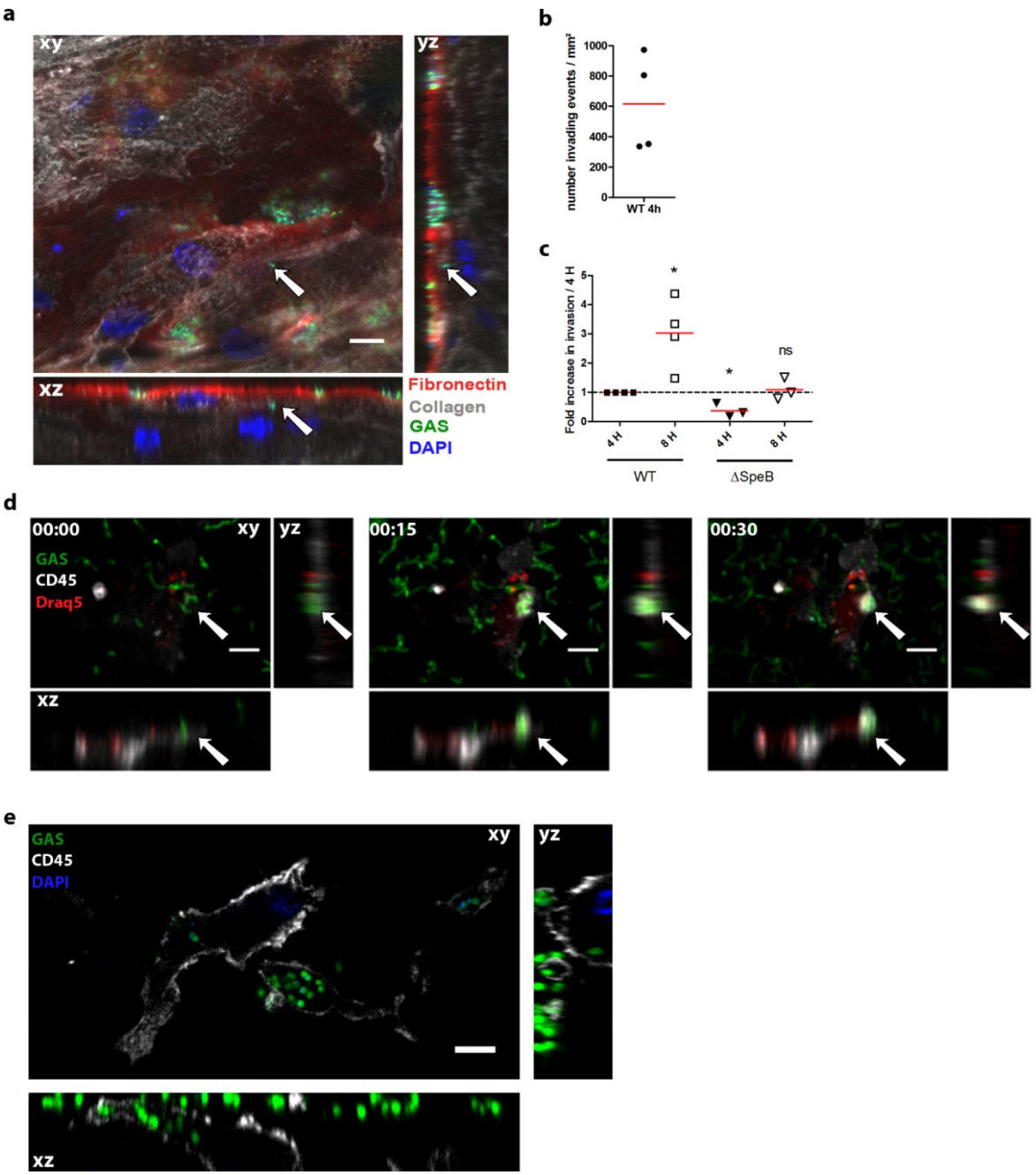

Figure 2. GAS invades the tissue using non-exclusively a protease activity and a Trojan horse mechanism. a, Orthogonal view of a tissue infected for 16 h. Arrows indicate an invading particle. Fibronectin, red; type IV collagen, grey; GAS, green; DAPI, blue. Scale bar: 10 µm. Magnification: 40X. **b**, Mean number of invading events per mm² at 4 h with the GFP-WT strain calculated using high throughput image analysis. Four subjects are shown. **c**, Ratio of GFP-WT and GFP-ΔSpeB invading events compared to WT at 4 h with the indicated strain at the indicated time. One-sample t-test to the WT at 4 h. N=4 GFP-WT, N=3 for GFP-ΔSpeB. *, $p<0.05$. **d**, Time lapse of an immune cell phagocytosing GAS *in situ*, with orthogonal view. Anti-CD45 (immune cell), grey; GAS, green; Draq5 (DNA), red. White arrow indicates the localization of the phagocytosis event. Scale bar: 10 µm. Magnification: 25X**. e**, GFP-WT inside the tissue and within an immune cell. Tissue infected under flow condition for 3 h. Anti-CD45, grey; bacteria, green; DAPI, blue. This image is taken 6 µm under the tissue surface. Scale bar: 5 µm. Magnification: 100 X..

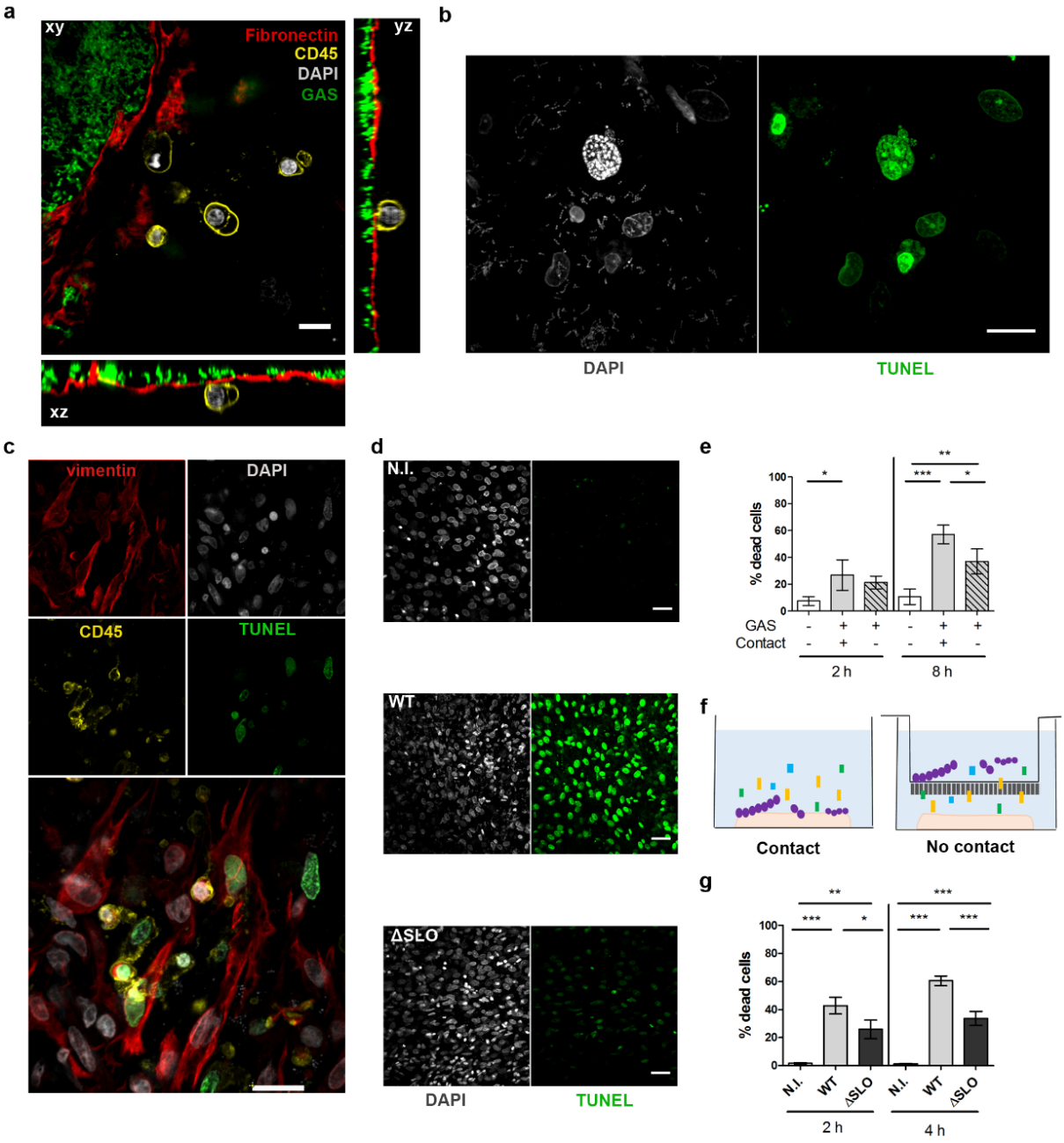
a
xy
Fibronectin
CD45
DAPI
GAS
yz
xz
b
DAPI
TUNEL
c
vimentin
DAPI
CD45
TUNEL
d
N.I.
WT
ΔSLO
DAPI
TUNEL
e
% dead cells
GAS
Contact
2 h
8 h
f
Contact
No contact
g
% dead cells
N.I.
WT
ΔSLO
2 h
4 h

Figure 3. GAS induces stromal and immune cells death via processes involving SLO and other secreted factors. a, Immune cells are affected by infection. Orthogonal view of a tissue prestained with anti-fibronectin (red) and anti-CD45 antibodies (yellow) and infected under static conditions 5 h with WT-GFP bacteria (green), and stained with DAPI (grey). CD45 positive cells present blebs and altered nuclear morphology. Scale bar: 10 µm, Magnification 40X. **b**, Immunofluorescence approach highlighting the state of the nuclei in a tissue after 16 h of static infection DNA, grey; TUNEL, green. Nuclei present altered morphology and DNA damages, as shown by the TUNEL staining. Scale bar: 10 µm. Magnification: 63X. **c**, All cells can be damaged. Immunofluorescence of tissue after 16 h of static infection. Decidual cells ($vimentin^+$, $CD45^-$) and immune cells ($CD45^+$) present damaged nuclei ($TUNEL^+$). Vimentin, red; DAPI, grey; CD45, yellow; TUNEL, green. Scale bar: 10 µm. Magnification: 40X. **d**, Immunofluorescence of tissue infected 4 h with the indicated strains. N.I., non-infected. DNA, grey (left panel), TUNEL, green (right panel). Scale bar: 40 µm. Magnification: 20X. **e,g** Percentage of dead cells. **e**, quantification of cytotoxicity, with 3 subjects; contact, + or -, in the absence or the presence of a Transwell® insert, respectively. **f**, Schematic representation of the experimental set-up with a Transwell® used in figure (**e**). Bacteria, mauve; tissue, beige; rectangles, secreted factors. **g**, Quantification of cytotoxicity, 4 subjects. Statistical analysis (**e** and **g**): Two-Way ANOVA with a Bonferroni post-test, *, $p<0.05$; **, $p<0.005$; ***, $p<0.001$

When growth occurred at the tissue surface, it was with similar kinetics (Fig. 1f,h); however, one tissue did not elicit bacterial growth at all (S#8, data not shown). Also, *in vitro* the conditioned media promoted either a 10,000-fold (S#2, S#3 and S#5) or a 10- to 100-fold CFU increase (S#1 and S#4) (Fig. 1i) suggesting that subject/tissue-peculiarities influence GAS capacity to establish infection. This correlates with the fact that host genetic factors favor GAS invasive infections[17] and suggests that the immunological state of the various tissues differs. We therefore analyzed the expression of 133 unique immune genes related to "Inflammatory cytokines and receptors" and "Human innate & adaptive response" pathways in four tissues. In the absence of infection, there is low to moderate expression of the majority of the genes tested (Fig. 4a). The 10% most highly expressed genes are related to "Macrophage" and "cytokine-mediated signaling pathway", reflecting the innate immune response capacity of the tissue. Interestingly, the basal expression levels of these genes are subject dependent (Fig. 4a, S3a) and those of S#4 tissue that supports low bacterial growth (Fig. 1i) differs from the others, its basal expression level of ten genes, including CD14, ITGAM, and SLC11A1, signing "macrophages" being markedly higher than those of the three other subjects (Fig. 4a,S3a). This suggests that initial presence of a high proportion of macrophage/phagocytic cells in the tissue impairs GAS capacity to establish infection.

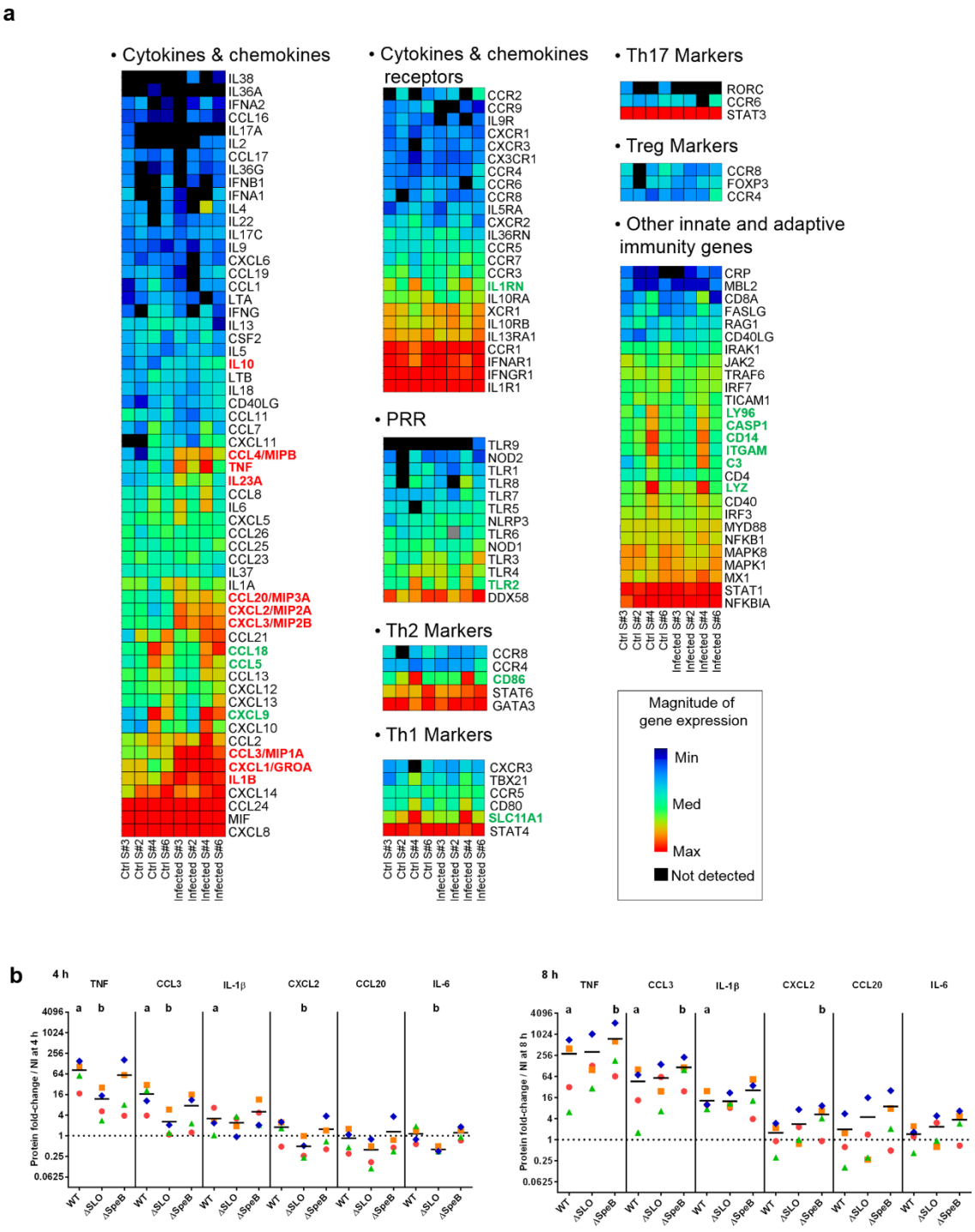
a
• Cytokines & chemokines
IL38
IL36A
IFNA2
CCL16
IL17A
IL2
CCL17
IL36G
IFNB1
IFNA1
IL4
IL22
IL17C
IL9
CXCL6
CCL19
CCL1
LTA
IFNG
IL13
CSF2
IL5
IL10
LTB
IL18
CD40LG
CCL11
CCL7
CXCL11
CCL4/MIPB
TNF
IL23A
CCL8
IL6
CXCL5
CCL26
CCL25
CCL23
IL37
IL1A
CCL20/MIP3A
CXCL2/MIP2A
CXCL3/MIP2B
CCL21
CCL18
CCL5
CCL13
CXCL12
CXCL13
CXCL9
CXCL10
CCL2
CCL3/MIP1A
CXCL1/GROA
IL1B
CXCL14
CCL24
MIF
CXCL8
Ctrl S#3
Ctrl S#2
Ctrl S#4
Ctrl S#6
Infected S#3
Infected S#2
Infected S#4
Infected S#6
• Cytokines & chemokines receptors
CCR2
CCR9
IL9R
CXCR1
CXCR3
CX3CR1
CCR4
CCR6
CCR8
IL5RA
CXCR2
IL36RN
CCR5
CCR7
CCR3
IL1RN
IL10RA
XCR1
IL10RB
IL13RA1
CCR1
IFNAR1
IFNGR1
IL1R1
• PRR
TLR9
NOD2
TLR1
TLR8
TLR7
TLR5
NLRP3
TLR6
NOD1
TLR3
TLR4
TLR2
DDX58
• Th2 Markers
CCR8
CCR4
CD86
STAT6
GATA3
• Th1 Markers
CXCR3
TBX21
CCR5
CD80
SLC11A1
STAT4
• Th17 Markers
RORC
CCR6
STAT3
• Treg Markers
CCR8
FOXP3
CCR4
• Other innate and adaptive immunity genes
CRP
MBL2
CD8A
FASLG
RAG1
CD40LG
IRAK1
JAK2
TRAF6
IRF7
TICAM1
LY96
CASP1
CD14
ITGAM
C3
CD4
LYZ
CD40
IRF3
MYD88
NFKB1
MAPK8
MAPK1
MX1
STAT1
NFKBIA
Magnitude of gene expression
Min
Med
Max
Not detected
b
4 h
TNF
CCL3
IL-1β
CXCL2
CCL20
IL-6
Protein fold-change / NI at 4 h
4096
1024
256
64
16
4
1
0.25
0.0625
WT
ΔSLO
ΔSpeB
8 h
Protein fold-change / NI at 8 h

Fig. 4. Host responses to GAS infection a, Heat-map of the results from the qRT-PCR screening using RT²qPCR "Inflammatory cytokines and receptors" and "Human innate & adaptive response" arrays on 4 subjects, control (Ctrl) or infected 8 h with the WT strain (Infected). Genes are regrouped according to their ontogeny, and classified top to bottom depending on the intensity of expression, the 10% most highly expressed genes are related to the ontology pathways "Macrophage" (ARCHS4 database[1], *p* values: 0.001) and "cytokine-mediated signaling pathway" (Gene Ontology Biology process GO:0019221, *p* value:3.48 10^{-16}). Genes that are significantly overexpressed after infection are in red and are related to "acute inflammatory response" and "macrophages" (GO:0002526, *p* value: 1.41 10^{-17}; ARCHS4, *p* value: 4.26 10^{-10}, respectively). Genes that are expressed differently at the basal level on subject S#4 are indicated in green and are related to a signature of macrophage (ARCHS4 database[1], *p* value: 4.26 10^{-10}). Statistical analysis: Student's two tailed *t*-distributed for paired samples; *, $p<0.05$. **b**, Fold-change increase in the concentration of the indicated cytokines compared to the non-infected condition (NI) at; left 4 h and right, 8 h post-infection on tissues from 4 different subjects. Mean is indicated with a black line. S#7, red circle; S#8, orange square; S#9, green. Statistical analysis: Friedman and post hoc pairwise comparison tests, a, $p<0.05$ as compared to NI; b, $p<0.05$ as compared to WT

We next investigated the host immune response during the early steps of GAS tissue infection by testing the change in expression of these 133 genes after 8 h of infection. Ten genes among the 133 (7.5%); they all encode cytokines and chemokines related to the ontology pathways, "acute inflammatory response" and "macrophages", showed a significantly overexpression (Fig. 4a, Table S1). To assess the breadth of this immune response, we compared our results to the already published response of human decidua to a GBS infection[18]. After 8 h of infection, GBS induced the expression of 32 genes that include 9 of the 10 genes overexpressed after a GAS infection (Table S1). The principal molecules activated specifically during the GBS infection are signaling molecules related to "cellular response to cytokine stimulus". This demonstrates that GAS impairs the tissue robust immune response normally elicited by a Streptococcus pathogen also involved in endometritis. Strikingly, the only gene specifically overexpressed by a GAS infection is IL10, an anti-inflammatory cytokine. Altogether, these results suggest that GAS specifically induces a low and limited inflammation during the initiation of infection.

To further analyze the host immune response and because GAS is able *in vitro* to modulate cytokine expression and accumulation[19–21], we quantified at 4 and 8 h the expression of seven of these ten genes and that of IL6, the classical pro-inflammatory cytokine, in five tissues and also the protein concentration of six cytokines in the explant supernatants of four subjects (Fig. S3b-c, 4b, S4, Table S2, S3). Overexpression of three genes, TNF, CCL20 and CCL3, occurs as soon as 4 h after infection; yet fewer genes are upregulated than at 8 h where the expression of CXCL2, CXCL1, and CCL4 is also increased (Fig. S3b). After GAS infection, the classical

pro-inflammatory cytokines IL6 and IL1b are not overexpressed in contrast to the observed overexpression with other pathogens including GBS at 8 h (Table S1)[22]. The basal level of accumulation of the six cytokines differ between subjects (Fig. S4). GAS infection increases significantly the accumulation of TNF, CCL3 and IL-1β as soon as at 4 h, and with a higher fold at 8 h (Fig. 4c). Interestingly, the overexpression of the CXCL2 gene at 4 h and of the CXCL2 and CCL20 genes at 8 h (Fig. S3) are not paralleled by an increase in the concentrations of these two proteins, suggesting that GAS also controls the immune response at the protein level (Fig. 4c).

GAS limiting the immune response at the transcriptional and post-transcriptional levels, we analyzed the potential roles of SLO and SpeB on that control. The ΔSLO strain yielded at 4 h a similar activation of the gene expressions than the WT strain (Fig. S3c). In contrast, it generated a lower accumulation of all cytokines except IL-1β and CCL20, indicating that the presence of SLO increases their secretion at 4 h but not at 8 h (Fig. 4c). In contrast, at 4 h the SpeB mutant has no effect on the accumulation of cytokines. Yet, at 8 h, it induced a higher accumulation of TNF, CCL3, and CXCL2 than the wild-type strain, indicating that SpeB tampers with cytokine accumulation. Overall, GAS controls the immune response at the RNA and protein levels as soon as 4 h post-infection and SLO and SpeB are involved in the control of the immune response at the protein level.

GAS was, until the 20th century, the major cause of infectious maternal death[1] while not being a colonizer of the vaginal flora[23], suggesting a particular propensity for GAS to elicit puerperal fever. A comprehension of the crucial initial steps of GAS invasive infections and in particular puerperal fever is lacking. GAS possesses a large collection of virulence factors mainly described for their implication in later stages of invasive infections, but their role in the initiation of these infections is discussed[24]. Furthermore, GAS human species specificity hinders the *in vivo* analysis of GAS infections. We therefore used the conjunction of *ex vivo* infection of a human decidua, bacterial genetic manipulation, state-of-the-art image and immune response analyses to dissect at the molecular level GAS capacity to establish puerperal fever. We demonstrate the remarkable capacity of GAS to colonize, invade and damage the decidua within the first hours of infections. Also, GAS simultaneously induces pro- and anti-inflammatory responses during the onset of infection. Moreover, an overall limited inflammation, including the production of an anti-inflammatory cytokine, is elicited; this tampering of the inflammation is supported by the comparison with GBS elicited response. This is in accordance with previous conclusions that the genuine role of several GAS effectors is to impair the immune system, favoring GAS colonization[25]. This constrained inflammation

may favor GAS infection initiation by delaying or decreasing the recruitment of immune cells. Altogether, our data account for the GAS – endometrium puerperal fever association.

We further show the involvement of two major virulence factors, SLO and SpeB, in the early steps of infection, both for the bacterial invasion process *per se* and the host response. The weaker efficiency of the mutant strains, for the tested phenotypes, together with the potential critical influence of the host basal immune stage on the GAS capacity to establish infection, point to the necessary equilibrium between pathogen and host factors for GAS infection to be successful.

Our holistic approach supported by the toolbox we developed can be applied to the study of the initial steps of GAS and other pathogens human infections on many tissues, and as such be a template for future *ex vivo* infections. GAS capacity to divert the host response during the early stages of decidua infection and to establish very early in the infection niche to resist antibiotics, such as intracellular bacteria and biofilms, confirms the necessity for prophylaxis. GAS remarkable efficiency to initiate invasive infections support the necessity for vaccination and the use of models such as ours to assess GAS potential targets.

Methods

Strains and culture conditions. The strains used in this study are described in Table S4. The M28PF1 strain is a clinical isolate responsible for an endometritis (French National Reference Center (CNR) for Streptococci, https://cnr-strep.fr/) that was selected on phenotypic and genotypic bases from a collection of 50 *emm28* independent clinical isolates[12]. GAS strains were grown under static condition at 37°C in Todd Hewitt broth supplemented with 0.2% Yeast Extract (THY) or on THY agar (THYA) plates. For GFP strains, the medium was supplemented with 10 µg/mL erythromycin.

Genetic constructions and generation of GFP-producing and SLO and SpeB deleted mutant strains. The strains harboring an integrated inducible *gfp* gene were constructed as follows. We sequentially cloned into the pG1 vector[26], the Perm - *gfp* transcriptional fusion surrounded by the KpnI and HindIII sites from pATΩgfp[27] giving rise to pG1-Perm-gfp. The *lacA-lacR* intergenic sequence, enabling a single cross-over in M28PF1 and derivatives, was amplified using the primers F_lacA and R_lacA and cloned by In-fusion© into pG1-Perm-gfp digested with EcoRI, giving rise to pG1-lacA-Perm-gfp. The *erm* promoter was replaced by the tetO tetR Pxyl promoter region by amplifying it from pTCV_TetO[28] using the primers F_tetO and R_tetO and cloning it into pG1-lacA-Perm-gfp previously digested with EcoRI-EcoRV, giving rise to pG1-lacA-PTetO-gfp. The plasmid was checked by sequencing and transferred into M28PF1 or derivatives by electroporation as previously described[29]. The correct localization of the construct was confirmed by sequencing the region using a primer outside the construct (R_extlacA) and one hybridizing to the vector, RP48. The uninduced GFP-producing strain, M28-GFP, grew like M28PF1 in laboratory THY. The construct was stable even in the absence of erythromycin for at least eight generations. The minimum anhydrotetracycline concentration required for full expression of the GFP is 20 ng/mL, the fluorescence is stable for at least 6 h when the bacteria are in the stationary growth phase. GFP fluorescence is observable when GAS is intra-cellular.

The ΔSLO and ΔSpeB strains correspond to in-frame deletion mutants of the genes *slo* and *speB* genes and were obtained by homologous recombination of the plasmid pG1-SLO and pG1-SpeB following the same protocol as previously [30]. The regions surrounding the construct were sequenced as described previously. The primers used for the generation of the plasmids pG1-SLO and pG1-SpeB are described in Table S5.

Antibodies. The following antibodies were used during this study: AlexaFluor 594 mouse anti-CD45 (Biolegend, clone M5E2), rabbit anti-Fibronectin (Sigma, #F3648), rabbit anti-vimentin (Abcam, ab92547), mouse anti-Type IV collagen (DSHB, M3F7), rabbit anti whole GAS, gift from I. Julkunen.

Human tissue collection. Human placenta with attached maternal-fetal membranes were collected from healthy women with an uncomplicated singleton pregnancy, undergoing a planned cesarean delivery prior the onset of active labor at term (between 38 and 40 weeks of pregnancy). The study of the human maternal-fetal membranes was approved by the local ethics committee (Comité de Protection des Personnes Ile de France III, n°Am5724-1-COL2991, 05/02/2013). All participants provided written informed consent prior to inclusion in the study at the Department of Obstetrics, Port Royal Maternity, Cochin University Hospital, Paris, France. Except for per-operatively administered antibiotics, women were excluded if prescription antibiotics were used during the two weeks preceding delivery. Table S6 indicates in which experiments each sample tissue was used.

Materno-fetal membrane processing. Within 15 min of collection, biological samples were processed in the laboratory. Maternal-fetal membranes were detached from placenta under sterile conditions, rinsed extensively in phosphate-buffered saline (PBS) and carefully examined. Pieces of membranes in RPMI, at distance of placenta and of the remodeling zone overlying the cervix[7], free of surface blood clots, were cut and glued to Petri dishes with a veterinary glue (Vetbond glue 3M, St Paul, MN), the fetal side sticking to the plastic.

Infection procedure. For all experiments, GAS strains were prepared as follows. GAS strains were diluted from an overnight culture, grown to the exponential phase at an OD = 0.5 in THY and diluted in RPMI. For GFP strains, exponential phase bacteria were diluted to an OD = 0.1 in THY supplemented with 10 µg/mL erythromycin and 20 ng/mL anhydrotetracyclin (Sigma), grown for 1 h 30 at 37°C and diluted in the specified medium.

Static: 1.5 cm² or 8 cm² of maternal-fetal membranes were glued (Vetbond 3M) by the fetal side in a 35mm Petri dish or on a glass coverslip respectively. When specified, tissues were pre-stained with 500 µL RPMI with 5 µL of anti-CD45 Alexafluor-594 coupled (Biolegend) for 30 minutes at 37°C, 5% CO_2. Tissues were infected with 0.2 mL/cm² of a solution of 1.7 10^8 bacteria/mL in RPMI, supplemented by 10 µg/mL erythromycin and 50 ng/mL anhydrotetracycline when GFP strains were used. After infection, tissues were washed and fixed in formalin for 24 h, and then stored in 70% ethanol at 4°C.

For cytotoxicity assay, 500 µl of RPMI were added to 1.5 cm² tissue glued to a coverslip in a 24-well plate. 100 µL of M28PF1 at 5.10^8 bacteria/mL was added directly or in the upper chamber of a 6.5 mm Transwell® insert (polycarbonate, 0.4 µm membrane, Costar). For the non-infected condition, 100 µL of RPMI was added directly. After the specified time of infection, tissues were washed with PBS and fixed in formalin for 24 h, and then stored in 70% ethanol at 4°C.

Flow infection condition: 8 cm² maternal-fetal explant were glued by the fetal side to 35 mm Petri dish and stained with Draq5 (1/2000, Biolegend) and anti-CD45 Alexafluor-594 coupled (Biolegend) in infection medium (RPMI without phenol, 10 µg/mL erythromycin, 50 ng/mL anhydrotetracycline (Sigma)) for 30 min at 37°C, 5% CO_2. Tissue was extensively washed with infection medium and 3 mL of GFP-producing bacteria (1.10^8 CFU/mL) in infection medium were added to the tissues in a 37°C microscopy chamber for 45 minutes until 20-30 % of tissue surface was covered by bacteria. Supernatant was then discarded, tissue was washed with infection medium to remove unattached bacteria, a peristaltic pump with circulating infection medium bubbled with 95% O_2 and 5% CO_2 was activated in an open circuit at 0.3 mL/min.

Immunofluorescence on fixed tissue. Fixed tissues were cut into 0.5 cm² pieces and glued to coverslips, permeabilized with 0.2% triton X100 (Sigma) for 30 minutes at 20°C. 500 µL of blocking solution (PBS+BSA 3%) was added for one hour at 20°C, and tissue were stained for 4 h at 20°C with 500 µL of blocking solution containing primary antibodies: 2 µL anti-fibronectin, 10 µL anti-type IV collagen, 2 µL of rabbit anti-Vimentin. Tissues were washed with PBS and secondary antibodies with DAPI (1/1000) in blocking solution were added for 1 hour at 20°C.

TUNEL staining protocol is based on a modified manufacturer's protocol (DeadEnd™ Fluorometric TUNEL System, Promega). Tissues fixed and glued to coverslips were permeabilized with 500 µL PBS with 0.2 % Triton X100 for 30 min at 20°C. 100 µL of equilibration buffer was added on the tissue in a wet chamber for 15 min, liquid was removed and 50 µL of labelling solution was added for 3-4 h at 37°C. Tissues were washed twice with saline-sodium citrate (SSC) 2X buffer (from the manufacturer's kit) and stained with DAPI (1/2000) for 15 min. For double vimentin and TUNEL staining, TUNEL staining was performed first.

Image acquisition of fluorescently labeled tissues. Live microscopy: infected tissue images were acquired with an upright confocal Leica Yokogawa CSU-X1 Spinning Disk (Yokogawa,

Tokyo, Japan) coupled with a DMI6000FS Leica microscope (Leica microsystems Gmbh, Wetzlar, Germany), with a 25X objective (NA 0.95, Olympus). Acquisitions were made with MetaMorph 7 software and an image was taken every 30 min for 3 h with a z-step of 2 µm. For long-term acquisition, axial drift was manually compensated after 3 h and acquisition was continued for another 3 h.

For fixed tissue, the maternal side of stained tissue was placed facing a 35 mm high glass bottom µ-dish (IBIDI) and directly imaged using a Yokogawa CSU-X1 Spinning Disk (Yokogawa, Tokyo, Japan) coupled with a DMI6000B Leica microscope (Leica microsystems Gmbh, Wetzlar, Germany). Acquisitions were made with MetaMorph 7 software.

For cytotoxicity quantification, images were acquired with a 20X objective (NA=0.7), 1 µm z-step and approximatively 70 slices per stack were acquired. For quantification of bacterial invasion, images were acquired with a 40X objective (NA=1.25), 0.3 µm z-step and approximatively 90 slices per stack were acquired.

Image treatments and data analysis. All images were processed with ImageJ. 3D drifts of live images were corrected with homemade routines. For surface area measurements, bacteria were segmented based on a threshold on the maximum intensity z projection images of the GFP signal at the different time points, with the same threshold for each time point. For local thickness measurement of the GFP signals corresponding to bacteria, whole field was subdivided in region of interest and a home-made ImageJ macro measured the full width at half maximum (FWHM) of the z-axis GFP signal. For thickness and surface measurements of bacteria, 3 to 12 fields per tissue were analyzed. For cytotoxicity measurements, TUNEL and DAPI positive nuclei of images were segmented and automatically counted. At least 5 fields per condition were analyzed. To measure bacterial invasion, another ImageJ macro was used to segment bacterial particles on z-max projection image of GFP signal. For each bacterial particle, the axial localization was determined and compared to fibronectin and type IV collagen localization. Any bacterial particle whose signal was below 1.2 µm to fibronectin or collagen signals was considered as an invasion event. 5 to 8 fields (153 x 169 x 30 µm) per conditions were analyzed. A GAS chain was considered to be in mean 4 cocci, corresponding to the mean size of invading particles. Taking into account surface and thickness of bacteria (mean thickness, 4 µm, bacterial coverage of a field: 90 %), we estimated the amount of invading chains.

Biofilm thickness 3D surface heat map was generated by a custom R code based on the plot-ly library.

A 3D image representation of the tissue was performed using Imaris 7.4 (Bitplane AG).

Immunohistofluorescence (IHC). After static infection, tissues were fixed in formol and embedded in paraffin; IHC was performed as described previously[8]. 10 µm-thick slices were cut and stained with home-made whole GAS rabbit antiserum and with DAPI.

Scanning electron microscopy. Tissues were infected 1 h as described above for static infections, washed once with RPMI, fresh RPMI was added for 3 h (1+3 h condition) or 7 h (1+7 h condition) and then the samples were fixed. Samples were immersed in a fixative solution (2.5% glutaraldehyde in 0.2 M sodium cacodylate buffer, pH 7.4)) and stored 1 h at 20°C and overnight at 4°C. The fixative was removed, and samples were rinsed three times for 10 min in a sodium cacodylate solution (0.1M, pH 7.4). The samples underwent progressive dehydration by soaking in a graded series of ethanol (50 to 100%) before critical-point drying under CO_2. Samples were mounted on aluminum stubs (10 mm diameter) with carbon adhesive discs (Agar Scientific, Oxford Instruments SAS, GOMETZ-LA-VILLE, France) and sputter coated with gold-palladium (Polaron SC7640, Milexia, Verrières-le-buisson, France) for 200 s at 10 mA. Samples were visualized by field emission gun scanning electron microscopy. They were viewed as secondary electron images (2 kV) with a Hitachi S4500 instrument (Milexia, Verrières-le-buisson, France). Scanning Electron Microscopy analyses were performed at the Microscopy and Imaging Platform MIMA2 (INRA, Jouy-en-Josas, France).

RNA extraction. After static infections, tissues were washed once and stored in TriReagents (Sigma) at -80°C until used. Total RNA was isolated using a Qiagen RNeasy Kit (Qiagen, Valencia, CA) according to the manufacturer's instructions. The purity and concentration of total RNA were evaluated using a Nanodrop spectrophotometer (Thermo Scientific, Waltham, MA), by measuring absorbance at 260 nm.

RT-qPCR analysis. RNA was treated with deoxyribonuclease (Invitrogen, Life Technologies, St Aubin, France) to remove any contaminating DNA. Four µg of total RNA were reverse transcribed using random primers and M-MLV Reverse Transcriptase (Invitrogen), according to the manufacturer's instructions. Quantitative PCR was carried out on a Light Cycler 480, 96 well apparatus (Roche Diagnostics, Manheim, Germany), with 160 ng of cDNA as a template, using the amplification kit SensiFAST SYBR No-Rox kit (Bioline, London, UK), according to the manufacturer's instructions. The RT^2 Profiler "Inflammatory cytokines and receptors" and

"Human innate and adaptive response" arrays PCR Arrays (Qiagen) were performed according to the manufacturer's instructions. Gene expression was normalized using a panel of 5 housekeeping genes: ACTB, B2M, GAPDH, HPRT1, RPLP0. ΔCt ranging from 0 and below to 6.0 were considered as maximum magnitude of gene expression, from 6.1 to 9.9 as moderate and from 10 to 15 as low. Primers for additional RT-PCR analysis were chosen using PRIMER3 software, based on published sequences (available upon request). Primers were obtained from Eurogentec (Angers, France) and used at 10 nM in the PCR reaction. In this series of experiment, the set of internal controls included the geometric mean of three different reference genes: SDHA, PPIA, and GAPDH.

Genes with a nominal p value ≤ 0.05 were considered to be differentially expressed. Genes showing > 2-fold variation were further considered in the analysis. Heatmaps were created using the MeV Package. Enrichr was used for pathways enrichment analysis, restricted to Gene Ontology (GO) terms and ARCHS4 databases.

GBS infection of maternal-fetal membranes microarray subanalysis. Data (Control 8 h: GSM2535518, GSM2535524, GSM2535529, GSM2535535 and GBS infection 8 h: GSM2535517, GSM2535526, GSM2535530, GSM2535536) from GSE96557 were extracted using GEO2R. After conversion of the Gene annotation using DAVID gene Id Conversion tool, fold-changes and p values for the 133 immune-related genes we previously analyzed with the RT²Profiler Arrays were retrieved from these 8 samples.

Protein analysis. After static infections, supernatants of explants were stored at − 80 °C until use. The levels of IL6, TNF, CCL20, CXCL2, CCL3, and IL-1 β were measured in a multiplex assay (Bio-Plex BIORAD). The concentrations are reported as pg/mL medium. The samples were quantified by duplicate according to the manufacturer's instruction.

***In vitro* bacterial growth measurement.** RPMI was added to materno-fetal tissues for 8 h at 37°C, 5% CO_2 and the supernatants (conditioned medium) were filtered and diluted 5 times with RPMI. A thousand bacteria/mL was added to these diluted tissue supernatants or to RPMI alone. After 8 h of incubation at 37°C, 5% CO_2, solutions were serially diluted and plated. After 24 h at 37°C, CFU were counted.

Computer code availability. Computer codes used for this work will be transferred upon request.

Statistical analyses. Data were analyzed by Prism 6 software (GraphPad Software, Inc. San Diego, CA) or Xlstat version 2018.1 (Addinsoft, Paris, France). When indicated, we used Two-

Way ANOVA. We used Student's t-test or non-parametric tests for quantitative variables as indicated in the text and Pearson's chi-square for qualitative variables, as appropriate. A *p*-value <0.05 was considered to be significant.

References

1. Anderson, B. L. Puerperal group a streptococcal infection: beyond semmelweis. *Obstet. Gynecol.* **123,** 874–82 (2014).
2. Carapetis, J. R., Steer, A. C., Mulholland, E. K. & Weber, M. The global burden of group A streptococcal diseases. *Lancet Infect. Dis.* **5,** 685–94 (2005).
3. Nelson, D. C., Garbe, J. & Collin, M. Cysteine proteinase SpeB from *Streptococcus pyogenes*– a potent modifier of immunologically important host and bacterial proteins. *Biol. Chem* **392,** 1077–1088 (2011).
4. Kapur, V. *et al.* A conserved *Streptococcus pyogenes* extracellular cysteine protease cleaves human fibronectin and degrades vitronectin. *Microb. Pathog.* **15,** 327–346 (1993).
5. Bricker, A. L., Cywes, C., Ashbaugh, C. D. & Wessels, M. R. NAD+-glycohydrolase acts as an intracellular toxin to enhance the extracellular survival of group A streptococci. *Mol. Microbiol.* **44,** 257–269 (2002).
6. Timmer, A. M. *et al.* Streptolysin O promotes group A streptococcus immune evasion by accelerated macrophage apoptosis. *J. Biol. Chem.* **284,** 862–871 (2009).
7. Marcellin, L. *et al.* Immune Modifications in Fetal Membranes Overlying the Cervix Precede Parturition in Humans. *J. Immunol.* **198,** 1345–1356 (2017).
8. Marcellin, L. *et al.* Endometriosis also affects the decidua in contact with the fetal membranes during pregnancy. *Hum. Reprod.* **30,** 392–405 (2015).
9. Green, N. M. *et al.* Genetic diversity among type *emm28* group A Streptococcus strains causing invasive infections and pharyngitis. *J. Clin. Microbiol.* **43,** 4083–91 (2005).
10. Byrne, J. L. B., Aagaard-Tillery, K. M., Johnson, J. L., Wright, L. J. & Silver, R. M. Group A streptococcal puerperal sepsis: initial characterization of virulence factors in association with clinical parameters. *J. Reprod. Immunol.* **82,** 74–83 (2009).
11. Plainvert, C. *et al.* Invasive group A streptococcal infections in adults, France (2006-2010). *Clin. Microbiol. Infect.* **18,** 702–10 (2012).
12. Longo, M. *et al.* Complete Genome Sequence of *Streptococcus pyogenes emm28* strain M28PF1, responsible of a puerperal fever. *Genome Announc.* **3,** e00750-15 (2015).
13. Sriskandan, S. Severe peripartum sepsis. *J. R. Coll. Physicians Edinb.* **41,** 339–346 (2011).
14. Winn, H. N. Group B Streptococcus Infection in Pregnancy. *Clin. Perinatol.* **34,** 387–392 (2007).
15. Fiedler, T., Koller, T. & Kreikemeyer, B. *Streptococcus pyogenes* biofilms formation, biology, and clinical relevance. *Front. Cell. Infect. Microbiol.* **5,** 1–11 (2015).
16. Siemens, N. *et al.* Biofilm in group A streptococcal necrotizing soft tissue infections. *JCI Insight* **1,** 151–157 (2016).
17. Kotb, M. *et al.* An immunogenetic and molecular basis for differences in outcomes of invasive group A streptococcal infections. *Nat. Med.* **8,** 1398–1404 (2002).
18. Park, H.-R. *et al.* Group B Streptococcus Activates Transcriptomic Pathways Related to Premature Birth in Human Extraplacental Membranes In Vitro. *Biol. Reprod.* **98,** 396–407 (2017).
19. Egesten, A. *et al.* SpeB of *Streptococcus pyogenes* differentially modulates antibacterial and receptor activating properties of human chemokines. *PLoS One* **4,** 1–9 (2009).
20. Zingaretti, C. *et al. Streptococcus pyogenes* SpyCEP: a chemokine-inactivating protease with unique structural and biochemical features. *FASEB J.* **24,** 2839–48 (2010).
21. Klenk, M. *et al.* Global epithelial cell transcriptional responses reveal *Streptococcus pyogenes* Fas regulator activity association with bacterial aggressiveness. *Cell. Microbiol.* **7,** 1237–1250 (2005).
22. Anders, A. P., Gaddy, J. A., Doster, R. S. & Aronoff, D. M. Current concepts in maternal-fetal immunology: Recognition and response to microbial pathogens by decidual stromal cells. *Am.*

J. Reprod. Immunol. **77,** e12623 (2017).
23. Mead, P. B. & Winn, W. C. Vaginal-rectal colonization with group A streptococci in late pregnancy. *Infect. Dis. Obstet. Gynecol.* **8,** 217–219 (2000).
24. Walker, M. J. *et al.* Disease manifestations and pathogenic mechanisms of group a Streptococcus. *Clin. Microbiol. Rev.* **27,** 264–301 (2014).
25. Hynes, W. & Sloan, M. *Secreted Extracellular Virulence Factors*. *Streptococcus pyogenes: Basic Biology to Clinical Manifestations* (2016).
26. Biswas, I., Gruss, A., Ehrlich, S. D. & Maguin, E. High-efficiency gene inactivation and replacement system for gram-positive bacteria. *J. Bacteriol.* **175,** 3628–35 (1993).
27. Clarebout, G. & Leclercq, R. Fluorescence assay for studying the ability of macrolides to induce production of ribosomal methylase. *Antimicrob. Agents Chemother.* **46,** 2269–2272 (2002).
28. Buscetta, M. *et al.* FbsC, a novel fibrinogen-binding protein, promotes Streptococcus agalactiae-host cell interactions. *J. Biol. Chem.* **289,** 21003–21015 (2014).
29. Caparon, M. G. & Scott, J. R. Genetic Manipulation of Pathogenic Streptococci. *Methods Enzymol.* **204,** 556–586 (1991).
30. Six, A. *et al.* Srr2, a multifaceted adhesin expressed by ST-17 hypervirulent Group B Streptococcus involved in binding to both fibrinogen and plasminogen. *Mol. Microbiol.* **97,** 1209–1222 (2015).
31. Longo, M. *et al.* Complete Genome Sequence of *Streptococcus pyogenes emm28* Clinical Isolate M28PF1, Responsible for a Puerperal Fever. *Genome Announc.* **3,** e00750-15 (2015).

Acknowledgements

We thank Louis Réot for the RT-PCR screening, Karine Bailly for the Luminex cytokine quantification, Sandra Brochet and Quentin Cece for the construction of the GFP strains, Clara Lambert for the Gram-positive culture tests in RPMI, Emmanuel Donnadieu, Sarah Barrin, Elisa Peranzoni, Vincent Feuillet and Alain Trautmann for advice in the imaging set-up, the Imag'IC and Cybio facilities of the Cochin Institute, all the personnel of the CIC Mère-Enfant Cochin-Necker. This work was supported by Université Paris Descartes (AW contract n° KL2UD) the Département Hospitalo-Universitaire Risks in Pregnancy (PRIDE 2014, AF & CM), INSERM, CNRS, Université Paris Descartes.

Supplementary figures

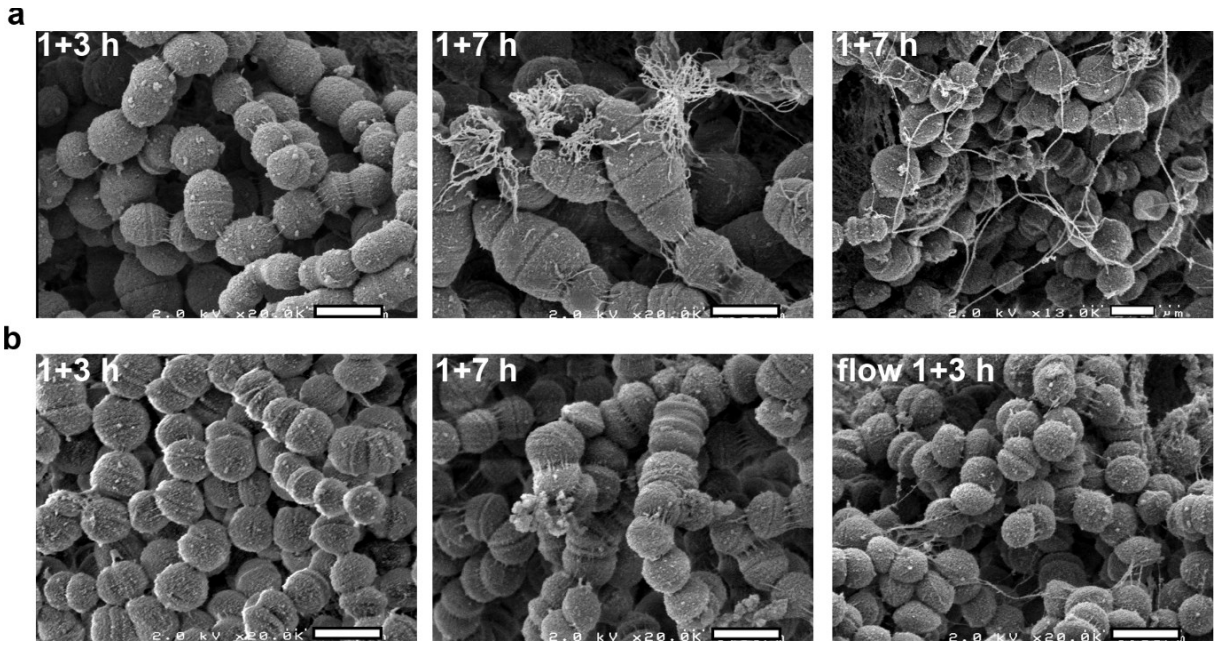

Figure S1. Kinetic of GAS biofilm formation at the surface of the tissue analyzed by scanning electron microscopy (SEM) with two subjects and different experimental conditions. After 1 h of infection, the tissues were washed and the experiment continued during indicated times **a**, Subject S#10. Morphological details of biofilm obtained under static conditions: left, after 3 h, thread-like structures, ~20 nm thick and ~200 nm long, but no filaments; middle: after 7 h, thread-like structures and micrometric webs; right: after 7 h, abundant filaments, ~30 nm thick and up to several µm. **b**, Subject S#5, displaying a different kinetic of biofilm formation. Under static condition: left, after 3 h, no thread-like structures nor filaments in contrast to S#10 (panel a); middle, after 7 h, thread-like structures, but no micrometric in contrast to S#10 in (panel a). Under flow condition, after 3 h, (right), thread-like structures and filaments absent in static conditions (S1b), showing that flow accelerates biofilm formation. Scale bar: 1 µm. Magnification: 20 000 X, except for figure (a) right panel, 13 000 X.

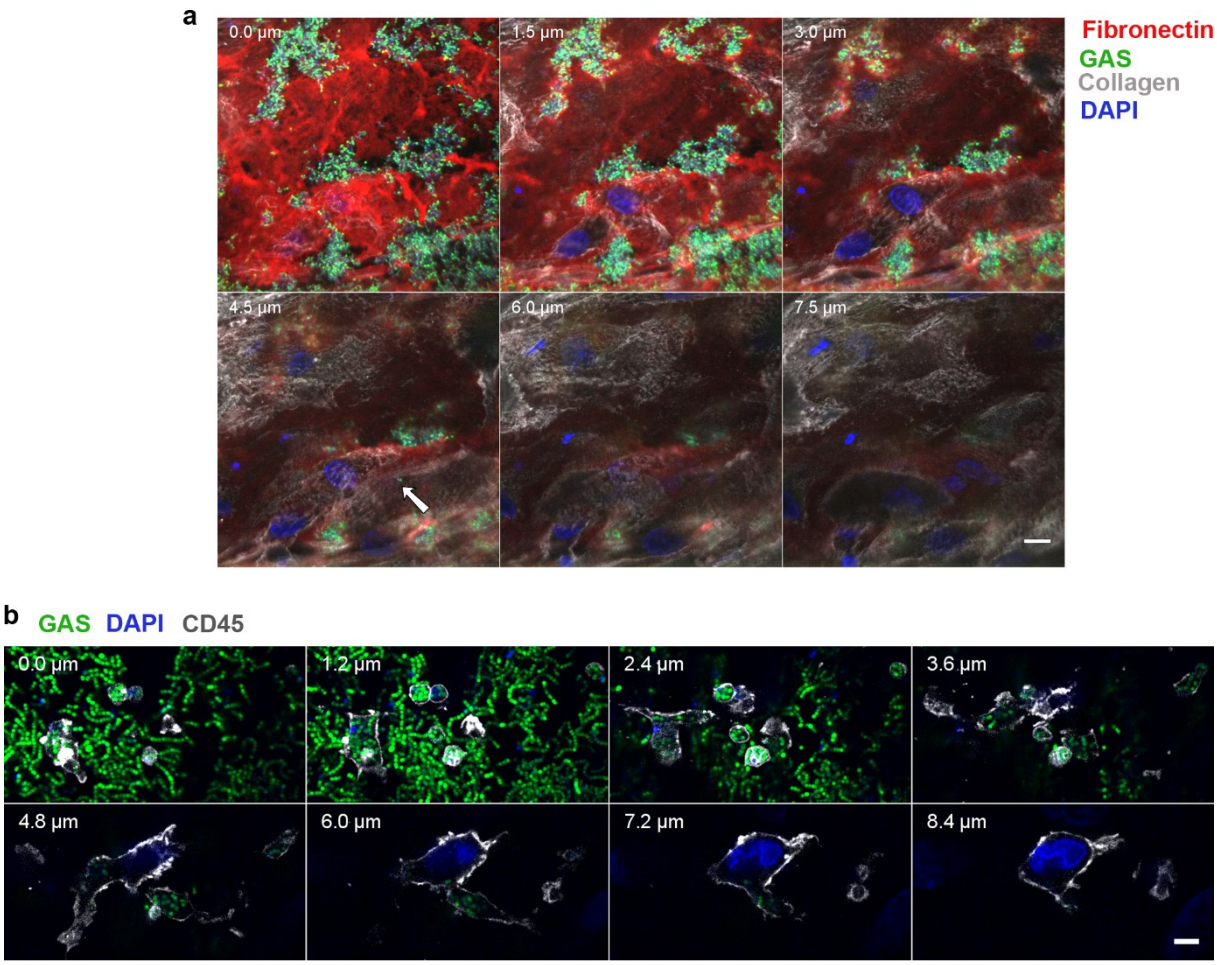

Figure S2. **GAS invades the tissue.** Montages of the same field at multiple depths. On both panels, the depth is indicated at the top left. 0 corresponds to the beginning of the GAS layer and is the first slice shown. **a**, ImageJ montage showing an example of GAS in the tissue. Tissue infected for 16 h under static conditions. Fibronectin, red; type IV collagen, grey; GFP-WT, green; DAPI, blue. A white arrow indicates the position of a GFP-WT coccus in the tissue. Scale bar: 10 µm. Magnification: 40X. Same sample as in Fig. 1a and 2a. **b**, ImageJ montage of GFP-WT inside the tissue and within an immune cell. Tissue infected under flow condition for 3 h. Anti-CD45, grey; GFP-WT, green; DAPI, blue. Scale bar: 5 µm. Magnification: 100 X. Same sample as in Fig. 2e.

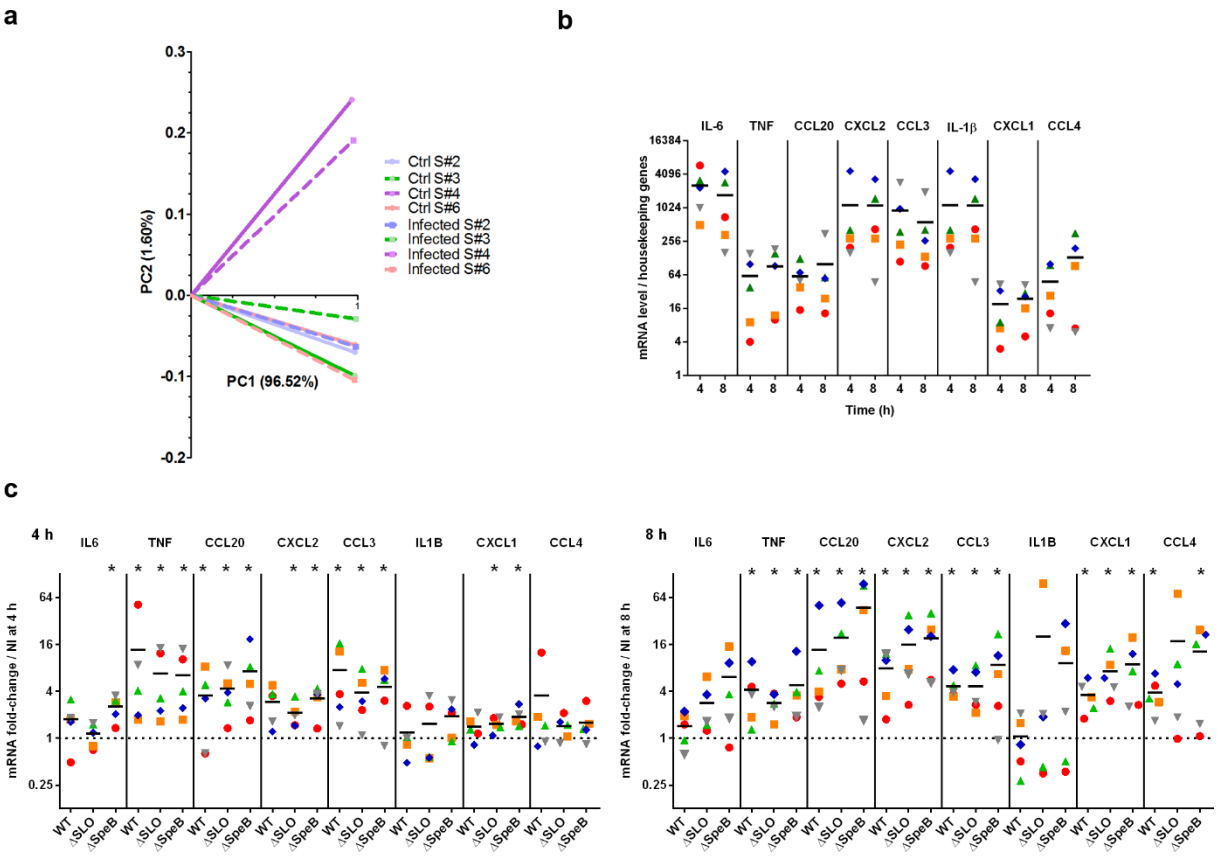

Figure S3. Basal levels and variation in expression of cytokine genes. a, principal component analysis of the basal expression of the 133 immune related genes across all samples showing that that of tissue #S4 differs from those of the other tissues. **b**, Basal level of expression of the indicated immune-related gene in the non-infected conditions compared to the housekeeping genes at 4 and 8 h. **c,** Fold-change variation of the expression of the immune-related genes after infection with the indicated strains for 4 h (left panel) and 8 h (right panel) compared to the non-infected expression. Axis is in log2. S#7, red circle; S#8, orange square; S#9, green triangle; S#10, blue diamond; S#11, grey triangle. Dotted lines correspond to the value of 1. Statistical analysis: Mann-Whitney U test; *, $p<0.05$ as compared to 1, ratio Strain-infected / non-infected conditions.

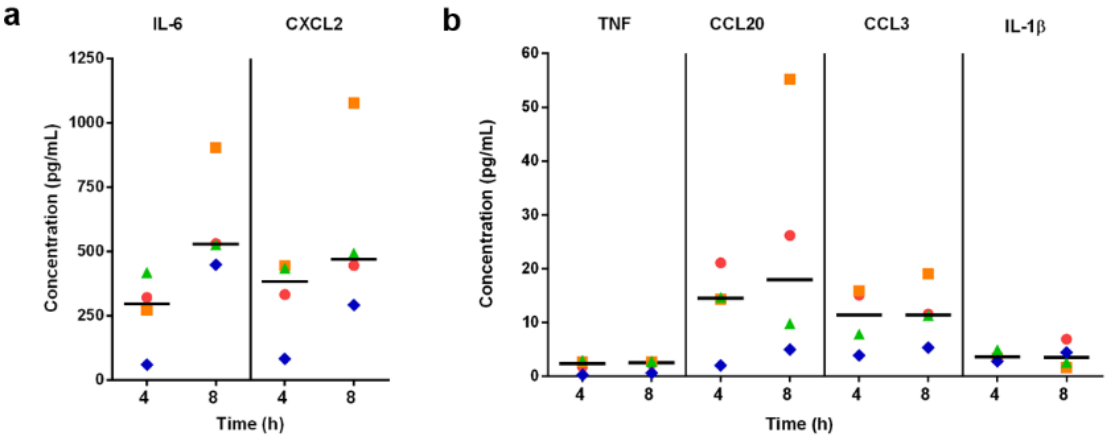

Figure S4. Basal levels of cytokine secretion. a-b, Basal levels of secretion of the indicated cytokine at the indicated time points for supernatant of non-infected decidual tissues. The scales of (**a)** and (**b)** are different. S#7, red circle; S#8, orange square; S#9, green triangle; S#10, blue diamond; S#11, grey triangle.

Table S1 Comparison of the overexpression of genes involved in the immune response

	GAS		GBS	
	mRNA Fold-change	*p-value*	mRNA Fold-change	*p-value*
IL6	3.44	0.2443517	20.08	0.0000001
IL1B	**6.06**	**0.0101306**	**7.79**	**0.0000004**
TNF	**40.37**	**0.0106377**	**32.25**	**0.0000016**
CXCL2	**29.34**	**0.0005470**	**10.46**	**0.0000044**
CCL20	**12.77**	**0.0005246**	**33.91**	**0.0000144**
CXCL8	1.90	0.0911197	4.80	0.0000319
IL1RN	0.94	0.9482826	3.96	0.0000747
CCL4	**111.43**	**0.0032225**	**12.69**	**0.0000815**
IL1A	1.83	0.4538192	6.85	0.0001290
NFKB1	1.11	0.6764782	2.25	0.0001450
ICAM1	2.08	0.4791674	5.01	0.0001730
NFKBIA	2.75	0.0500612	5.51	0.0001780
CXCL3	**28.34**	**0.0000184**	**9.92**	**0.0001850**
TLR2	1.26	0.7816158	4.52	0.0002380
TLR6	1.15	0.7529346	0.43	0.0017900
CCL13	0.76	0.7698270	0.47	0.0018400
NLRP3	2.36	0.0521823	4.39	0.0022200
CCR7	2.62	0.1155378	3.36	0.0064500
CCR1	2.00	0.0623347	0.36	0.0065000
CCL3	**14.52**	**0.0009604**	**4.88**	**0.0072300**
CD80	1.61	0.5656690	3.08	0.0081700
CD14	0.53	0.5807491	0.64	0.0084000
IFNA2	0.84	0.8758766	0.71	0.0125000
CCL2	2.58	0.2099790	2.38	0.0137000
CCL8	1.71	0.5478146	3.10	0.0146000
IL10RA	0.56	0.2238125	1.55	0.0186000
CXCL1	**14.52**	**0.0007640**	**3.20**	**0.0200000**
TICAM1	0.87	0.7283693	1.69	0.0226000
IL23A	**9.47**	**0.0229023**	**13.52**	**0.0229000**
CXCL5	1.48	0.5061415	2.98	0.0233000
IL37	0.64	0.1534900	0.68	0.0356000
CD40LG	2.38	0.3139426	0.74	0.0411000
IL18	1.19	0.7368512	2.15	0.0510000
LTA	0.35	0.2617627	1.42	0.0511000
TLR8	0.94	0.9689146	1.72	0.0609000
CXCR2	0.51	0.3713690	0.54	0.0629000
NOD1	0.78	0.5487833	0.60	0.0639000
CXCR3	1.58	0.4743766	0.77	0.0803000
IL9R	0.23	0.1263553	1.27	0.0815000
IRAK1	0.69	0.3244791	0.74	0.0861000
TLR4	1.40	0.4818540	0.63	0.0879000
TBX21	1.09	0.9344079	0.75	0.0966000
RAG1	0.74	0.5642718	0.80	0.1000000
CSF2	1.18	0.8418437	1.33	0.1030000
IFNGR1	0.74	0.3574953	1.25	0.1120000
STAT3	1.21	0.4820490	1.27	0.1330000
CXCL10	3.57	0.4609962	5.21	0.1360000
TLR1	0.93	0.9379901	0.70	0.1380000
CASP1	0.76	0.7458079	1.42	0.1440000
CD86	0.94	0.9553241	0.64	0.1730000
IL10	**4.73**	**0.0490744**	**1.43**	**0.2190000**

In green and bold the genes significantly upregulated after infection with GAS and GBS compared to tissue non infected; in orange the genes significantly only upregulated after infection with GBS[18]. In red and bold genes only upregulated after GAS infection. Several genes only overexpressed by GBS, such as NFKB1, ICAM, NFKBIA, TLR2, NLRP3, CD80, are related to the ontogeny pathways "cellular response to cytokine stimulus" (GO:0071345, *p* value= $2.4\ 10^{-31}$). Hits were classified in the decreasing order of *p-value* for GBS, until no gene was significantly differentially regulated for GAS and GBS. n=4 for GAS and for GBS.

Table S2 Concentration of inflammatory molecules in the supernatants at 4 h

	4H			
	CT	WT	ΔSlo	ΔSpeB
CXCL2	**323** (81-444 ±84)	**544** (158-1091 ±222)	**167** (42-441 ±92)	**340** (132-629 ±104)
IL1b	**3.7** (2.8-4.9 ±0.44)	**11** (5.2-25 ±4.5)	**9.7** (2.6-18 ±3.3)	**18** (5.7-39 ±7.4)
IL-6	**267** (60-417 ±75)	**346** (46-778 ±159)	**106** (21-145 ±29)	**279** (107-393 ±68)
CCL3	**11** (3.9-16 ±2.9)	**186** (40-481 ±102)	**31** (8-92 ±20)	**82** (18-250 ±56)
CCL20	**13** (2-21 ±4)	**9.6** (2.2-23 ±4.6)	**3.5** (1.6-7.1 ±1.3)	**8.2** (5.1-11 ±1.2)
TNF	**1.9** (0.25-21 ±2.9)	**130** (31-23 ±287)	**23** (3.7-7.1 ±70)	**58** (6.9-11 ±161)

Concentration in pg/mL. Results are expressed as: Mean (minimum-maximum ± standard error). 5 subjects.

Table S3 Concentration of inflammatory molecules in the supernatants at 8 h

	8H			
	CT	WT	ΔSlo	ΔSpeB
CXCL2	**576** (291-1077 ±172)	**932** (153-2311 ±482)	**1115** (487-2115 ±351)	**3078** (410-7190 ±1453)
IL1b	**3.9** (1.6-6.9 ±1.2)	**43** (19-69 ±10)	**49** (15-97 ±18)	**75** (27-154 ±29)
IL-6	**602** (448-904 ±102)	**951** (222-2203 ±432)	**1202** (495-2127 ±401)	**2274** (359-4283 ±853)
CCL3	**12** (5.4-19 ±2.8)	**616** (18-1908 ±437)	**503** (73-761 ±158)	**1202** (279-2192 ±391)
CCL20	**24** (5-55 ±11)	**33** (1.6-85 ±18)	**33** (3.1-79 ±17)	**147** (13-429 ±98)
TNF	**2.1** (0.6-55 ±2.8)	**401** (17-85 ±1090)	**320** (83-79 ±622)	**938** (152-429 ±1798)

Concentration in pg/mL. Results are expressed as: Mean (minimum-maximum ± standard error). 5 subjects.

Table S4 Strains and plasmids used in this study

Strains or plasmid	Relevant properties	Source or reference
Streptococcus pyogenes		
M28PF1	Wild-type representative *emm28* clinical isolate	[31]
ΔSpeB	M28PF1 lacking the *speB* gene coding for SpeB	This study
ΔSLO	M28PF1 lacking the *slo* gene coding for SLO	This study
M28PF1-GFP	M28PF1 with the integrated pG1-lacA-PTetO-gfp	This study
ΔSpeB-GFP	ΔSpeB with the integrated pG1-lacA-PTetO-gfp	This study
Plasmids		
pG+host5	Erm; ColE1 replicon, thermosensitive derivative of pGK12; MCS pBluescript	[26]
pATΩgfp	pAT28 derivative containing the *gfp* gene	[27]
pTCV_TetO	Plasmid containing the tetO tetR Pxyl promoter , inducible with anhydrotetracycline	[28]
pG1-Perm-gfp	pG+host5 containing the *gfp* gene from pATΩgfp	This study
pG1-lacA-Perm-gfp	pG1-Perm-gfp with the lacA intergenic region to allow stable integration in GAS genome	This study
pG1-lacA-PTetO-gfp	pG1-lacA-Perm-gfp with the Erm promoter replaced by the tetO tetR Pxyl promoter of pTCV_TetO. Can be integrated in GAS genome for anhydrotetracycline inducible *gfp* expression	This study

Table S5. Primers used in this study for cloning and checking cloning

Primer Name	Sequence*
F_tetO	GTGGAATTGTGAGCGGATAAC
R_tetO	**GGTACC**TTTTCACTCGTTAAAAAGTTTTGAGAATATTTTATATTTTTG TTCATGTAATCACTCCTTCTTAATCTGTTAACGCTACGATCTAGCT
F_lacA	ACATGATTACGAATTTCAACGACTTCGTATTTACCTT
R_lacA	ACACTCTTAAGAATTCGCGGTCATATCTGAGATGTT
R_extlacA	CCACCATGGGTCCTGATA
RP48	AGCGGATAACAATTTCACACAGGA
SLO-F1	GACTCTAGA**GGATCC**GGTGCCAAAGGGTTTAGAA
SLO-R1	CTCAGGGGGATAAGAGCTGCCGTTAGTAG
SLO-F2	TCTTATCCCCTGAGCCCATATGGTTCGAT
SLO-R2	CATGATTAC**GAATTC**GGGACAGTTGGGGTCAAATC
SpeB-F1	GACTCTAGA**GGATCC**GAGCATCTACTAGCCACAATA
SpeB-R1	GGGTTAGCAAGAACAAATCC
SpeB-F2	TGTTCTTGCTAACCCTTCAACGGTTACCAAAGTGC
SpeB-R2	CATGATTAC**GAATTC**ATTAGTAGGCGTTGATGACC

* restriction enzyme sites are highlighted in bold and sequences used for the In-fusion© cloning are shown in red.

Table S6 List of experiments in which each tissue sample was used

Subject	Figure
S#1	Fig. 1i
S#2	Fig. 1i, Fig. 2b-c, Fig. 4a, Fig. S3a
S#3	Fig. 1i, Fig. 4a, Fig. S3a
S#4	Fig. 1i, Fig. 4a, Fig. S3a
S#5	Fig. 1i, Fig. 2e, Fig. 3e, Fig. S1, Fig. S2b
S#6	Fig. 4a, Fig. S3a
S#7	Fig. 1h, Fig. 3c, Fig. 4c, Fig. S3b-c, Fig. S4, Table S3-4
S#8	Fig. 2b-c, Fig. 4c, Fig. S3b-c, Fig. S4,Table S3-4
S#9	Fig. 1c-d, Fig. 1g-h, Fig. 2b-d, Fig. 4c, Fig. S3b-c, Fig. S4, Table S3-4, Supp video 1
S#10	Fig. 1d, Fig. 1h, Fig. 1k, Fig. 4c, Fig. S1, Fig. S3b-c, Fig. S4, Table S3-4, Supp video 3
S#11	Fig. S3b-c
S#12	Fig. 3g
S#13	Fig. 3e
S#14	Fig. 3e
S#15	Fig. 3g
S#16	Fig. 1a, Fig. 1h, Fig. 2a-c, Fig. 3a, Fig. S2a
S#17	Fig. 1h, Fig. 3d, Fig. 3g
S#18	Fig. S1d-f, Supp video 2
S#19	Fig. 1f, Fig. 3b, Supp video 4
S#20	Fig. 1b
S#21	Fig. 3g

The numbering does not correspond to the order in which subjects were included in the study

Supplementary video:

Supp video 1. GAS multiplication at the tissue surface
Live confocal microscopy. GAS is in green. Magnification: 25X. Scale bar: 20 µm. Time step= 30 minutes. The images are the same as in Fig. 1c.

Supp video 2. Isolated GAS multiplication at the tissue surface
Live confocal microscopy GAS is in green. Magnification: 25X. Scale bar: 5 µm. Time step= 30 minutes. The images are the same as in Fig. 1e.

Supp video 3. Real-time *in situ* phagocytosis of GAS
Live confocal microscopy. GAS in green, CD45 in grey and DNA in blue. Magnification: 25X. Scale bar = 5 µm. Time step= 30 minutes. The images are the same as in Fig. 2d.

Supp video 4. Immune cell blebbing and death after infection
Live confocal microscopy of tissue infected under flow conditions. Intact nucleus, red; permeabilized nucleus (dead cell), blue; CD45, yellow. Magnification: 25X. Scale bar: 10 µm. Time step= 30 minutes.

Additional results and experimental approaches related to manuscript 2

Additional results to Manuscript 2

Involvement of decidual cells in the *ex vivo* bacterial growth

Decidual explants trigger bacterial growth *ex vivo* (Manuscript 2, Fig. 1). While the overall kinetic is conserved between donors (Manuscript 2, Fig. 1d), we observed discrepancies over the 9 fields acquired on one donor tissue (Fig. 1a). Two groups of fields can be distinguished, one that induced high bacterial growth and the other which induced low bacterial growth. We wandered if the immune cell types in the different fields could suggest the origin of such differences. There was no correlation between the number of CD45 positive cells within a field and the growth of GAS (data not shown). However, there was a direct correlation between the number of decidual cells per field and the capacity of bacteria to multiply (Fig. 1b). We therefore investigated if elements secreted by decidual stromal cells were sufficient to trigger bacterial growth. We used primary decidual cells isolated from two donors, and we observed that decidual stromal cells conditioned media were sufficient to trigger GAS growth (Fig. 1c). In conclusion, our results suggest that secreted elements by tissue decidual cells are involved in GAS growth.

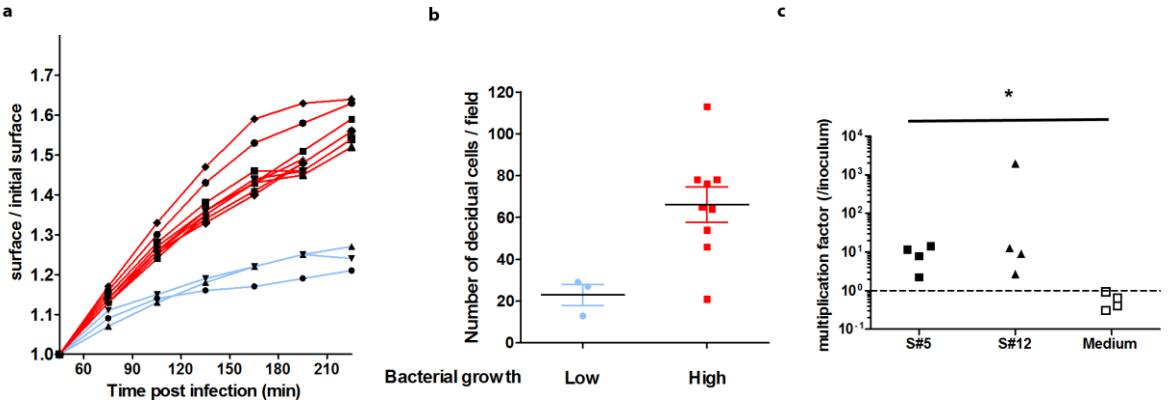

Figure 1 Secreted elements by decidual stromal cells are sufficient to trigger bacterial cell growth a, The increase in the area covered by GFP-producing bacteria on 9 fields of the same acquisition of the same tissue (S#9) are represented. The color code is meant to highlight fields inducing high (red) and low (blue) growth. b, number of decidual stromal cells (vimentin$^+$, CD45$^-$) in each field of (a). c, *in vitro* growth of GAS in primary decidual cells conditioned medium, from two donors (S#5 and S#12). Each experiment was performed 4 times independently in duplicates. Medium corresponds to RPMI. Friedman test with Dunn's multiple comparison test. *, $p<0.05$.

In situ phagocytosis

We observed that two types of cells phagocytosed GAS in infected decidua: large CD45 cells (Manuscript 2, Fig. 2d-e) and neutrophil-like cells (Additional results Fig. 2a). Using live-confocal imaging, we witnessed in real-time in situ phagocytosis of GAS (Manuscript 2, Fig. 2a and supplementary video 3). This suggests that PMN-like cells reach the surface within 15 minutes and phagocytose GAS. We observed neutrophil-like cells (Fig. 2b) filled with GAS in CD45+ vacuoles. The nuclei are condensed and there is a rupture of the plasma membrane in one of the two cells (Fig. 2b).

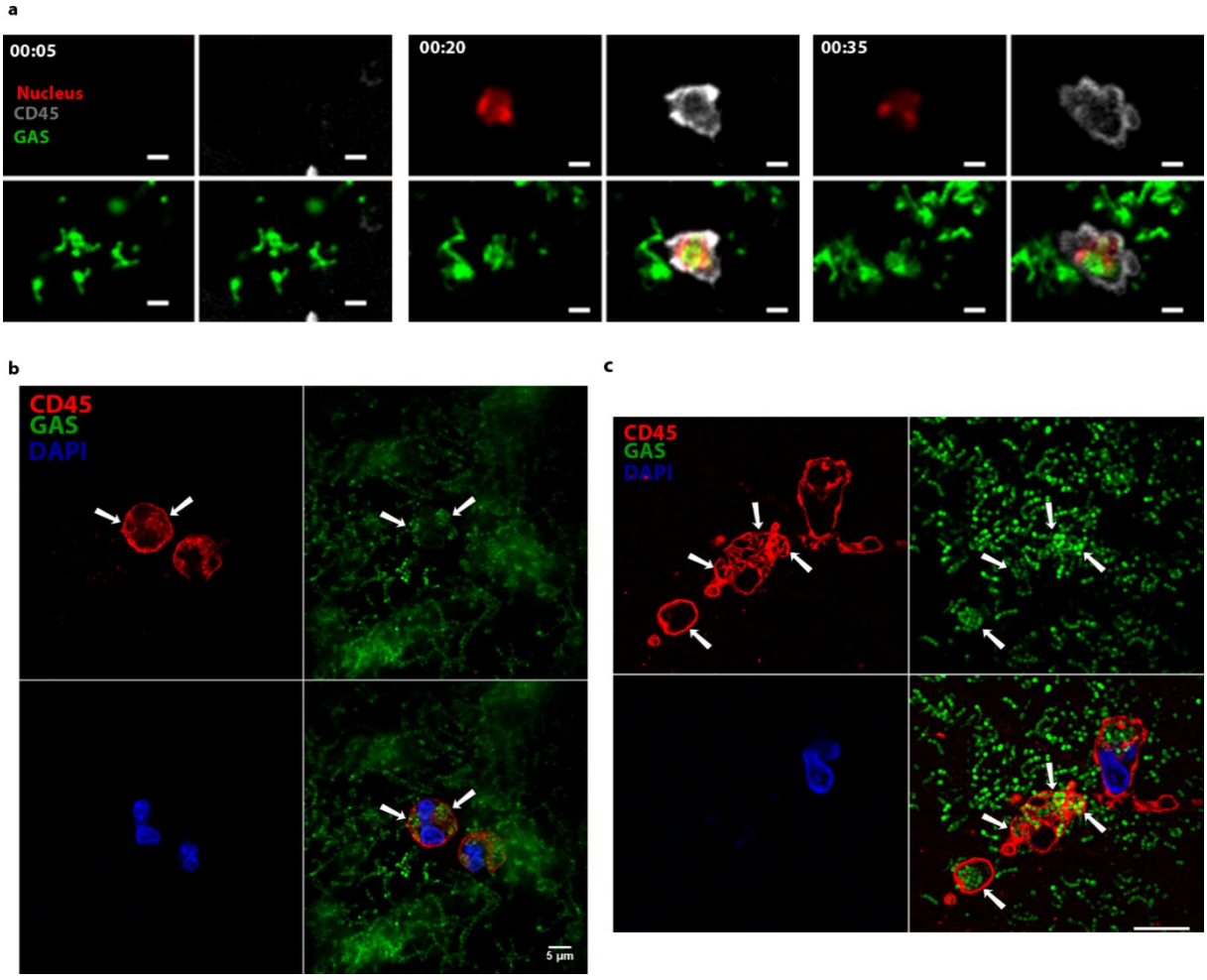

Figure 2 Real-time phagocytosis of GAS and intracellular bacteria surrounded by vacuoles. a, PMN-like CD45+ cells with intracellular GAS at the tissue surface in live confocal microscopy. Live acquisition of an immune cell phagocytosing bacteria on tissue of subject S#7. CD45 in grey; Draq5 in red and GAS in green. Scale bar: 5µm. Magnification: 25X. b, Tissue pre-stained with anti-CD45 antibodies, infected 4 h under static conditions (S#19) showing a neutrophil-like cells with GAS in vacuoles. The arrow shows the membrane rupture. Scale bar: 10 µm; Magnification: 100X. c, Pre-stained tissue (S#5) was infected with GFP-producing bacteria for 1h under static conditions, then 3 h under flow conditions. Macrophage-like cell with GAS in vacuoles, as indicated by arrows. Scale bar: 5 µm; magnification: 100X. GAS in green; CD45 in red; DAPI in blue for b and c.

Large CD45+ cells with large extension present multiple GAS within CD45+ membranes. Since we incubated the sample with anti-CD45 antibodies before the infection, the CD45+ vacuole

corresponds to plasma membrane engulfed with bacteria, suggesting phagocytosis. Cells are filled with bacteria and present an altered nucleus morphology with high condensation, suggesting the phagocytic cell died (Fig. 2c).

We therefore observed GFP-producing bacteria within vacuoles in macrophages and neutrophils *in situ*, suggesting that phagocytic cells efficiently phagocytose GAS. These bacteria appear to escape from these cells after cell lysis through mechanisms we did not assess.

Experimental procedure

***In vitro* growth in decidual cell supernatant.** Decidual cells were isolated and cultured as described in the experimental procedure of Manuscript 1. Decidual cells from two different donors were starved to eliminate residual FBS by removing culture medium, washing once with PBS and adding RPMI 8 h. RPMI was then removed and fresh RPMI was added overnight. Supernatant was collected, and 10^3 bacteria in exponential growth phase were added to 1 mL of decidual cell supernatant or fresh RPMI and incubated 8 h at 37°C, 5% CO_2. GAS was plated and cfus were numbered as described in the experimental procedure of Manuscript 2.

Computer codes used in Manuscript 2

Thickness measurement

This macro takes advantage of the fact that the thickness of an object is proportional to the full width at half maximum (FWHM) of the Gaussian curve of the intensity plot in the axial (depth) direction.

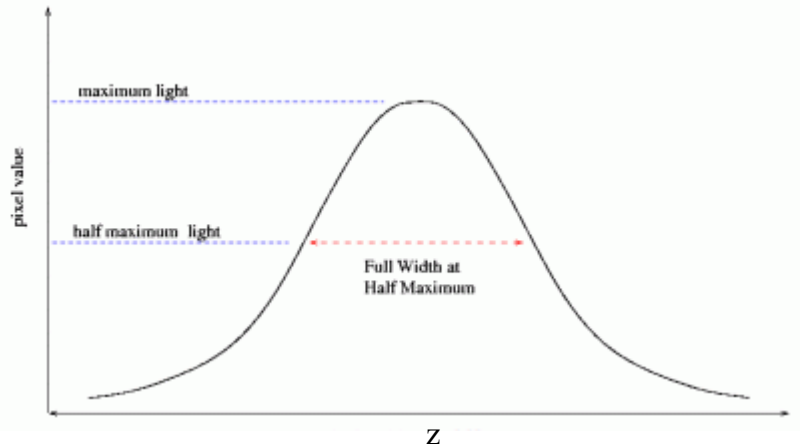

We can therefore estimate the thickness of a bacterial layer by:

- fitting a Gaussian curve
- calculating the FWHM
- transforming this value in µm: for this we calculated the FWHM of isolated bacteria and considered their diameter to be 1 µm

Single bacteria display an intensity curve that is a perfect Gaussian curve in the axial direction (z-axis). However, aggregates of bacteria present a Gaussian curve in the z axis only if the distance between single objects is inferior to the axial resolution, 500 nm. This is locally correct on dense aggregates. Moreover, the bacterial layer is not perfectly flat and homogenous. We therefore need to locally fit a Gaussian curve, on small regions to have accurate measurements of the thickness.

The macro basically subdivides the field in 2500 regions of interest, and fit a Gaussian curve to the z-axis plot of intensity of the GFP signal (bacteria), from which the FWHM is extracted. The macro filters results for Gaussian curves that are incorrectly fitted (R^2 too low etc…). Finally, we have for each of the 2500 regions a value in pixel that is transformed in µm. We then extract the mean value, and repeat the analysis for each time-point of each stage for each donor tissue.

```
//ScanSlideThickness.
//The purpose of this macro is to measure the local thickness of a bacterial layer.
//This macro will fit a gaussian to a zplot signal of a subrectangle of an image and will measure the FWHM of the gaussian, and the complete image will be scanned by this rectangle.
//Written by Antonin Weckel, Institut Cochin, Barriers and Pathogens. February 2018.

start = getTime();
Image_Name = getTitle();
getDimensions(image_width, image_height, image_channels, image_slices, image_frames);
getVoxelSize(voxel_width, voxel_height, voxel_depth, voxel_unit);
//image_slices=image_slices*2;


dir = getDirectory("Choose directory");

u=50;                                   //decide the size of the rectangle for the scanning. u is the division factor, the number of rectangles is u²
dividerW=(image_width/u);
dividerH=(image_height/u);
maxW=dividerW*(u);
maxH=dividerH*(u);

for(frame=1;frame<=image_frames;frame++){    //here one frame is one time point
    setBatchMode(true);
    Stack.setPosition(1, 1, slice);

        if (isOpen("Log")) {
        selectWindow("Log");
        run("Close");
         }

    for (width=0;width<=maxW;width+=dividerW){          //scanning in width
        for (height=0;height<=maxH;height+=dividerH){       // scanning in height
            selectWindow(Image_Name);
            makeRectangle(width, height, dividerW, dividerH);
            fitGaussian();                  // see end of the code for the details. It prints the FWHM in the Log window for each rectangle.
                }                       // end of the loop for the width
            }                           //end of the loop for the height
    selectWindow("Log");
    saveAs("text",dir+"FWHM"+"_"+Image_Name+"_"+slice+".csv");

}             //end of the loop for the slices
```

```
print((getTime()-start)/1000);
////////////////////////////////////////////////////////////////////////////////////////////////////////////////////
function fitGaussian(){                                    //this function calculates the FWHM from the z-axis profile of intensity.
    run("Plot Z-axis Profile", "profile=z-axis");
    rename("Zplot");
        Plot.getValues(x,y);
        selectWindow("Zplot");
    Fit.doFit("Gaussian", x, y) ;
    Fit.plot;
    max=Fit.p(1);                   //max value
    min=Fit.p(0);                   //min value
    delta=max-min;                  // amplitude
    zposition=Fit.p(2);             //position of the max
    //print("max="+max);
    //print("zmax="+zposition);

    sortedParameter = Fit.p(3); // parameter d of gaussian
    rSquared = Fit.rSquared ;
    close();

    FWHM = (2 * sqrt( 2 * log(2) ) ) * sortedParameter ;// http://fr.wikipedia.org/wiki/Largeur_%C3%A0_mi-hauteur
    bact=0;

// here we will filter the results to avoid bad/uncorrect fitting

    if (rSquared>0.7){                  // bad fitting means artefactual fitting
        if(delta>20){                 //amplitude. too small signal corresponds to noise
                if(max<10000){          //too big gaussian
                        if(min>0){     // a signal should not be negative
                            if (zposition>=0 && zposition<=(image_slices*2)){     //zmax peak position. must be within 0 and the nb of slices
                                print("FWHM"+"_"+width+"_"+height+"="+FWHM);          //give the position and value of the FWHμ
                                bact=1;
                            }
                        }
                    }
                }
            }
        if (bact==0){                               //when no bacteria, FWHM=0
            print("FWHM="+0);
                }
    selectWindow("Zplot");
    close();
    }
```

R code for 3D surface heat map.

This surface is generated from the 2500 values of local thickness (from FWHM). To smooth out the surface, every single region was attributed the mean of the values of 4 adjacent tiles.

```
library(plotly)

pathPrep <- function(path = "clipboard") {
  y <- if (path == "clipboard") {
    readClipboard()
  } else {
    cat("Please enter the path:\n\n")
    readline()
  }
  x <- chartr("\\", "/", y)
  writeClipboard(x)
  return(x)
}
pathPrep()
#Replace "Downloads" with the directory where your input file is
folder = pathPrep()

x <- seq_len(nrow(volcano)) + 50
y <- seq_len(ncol(volcano)) + 50
col3 <- c(`0` = "blue", `5`="white", `10` = "orange", `20` = "red", `30` = "black")
axx <- list(
  nticks = 10,
  range = c(50,100)
)

axy <- list(
  nticks = 10,
  range = c(50,92),
  title=" "
)

axz <- list(
  title="m",
  nticks = 5,
  range = c(0,15)
)
m <- list(
  l = 0,
  r = 0,
  b = 0,
  t = 0,
  pad = 0)

input.file = "FWHM value T10.csv"
lieu<-paste(folder,"/",input.file,sep="")
mat2 <- read.csv(lieu,header=FALSE,sep=";")
test<-as.matrix(mat2)
p=plot_ly(x = ~x, y = ~y, z =test,text= "T10", width = 900, height = 300,
type="surface",showscale=T, cmin=0, cmax=9, cauto = F, autocolorscale=F,colorscale=col3

        )%>%layout(autosize=F, margin = m, scene = list(aspectmode = "manual", aspectratio =
list(x=1.5, y=1.05, z=0.225),xaxis=axx,yaxis=axy,zaxis=axz, camera=list(eye = list(x = 0.005, y
= 1, z = 0.5))))
p
```

Measurement of cytotoxicity

This macro is a 3D segmentation of nuclei based on intensity and morphology (Plug-in 3D object counter) to count TUNEL positive (dead cells) and DAPI positive nuclei (all cells). To avoid false positive in the DAPI channel that also contains the signals from bacteria that could be interpreted as nuclei, there is a small step where we exclude the first stacks of the image containing only bacterial signal, and an “open” treatment of the binary signal (which “erases” sharp structures such as bacteria).

```
// macro tunnel counting made for 20X pictures, bin=2
//CHANGE are places where the user needs to change in the text the value for each image analysis. Not user friendly, sorry. lines 41,45,81
//Copyright Antonin Weckel, Institut Cochin

//unspecific setting up
run("Close All");
setForegroundColor(0,0,0);
setBackgroundColor(255,255,255);
setOption("BlackBackground", true);

if (isOpen("Log")) {
     selectWindow("Log");
     run("Close");}

// specific set up
dir = getDirectory("Choix du r@pertoire contenant les images");

Dialog.create("nom de la manip");
Dialog.addMessage("attention aux caracteres utilises,pas nom du canal");
    Dialog.addString("nom manip","a remplacer");
    Dialog.show();
filename=Dialog.getString();

Dialog.create("nombre de fichier à mesurer");
    Dialog.addString("nombre","a remplacer");
    Dialog.show();
nb=Dialog.getString();

// beginning of the macro
//the channel with TUNEL staining is analyzed with 3D bject counter
for (h=1;h<=nb;h++){
        numero=h;
    filenamenumber=filename+numero;
    name488=filenamenumber+"_w2491"+".TIF";
    direct488=dir+name488;
    open(direct488);
```

```
    open(direct488);
    selectWindow(name488);
    run("Subtract Background...", "rolling=30 stack");
// security check: 3D oject counter induces bugs if you have thresholded above the maximun value presented in the image. So the macro can only be run if one px>threshold
    run("Z Project...", "projection=[Max Intensity]");
    getRawStatistics(nPixels, mean, min, max);
    if (max>=220){                                  //the maximum value of the zprojection is the maximum px present in all the image. CHANGE
        close();
        selectWindow(name488);
    run("3D Objects Counter", "threshold=300 slice=33 min.=700 max.=16233360 objects summary");}       //CHANGE the threshold
    else {                      //if no px above threshold,no positive nuclei
        print(name488+"no object");}
    }

selectWindow("Log");

savefilename=filename+"_"+"number TUNEL positive nuclei"+".csv";
    saveAs("text",dir+savefilename);
    close();

if (isOpen("Log")) {
     selectWindow("Log");
     run("Close");}

// beginning of the analysis of the DAPI image: all the nuclei
count405=newArray(0);
h=getNumber("if bacteria, say 1, else 0",1);
for (i=1;i<=nb;i++){
    filenamenumber=filename+i;
    name405=filenamenumber+"_w3405"+".TIF";
    direct405=dir+name405;
    open(direct405);
    selectWindow(name405);
    z=nSlices;
    slicestart=1;
```

```
    slicestart=1;

    if (h==1){                                                  //image with bacteria which are not nuclei but DAPI+
    waitForUser("choose the number of the first slice to start analysis");
slicestart=getNumber("slice start",1);
    }
run("Duplicate...", "title=subs duplicate range=" + slicestart + "-" + z);          // we analyze the image starting at the top of nuclei, not top of bacteria
rename("subs"+name405);
    run("Subtract Background...", "rolling=30 stack");
    setAutoThreshold("Default dark");
//run("Threshold...");
setThreshold(60, 4800);                                                 // CHANGE
setOption("BlackBackground", true);
run("Convert to Mask", "method=Default background=Default black");
run("Options...", "iterations=2 count=1 black pad edm=8-bit do=Open stack");                // small trick to get rid of non ellipsoid small patches of bacteria
run("3D Objects Counter", "threshold=128 slice=28 min.=700 max.=13773760 objects summary");
}
selectWindow("Log");
savefilename=filename+"_"+"nombre noyau"+".csv";
    saveAs("text",dir+savefilename);
run("Close All");
```

Analysis of the 3D position of GAS

This macro segments bacterial particles from the maximum z-projection of the GFP signal. Each particle is a Region of Interest (ROI).

For each particle, the z-position is calculated from the maximum of the z-axis intensity plot (Find Peak plug-in on the z-axis profile). The position of collagen and fibronectin is analyzed at the same ROI in a similar way. Z-position of the different elements are compared: if the z-position of the bacterial particle is lower than collagen or fibronectin (the most superficial element), with a distance superior to 1.2 µm, the bacteria is considered as “invading particle”. Though we did not use it in the manuscript, this macro also exports the distances between invading particles and the topical signal, and the size of the particles.

Since cellular granules have sometime the same intensity as GFP-producing bacteria (due to autofluorescence, autoF), particles are filtered to check they are bacteria by analyzing the presence of a DAPI (DNA) signal in the vicinity of the GFP signal (they should overlap).

```
//macro3Dbacteriaposition. Developped by Antonin Weckel, INSERM u1016, Institut Cochin, Paris, FRANCE. Last modified:March 2018
//Objectives: Identify the number of bacterial particule found within the tissue
// Pipeline: 1) bacteria are thresholded in a z-max projection of the 491 channel, particules are segmented and ROI list is saved.
//  2) For each ROI, the z position of the bacteria (zbact) is determined through the "Find peaks" plugin applied to Z-axis profile. If two bacteria are one on another (two peaks), the zbact corresponds to the deepest peak.
//  3) ROI are checked for behind real bacterial signal and not autofluorescence. For each ROI, DNA peaks are analyzed and the absence of a DNA peaks in the vicinity of the bacterial peaks exclude the ROI of the macro. The number of excluded events is indic
//ROI number of excluded events can be retrieved with a specified line.
//  4) Z position of objects of interest in the channel 635 and 591 are determined (z591 and z635) with "Find Peaks". This time, the closest object to the surface (smaller z) is kept.
//  5) Z position of filtered ROI is compared to z635 and z591, in this order. Bacteria are considered below z635 and z591 if they are 3 stacks below (1.2 µm ).

setForegroundColor(0,0,0);
setBackgroundColor(255,255,255);
setOption("BlackBackground", true);
dir = getDirectory("Folder containing images");              // folder where images are, and where the output files will be saved
list = getFileList(dir);
firstimage=0;
for (fileposition=0;fileposition<list.length;fileposition++){   //this a line which gives me automatically the name of all the files in a folder
    if (endsWith(list[fileposition],"nd")==1){
        filenamenumber=substring(list[fileposition],0,9);          //check this line, depends on the length of the name
        name488=filenamenumber+"_w3491"+".TIF";
    name561=filenamenumber+"_w2561"+".TIF";
    name635=filenamenumber+"_w1635"+".TIF";
    name405=filenamenumber+"_w4405"+".TIF";

    direct488=dir+name488;                    //image directory
    direct635=dir+name635;
    direct561=dir+name561;
    direct405=dir+name405;

    print(name488);// the value to segment images is only determined on the firstimage
                // This is the different file Main loop.

    //Initiation of the macro
    if (isOpen("Results")) {
     selectWindow("Results");
     run("Close");
     }
      if (isOpen("Log")) {
         selectWindow("Log");
         run("Close");
     }

     if (isOpen("Plot Values")) {
         selectWindow("Plot Values");
         run("Close");
     }
    if (isOpen("NumÃ®ro des particules en invasion")) {
         selectWindow("NumÃ®ro des particules en invasion");
         selectWindow("NumÃ®ro des particules en invasion");
         run("Close");
     }
    if (isOpen("ROI Manager")) {
         selectWindow("ROI Manager");
         run("Close");

     }
     if (isOpen("NumerobactérieInv")) {
         selectWindow("NumerobactérieInv");
         run("Close");
     }

//Initiation of the variables
        nbpartunder=0;
        nbbactunder=0;
        nbbactériesunder=0;
        nbpartcolo=0;
        nbbactcolo=0;
        nbmatrice=0;
        nbbactmatrice=0;
        Nbpart=0;
        m=0;

//to be checked for every acquisition
amplitude488=40;
amplitude405=30;
amplitude635=80;
amplitude561=30;

filenamenumber=filename+h;                  //incrementation of the filename
name488=filenamenumber+"_w3491"+".STK";
name561=filenamenumber+"_w2561"+".STK";
name635=filenamenumber+"_w1635"+".STK";
name405=filenamenumber+"_w4405"+".STK";

direct488=dir+name488;                      //image directory
direct635=dir+name635;
direct561=dir+name561;
direct405=dir+name405;
if (File.exists(direct488)) {
open(direct488);

run("Duplicate...", "duplicate");                  // I work on a duplicated image to apply a threshold on it
rename("488analyse");

// the deeper we get, the bigger chance we have to find autoF granules. Since no bacteria can be found very deep, we only look for bacteria on the first 30µm
```

```
// the deeper we get, the bigger chance we have to find autof granules. Since no bacteria can be found very deep, we only look for bacteria on the first 30µm
if (nSlices>90){
run("Z Project...", "stop=90 projection=[Max Intensity]");
}
else {run("Z Project...", "projection=[Max Intensity]");}


run("Mean...", "radius=1");
 setAutoThreshold("Default dark");

//If it is the first image, the user is asked to give a threshold value (minthreshold)
if (firstimage==0){
    beep;
    waitForUser("Check threshold ");
    Dialog.create("min threshold bacteria");
Dialog.addMessage("it must be a number");
    Dialog.addString("min threshold value","200");
    Dialog.show();
minthreshold=Dialog.getString();
firstimage=1;                          //at the next image h, the thresh will not be asked
}

//run("Threshold...");
setThreshold(minthreshold, 4200);
setOption("BlackBackground", true);
run("Convert to Mask");
run("Watershed");                          // I add a Watershed to decrease the size of the particles analyzed
run("Analyze Particles...", "size=30-Infinity showsNothing display clear include summarize add");
roiManager("Show All with labels");

n = roiManager("count");          // n is the number of particules
Arrayunder = newArray(n);    //array containing the particules invading


open(direct635);
open(direct561);
open(direct405);

//on the microscope I use, the 405 channel is not at the same z position as the other channels so it is essential to correct it through a translation of 4 voxels. Noise induces false peaks, always better with a substract background
selectWindow(name405);
run("Subtract Background...", "rolling=50 stack");
run("Transform2 Translate", "x-distance=0.0 y-distance=0.0 z-distance=4 voxel interpolation=Linear background=0.0");
rename("405translated");
setMinAndMax(0, 1306);

 selectWindow(name405);
    run("Close");
```

```
    run("Close");


// Step 2. Loop on every single ROI
for (i=0; i<n ; i++) {
    tooclose=0;
    z635=0;
    nopeaks635=0;
    nopeaks561=0;
    z561=0;
    zbact=0;
    Zint=0;
    Zint561=0;
    tempzbact=0;
    a1=newArray(1);
    selectWindow(name488);
    roiManager("Select", i);
    getStatistics(area);
    m=area;
    run("Plot Z-axis Profile");
    rename("Z-axis profile"+name488);
    run("Find Peaks", "min._peak_amplitude=&amplitude488 min._peak_distance=0 min._value=[] exclude max._value=10 list");          //The amplitude depends on every acquisition. Change it before the run
    selectWindow("Z-axis profile"+name488);
    run("Close");
    selectWindow("Plot Values");
    listbacteria=FindPeaksList(a1);        //listbacteria contains the value of the peaks of bacteria. See function description for details


    if (listbacteria.length>1){            // if more than one peak, we check if the peaks are close or not. when too close, DNA peaks can't be resolved
        for(u=1;u<a1.length;u++){
                tempu=u+1;
                delta=abs(parseInt(listbacteria[u])-parseInt(listbacteria[tempu]));
                if ((parseInt(delta))<9){
                            tooclose=1;               //this is a security. Too close peaks in 491 sometimes induce DNA peaks tha merge.
                        }
            }
    }
    if(listbacteria.length==1 && listbacteria[0]!=0){
        zbact=parseInt(listbacteria[0]);      //when there is one peak, zbact equal to the only peak position
    }

    if(listbacteria.length>1) {
        Array.getStatistics(listbacteria, min, max, mean, stdDev);
        zbact=parseInt(max);                        // when several peaks, the deepest is taken (max value of listbacteria1)
                    }

     close("Peaks*");
```

```
    close("Peaks*");
    //canal DNA 405. Step 3              Here the main idea is that cells granules are highly autof, and the peak of a granule can be mistaken as bacteria. There is no DNA in a granule, in contrast to bacteria
    bact=0;         // when 0, bacteria is not a bacteria. when 1, we have confirmed it is a bacterium.
    selectWindow("405translated");
    roiManager("Select", i);
    run("Plot Z-axis Profile");
    rename("Z-axis profile"+"name405");
    run("Find Peaks", "min._peak_amplitude=&amplitude405 min._peak_distance=0 min._value=[] exclude max._value=10 list");
    selectWindow("Z-axis profile"+"name405");
    run("Close");
    selectWindow("Plot Values");
    a1=newArray(1);
    listdna=FindPeaksList(a1);

    if(tooclose==0){
        if(listdna.length==1 && listdna[0]!=-1){              //there is only one DNA peak
        zDNA=parseInt(listdna[0]);
            if ((zbact-8)<=zDNA && (zbact+8)>=zDNA) {          //the DNA peak is close to the bacteria peak
                bact=1;                                 // when bact==1, we confirm the ROI is a bacterium
                }
            else if (listbacteria.length>1){               //there is more than a bacteriapeak
            for (t=0;t<listbacteria.length;t++){              // we go back to the list of bacteria peak to check if one correspond to the DNA peak
            tempzbact=parseInt(listbacteria[t]);
                if ((tempzbact-8)<=zDNA && (tempzbact+8)>=zDNA) {
                bact=1;
                zbact=tempzbact;                    // the "correct" bact peak is saved. if it exists
                }
            }
        }
    }


        if (listdna.length>1 && listbacteria[0]!=-1){                    // there are several DNA peaks. Some can come from nuclei.
            for (t=0;t<listbacteria.length;t++){                 // we check if any bacterial peak correspond
                tempzbact=parseInt(listbacteria[t]);
                    for (g=0;g<listdna.length;g++){                    //we check all the dna peaks correspondence to a bacterial peak.
                if ((tempzbact-8)<=listdna[g] && (tempzbact+8)>=listdna[g]) {
                    zbact=tempzbact;
                    bact=1;
                        }
                }
            }
        }
    }

    if (bact==0){                               // this is to check the particule that were disqualified as no DNA
        print("Not a bacterium"+i+1);
```

```
    }

    //channel 561 (beginning of step 4)
    selectWindow(name561);
    roiManager("Select", i);
    run("Plot Z-axis Profile");
    rename("Z-axis profile"+name561);
    run("Find Peaks", "min._peak_amplitude=&amplitude561 min._peak_distance=0 min._value=[] exclude max._value=10 list");     //this is the line to change at ever acquisition. Amplitude varies
    selectWindow("Z-axis profile"+name561);
    run("Close");
    selectWindow("Plot Values");
    a1=newArray(1);
    list561=FindPeaksList(a1);

    if(list561.length==1){                // either there is no peak, or one peak
        if(list561[0]==-1){               // no peak
        nopeaks561=1;
        }
        else {
    z561=parseInt(list561[0]);            // one peak, so z561 gets this unique value
        }
    }

    if (list561.length>1){                //several 561 peaks
        Array.getStatistics(list561, min, max, mean, stdDev);
        z561=parseInt(min);            //the peak the closest to the surface is taken into account
        }


    close("Peaks*");

    //canal fibronectine 635
    selectWindow(name635);
    roiManager("Select", i);
    run("Plot Z-axis Profile");
    rename("Z-axis profile"+name635);
    run("Find Peaks", "min._peak_amplitude=&amplitude635 min._peak_distance=0 min._value=[] exclude max._value=10 list");
    selectWindow("Z-axis profile"+name635);
    run("Close");
    selectWindow("Plot Values");
    a1=newArray(1);
    list635=FindPeaksList(a1);

    if(list635.length==1){                //symetric to 561 analysis
        if(list635[0]==-1){;
        nopeaks635=1;
        }
```

```
        }
        else {
    z635=parseInt(list635[0]);
        }
    }

    if (list635.length>1){
        Array.getStatistics(list635, min, max, mean, stdDev);
        z635=parseInt(min);
        }

    //Step 5. the zbacteria position is compared to the other elements of the tissue
    if(bact==1) {                  //it is a bacterium with a 491 peak and a DNA peak
        if(nopeaks635==1){                 // no 635 element
            if(nopeaks561==0) {               // but a 561 element
                if (zbact-3>z561){
                nbpartunder=(nbpartunder+1);
                    nbbactunder=nbbactunder+(m/37);
                    Zint561=((zbact-z561)*0.3);
                        print("ROI under 561 signal"+i+1+" &"+" distance to 561 peak= "+Zint561);
                }
                else if   (zbact-3<=z561) {
                nbpartcolo=nbpartcolo+1;
                nbbactcolo=nbbactcolo+(m/37);
                    }
            }
                if(nopeaks561==1){                // no 561 element
                nbpartcolo=nbpartcolo+1;
                nbbactcolo=nbbactcolo+(m/37);
            }
        }

        if(nopeaks635==0){                //a 635 peak
                if(nopeaks561==0) {               // and a 561 peak
                    if(zbact-3>z561){             //bacteria below 561
                    nbpartunder=(nbpartunder+1);
                    nbbactunder=nbbactunder+(m/37);
                        if (z561<=z635){                //when 635 peak is above 561 peak
                            Zint561=((zbact-z561)*0.3);
                            print("ROI under 561 signal is:"+i+1+" &"+" distance to 561 = "+Zint561);             // distance bacteria to surface = distance bacteria 561
                        }
                        if (z561>z635){                                 // distance bacteria to surface= distance to 635
                            Zint561=((zbact-z635)*0.3);
                            print("ROI under 561 signal is:"+i+1+" &"+" distance to 635= "+Zint561);
                        }

                    }
```

```
                }
                else if ((zbact-3)>z635){
                nbmatrice=nbmatrice+1;
            nbbactmatrice=nbbactmatrice+(m/37);
            Zint=((zbact-z635)*0.3);
                    print("ROI under 635 signal is:"+i+1+" &"+" distance to 635 = "+Zint);
                    }
            else if((zbact-3)<=z561){           // we consder z635>z561
            nbpartcolo=nbpartcolo+1;
            nbbactcolo=nbbactcolo+(m/37);
                    }
                }

            if(nopeaks561==1){     //635 peak but no 561 peak
                if ((zbact-3)>z635){
                nbmatrice=nbmatrice+1;
            nbbactmatrice=nbbactmatrice+(m/37);
            Zint=(zbact-z635)*0.3;
                    print("ROI under 635 signal is:"+i+1+" &"+" distance to 635= "+Zint);
                                    }
            if((zbact-3)<=z635){
                            nbpartcolo=nbpartcolo+1;
            nbbactcolo=nbbactcolo+(m/37);
                    }
                }
            }
        }

    close("Peaks*");
}
Nbpartinv=nbpartunder+nbmatrice;
Nbbactinv= nbbactmatrice+nbbactunder;
Nbpart=(nbpartcolo+Nbpartinv);
Nbbact=(Nbbactinv+nbbactcolo);

print(filenamenumber);
print("");
print ("Number of particles invading= "+Nbpartinv);
print ("Number of particle colonising= "+nbpartcolo);
print("Total number of particules= "+Nbpart);
print("");
print("Number of bacteria invading= "+nbbactmatrice);
print("Number of bacteria colonising= "+nbbactcolo);
print("Total number of bacteria="+Nbbact);

print("");
print("threshold GFP= "+ minthreshold);
```

```
print("");
print("threshold GFP= "+ minthreshold);
print("amplitude 488= "+ amplitude488);
print("amplitude 405= "+amplitude405);
print("amplitude 561= "+amplitude561);
print("amplitude 635= "+amplitude635);

if(Nbpart!=n){
    print(Nbpart-n);
}
selectWindow("Log");
saveAs("text",dir+"macropos"+filenamenumber+".csv");

roiManager("deselect");
     roiManager("save", dir+"macropos"+filenamenumber+".zip")

run("Close All");
beep;
// end of the Loop for the particules
}
}// end of the Loop for the particules
}
beep;
print((getTime()-start)/1000);
//////////////////////////////////////////////////////////////////////////////////////////////////////////////////////////////////////////////////////////////////////////////////////////////////////////
function FindPeaksList(a1){

    lines = split(getInfo(), "\n");                  //creates an array (named Lines) that contains all the value of the columns of the Plot Values window which is the output window of the "Find peaks" plugin
    values = split(lines[1], "\t");          // values contains an array with the data of the first Line.
    N=values.length;             // N corresponds to the number of columns in the second Line of the array "Lines", because Lines[0] are the head

    if (N<4){                // there is no peak found. Therefore we give to a1[0] a negative value.
    a1[0]=-1;
    }
    if (N>=4){          //when there is no peak, N=2. One peak: N=4. More than one peak: N>4. nobact=1 only if there is a peak of bacteria that is found.
        a1[0]=values[2];                //a1 is the initiation values of the peaks position of the different bacteria in a ROI. values[2] is the position of the first peak
        for(u=2;u<=10;u++){            //scan all the Lines (zpeak position and y value). There is never more than 10 peaks
            valuesbis = split(lines[u], "\t");       // valuesbis contains the data of the u Line
            Nbis= valuesbis.length;
            if (Nbis>=4){                  // there is a u-th peak
                r=valuesbis[2];              // r will change at every u position. It is the value of the u-th peak found.
                a1=Array.concat(a1,r);            // this array concatenate all the z position of the peaks
                }
            }
    }
                return a1;
}
```

Discussion

Discussion and perspectives

GAS is responsible for a wide range of diseases and is able to infect multiple and diverse tissues (skin, pharynx, endometrium). It infects people of all age groups, ethnicities and sex. More than 200 GAS *emm*-types have been described (15), they present diverse and distinct repertoires of virulence factors. There is no single hypervirulent strain of GAS and the proportion of the different *emm*-types involved in invasive infections is dynamic, with several clones emerging in the past decades, after acquisition or loss of different factors (capsule, Sda1 etc…). These emerging clones are involved in the increase of the number of GAS invasive infections in developed countries (580, 581) and they indicate that GAS strains are still evolving and adapting to the human host. GAS harbors a very complex network of virulence factors acting with one another. These factors present functional redundancy, as shown with the number of fibronectin binding proteins. Moreover, GAS virulence factors are tightly regulated (Introduction 2.2). Consequently, GAS is fully equipped to face various environments. Host genetic background (528) and local parameters (inflammation, trauma, breach, post-partum) are already-known risk factors for superficial and/or invasive infections. Yet why certain individuals suffer from invasive infections is still not understood.

The main focus of our research team is the establishment of GAS invasive infections, with the endometritis as a model. Interestingly, GAS barely colonizes the human vagina in contrast to other bacteria (539). A recent report showed that women with previous GAS genital infections had a higher carrier stage than a control group, suggesting that particularities in some women favor their colonization with GAS, increasing the risk for GAS endometritis (582). GAS appears to take particularly advantage of the postpartum compared to other bacteria colonizing the woman gyneco-obstetrical sphere and the number of cases dropped due to current prophylactic measures (31). To understand the origin of GAS infections in the postpartum, it is important to consider the specificity of this context, and how it favors GAS infections (583). While in our studies we considered the specific cells from the tissues involved in the onset of GAS endometritis (cervical, endometrial, decidual stromal and immune cells), we did not consider other factors that are very specific of the postpartum, such as the pH, that could be critical for GAS pathogenesis (583).

To explore the mechanisms involved in GAS endometritis, we developed during this PhD two complementary research axes analyzing diverse aspects of GAS pathogenesis. Binding to host epithelium (endometrium, skin or pharynx), through R28 among other direct

and indirect adhesin-mediated bindings, is critical to infection. In the presence of a breach, after epithelium disruption or in any situation where the stroma is accessible to GAS, the multiple steps we characterized are critical.

Direct interactions with integrins and their implications in pathogenesis

The N-terminal domain of R28 binds to three integrins, α3β1, α6β1 and α6β4. Integrins are plasma membrane dimers with one β and one α subunit; there are 9 types of β subunits and 24 types of α subunits and altogether 24 different integrins (584). Integrins promote cell binding to the extracellular matrix, and their ligands are fibronectin, vitronectin and laminins (585). α3β1, α6β1 and α6β4 integrins are laminin binding integrins (586). We could investigate if R28 competes with laminins (and *vice-versa*) to bind integrins.

Integrins exist under two conformations, active or inactive and natural ligands often bind a defined biochemical region overlapping the α and β subunits, accessible only when the integrin is in the active form (584). Divalent cations change the conformation of integrins to the active form and the binding of ligands to integrins is partly mediated by these divalent cations. $R28_{Nt}$ does not require divalent ions to bind integrins indicating it can bind the inactive form of integrins. Since $R28_{Nt}$ binds to a lesser extent integrins α3β1 and α6β1 in the presence of divalent cations, this suggests that the affinity of $R28_{Nt}$ for integrins is lower in the active form than in the inactive form. All this indicates that R28 does not bind to the exact same site as laminins.

Intracellular domains of integrins bind to the cytoskeleton and are involved in the transduction of outside-in signals: α3β1 and α6β1 bind to actin, and α6β4 to intermediate filaments (585). Binding of natural ligands or inside-out signals induce integrins to change from the inactive to the active form. In our experiments, $R28_{Nt}$ did not induced intracellular transduction of signals as evaluated by assaying the phosphorylation of several proteins of classical downstream pathways of integrin activation (such as FAK), but our results were not conclusive and will require more sensitive approaches. Ligand binding to integrins can induce the internalization of bound elements (see Introduction 3.1.3). We looked for the effect of $R28_{Nt}$ on the internalization of coated beads and found no difference between $R28_{Nt}$-coated beads and the controls. In contrast to natural ligands such as laminins, $R28_{Nt}$ may bind to a domain on integrins that does not change the activation state of the integrins, explaining absence of effects on the internalization and intracellular transduction.

The integrins α3β1, α6β1 and α6β4 are receptors of $R28_{Nt}$ and are most probably not its sole receptors. Silencing simultaneously the β1 and β4 integrins did not significantly reduce the binding of $R28_{Nt}$ to HEC-1-A cells (data not shown). $R28_{Nt}$ significantly binds to K562 hematopoietic cells, which express only the α5β1 integrin (data not shown). This confirms that on HEC-1-A cells and other cell lines, α3β1, α6β1 and α6β4 might not be the sole receptors of $R28_{Nt}$.

Few GAS proteins bind directly to integrins: so far, only one variant of SpeB and the SclI proteins have been shown to bind to integrins (93, 330, 331); GAS interaction with α3β1, α6β1 or α6β4 was not described. Therefore R28 completes the vast repertoire of adhesins of *emm28* strains by binding to integrins not bound by already described adhesins, promoting adhesion to several epitheliums.

To our knowledge few bacterial adhesins bind directly α3β1, α6β1 or α6β4 integrins. Only *Yersinia pestis* invasin directly binds to both the integrins α3β1 and α6β1 (587) and the BBB07 and BB172 proteins of *Borrelia burgdorferi* directly bind to α3β1 (588, 589). Among viral proteins, the glycoprotein B (gB) of *Herpesviridae* binds directly to α3β1 and α6β1, the gB of cytomegalovirus directly binds to α6β1 (590, 591) and Adenovirus Serotype 5 penton base protein directly binds to α3β1 (592). No direct interaction between a viral, fungal or bacterial protein with α6β4 has been described so far. No bacterial interaction with cells was described to involve α6β4, but several viruses might interact with this integrin (593). A protein binding any of these three integrins is not only unique among GAS, but also rare among bacterial and viral pathogens. The mechanism of $R28_{Nt}$ binding to these integrins has therefore no equivalent in other organisms and this interaction warrants further structural, biochemical and mechanistic studies.

Ex vivo infection of the decidua: strength and limits of an original model

We developed a novel model of *ex vivo* infection of a human tissue, the decidua. The tissue comes from healthy subjects, it is a normally sterile tissue. The fibronectin layer provides an early abundant source of adhesion, which allows the infectious bacteria to settle. Decidualization is the differenciation of stromal endometrial cells in specialized cells, which support embryo growth and maintain early pregnancy (594). As described in the introduction, half of the endometritis in France are in the context of postabortum, postpartum, *in vitro* fertilization, and intra-uterine device: in all these contexts the endometrium is decidualized. Moreover, decidualization starts at the 18^{th} day of the menstrual cycle. The decidua is therefore

a good model to study endometritis. It is immunotolerant to the fetus until labor, through the presence, among other factors, of fetal specific T regulatory lymphocytes (595, 596). However, it contains multiple cell types thought to react/control the infection of materno-fetal membrane: the decidua is an "immune-competent" tissue (583, 597, 598). These membranes constitute an immune barrier protecting mother from fetal infection, and the fetus from maternal infection. It is therefore a good model to study immune response in a tissue barrier. We infected the tissues less than three hours following the caesarians to avoid stress due to changes from *in vivo* conditions. We used a high inoculum and only 10 % of the bacteria adhere to the tissue within the first hour in static conditions. Moreover, static infection implies accumulation of host and bacterial elements, enhancing their effects on the host tissue and the bacteria. During the *in vivo* routes of infection, the initial inoculum and the concentration of effectors are probably lower than the one we used in our model. However, such a high inoculum allows the appearance of reproducible phenotypes despite inherent differences between the tissues we study. In contrast, in the experimental set-up with flow conditions, we washed the tissue after 45 minutes to let a ~20% initial colonization; the wash and the flow removed bacteria in the supernatant. In these conditions, there is dilution of host and bacterial elements. *In vivo* conditions are probably reflected in part by the static and in part by the flow conditions, and both are complementary to study GAS pathogenesis.

GAS 3D colonization and multiplication at the tissue surface

In contrast to all other Gram-positive bacteria tested, GAS does not multiply in RPMI. Metabolic needs and pathways differ between these Gram-positive bacteria. Tissue secreted elements promote bacterial growth; furthermore, the supernatants of primary decidual stromal cells of HEC-1-A cells (data not shown) are sufficient to sustain it. Our study is different from Baruch and collaborators' (57), since they used a chemically defined medium devoid of the essential amino acid asparagine; the endoplasmic reticulum stress due to SLO and SLS releases asparagine, enabling bacterial growth. Our current hypothesis is that amino acid residues are not lacking in RPMI: all 20 amino acids are present, we inoculated a thousand bacteria per mL and there is no multiplication. Adding asparagine to RPMI did not trigger GAS growth (laboratory unpublished results). The only way we were able to restore bacterial growth in RPMI was by adding HEC-1-A and decidual stromal cells supernatant, the laboratory medium THY or BSA. We hypothesized that peptides, most probably di/tri/hexa peptides released by cells and imported in GAS (through the Dpp or Opp permeases) could be the missing elements for bacterial growth in RPMI. We are currently investigating whether small peptides enable

bacterial growth in RPMI. Either GAS exploits small peptides in conditioned medium, or it degrades proteins into small peptides. We will perform dialysis to remove small peptides from RPMI and test *in vitro* GAS multiplication in these depleted media. How GAS exploits host molecules for bacterial growth *in vivo* in the early steps of infections is scarcely investigated. However, multiplication is a fundamental for virulence and there is a relation between Dpp/Opp and the activation of several virulence pathways, notably the production of SpeB [(464), Introduction 3.1.4]. Therefore, acting on GAS metabolism or sensing of the host could unravel new opportunities for the development of treatments against GAS infections.

We showed that GAS is able to form biofilms at the surface of the decidua; we analyzed the dynamics of this formation and the EPS structures involved in it. Several reports describe the involvement of extracellular DNA and carbohydrates in these structures (405, 406). In our model, we did not detect extracellular DNA by DAPI staining in contrary to Siemens and collaborators (413), nor inter-bacterial concanavalin A (ConA) positive structures and we did not look at lipids. However, most already-published descriptions of GAS biofilms were made after 24-48 h after inoculation: late structures may contain extracellular DNA that 8 h biofilms do not possess. We observed ConA labelling of bacteria after infection of the decidua, but the ConA also labels several host elements. Furthermore, GAS aggregates were stained by ConA after one hour of infection, though we did not observe any EPS under SEM analysis at one hour, suggesting that ConA labels GAS surface. Considering the size of the biofilm that is present after 8 h, the structures we observe under SEM might be carbohydrates; that was not confirmed during immunofluorescence experiments, but the amount of material produced or the immunofluorescence resolution may not be sufficient to observe them. To study GAS biofilm, Lembke and collaborators (408) used multiple M-types on different *in vitro* surfaces and under static or flow conditions and assessed the biofilm structures after 24-72 h. While their conditions are unrelated to ours, they also observed at low resolution (3500X) “thread-like” structures. In their experimental approach, they only see these structures with a M2 strain seeded on a fibronectin-coated surface and under flow conditions. We also found that biofilm formation is different under flow and static conditions, with more EPS structures under flow than it its absence. Several hypotheses could explain this difference. First, some bacterial and host effectors could accumulate in static but not in flow conditions and degrade or repress the synthesis of these structures. Of note, it has been suggested that quorum sensing might be involved in biofilm formation (413). If the quorum sensing inhibits biofilm formation, diluting the supernatant with flow would decrease the amount of quorum sensing pheromones,

enhancing biofilm formation. However, this would be the opposite to what was demonstrated *in vitro*, where quorum sensing is described as an activator of biofilm formation (408). We did not observe significant changes in the dynamic of appearance of biofilm structures with the ΔSpeB mutant, compared to the wild-type strain, under SEM (data not shown), confirming that SpeB is not critical for biofilm formation as shown on 3D organotypic skin tissue (413). The flow imposed in our chamber set-up (0.3 mL/min) was only to compensate medium evaporation for confocal live imaging which probably does not provide a significant shear stress. We therefore think that the shear stress from the flow does not explain the difference in biofilm presence. Our main hypothesis is that supply in nutrients in flow conditions might lead to bacteria with differentially regulated metabolisms and different levels of production of EPS.

We identified three structures: thread-like structures, filaments and micrometric webs. Thread-like structures and filaments do not present the same diameter (20 nm vs 30 nm), localization (intra-chain vs inter-chains) and length (~200 nm vs > 1µm). We hypothesize that thread-like structures and filaments correspond to structures of different origins and perhaps of nature. Webs may be a late stage of filaments structures intertwined. We still distinguish these two structures because we observed filaments in several conditions, but webs only at 7 h on the subject (S#10). To further study these structures, we could compare early formation of biofilm *in vitro* in a conditioned tissue/cell medium on a fibronectin coated, or not, surface, and compare it to formation in a laboratory culture medium, BHI (409). Though GAS multiplies in both media, there could be striking differences in the amount of biofilm and structures produced due to specific signals in the conditioned media. Using only fibronectin would also avoid other host elements that are secreted by the tissue and that cover the bacteria, such as small amount of plasma derived components, enabling more precise identification of prokaryotic structures. Finally, we used SEM on ethanol fixed samples, which alters the appearance of the small structures, especially the hydrated structures. Recent advances in SEM allow acquiring samples without ethanol fixation and this would give insights on the native structures of the biofilm. Finally, we could investigate the biochemical nature of the EPS structures we observe by treating infected decidua with protease, DNAse or metaperiodate (405).

We observed different kinetics of appearance of structures depending on the subjects. This could be due to different growth kinetics, higher secretion of host elements degrading the structures or promoting their synthesis, or less signals triggering biofilm formation. Host factors appear critical in the establishment of GAS biofilms in NF biopsies (413). To identify key

elements governing the formation of biofilm structures, and correlation with other phenotypes such as bacterial growth at the tissue surface, will require studying tissues from more subjects.

Invasion of the tissue and the intracellular state of GAS

Clinical samples of GAS invasive infections show high infiltration of GAS, indicating GAS can penetrate host tissue. However, studying GAS invasion of stromal tissue requires a 3D matrix, which is provided by explants. There are more invading events at 8 h than at 4 h. From all the "invading particles", a basal level corresponds to artefacts due to the imaging and the quantification, and small breaches may enable a basal level of unspecific invading particles in the early time-points. The fact that GAS wild-type and ΔSpeB invade more at 8 h than at 4 h could have two origins. Either the tissue is more degraded at 8 h than 4 h due directly to GAS effectors, or the tissue is degraded by host metalloproteases, activated by host inflammation or by bacterial effectors. To analyze if host elements of the tissue increase the permeability of the tissue overtime, we could compare the invasion on fresh tissue and on tissue preincubated for 8 h, in which host factors could have accumulated and affected the tissue integrity. In static conditions of infection and when analyzing the invasion process, we used an excess amount of bacteria to minimize differences in colonization between the wild-type and ΔSpeB strains that could explain differences in invasion. The ΔSpeB invades less at 4 h than the wild-type, and there is a similar trend at 8 h. Therefore the level of invasion of the WT strain at 4 h is not only due to passive penetration and before 4 h, bacterial effectors, including SpeB, already exert their effects. SpeB degrades fibronectin, which we hypothesize is the major explanation for the decreased of invasion of the SpeB mutant. However, since SpeB is a broad-spectrum protease, its absence induces multiple distinct changes, and discriminating which change(s) is involved in the decreased invasion of the ΔSpeB strain is difficult to assess. Of note, SpeB regulates the GAS proteome [(401) and Introduction 2.2.4]. It would be interesting to analyze if SpeB readily degrades *ex vivo* the surface fibronectin of decidual tissue or *in vitro* a fibronectin layer. Treatment of the tissue with purified SpeB prior to infection with the ΔSpeB strain or the wild-type strain with the cysteine protease inhibitor E64 might confirm the importance of GAS degradation of the tissue for invasion. Finally, we could analyze the invasion of a SpeB expressing *Lactococcus lactis* strain compared to a control strain. The invasion events are rare at the 8 h time point, but they could be critical for GAS invasive infections. Our results confirm that during infection, GAS produces factors favoring invasion of the tissue. Clinically, this might be important events for invasive infections, where GAS penetrates the tissue, favoring the access to new sources of nutrients and increasing bacterial loads.

We were able to follow in real-time and at high resolution phagocytosis by two different types of phagocytic cells. Cytometric analysis of uninfected tissue so far did not seek neutrophils since they represent a low fraction of all cells. Our image analysis showed that these cells are highly mobile in the tissue and sometimes recruited to the surface to phagocytose bacteria. We also showed large $CD45^+$ phagocytic cells with surface protrusion capture surface bacteria. We are currently investigating which type(s) of immune cells, CD11b/c+ and $CD14^+$ performs this phagocytosis. Moreover, different reports highlight GAS capacity to survive in phagocytic cells (501), but the molecular mechanisms are still under investigation, with the M1 protein and SLO incriminated (502–506). Also, some GAS bacteria are found trapped in $CD45^+$ vacuoles at very late time-points, which shows that not all bacteria escape these vacuoles. GFP-GAS trapped in these vacuoles maintained their fluorescence over several hours, which suggests the vacuole is not fully acidified, providing an explanation for their survival. Survival in phagocytic cells could also originate from a more global dysfunction of the cells, due to the stress induced by GAS pore-forming toxins and other effectors, highly suggested by our observation that several macrophage-like cells produce blebs after phagocytosis. We will track phagocytosis events at higher time/spatial resolution *in situ* and for longer periods (using 40X objective instead of 25X, and time steps of 5 minutes instead of 15 minutes), to track the bacterial future and analyze if they survive to phagocytosis and multiply inside the phagocytic cells.

GAS consequences on host cells and cytotoxicity

GAS induces dramatic cell-death through secreted molecules, including SLO. The Transwell® system avoids the contact between bacteria and the tissue. However, it also increases the distance between GAS and the tissue, potentially decreasing the diffusion of GAS effectors and explaining the slightly lower cytotoxicity when infection was carried out in the Transwell® system instead of a direct contact with the tissue.

More than half the cells are killed during a 4 h GAS infection. Of note, there is a gradient of cytotoxicity: we observed that the cells the closest to the surface are the first to die. The most abundant cells in the decidua are from top to bottom: stromal cells, then stromal and immune cells (mainly lymphocytes) and finally lymphocytes with macrophage-like cells. This might be important regarding the immune response: macrophages are the latest to suffer from the infection, and at 4 h a significant proportion of macrophages might not be affected. To confirm this hypothesis, we will specifically label macrophages (CD14), other immune cells (CD3 and

CD4) and decidual cells (Vimentin) in addition to TUNEL staining, and we will quantify the proportion of each cell type that is killed at different time-points and depending on their depth.

We observed blebbing of cells during infection with GAS. These dramatic morphological changes could arise from two mechanisms: ectocytosis, as a resistance mechanism to pore formation (Introduction, Figure 10), or cell death (599). These blebs are rare on non-infected compared to infected tissue under static conditions. However, we observed also blebbing on non-infected tissue during live acquisition, but to a lesser extent than in the presence of GAS. Since UVs from the live acquisitions (for DAPI imaging) induce apoptosis, we will compare blebbing formation between infected and non-infected tissue in the absence of UV excitation. Several events of blebbing are concomitant with DAPI incorporation in flow conditions, and for lymphocytes, nuclear shrinkage appears before blebbing: this suggests that the blebbing is linked to cell death pathways. Some of the events observed during live microscopy may be apoptotic events: we observed the formation of beaded apoptopodia on some infected tissues (data not shown), a feature of apoptosis (600). We could analyze the Caspase 3 and 7 activation on the whole tissue as an indication of apoptosis/pyroptosis, and compare the activation after infection with several mutants and in uninfected tissue. In live microscopy, we could use Nucview to follow in real-time the activation of caspases. However, we observed large blebs originating from $CD45^+$ cells, which resemble macrophages, and these blebs are formed before cell death. These structures could correspond to ectocytosis and blebs as previously described (62, 63). We tried to label the A1 annexin recruitment in blebs as a marker of ectocytosis, but this was not conclusive and needs further development. We showed that both immune and non-immune cells are killed. Our approach did not allow following in real-time stromal cells death nor blebbing because there is no specific cell surface marker to label stromal cells and because DAPI is weakly excluded from these cells under flow conditions. We tried several unspecific labelling of cells: lipid dyes do not penetrate homogenously in the tissue and molecules such as Celltracker require metabolic activity and did not stain efficiently decidual stromal cells. We could use cytometric analyses for quantifying cell death, but these analyses are highly biased, since dead cells are more sensitive to the mechanical disruption of the tissue used for the generation of the cell suspension. Such cytometric analysis would thus probably underestimates the amount of dead cells. We already performed multiple tests on the decidua, which appears to be very sensitive to all tested disruption protocols, and this was even more complicated on infected tissue with many cells lyzed during the disruption of the tissue. As for phagocytosis of bacteria, our imaging set up

was not optimized to follow in real-time membrane modifications. The concomitant use of DAPI incorporation, membrane labelling (CD14, CD3 and CD4), real-time marker of apoptosis and high time and spatial resolution might indicate different changes in membranes depending on the immune cell type, and if blebbing is associated to cell death, or a form of ectocytosis.

Our Transwell® system suggests that the elements involved in cytotoxicity are secreted. SLO is a well described pore-forming toxin, but as shown in our study, though its deletion reduces significantly the cytotoxic effect of GAS, it is not the only source of cytotoxicity. Three candidates are SLS, NADase and SP-SPT (75, 76, 160, 488). We could perform the same analysis we did with strains deleted for one or many of these secreted molecules. Moreover, we could compare blebbing in live acquisition between a wild-type strain and a ΔSLO, or other mutants, which might highlight a direct involvement of bacterial effectors in the triggering of cell blebbing.

GAS pathogenesis and the host response: an intimate relation depending on the context

GAS is well-known for inducing strong inflammatory responses during invasive diseases, such as necrotizing fasciitis, potentially leading to STSS (517). Regarding GAS and puerperal fever, there are very few reports that analyzed the immune response to this infection. In a murine model of vaginal colonization, IL-17A is important for GAS colonization (601). In our model and during decidua infection with GBS, IL-17A was not upregulated, and is probably not critical for the early response to these infections (602).

GAS has a strong capacity to control, delay or destabilize the immune responses, increasing GAS ability to colonize and infect (523). In our model, GAS induces an overexpression of very few immune-related genes, less than GBS for instance (602). We infected the decidua with a higher amount of bacteria than Park *et al.*, however they used FBS in the medium which might promote bacterial growth yielding a number of bacteria equal or higher to that we used. We will analyze the overexpression of several genes after infection with GBS in the same condition as GAS to refine our comparison between GAS and GBS infections. The latter activates the expression of 32 genes out of 133, 9 in common with GAS infection. Notably, GBS specifically activates the expression of IL-6, TLR2, TLR6, NLRP3 and NFKPB1, CD80. The fact IL-6 is not activated ($p=0.24$ by GAS compared to $p=0.0000001$ for GBS) is the most striking result: TNF is highly overexpressed and together with IL-6 they correspond to the early acute response to infection. CD80 is a marker of activation of antigen presenting cells, required for the activation of effector T cells (603). Since recruitment of

circulating immune cells is impossible in explants, an increase in whole tissue of $CD80^+$ cells indicates a differentiation of some of immune cells, consequent to inflammation and/or microbial recognition. Leucocytes represent 40 % of the tissue cells, and 70 % of these leucocytes are lymphocytes but no lymphocyte is naïve (personal communication). The absence of significant overexpression of TLR, NLRP and NFKB shows that lymphocyte did not respond to GAS infection in contrast to GBS. Either these cells are more sensitive to GBS than to GAS antigens, or GAS is able to inhibit their activation. After infection with GAS, there is only the primary tissue response (cytokines, including many chemokines of the same family, the MIP), but no development of the long-term immune response. Finally, the only cytokine overexpressed in GAS but not in GBS is IL-10, an anti-inflammatory cytokine. It is striking that an infection triggers the production of an anti-inflammatory molecule early during the infection. However, superantigens are known to induce the secretion of IL-10 in immune cells (521), which could contribute to the overall tempering of the immune response. We will test the ability of GAS to temper the immune response by co-infecting the tissue with GAS and GBS, and compare the activation of several cytokine genes (genes coding for IL-6, IL-1β, TNF, Nlrp3 etc..) to uninfected tissue, GAS or GBS infections at 8 h. GAS ability to silence lymphocyte (re)activation could occur by multiple mechanisms, either by killing these cells before they can react, or by the secretion of superantigens that induces anergy to lymphocytes (520). Moreover, GAS infection results in a significant increase in the concentration of several pro-inflammatory molecules: TNF, CCL3 and IL-1β. While higher than in the absence of infection, the levels of these cytokines could still be lowered by GAS. The difference we observed when the infections were carried out with the SLO and SpeB mutant strains are very minor compared to the overall control of the immune response. We should therefore test the importance of other GAS factors, such as superantigens, to understand how GAS controls the tissue response.

One major limitation of our study is that we used whole RNA analysis, which limits the sensitivity, and we could miss important changes in expression in small cell subsets. As shown with the infection of the decidua with GBS, this approach still allows to identify many genes upregulated after infection with a pathogen (602). RNA analysis after cell sorting could enrich for immune cells. However, this approach involves enzymatic and mechanical disruption of the tissue, which eliminates fragile or damaged cells. We could use *in situ* hybridization to identify which cells express/overexpress specific genes on the whole tissue after infections (604).

In contrast to infection with the wild-type strain and the SpeB mutant, infection with the SLO mutant yielded lower concentration of cytokines in the supernatant than in the absence of infection. This indicates that the absence of accumulation of cytokines with the wild-type strain is the concomitant result of mechanisms that increase and decrease the amounts of cytokines, and that SLO is involved in a pro-inflammatory response. Stressed and dead cells release pro-inflammatory signals, and by having a delayed kinetic and lower intensity of cytotoxicity, the infection in the absence of SLO could result in lower induction of inflammation (605). In apparent contrast, at 8 h, in experiments on three subjects out of four, the amounts of cytokines accumulated after infection is higher in the absence of SLO than in its presence. We hypothesize that SLO mediated cell-death affects the 8 h time-point immune population involved in the secretion of these cytokines. By reducing the pool of secreting cells, SLO reduces the mounting of the inflammatory response.

The SpeB mutant presents higher accumulation of cytokine at 8 h but not 4 h. SpeB degrades several pro-inflammatory cytokines, including the overexpressed CXCL1, CXCL2 and CCL20 (101). However, by acting on some but not all cytokines, SpeB might reduce the activation of immune cells, further decreasing the production of cytokines. One reason for SpeB absence of effect at 4 h might result from its lower gene expression since *speB* is highly expressed during the stationary phase. Lower concentrations of SpeB and cytokines at 4 h than at 8 h may not be sufficient to observe an effect of SpeB on cytokine accumulation at 4 h. SpeB is not the only protease involved in the degradation of cytokines; we could test the importance of SpyCEP on cytokine accumulation (167).

Finally, we only tested the effect of mutant strains on genes that were overexpressed during infections with the wild-type strain. However, some genes not overexpressed in these conditions may be overexpressed during infection with the SLO and SpeB mutants, and similarly for the accumulation of different cytokines. RT-profiling with the mutants at 8 h could be performed to analyze these possibilities.

The implication of differences in host and bacterial genetic backgrounds in the pathogenesis

GAS efficiently multiplies at the tissue surface except with one subject (S#7). *In vitro* growth in the supernatant of uninfected tissue depends on the subject and one of them that elicited lower growth, compared to other subjects, presented a higher amount of cells with a “macrophage” signature. The levels of expression and production of cytokines in the absence

of infection differ between the subjects, demonstrating difference in the immune status of the subjects. We analyzed the available clinical information on patients, and nothing was significantly different from the other subjects: it is crucial to analyze the specificities of each subject at the tissue level to understand the differences of bacterial phenotypes. We could better characterize the tissue in the absence of infection, by flow cytometry to enumerate the different cell subsets, by analyzing the levels of expression of key genes by qPCR, by analyzing the tissue secretion of anti-microbial peptides, which might enlighten our understanding of host properties favoring or limiting GAS pathogenesis. In a longer time, we could also compare the differences between the genetic backgrounds of the subjects (528).

We focused our study on the *emm28* genotypes, which is an E pattern genotype highly prevalent in Europe but poorly studied in comparison to the *emm1*, *emm6*, *emm3* (A pattern) or *emm89* strains (E pattern). All *emm*-genotypes harbor specific repertoires of virulence factors and the *emm28* might be specifically equipped for infection of the gyneco-obstetrical sphere. The high efficiency of infection we observed on the decidua might be specific to this genotype. For example, the capacity of formation of biofilm might be *emm28*-specific. *In vitro* studies on GAS formation of biofilm point out that some strains are, or not, biofilm producers (408, 409). Moreover, the *in vitro* capacity of GAS strains to form biofilm does not correlate with their ability to form biofilms in biopsies (413). While R28 is specific to *emm28* strains, the study we performed on the tissue did not focus on *emm28*-specific factors: SpeB and SLO are expressed by all clinical strains. However, the factors influencing the regulation of expression of *slo* and *speB* depend on the genotype considered (see Introduction 2.2). Although being expressed by all strains, their importance in the infection may be different in other *emm*-types. We could perform infection of the decidua with strains from other *emm*-types to study the specificity of the *emm28* wild-type phenotypes. In addition, we used a representative strain of a collection of *emm28* strains, and we could compare the phenotypes of different strains of this collection.

We explored the possibility that R28 contributes to GAS *emm28* strains association with endometritis. We showed that R28 might be involved in the *emm28* association with endometritis by increasing adhesion to cells of the gyneco-obstetrical sphere. Studying factors independently may hide that a combination of factors promotes infections in the specific environment of the gyneco-obstetrical sphere. Surface proteins like M28, Mrp28, Enn28, Epf or RD2-encoded proteins such as, in addition to R28, Ag I/II and other yet uncharacterized putative surface proteins, might contribute, alone or together, to increasing adhesion to cells of gyneco-obstetrical sphere. However, our understanding of GAS *emm28* association with

endometritis might not rely uniquely on its capacity to adhere, and other specificities of this environment might specifically favor this *emm*-type, such as the acidity, osmolality of the endometrium.

General perspectives

This study was performed on human explants. As specified in the introduction, only few studies of GAS were done on human explants, such as skin and tonsil. However, our study developed numerous tools that could be applied to these other tissues and might improve our understanding of the early steps of skin/throat infections. We can apply similar approaches on other explants to determine the specificity of the decidua in the phenomena described and we could extend our discoveries to other superficial and invasive infections.

Explant studies provide the ability to analyze the tissue-specific response without being "polluted" by recruitment of circulating cells. Yet, this also implies that we see differential secretion of cytokines without analyzing if it actually significantly delays the immune response, for example by decreasing the immune cells recruitment. The only highly motile cells in the tissue are cells with several nucleus lobes, probably neutrophils. However, these cells are rare and the few movements in the tissue we analyzed were hectic and complex since the tissue is not flat and the time steps we used were too long (30 minutes) to track cells. Apart from isolated events, we did not witness significant immune cell recruitment, and to analyze it, we could use xenografting of explants on mice, as already done with skin samples (See introduction 4.2.1).

This study mainly focused on the endometritis. However, several phenomena we describe may not rely on properties specific to the decidua and may consequently reflect what occurs during GAS invasive infections. What struck us when performing this study on the decidua was, despite inherent genetic differences between subjects, the robustness of all the phenotypes we analyzed: this reminds the fact that GAS is a remarkable and well-equipped bacterium able to face various situations with high efficiency. GAS is a rare example of a widely spread human-specific pathogen which is not a commensal and has a parasitic mode of dissemination: its main dissemination route is superficial infections of the skin and the throat. Its rare lifestyle makes this pathogen an interesting source of fundamental questions on co-evolution and virulence strategies, while making highly complex the battle to reduce this pathogen burden on health and disease.

References

References

1. Semmelweis, I. (1987) The Etiology, Concept, and Prophylaxis of Childbed Fever. *J. Public Health Policy*. **8**, 582
2. Theodor, B. (1874) *Untersuchungen über die Vegetationsformen von Coccobacteria septica und den Antheil, welchen sie an der Entstehung und Verbreitung der accidentellen Wundkrankheiten haben : Versuch einer wissenschaftlichen Kritik der verschiedenen Methoden antisept*, Berlin : G. Reimer
3. Perrin, M. (1879) Septicémie. *Bull. Acad. Natl. Med.* **2**, pp 47-55
4. Pasteur, L. (1879) Sépticémie puerpérale. *Bull. Acad. Natl. Med.*
5. Rosenbach, F. J. (1884) Mikro-organismen bei den Wund-Infections-Krankheiten des Menschen. *Wiesbad. Bergmann*
6. Lancefield, R. (1933) A serological differentiation of human and other groups of hemolytic streptococci. *J. Exp. Med.* **1919**, 571–595
7. Davies, H. C., Karush, F., Joanne, H., and Rudd, J. H. (1965) Effect of Amino Acids on Steady-State Growth of a Group A Hemolytic Streptococcus
8. Farrell, M. A. (1935) Studies on the Respiratory Mechanism of the Streptococci. *J. Bacteriol.* **29**, 411–35
9. Pancholi, V., and Caparon, M. (2016) *Streptococcus pyogenes* Metabolism. *Streptococcus pyogenes Basic Biol. to Clin. Manifestations*
10. Beres, S. B., and Musser, J. M. (2007) Contribution of Exogenous Genetic Elements to the Group A Streptococcus Metagenome. *PLoS One*. **2**, e800
11. Todd, E. W., and Lancefield, R. C. (1928) Variants of hemolytic streptococci; their relation to type-specific substance, virulence, and toxin. *J. Exp. Med.* **48**, 751–67
12. Martin, W. J., Steer, A. C., Smeesters, P. R., Keeble, J., Inouye, M., Carapetis, J., and Wicks, I. P. (2015) Post-infectious group A streptococcal autoimmune syndromes and the heart. *Autoimmun. Rev.* **14**, 710–725
13. Beachey, E. H., Seyer, J. M., Dale, J. B., Simpson, W. A., and Kang, A. H. (1981) Type-specific protective immunity evoked by synthetic peptide of *Streptococcus pyogenes* M protein. *Nature*. **292**, 457–459
14. Beall, B., Facklam, R., and Thompson, T. (1995) Sequencing *emm* -specific polymerase chain reaction products for routine and accurate typing of group A Streptococci. *J.Clin.Microbiol.* **34**, 953–958
15. Li, Z., Sakota, V., Jackson, D., Franklin, A. R., and Beall, B. (2003) Array of M protein gene subtypes in 1064 recent invasive group A streptococcus isolates recovered from the active bacterial core surveillance. *J. Infect. Dis.* **188**, 1587–92
16. Oliver, J., Malliya Wadu, E., Pierse, N., Moreland, N. J., Williamson, D. A., and Baker, M. G. (2018) Group A Streptococcus pharyngitis and pharyngeal carriage: A meta-analysis. *PLoS Negl. Trop. Dis.* **12**, 1–17
17. Kaplan, E. L. (1980) Group A streptococcal upper respiratory carrier state: An enigma. *J. Pediatr.* **97**, 337–345
18. Shulman, S. T., Bisno, A. L., Clegg, H. W., Gerber, M. A., Kaplan, E. L., Lee, G., Martin, J. M., and Van Beneden, C. (2012) Executive summary: Clinical practice guideline for the diagnosis and management of group a streptococcal pharyngitis: 2012 update by the infectious diseases society of America. *Clin. Infect. Dis.* **55**, 1279–1282
19. Martin, J. M. (2004) Group A Streptococci Among School-Aged Children: Clinical Characteristics and the Carrier State. *Pediatrics*. **114**, 1212–1219
20. Komaroff, A. L., Pass, T. M., Aronson, M. D., Ervin, C. T., Cretin, S., Winickoff, R. N., and Branch, W. T. (1986) The prediction of streptococcal pharyngitis in adults. *J. Gen. Intern. Med.* **1**, 1–7
21. Carapetis, J. R., Steer, A. C., Mulholland, E. K., and Weber, M. (2005) The global burden of group A streptococcal diseases. *Lancet Infect. Dis.* **5**, 685–94
22. Lepoutre, A., Doloy, A., Bidet, P., Leblond, A., Perrocheau, A., Bingen, E., Trieu-Cuot, P., Bouvet, A., Poyart, C., and Lévy-Bruhl, D. (2011) Epidemiology of invasive *Streptococcus pyogenes* infections in France in 2007. *J. Clin. Microbiol.* **49**, 4094–4100
23. McHenry, C. R., Piotrowski, J. J., Petrinic, D., and Malangoni, M. A. (1995) Determinants of mortality for necrotizing soft-tissue infections. *Ann. Surg.* **221**, 558–565
24. O'Brien, K. L., Beall, B., Barrett, N. L., Cieslak, P. R., Reingold, A., Farley, M. M., Danila, R., Zell, E. R., Facklam, R., Schwartz, B., and Schuchat, A. (2002) Epidemiology of invasive group a streptococcus disease in the United States, 1995-1999. *Clin. Infect. Dis.* **35**, 268–76
25. Young, M. H., Aronoff, D. M., and Engleberg, N. C. (2005) Necrotizing fasciitis: pathogenesis and treatment. *Expert Rev. Anti. Infect. Ther.* **3**, 279–94
26. Maharaj, D. (2007) Puerperal pyrexia: A review. Part I. *Obstet. Gynecol. Surv.* **62**, 393–399
27. Leonard, A., Wright, A., Saavedra-Campos, M., Lamagni, T., Cordery, R., Nicholls, M., Domoney, C., Sriskandan, S., and Balasegaram, S. (2018) Severe group A streptococcal infections in mothers and their newborns in London and the South East, 2010-2016: assessment of risk and audit of public health management. *BJOG*. 10.1111/1471-0528.15415

28. Deutscher, M., Lewis, M., Zell, E. R., Taylor, T. H., Van Beneden, C., and Schrag, S. (2011) Incidence and severity of invasive streptococcus pneumoniae, group a streptococcus, and group b streptococcus infections among pregnant and postpartum women. *Clin. Infect. Dis.* **53**, 114–123

29. Axelsson, D., and Blomberg, M. (2014) Prevalence of postpartum infections: A population-based observational study. *Acta Obstet. Gynecol. Scand.* **93**, 1065–1068

30. Knowles, S. J., O'Sullivan, N. P., Meenan, A. M., Hanniffy, R., and Robson, M. (2015) Maternal sepsis incidence, aetiology and outcome for mother and fetus: A prospective study. *BJOG An Int. J. Obstet. Gynaecol.* **122**, 663–671

31. Anderson, B. L. (2014) Puerperal group a streptococcal infection: beyond semmelweis. *Obstet. Gynecol.* **123**, 874–82

32. Guilherme, L., Kalil, J., and Cunningham, M. (2006) Molecular mimicry in the autoimmune pathogenesis of rheumatic heart disease. *Autoimmunity*. **39**, 31–39

33. Smeesters, P. R., Dramaix, M., and Van Melderen, L. (2010) The *emm*-type diversity does not always reflect the M protein genetic diversity-Is there a case for designer vaccine against GAS. *Vaccine*. **28**, 883–885

34. Steer, A. C., Law, I., Matatolu, L., Beall, B. W., and Carapetis, J. R. (2009) Global *emm* type distribution of group A streptococci: systematic review and implications for vaccine development. *Lancet Infect. Dis.* **9**, 611–616

35. Gherardi, G., Vitali, L. A., and Creti, R. (2018) Prevalent *emm* Types among Invasive GAS in Europe and North America since Year 2000. *Front. Public Heal.* **6**, 59

36. Sumby, P., Porcella, S. F., Madrigal, A. G., Barbian, K. D., Virtaneva, K., Ricklefs, S. M., Sturdevant, D. E., Graham, M. R., Vuopio- Varkila, J., Hoe, N. P., and Musser, J. M. (2005) Evolutionary Origin and Emergence of a Highly Successful Clone of Serotype M1 Group A *Streptococcus* Involved Multiple Horizontal Gene Transfer Events. *J. Infect. Dis.* **192**, 771–782

37. Turner, C. E., Abbott, J., Lamagni, T., Holden, M. T. G., David, S., Jones, M. D., and Game, L. (2015) Emergence of a New Highly Successful Acapsular Group A Streptococcus Clade of Genotype *emm89* in the United Kingdom. **6**, 1–11

38. Bessen, D. E. (2016) Tissue tropisms in group A Streptococcus: what virulence factors distinguish pharyngitis from impetigo strains? *Curr. Opin. Infect. Dis.* **29**, 295–303

39. McGregor, K. F., Spratt, B. G., Kalia, A., Bennett, A., Bilek, N., Beall, B., and Bessen, D. E. (2004) Multilocus sequence typing of Streptococcus pyogenes representing most known *emm* -types and distinctions among subpopulation genetic structures. *J. Bacteriol.* **186**, 4285–4294

40. Bessen, D. E., Sotir, C. M., Readdy, T. L., and Hollingshead, S. K. (1996) Genetic correlates of throat and skin isolates of group A streptococci. *J. Infect. Dis.* **173**, 896–900

41. Courtney, H., Ofek, I., Penfound, T., Nizet, V., Pence, M. A., Kreikemeyer, B., Podbielbski, A., Hasty, D. L., and Dale, J. B. (2009) Relationship between expression of the family of M proteins and lipoteichoic acid to hydrophobicity and biofilm formation in *Streptococcus pyogenes*. *PLoS One*. 10.1371/journal.pone.0004166

42. McMillan, D. J., Drèze, P.-A., Vu, T., Bessen, D. E., Guglielmini, J., Steer, A. C., Carapetis, J. R., Van Melderen, L., Sriprakash, K. S., and Smeesters, P. R. (2013) Updated model of group A Streptococcus M proteins based on a comprehensive worldwide study. *Clin. Microbiol. Infect.* **19**, E222-9

43. Plainvert, C., Doloy, A., Loubinoux, J., Lepoutre, A., Collobert, G., Touak, G., Trieu-Cuot, P., Bouvet, A., and Poyart, C. (2012) Invasive group A streptococcal infections in adults, France (2006-2010). *Clin. Microbiol. Infect.* **18**, 702–10

44. Colman, G., Tanna, A., Efstratiou, A., and Gaworzewska, E. T. (1993) The serotypes of *Streptococcus pyogenes* present in Britain during 1980-1990 and their association with disease. *J. Med. Microbiol.* **39**, 165–178

45. Green, N. M., Zhang, S., Porcella, S. F., Nagiec, M. J., Barbian, K. D., Beres, S. B., LeFebvre, R. B., and Musser, J. M. (2005) Genome sequence of a serotype M28 strain of group a streptococcus: potential new insights into puerperal sepsis and bacterial disease specificity. *J. Infect. Dis.* **192**, 760–70

46. Byrne, J. L. B., Aagaard-Tillery, K. M., Johnson, J. L., Wright, L. J., and Silver, R. M. (2009) Group A streptococcal puerperal sepsis: initial characterization of virulence factors in association with clinical parameters. *J. Reprod. Immunol.* **82**, 74–83

47. Golińska, E., van der Linden, M., Więcek, G., Mikołajczyk, D., Machul, A., Samet, A., Piórkowska, A., Dorycka, M., Heczko, P. B., and Strus, M. (2016) Virulence factors of *Streptococcus pyogenes* strains from women in peri-labor with invasive infections. *Eur. J. Clin. Microbiol. Infect. Dis.* **35**, 747–754

48. Stålhammar-Carlemalm, M., Areschoug, T., Larsson, C., and Lindahl, G. (1999) The R28 protein of *Streptococcus pyogenes* is related to several group B streptococcal surface proteins, confers protective immunity and promotes binding to human epithelial cells. *Mol. Microbiol.* **33**, 208–19

49. Green, N. M., Beres, S. B., Graviss, E. A., Allison, J. E., McGeer, A. J., Vuopio-Varkila, J., LeFebvre, R. B., and Musser, J. M. (2005) Genetic diversity among type *emm28* group A Streptococcus strains causing invasive infections and pharyngitis. *J. Clin. Microbiol.* **43**, 4083–91

50. Baker, C. J., Goroff, D. K., Alpert, S., Crockett, V. A., Zinner, S. H., Evrard, J. R., Rosner, B., and McCormack, W. M. (1977) Vaginal colonization with group B streptococcus: a study in college women. *J. Infect. Dis.* **135**, 392–7

51. Rosenow, E. C. (1907) Human Pneumococcal Opsonin and the Antiopsonic Substance in Virulent Pneumococci. *J. Infect. Dis.* **4**, 285–296

52. Casadevall, A., and Pirofski, L. (1999) Host-pathogen interactions: redefi ning the basic concepts of virulence and pathogenicity. *Infect. Immun.* **67**, 3703–3713

53. Bhakdi, S., Tranum-Jensen, J., and Sziegoleit, A. (1985) Mechanism of membrane damage by streptolysin-O. *Infect. Immun.* **47**,

52–60

54. Mozola, C. C., and Caparon, M. G. (2015) Dual modes of membrane binding direct pore formation by Streptolysin O. *Mol. Microbiol.* **97**, 1036–1050

55. Shewell, L. K., Harvey, R. M., Higgins, M. A., Day, C. J., Hartley-Tassell, L. E., Chen, A. Y., Gillen, C. M., James, D. B. A., Alonzo, F., Torres, V. J., Walker, M. J., Paton, A. W., Paton, J. C., and Jennings, M. P. (2014) The cholesterol-dependent cytolysins pneumolysin and streptolysin O require binding to red blood cell glycans for hemolytic activity. *Proc. Natl. Acad. Sci.* **111**, E5312–E5320

56. Cywes-Bentley, C., Hakansson, A., Christianson, J., and Wessels, M. R. (2005) Extracellular group A Streptococcus induces keratinocyte apoptosis by dysregulating calcium signalling. *Cell. Microbiol.* **7**, 945–955

57. Baruch, M., Belotserkovsky, I., Hertzog, B. B., Ravins, M., Dov, E., McIver, K. S., Le Breton, Y. S., Zhou, Y., Cheng, C. Y., Chen, C. Y., and Hanski, E. (2014) An extracellular bacterial pathogen modulates host metabolism to regulate its own sensing and proliferation. *Cell*. **156**, 97–108

58. Rodríguez, A., Webster, P., Ortego, J., and Andrews, N. W. (1997) Lysosomes Behave as Ca 2. *Cell*. **137**, 93–104

59. Idone, V., Tam, C., Goss, J. W., Toomre, D., Pypaert, M., and Andrews, N. W. (2008) Repair of injured plasma membrane by rapid Ca2+ dependent endocytosis. *J. Cell Biol.* **180**, 905–914

60. Rao, S. K., Huynh, C., Proux-Gillardeaux, V., Galli, T., and Andrews, N. W. (2004) Identification of SNAREs Involved in Synaptotagmin VII-regulated Lysosomal Exocytosis. *J. Biol. Chem.* **279**, 20471–20479

61. Tam, C., Idone, V., Devlin, C., Fernandes, M. C., Flannery, A., He, X., Schuchman, E., Tabas, I., and Andrews, N. W. (2010) Exocytosis of acid sphingomyelinase by wounded cells promotes endocytosis and plasma membrane repair. *J. Cell Biol.* **189**, 1027–1038

62. Babiychuk, E. B., Monastyrskaya, K., Potez, S., and Draeger, A. (2011) Blebbing confers resistance against cell lysis. *Cell Death Differ.* **18**, 80–89

63. Keyel, P. A., Loultcheva, L., Roth, R., Salter, R. D., Watkins, S. C., Yokoyama, W. M., and Heuser, J. E. (2011) Streptolysin O clearance through sequestration into blebs that bud passively from the plasma membrane. *J. Cell Sci.* **124**, 2414–2423

64. Cassidy, S. K. B., and O'Riordan, M. X. D. (2013) More than a pore: The cellular response to cholesterol-dependent cytolysins. *Toxins (Basel).* **5**, 618–636

65. Ghosh, J., and Caparon, M. G. (2006) Specificity of *Streptococcus pyogenes* NAD+ glycohydrolase in cytolysin-mediated translocation. *Mol. Microbiol.* **62**, 1203–1214

66. Madden, J. C., Ruiz, N., Caparon, M., and Louis, S. (2001) A Functional Equivalent of Type III Secretion in Gram-Positive Bacteria. **104**, 143–152

67. Yoon, J. Y., An, D. R., Yoon, H.-J., Kim, H. S., Lee, S. J., Im, H. N., Jang, J. Y., and Suh, S. W. (2013) High-resolution crystal structure of Streptococcus pyogenes β-NAD + glycohydrolase in complex with its endogenous inhibitor IFS reveals a highly water-rich interface. *J. Synchrotron Radiat.* **20**, 962–967

68. Kimoto, H., Fujii, Y., Hirano, S., Yokota, Y., and Taketo, A. (2006) Genetic and biochemical properties of streptococcal NAD-glycohydrolase inhibitor. *J. Biol. Chem.* **281**, 9181–9189

69. Young Yoon, J., Ri An, D., Yoon, H.-J., Sook Kim, H., Jae Lee, S., Na Im, H., Young Jang, J., and Won Suh, S. (2013) diffraction structural biology High-resolution crystal structure of *Streptococcus pyogenes* b-NAD + glycohydrolase in complex with its endogenous inhibitor IFS reveals a highly water-rich interface. *J. Synchrotron Rad*. **20**, 962–967

70. Magassa, N., Chandrasekaran, S., and Caparon, M. G. (2010) *Streptococcus pyogenes* cytolysin-mediated translocation does not require pore formation by streptolysin O. *EMBO Rep.* **11**, 400–5

71. Ghosh, J., Anderson, P. J., Chandrasekaran, S., and Caparon, M. G. (2010) Characterization of *Streptococcus pyogenes* β-NAD+ glycohydrolase: Re-evaluation of enzymatic properties associated with pathogenesis. *J. Biol. Chem.* **285**, 5683–5694

72. Chandrasekaran, S., and Caparon, M. G. (2016) The NADase-Negative Variant of the *Streptococcus pyogenes* Toxin NAD + Glycohydrolase Induces JNK1-Mediated Programmed Cellular Necrosis. *MBio*. **7**, e02215-15

73. Hancz, D., Westerlund, E., Bastiat-Sempe, B., Sharma, O., Valfridsson, C., Meyer, L., Love, J. F., O'Seaghdha, M., Wessels, M. R., and Persson, J. J. (2017) Inhibition of Inflammasome-Dependent Interleukin 1β Production by Streptococcal NAD + -Glycohydrolase: Evidence for Extracellular Activity. *MBio*. **8**, e00756-17

74. Datta, V., Myskowski, S. M., Kwinn, L. A., Chiem, D. N., Varki, N., Kansal, R. G., Kotb, M., and Nizet, V. (2005) Mutational analysis of the group A streptococcal operon encoding streptolysin S and its virulence role in invasive infection. *Mol. Microbiol.* **56**, 681–695

75. Ofek, I., Zafriri, D., Goldhar, J., and Eisenstein, B. I. (1990) Inability of toxin inhibitors to neutralize enhanced toxicity caused by bacteria adherent to tissue culture cells. *Infect. Immun.* **58**, 3737–3742

76. Flaherty, R. A., Puricelli, J. M., Higashi, D. L., Park, C. J., and Lee, S. W. (2015) Streptolysin S promotes programmed cell death and enhances inflammatory signaling in epithelial keratinocytes during group A Streptococcus infection. *Infect. Immun.* **83**, 4118–4133

77. Nizet, V. (2002) Streptococcal β-hemolysins: Genetics and role in disease pathogenesis. *Trends Microbiol.* **10**, 575–580

78. Ginsburg, I. (1963) Oxygen-stable hemolysins of group a streptococci: I. the role of various agents in the production of the hemolysins. *J. Exp. Med.* **118**, 905–917

79. Higashi, D. L., Biais, N., Donahue, D. L., Mayfield, J. A., Tessier, C. R., Rodriguez, K., Ashfeld, B. L., Luchetti, J., Ploplis, V. A.,

Castellino, F. J., and Lee, S. W. (2016) Activation of band 3 mediates group A Streptococcus streptolysin S-based beta-haemolysis. *Nat. Microbiol.* **1**, 1–6

80. Bohach, G. A., Hauser, A. R., and Schlievert, P. M. (1988) Cloning of the gene, speB, for streptococcal pyrogenic exotoxin type B in Escherichia coli. *Infect. Immun.* **56**, 1665–1667

81. Chen, C. Y., Luo, S. C., Kuo, C. F., Lin, Y. S., Wu, J. J., Lin, M. T., Liu, C. C., Jeng, W. Y., and Chuang, W. J. (2003) Maturation processing and characterization of streptopain. *J. Biol. Chem.* **278**, 17336–17343

82. Liu, T. Y., and Elliott, S. D. (1965) Activation of streptococcal proteinase and its zymogen by bacterial cell walls. *Nature*. **206**, 33–34

83. Liu, T. Y., and Elliott, S. D. (1965) Streptococcal proteinase: the zymogen to enzyme transfromation. *J. Biol. Chem.* **240**, 1138–42

84. Musser, J. M., Stockbauer, K., Kapur, V., and Rudgers, G. W. (1996) Substitution of cysteine 192 in a highly conserved *Streptococcus pyogenes* extracellular cysteine protease (interleukin 1β convertase) alters proteolytic activity and ablates zymogen processing. *Infect. Immun.* **64**, 1913–1917

85. Luca-Harari, B., Darenberg, J., Neal, S., Siljander, T., Strakova, L., Tanna, A., Creti, R., Ekelund, K., Koliou, M., Tassios, P. T., Van Der Linden, M., Straut, M., Vuopio-Varkila, J., Bouvet, A., Efstratiou, A., Schalén, C., Henriques-Normark, B., and Jasir, A. (2009) Clinical and Microbiological Characteristics of Severe *Streptococcus pyogenes* Disease in Europe. *J. Clin. Microbiol.* **47**, 1155–1165

86. Kagawa, T. F., Cooney, J. C., Baker, H. M., McSweeney, S., Liu, M., Gubba, S., Musser, J. M., and Baker, E. N. (2000) Crystal structure of the zymogen form of the group A Streptococcus virulence factor SpeB: an integrin-binding cysteine protease. *Proc. Natl. Acad. Sci. U. S. A.* **97**, 2235–40

87. Olsen, J. G., Dagil, R., Niclasen, L. M., Sørensen, O. E., and Kragelund, B. B. (2009) Structure of the Mature Streptococcal Cysteine Protease Exotoxin mSpeB in Its Active Dimeric Form. *J. Mol. Biol.* **393**, 693–703

88. Persson, H., Vindebro, R., and Von Pawel-Rammingen, U. (2013) The streptococcal cysteine protease SpeB is not a natural immunoglobulin-cleaving enzyme. *Infect. Immun.* **81**, 2236–2241

89. Nelson, D. C., Garbe, J., and Collin, M. (2011) Cysteine proteinase SpeB from *Streptococcus pyogenes*– a potent modifier of immunologically important host and bacterial proteins. *Biol. Chem.* **392**, 1077–1088

90. Rasmussen, M., Müller, H. P., and Björck, L. (1999) Protein GRAB of *Streptococcus pyogenes* regulates proteolysis at the bacterial surface by binding α2-macroglobulin. *J. Biol. Chem.* **274**, 15336–15344

91. Nyberg, P., Rasmussen, M., and Björck, L. (2004) α2-Macroglobulin-proteinase complexes protect *Streptococcus pyogenes* from killing by the antimicrobial peptide LL-37. *J. Biol. Chem.* **279**, 52820–52823

92. Hytönen, J., Haataja, S., Gerlach, D., Podbielski, A., and Finne, J. (2001) The SpeB virulence factor of *Streptococcus pyogenes*, a multifunctional secreted and cell surface molecule with strepadhesin, laminin-binding and cysteine protease activity. *Mol. Microbiol.* **39**, 512–519

93. Stockbauer, K. E., Magoun, L., Liu, M., Burns, E. H., Gubba, S., Renish, S., Pan, X., Bodary, S. C., Baker, E., Coburn, J., Leong, J. M., and Musser, J. M. (1999) A natural variant of the cysteine protease virulence factor of group A Streptococcus with an arginine-glycine-aspartic acid (RGD) motif preferentially binds human integrins alphavbeta3 and alphaIIbbeta3. *Proc. Natl. Acad. Sci. U. S. A.* **96**, 242–247

94. Collin, M., and Olsén, A. (2001) Effect of SpeB and EndoS from *Streptococcus pyogenes* on human immunoglobulins. *Infect. Immun.* **69**, 7187–7189

95. Collin, M., Svensson, M. D., Sjöholm, A. G., Jensenius, J. C., Sjöbring, U., and Olsén, A. (2002) EndoS and SpeB from *Streptococcus pyogenes* inhibit immunoglobulin-mediated opsonophagocytosis. *Infect. Immun.* **70**, 6646–6651

96. Eriksson, A., and Norgren, M. (2003) Cleavage of antigen-bound immunoglobulin G by SpeB contributes to streptococcal persistence in opsonizing blood. *Infect. Immun.* **71**, 211–217

97. Collin, M., and Olsén, A. (2001) EndoS, a novel secreted protein from *Streptococcus pyogenes* with endoglycosidase activity on human IgG. *EMBO J.* **20**, 3046–3055

98. Kuo, C. F., Lin, Y. S., Chuang, W. J., Wu, J. J., and Tsao, N. (2008) Degradation of complement 3 by streptococcal pyrogenic exotoxin B inhibits complement activation and neutrophil opsonophagocytosis. *Infect. Immun.* **76**, 1163–1169

99. Terao, Y., Mori, Y., Yamaguchi, M., Shimizu, Y., Ooe, K., Hamada, S., and Kawabata, S. (2008) Group A streptococcal cysteine protease degrades C3 (C3b) and contributes to evasion of innate immunity. *J. Biol. Chem.* **283**, 6253–6260

100. Tsao, N., Tsai, W. H., Lin, Y. S., Chuang, W. J., Wang, C. H., and Kuo, C. F. (2006) Streptococcal pyrogenic exotoxin B cleaves properdin and inhibits complement-mediated opsonophagocytosis. *Biochem. Biophys. Res. Commun.* **339**, 779–784

101. Egesten, A., Olin, A. I., Linge, H. M., Yadav, M., Mörgelin, M., Karlsson, A., and Collin, M. (2009) SpeB of *Streptococcus pyogenes* differentially modulates antibacterial and receptor activating properties of human chemokines. *PLoS One*. **4**, 1–9

102. Kapur, V., Majesky, M. W., Li, L. L., Black, R. A., and Musser, J. M. (1993) Cleavage of interleukin 1 beta (IL-1 beta) precursor to produce active IL-1 beta by a conserved extracellular cysteine protease from *Streptococcus pyogenes*. *Proc. Natl. Acad. Sci. U. S. A.* **90**, 7676–80

103. Herwald, H., Collin, M., Müller-Esterl, W., and Björck, L. (1996) Streptococcal cysteine proteinase releases kinins: a virulence mechanism. *J. Exp. Med.* **184**, 665–673

104. Elliott, S. D. (1945) A Proteolytic Enzyme Produced By Group A Streptococci With Special Reference To Its Effect On The Type-Specific M Antigen. *J. Exp. Med.* **81**, 573–92

105. Matsuka, Y. V., Pillai, S., Gubba, S., Musser, J. M., and Olmsted, S. B. (1999) Fibrinogen cleavage by the *Streptococcus pyogenes* extracellular cysteine protease and generation of antibodies that inhibit enzyme proteolytic activity. *Infect. Immun.* **67**, 4326–4333

106. Cole, J. N., McArthur, J. D., McKay, F. C., Sanderson-Smith, M. L., Cork, A. J., Ranson, M., Rohde, M., Itzek, A., Sun, H., Ginsburg, D., Kotb, M., Nizet, V., Chhatwal, G. S., and Walker, M. J. (2006) Trigger for group A streptococcal M1T1 invasive disease. *FASEB J.* **20**, 1745–1747

107. Kapur, V., Topouzis, S., Majesky, M. W., Li, L. L., Hamrick, M. R., Hamill, R. J., Patti, J. M., and Musser, J. M. (1993) A conserved *Streptococcus pyogenes* extracellular cysteine protease cleaves human fibronectin and degrades vitronectin. *Microb. Pathog.* **15**, 327–346

108. Wolf, B. B., Gibson, C. A., Kapur, V., Hussaini, I. M., Musser, J. M., and Gonias, S. L. (1994) Proteolytically active streptococcal pyrogenic exotoxin B cleaves monocytic cell urokinase receptor and releases an active fragment of the receptor from the cell surface. *J. Biol. Chem.* **269**, 30682–7

109. Burns Jr., E. H., Marciel, A. M., and Musser, J. M. (1996) Activation of a 66-kilodalton human endothelial cell matrix metalloprotease by *Streptococcus pyogenes* extracellular cysteine protease. *Infect Immun.* **64**, 4744–4750

110. Tamura, F., Nakagawa, R., Akuta, T., Okamoto, S., Hamada, S., Maeda, H., Kawabata, S., and Akaike, T. (2004) Proapoptotic effect of proteolytic activation of matrix metalloproteinases by *Streptococcus pyogenes* thiol proteinase (Streptococcus pyrogenic exotoxin B). *Infect. Immun.* **72**, 4836–4847

111. Schmidtchen, A., Frick, I. M., and Björck, L. (2001) Dermatan sulphate is released by proteinases of common pathogenic bacteria and inactivates antibacterial α-defensin. *Mol. Microbiol.* **39**, 708–713

112. Meinert Niclasen, L., Olsen, J. G., Dagil, R., Qing, Z., Sørensen, O. E., and Kragelund, B. B. (2011) Streptococcal pyogenic exotoxin B (SpeB) boosts the contact system via binding of α-1 antitrypsin. *Biochem. J.* **434**, 123–132

113. Fraser, J. D., and Proft, T. (2008) The bacterial superantigen and superantigen-like proteins. *Immunol. Rev.* **225**, 226–243

114. Proft, T., and Fraser, J. D. (2016) *Streptococcal Superantigens: Biological properties and potential role in disease*

115. Watson, D. W. (1960) Host-parasite factors in group A streptococcal infections. Pyrogenic and other effects of immunologic distinct exotoxins related to scarlet fever toxins. *J. Exp. Med.* **111**, 255–84

116. Kim, Y. B., and Watson, D. W. (1970) A purified group A streptococcal pyrogenic exotoxin. Physiochemical and biological properties including the enhancement of susceptibility to endotoxin lethal shock. *J. Exp. Med.* **131**, 611–22

117. Mollick, J. A., Miller, J. M., Cook, R. G., Grossman, D., and Rich, R. R. (1993) A novel superantigen isolated from pathogenic strains of *Streptococcus pyogenes* with aminoterminal homolgy to staphylococcal enterooxins B and C. *J Clin Invest.* **92**, 710–719

118. Beres, S. B., Sylva, G. L., Barbian, K. D., Lei, B., Hoff, J. S., Mammarella, N. D., Liu, M.-Y., Smoot, J. C., Porcella, S. F., Parkins, L. D., Campbell, D. S., Smith, T. M., McCormick, J. K., Leung, D. Y. M., Schlievert, P. M., and Musser, J. M. (2002) Genome sequence of a serotype M3 strain of group A Streptococcus: Phage-encoded toxins, the high-virulence phenotype, and clone emergence. *Proc. Natl. Acad. Sci.* **99**, 10078–10083

119. Smoot, L. M., McCormick, J. K., Smoot, J. C., Hoe, N. P., Strickland, I., Cole, R. L., Barbian, K. D., Earhart, C. A., Ohlendorf, D. H., Veasy, L. G., Hill, H. R., Leung, D. Y. M., Schlievert, P. M., and Musser, J. M. (2002) Characterization of two novel pyrogenic toxin superantigens made by an acute rheumatic fever clone of *Streptococcus pyogenes* associated with multiple disease outbreaks. *Infect. Immun.* **70**, 7095–104

120. Proft, T., Webb, P. D., Handley, V., Fraser, D., and Fraser, J. D. (2003) Two Novel Superantigens Found in Both Group A and Group C Streptococcus Two Novel Superantigens Found in Both Group A and Group C Streptococcus. *Infect. Immun.* **71**, 1361–1369

121. Proft, T., Arcus, V. L., Handley, V., Baker, E. N., and Fraser, J. D. (2001) Immunological and biochemical characterization of streptococcal pyrogenic exotoxins I and J (SPE-I and SPE-J) from *Streptococcus pyogenes*. *J. Immunol.* **166**, 6711–6719

122. Proft, T., Moffatt, S. L. L., Berkahn, C. J. J., and Fraser, J. D. D. (1999) Identification and characterization of novel superantigens from *Streptococcus pyogenes*. *J. Exp. Med.* **189**, 89–101

123. Turner, C. E., Sommerlad, M., McGregor, K., Davies, F. J., Pichon, B., Chong, D. L. W. W., Farzaneh, L., Holden, M. T. G. G., Spratt, B. G., Efstratiou, A., and Sriskandan, S. (2012) Superantigenic activity of emm3 Streptococcus pyogenes is abrogated by a conserved, naturally occurring smeZ mutation. *PLoS One*. **7**, e46376

124. Proft, T., Moffatt, S. L., Weller, K. D., Paterson, A., Martin, D., and Fraser, J. D. (2000) The streptococcal superantigen SMEZ exhibits wide allelic variation, mosaic structure, and significant antigenic variation. *J. Exp. Med.* **191**, 1765–76

125. Friães, A., Pinto, F. R., Silva-Costa, C., Ramirez, M., and Melo-Cristino, J. (2013) Superantigen gene complement of *Streptococcus pyogenes* - Relationship with other typing methods and short-term stability. *Eur. J. Clin. Microbiol. Infect. Dis.* **32**, 115–125

126. Longo, M., De Jode, M., Plainvert, C., Weckel, A., Hua, A., Château, A., Glaser, P., Poyart, C., Fouet, A., Huaa, A., Château, A., Glaser, P., Poyart, C., and Fouet, A. (2015) Complete Genome Sequence of *Streptococcus pyogenes emm28* strain M28PF1, responsible of a puerperal fever. *Genome Announc.* **3**, e00750-15

127. Arad, G., Levy, R., Nasie, I., Hillman, D., Rotfogel, Z., Barash, U., Supper, E., Shpilka, T., Minis, A., and Kaempfer, R. (2011) Binding of superantigen toxins into the CD28 homodimer interface is essential for induction of cytokine genes that mediate lethal shock. *PLoS Biol.* 10.1371/journal.pbio.1001149

128. Müller-Alouf, H., Carnoy, C., Simonet, M., and Alouf, J. E. (2001) Superantigen bacterial toxins: State of the art. *Toxicon*. **39**, 1691–1701

129. Sumby, P., Barbian, K. D., Gardner, D. J., Whitney, A. R., Welty, D. M., Long, R. D., Bailey, J. R., Parnell, M. J., Hoe, N. P.,

Adams, G. G., DeLeo, F. R., and Musser, J. M. (2005) Extracellular deoxyribonuclease made by group A Streptococcus assists pathogenesis by enhancing evasion of the innate immune response. *Proc. Natl. Acad. Sci.* **102**, 1679–1684

130. Buchanan, J. T., Simpson, A. J., Aziz, R. K., Liu, G. Y., Kristian, S. A., Kotb, M., Feramisco, J., and Nizet, V. (2006) DNase expression allows the pathogen group A Streptococcus to escape killing in neutrophil extracellular traps. *Curr. Biol.* **16**, 396–400

131. Matsumoto, M., Sakae, K., Hashikawa, S., Torii, K., Hasegawa, T., Horii, T., Endo, M., Okuno, R., Murayama, S., Hirasawa, K., Suzuki, R., Isobe, J., Tanaka, D., Katsukawa, C., Tamaru, A., Tomita, M., Ogata, K., Ikebe, T., Watanabe, H., Ohta, M., Saito, H., Otani, K., Oguro, M., Fujisaki, J., Sugama, K., Hosorogi, S., Sakaki, M., Kasama, Y., Tanaka, H., Sunahara, C., Shimizu, T., Moroishi, S., Abe, Y., and Kudaka, J. (2005) Close correlation of streptococcal DNase B (sdaB) alleles with *emm* genotypes in *Streptococcus pyogenes*. *Microbiol. Immunol.* **49**, 925–929

132. Hasegawa, T., Minami, M., Okamoto, A., Tatsuno, I., Isaka, M., and Ohta, M. (2010) Characterization of a virulence-associated and cell-wall-located DNase of *Streptococcus pyogenes*. *Microbiology*. **156**, 184–190

133. Walker, M. J., Hollands, A., Sanderson-Smith, M. L., Cole, J. N., Kirk, J. K., Henningham, A., McArthur, J. D., Dinkla, K., Aziz, R. K., Kansal, R. G., Simpson, A. J., Buchanan, J. T., Chhatwal, G. S., Kotb, M., and Nizet, V. (2007) DNase Sda1 provides selection pressure for a switch to invasive group A streptococcal infection. *Nat. Med.* **13**, 981–985

134. Venturini, C., Ong, C. lynn Y., Gillen, C. M., Ben-Zakour, N. L., Maamary, P. G., Nizet, V., Beatson, S. A., and Walker, M. J. (2013) Acquisition of the Sda1-encoding bacteriophage does not enhance virulence of the serotype M1 *Streptococcus pyogenes* strain SF370. *Infect. Immun.* **81**, 2062–2069

135. Zhou, Y., Hanks, T. S., Feng, W., Li, J., Liu, G., Liu, M., and Lei, B. (2013) The sagA/pel locus does not regulate the expression of the M protein of the M1T1 lineage of group A Streptococcus. *Virulence*. **4**, 698–706

136. Liu, G., Feng, W., Li, D., Liu, M., Nelson, D. C., and Lei, B. (2015) The Mga Regulon but Not Deoxyribonuclease Sda1 of Invasive M1T1 Group A Streptococcus Contributes to In Vivo Selection of CovRS Mutations and Resistance to Innate Immune Killing Mechanisms. *Infect. Immun.* **83**, 4293–303

137. Korczynska, J. E., Turkenburg, J. P., and Taylor, E. J. (2012) The structural characterization of a prophage-encoded extracellular DNase from *Streptococcus pyogenes*. *Nucleic Acids Res.* **40**, 928–938

138. McShan, W. M., Ferretti, J. J., Karasawa, T., Suvorov, A. N., Lin, S., Qin, B., Jia, H., Kenton, S., Najar, F., Wu, H., Scott, J., Roe, B. A., and Savic, D. J. (2008) Genome sequence of a nephritogenic and highly transformable M49 strain of *Streptococcus pyogenes*. *J. Bacteriol.* **190**, 7773–7785

139. Sjögren, J., Struwe, W. B., Cosgrave, E. F. J., Rudd, P. M., Stervander, M., Allhorn, M., Hollands, A., Nizet, V., and Collin, M. (2013) EndoS $_2$ is a unique and conserved enzyme of serotype M49 group A *Streptococcus* that hydrolyses N-linked glycans on IgG and α_1 -acid glycoprotein. *Biochem. J.* **455**, 107–118

140. Akesson, P., Moritz, L., Truedsson, M., Christensson, B., and von Pawel-Rammingen, U. (2006) IdeS, a Highly Specific Immunoglobulin G (IgG)-Cleaving Enzyme from *Streptococcus pyogenes*, Is Inhibited by Specific IgG Antibodies Generated during Infection. *Infect. Immun.* **74**, 497–503

141. Von Pawel-Rammingen, U., Johansson, B. P., and Björck, L. (2002) IdeS, a novel streptococcal cysteine proteinase with unique specificity for immunoglobulin G. *EMBO J.* **21**, 1607–1615

142. Agniswamy, J., Lei, B., Musser, J. M., and Sun, P. D. (2004) Insight of host immune evasion mediated by two variants of group A Streptococcus Mac protein. *J. Biol. Chem.* **279**, 52789–52796

143. Terao, Y., Kawabata, S., Nakata, M., Nakagawa, I., and Hamada, S. (2002) Molecular characterization of a novel fibronectin-binding protein of *Streptococcus pyogenes* strains isolated from toxic shock-like syndrome patients. *J. Biol. Chem.* **277**, 47428–47435

144. Lei, B., DeLeo, F. R., Hoe, N. P., Graham, M. R., Mackie, S. M., Cole, R. L., Liu, M., Hill, H. R., Low, D. E., Federle, M. J., Scott, J. R., and Musser, J. M. (2001) Evasion of human innate and acquired immunity by a bacterial homolog of CD11b that inhibits opsonophagocytosis. *Nat. Med.* **7**, 1298–1305

145. Hynes, W. L., Dixon, A. R., Walton, S. L., and Aridgides, L. J. (2000) The extracellular hyaluronidase gene (hylA) of *Streptococcus pyogenes*. *FEMS Microbiol. Lett.* **184**, 109–112

146. Hynes, W. L., Hancock, L., and Ferretti, J. J. (1995) Analysis of a second bacteriophage hyaluronidase gene from Strptococcus pyogenes: Evidence for a third hyaluronidase involved in extracellular enzymatic activity. *Infect. Immun.* **63**, 3015–3020

147. Hynes, W., Johnson, C., and Stokes, M. (2009) A single nucleotide mutation results in loss of enzymatic activity in the hyaluronate lyase gene of *Streptococcus pyogenes*. *Microb. Pathog.* **47**, 308–313

148. Henningham, A., Yamaguchi, M., Aziz, R. K., Kuipers, K., Buffalo, C. Z., Dahesh, S., Choudhury, B., Van Vleet, J., Yamaguchi, Y., Seymour, L. M., Ben Zakour, N. L., He, L., Smith, H. V., Grimwood, K., Beatson, S. A., Ghosh, P., Walker, M. J., Nizet, V., and Colea, J. N. (2014) Mutual exclusivity of hyaluronan and hyaluronidase in invasive group a Streptococcus. *J. Biol. Chem.* **289**, 32303–32315

149. Fernie-King, B. A., Seilly, D. J., Willers, C., Würzner, R., Davies, A., and Lachmann, P. J. (2001) Streptococcal inhibitor of complement (SIC) inhibits the membrane attack complex by preventing uptake of C567 onto cell membranes. *Immunology*. **103**, 390–398

150. Frick, I. M., Åkesson, P., Rasmussen, M., Schmidtchen, A., and Björck, L. (2003) SIC, a secreted protein of *Streptococcus pyogenes* that inactivates antibacterial peptides. *J. Biol. Chem.* **278**, 16561–16566

151. Fernie-King, B. A., Seilly, D. J., and Lachmann, P. J. (2004) The interaction of streptococcal inhibitor of complement (SIC) and its proteolytic fragments with the human beta defensins. *Immunology*. **111**, 444–452

152. Fernie-King, B. A., Seilly, D. J., Davies, A., and Lachmann, P. J. (2002) Streptococcal inhibitor of complement inhibits two

additional components of the mucosal innate immune system: Secretory leukocyte proteinase inhibitor and lysozyme. *Infect. Immun.* **70**, 4908–4916

153. Egesten, A., Eliasson, M., Johansson, H. M., Olin, A. I., Mörgelin, M., Mueller, A., Pease, J. E., Frick, I., and Björck, L. (2007) The CXC Chemokine MIG/CXCL9 Is Important in Innate Immunity against *Streptococcus pyogenes*. *J. Infect. Dis.* **195**, 684–693

154. Frick, I. M., Shannon, O., Åkesson, P., Mörgelin, M., Collin, M., Schmidtchen, A., and Björck, L. (2011) Antibacterial activity of the contact and complement systems is blocked by SIC, a protein secreted by *Streptococcus pyogenes*. *J. Biol. Chem.* **286**, 1331–1340

155. Pence, M. A., Rooijakkers, S. H. M., Cogen, A. L., Cole, J. N., Hollands, A., Gallo, R. L., and Nizet, V. (2010) Streptococcal inhibitor of complement promotes innate immune resistance phenotypes of invasive M1T1 group A Streptococcus. *J. Innate Immun.* **2**, 587–595

156. Binks, M., McMillan, D., and Sriprakash, K. S. (2003) Genomic Location and Variation of the Gene for CRS, a Complement Binding Protein in the M57 Strains of *Streptococcus pyogenes*. *Infect. Immun.* **71**, 6701–6706

157. Binks, M., and Sriprakash, K. S. (2004) Characterization of a complement-binding protein, DRS, from strains of *Streptococcus pyogenes* containing the emm12 and emm55 genes. *Infect. Immun.* **72**, 3981–3986

158. Agarwal, S., Agarwal, S., Pancholi, P., and Pancholi, V. (2011) Role of serine/threonine phosphatase (SP-STP) in *Streptococcus pyogenes* physiology and virulence. *J. Biol. Chem.* **286**, 41368–41380

159. Jin, H., and Pancholi, V. (2006) Identification and biochemical characterization of a eukaryotic-type serine/threonine kinase and its cognate phosphatase in *Streptococcus pyogenes*: Their biological functions and substrate identification. *J. Mol. Biol.* **357**, 1351–1372

160. Agarwal, S. S., Agarwal, S. S., Jin, H., Pancholi, P., and Pancholi, V. (2012) Serine/threonine phosphatase (SP-STP), secreted from *Streptococcus pyogenes*, is a pro-apoptotic protein. *J. Biol. Chem.* **287**, 9147–9167

161. Kant, S., Agarwal, S., Pancholi, P., and Pancholi, V. (2015) The *Streptococcus pyogenes* orphan protein tyrosine phosphatase, SP-PTP, possesses dual specificity and essential virulence regulatory functions. *Mol. Microbiol.* **97**, 515–540

162. Coye, L. H., and Collins, C. M. (2004) Identification of SpyA, a novel ADP-ribosyltransferase of *Streptococcus pyogenes*. *Mol. Microbiol.* **54**, 89–98

163. Icenogle, L. M., Hengel, S. M., Coye, L. H., Streifel, A., Collins, C. M., Goodlett, D. R., and Moseley, S. L. (2012) Molecular and biological characterization of streptococcal SpyA-mediated ADP-ribosylation of intermediate filament protein vimentin. *J. Biol. Chem.* **287**, 21481–21491

164. Korotkova, N., Hoff, J. S., Becker, D. M., Quinn, J. K. H., Icenogle, L. M., and Moseley, S. L. (2012) SpyA is a membrane-bound ADP-ribosyltransferase of *Streptococcus pyogenes* which modifies a streptococcal peptide, SpyB. *Mol. Microbiol.* **83**, 936–952

165. Edgar, R. J., Chen, J., Kant, S., Rechkina, E., Rush, J. S., Forsberg, L. S., Jaehrig, B., Azadi, P., Tchesnokova, V., Sokurenko, E. V., Zhu, H., Korotkov, K. V., Pancholi, V., and Korotkova, N. (2016) SpyB, a Small Heme-Binding Protein, Affects the Composition of the Cell Wall in *Streptococcus pyogenes*. *Front. Cell. Infect. Microbiol.* **6**, 1263389–126

166. Lin, A. E., Beasley, F. C., Keller, N., Hollands, A., Urbano, R., Troemel, E. R., Hoffman, H. M., and Nizet, V. (2015) A group a Streptococcus ADP-ribosyltransferase toxin stimulates a protective interleukin 1β-dependent macrophage immune response. *MBio*. **6**, 1–12

167. Zingaretti, C., Falugi, F., Nardi-Dei, V., Pietrocola, G., Mariani, M., Liberatori, S., Gallotta, M., Tontini, M., Tani, C., Speziale, P., Grandi, G., and Margarit, I. (2010) *Streptococcus pyogenes* SpyCEP: a chemokine-inactivating protease with unique structural and biochemical features. *FASEB J.* **24**, 2839–48

168. Zinkernagel, A. S., Timmer, A. M., Pence, M. A., Locke, J. B., Buchanan, J. T., Turner, C. E., Mishalian, I., Sriskandan, S., Hanski, E., and Nizet, V. (2008) The IL-8 Protease SpyCEP/ScpC of Group A Streptococcus Promotes Resistance to Neutrophil Killing. *Cell Host Microbe*. **4**, 170–178

169. Andreoni, F., Ogawa, T., Ogawa, M., Madon, J., Uchiyama, S., Schuepbach, R. a, and Zinkernagel, A. S. (2014) The IL-8 protease SpyCEP is detrimental for Group A Streptococcus host-cells interaction and biofilm formation. *Front. Microbiol.* **5**, 339

170. Zhu, H., Liu, M., Sumby, P., and Lei, B. (2009) The secreted esterase of group A Streptococcus is important for invasive skin infection and dissemination in mice. *Infect. Immun.* **77**, 5225–5232

171. Hayano, S., and Tanaka, A. (1973) Extracellular esterases of group A streptococci. *Infect. Immun.* **7**, 561–566

172. Feng, W., Minor, D., Liu, M., and Lei, B. (2017) Requirement and synergistic contribution of platelet-activating factor acetylhydrolase Sse and streptolysin S to inhibition of neutrophil recruitment and systemic infection by hypervirulent emm3 group A Streptococcus in subcutaneous infection of mice. *Infect. Immun.* **85**, e00530-17

173. Liu, M., Zhu, H., Li, J., Garcia, C. C., Feng, W., Kirpotina, L. N., Hilmer, J., Tavares, L. P., Layton, A. W., Quinn, M. T., Bothner, B., Teixeira, M. M., and Lei, B. (2012) Group A Streptococcus Secreted Esterase Hydrolyzes Platelet-Activating Factor to Impede Neutrophil Recruitment and Facilitate Innate Immune Evasion. *PLoS Pathog.* **8**, e1002624

174. Boxrud, P. D., Verhamme, I. M., and Bock, P. E. (2004) Resolution of conformational activation in the kinetic mechanism of plasminogen activation by streptokinase. *J. Biol. Chem.* **279**, 36633–36641

175. Boxrud, P. D., Fay, W. P., and Bock, P. E. (2000) Streptokinase binds to human plasmin with high affinity, perturbs the plasmin active site, and induces expression of a substrate recognition exosite for plasminogen. *J. Biol. Chem.* **275**, 14579–14589

176. Nolan, M., Bouldin, S. D., and Bock, P. E. (2013) Full time course kinetics of the streptokinase-plasminogen activation pathway. *J. Biol. Chem.* **288**, 29482–29493

177. Boxrud, P. D., and Bock, P. E. (2004) Coupling of conformational and proteolytic activation in the kinetic mechanism of plasminogen activation by streptokinase. *J. Biol. Chem.* **279**, 36642–36649

178. Fischetti, V. A. (1989) Streptococcal M protein: molecular design and biological behavior. *Clin. Microbiol. Rev.* **2**, 285–314

179. Fischetti, V. A., Pancholi, V., and Schneewind, O. (1990) Conservation of a hexapeptide sequence in the anchor region of surface proteins from Gram-positive cocci. **4**, 1603–1605

180. Hollingshead, S. K., Arnold, J., Readdy, T. L., and Bessenz, D. E. (1994) Molecular evolution of a multigene family in group A streptococci. *Mol. Biol. Evol.* **11**, 208–219

181. Ermert, D., Weckel, A., Magda, M., Mörgelin, M., Shaughnessy, J., Rice, P. A., Björck, L., Ram, S., and Blom, A. M. (2018) Human IgG Increases Virulence of Streptococcus pyogenes through Complement Evasion. *J. Immunol.* **200**, 3495–3505

182. Ghosh, P. (2011) The nonideal coiled coil of M protein and its multifarious functions in pathogenesis. in *Advances in Experimental Medicine and Biology* (Linke, D., and Goldman, A. eds), pp. 197–211, Advances in Experimental Medicine and Biology, Springer Netherlands, Dordrecht, **715**, 197–211

183. Nilson, B. H. K., Frick, I.-M. M., Akesson, P., Forsén, S., Björck, L., Akerström, B., Wikström, M., Aakesson, P., Forsen, S., Bjoerck, L., Aakerstroem, B., and Wikstroem, M. (1995) Structure and Stability of Protein H and the M1 Protein from *Streptococcus pyogenes*. Implications for Other Surface Proteins of Gram-Positive Bacteria. *Biochemistry*. **34**, 13688–13698

184. McNamara, C., Zinkernagel, A. S., Macheboeuf, P., Cunningham, M. W., Nizet, V., and Ghosh, P. (2008) Coiled-Coil Irregularities and Instabilities in Group A Streptococcus M1 Are Required for Virulence. *Science (80-.).* **319**, 1405–1408

185. Stewart, C. M., Buffalo, C. Z., Valderrama, J. A., Henningham, A., Cole, J. N., Nizet, V., and Ghosh, P. (2016) Coiled-coil destabilizing residues in the group A *Streptococcus* M1 protein are required for functional interaction. *Proc. Natl. Acad. Sci.* **113**, 9515–9520

186. Uchiyama, S., Andreoni, F., Zürcher, C., Schilcher, K., Ender, M., Madon, J., Matt, U., Ghosh, P., Nizet, V., Schuepbach, R. A., and Zinkernagel, A. S. (2013) Coiled-coil irregularities of the M1 protein structure promote M1-fibrinogen interaction and influence group A Streptococcus host cell interactions and virulence. *J. Mol. Med. (Berl).* **91**, 861–9

187. Horstmann, R. D., Sievertsen, H. J., Knobloch, J., and Fischetti, V. A. (1988) Antiphagocytic activity of streptococcal M protein: selective binding of complement control protein factor H. *Proc. Natl. Acad. Sci. U. S. A.* **85**, 1657–61

188. Johnsson, E., Bergård, K., Kotarsky, H., Hellwage, J., Zipfel, P., Sjöbring, U., and Lindahl, G. (1998) Role of the hypervariable region in streptococcal M proteins: Binding of a human complement regulator. *Mol. Immunol.* **35**, 369

189. Suvilehto, J., Jarva, H., Seppänen, M., Siljander, T., Vuopio-Varkila, J., and Meri, S. (2008) Binding of complement regulators factor H and C4b binding protein to group A streptococcal strains isolated from tonsillar tissue and blood. *Microbes Infect.* **10**, 757–63

190. Kotarsky, H., Hellwage, J., Johnsson, E., Skerka, C., Svensson, H. G., Lindahl, G., Sjöbring, U., Peter, F., and Zipfel, P. F. (1998) Identification of a Domain in Human Factor H and Factor H-Like Protein-1 Required for the Interaction with Streptococcal M Proteins. *J. Immunol.* **160**, 3349 LP-3354

191. Bessen, D. E. (1994) Localization of immunoglobulin A-binding sites within M or M-like proteins of group A streptococci. *Infect. Immun.* **62**, 1968–1974

192. Hollingshead, S. K., Fischetti, V. A., and Scott, J. R. (1987) A highly conserved region present in transcripts encoding heterologous M proteins of group A streptococci. *Infect. Immun.* **55**, 3237–3239

193. Sandin, C., Carlsson, F., and Lindahl, G. (2006) Binding of human plasma proteins to *Streptococcus pyogenes* M protein determines the location of opsonic and non-opsonic epitopes. *Mol. Microbiol.* **59**, 20–30

194. Ringdahl, U., and Sjöbring, U. (2000) Analysis of plasminogen-binding M proteins of *Streptococcus pyogenes*. *Methods*. **21**, 143–150

195. Sanderson-Smith, M., De Oliveira, D. M. P. P., Guglielmini, J., McMillan, D. J., Vu, T., Holien, J. K., Henningham, A., Steer, A. C., Bessen, D. E., Dale, J. B., Curtis, N., Beall, B. W., Walker, M. J., Parker, M. W., Carapetis, J. R., Van Melderen, L., Sriprakash, K. S., Smeesters, P. R., Génétique, L. De, Batzloff, M., Towers, R., Goossens, H., Malhotra-Kumar, S., Guilherme, L., Torres, R., Low, D., McGeer, A., Krizova, P., El Tayeb, S., Kado, J., Van Der Linden, M., Erdem, G., Moses, A., Nir-Paz, R., Ikebe, T., Watanabe, H., Sow, S., Tamboura, B., Kittang, B., Melo-Cristino, J., Ramirez, M., Straut, M., Suvorov, A., Totolian, A., Engel, M., Mayosi, B., Whitelaw, A., Darenberg, J., Normark, B. H., Ni, C. C., Wu, J. J., De Zoysa, A., Efstratiou, A., Shulman, S., and Tanz, R. (2014) A Systematic and Functional Classification of *Streptococcus pyogenes* That Serves as a New Tool for Molecular Typing and Vaccine Development. *J. Infect. Dis*. **210**, 1325–38

196. Lauth, X., von Köckritz-Blickwede, M., McNamara, C. W., Myskowski, S., Zinkernagel, A. S., Beall, B., Ghosh, P., Gallo, R. L., and Nizet, V. (2009) M1 Protein Allows Group A Streptococcal Survival in Phagocyte Extracellular Traps through Cathelicidin Inhibition. *J. Innate Immun.* **1**, 202–214

197. Nilsson, M., Wasylik, S., Mörgelin, M., Olin, A. I., Meijers, J. C. M., Derksen, R. H. W. M., de Groot, P. G., and Herwald, H. (2008) The antibacterial activity of peptides derived from human beta-2 glycoprotein I is inhibited by protein H and M1 protein from *Streptococcus pyogenes*. *Mol. Microbiol.* **67**, 482–492

198. Courtney, H. S., Von Hunolstein, C., Dale, J. B., Bronze, M. S., Beachey, E. H., and Hasty, D. L. (1992) Lipoteichoic acid and M protein: dual adhesins of group A streptococci. *Microb. Pathog.* **12**, 199–208

199. Wang, J. R., and Stinson, M. W. (1994) M protein mediates streptococcal adhesion to HEp-2 cells. *Infect. Immun.* **62**, 442–448

200. Cue, D., Lam, H., and Cleary, P. P. (2001) Genetic dissection of the *Streptococcus pyogenes* M1 protein: regions involved in fibronectin binding and intracellular invasion. *Microb. Pathog.* **31**, 231–42

201. Okada, N., Liszewski, M. K., Atkinson, J. P., and Caparon, M. (1995) Membrane cofactor protein (CD46) is a keratinocyte receptor for the M protein of the group A streptococcus. *Proc. Natl. Acad. Sci. U. S. A.* **92**, 2489–93

202. Giannakis, E., Male, D. A., Ormsby, R. J., Loveland, B. E., and Gordon, D. L. (2002) Identification of the streptococcal M protein binding site on membrane cofactor protein (CD46). *J. Immunol.* **168**, 4585–4592

203. Berkower, C., Ravins, M., Moses, A. E., and Hanski, E. (1999) Expression of different group A streptococcal M proteins in an isogenic background demonstrates diversity in adherence to and invasion of eukaryotic cells. *Mol. Microbiol.* **31**, 1463–1475

204. Frick, I. M., Schmidtchen, A., and Sjöbring, U. (2003) Interactions between M proteins of *Streptococcus pyogenes* and glycosaminoglycans promote bacterial adhesion to host cells. *Eur. J. Biochem.* **270**, 2303–2311

205. Frick, I. M., Mörgelin, M., and Björck, L. (2000) Virulent aggregates of *Streptococcus pyogenes* are generated by homophilic protein-protein interactions. *Mol. Microbiol.* **37**, 1232–1247

206. Caparon, M. G., Stephens, D. S., Olsein, A., and Scott, J. R. (1991) Role of M Protein in Adherence of Group A Streptococci. **6**, 1811–1817

207. Guilherme, L., Faé, K. C., Oshiro, S. E., Tanaka, A. C., Pomerantzeff, P. M. a, and Kalil, J. (2007) T cell response in rheumatic fever: crossreactivity between streptococcal M protein peptides and heart tissue proteins. *Curr. Protein Pept. Sci.* **8**, 39–44

208. Sanderson-Smith, M. L., Dowton, M., Ranson, M., and Walker, M. J. (2007) The plasminogen-binding group A streptococcal M protein-related protein Prp binds plasminogen via arginine and histidine residues. *J. Bacteriol.* **189**, 1435–1440

209. Sanderson-Smith, M. L., Walker, M. J., and Ranson, M. (2006) The maintenance of high affinity plasminogen binding by group A streptococcal plasminogen-binding M-like protein is mediated by arginine and histidine residues within the a1 and a2 repeat domains. *J. Biol. Chem.* **281**, 25965–25971

210. Berge, A., and Sjobring, U. (1993) PAM, a novel plasminogen-binding protein from *Streptococcus pyogenes*. *J. Biol. Chem.* **268**, 25417–25424

211. Åkesson, P., Schmidt, K. H., Cooney, J., and Björck, L. (1994) M1 protein and protein H: IgGFc- and albumin-binding streptococcal surface proteins encoded by adjacent genes. *Biochem. J.* **300**, 877–886

212. Cue, D., Dombek, P. E., Lam, H., and Cleary, P. P. (1998) *Streptococcus pyogenes* serotype M1 encodes multiple pathways for entry into human epithelial cells. *Infect. Immun.* **66**, 4593–4601

213. Ben Nasr, A. B., Herwald, H., Müller-Esterl, W., and Björck, L. (1995) Human kininogens interact with M protein, a bacterial surface protein and virulence determinant. *Biochem. J.* **305**, 173–180

214. Gubbe, K., Misselwitz, R., Welfle, K., Reichardt, W., Schmidt, K.-H., and Welfle, H. (1997) C-repeats of streptococcal M1 protein achieve the human serum albumin binding ability by flanking regions which stabilize the coiled coil conformation. *Biochemistry*. **36**, 8107–8113

215. Reichardt, W., Schmidt, K.-H., Amberg, C., and Gubbe, K. (1997) Mapping of Binding Sites for Human Serum Albumin and Fibrinogen on the M3-Protein BT - Streptococci and the Host (Horaud, T., Bouvet, A., Leclercq, R., de Montclos, H., and Sicard, M. eds), pp. 577–579, Springer US, Boston, MA, 10.1007/978-1-4899-1825-3_133

216. Price, J. D., Schaumburg, J., Sandin, C., Atkinson, J. P., Lindahl, G., and Kemper, C. (2005) Induction of a Regulatory Phenotype in Human CD4+ T Cells by Streptococcal M Protein. *J. Immunol.* **175**, 677–684

217. Waldemarsson, J., Stålhammar-Carlemalm, M., Sandin, C., Castellino, F. J., and Lindahl, G. (2009) Functional Dissection of Streptococcus pyogenes M5 Protein: the Hypervariable Region is Essential for Virulence. *PLoS One*. **4**, e7279

218. Whitnack, E., and Beachey, E. H. (1985) Inhibition of complement-mediated opsonization and phagocytosis of *Streptococcus pyogenes* by D fragments of fibrinogen and fibrin bound to cell surface M protein. *J. Exp. Med.* **162**, 1983–1997

219. Horstmann, R. D., Sievertsen, H. J., Leippe, M., and Fischetti, V. A. (1992) Role of fibrinogen in complement inhibition by streptococcal M protein. *Infect. Immun.* **60**, 5036–5041

220. Perez-Casal, J., Okada, N., Caparon, M. G., and Scott, J. R. (1995) Role of the conserved C-repeat region of the M protein of *Streptococcus pyogenes*. *Mol. Microbiol.* **15**, 907–916

221. Fischetti, V. A., Horstmann, R. D., and Pancholi, V. (1995) Location of the complement factor H binding site on streptococcal M6 protein. *Infect. Immun.* **63**, 149–153

222. Okada, N., Pentland, A. P., Falk, P., and Caparon, M. G. (1994) M protein and protein F act as important determinants of cell-specific tropism of *Streptococcus pyogenes* in skin tissue. *J. Clin. Invest.* **94**, 965–977

223. Retnoningrum, D. S., and Cleary, P. P. (1994) M12 protein from *Streptococcus pyogenes* is a receptor for immunoglobulin G3 and human albumin. *Infect. Immun.* **62**, 2387–2394

224. Whitnack, E., and Beachey, E. H. (1985) Biochemical and biological properties of the binding of human fibrinogen to M protein in group A streptococci. *J. Bacteriol.* **164**, 350–8

225. Boyle, M. D. P., Weber-Heynemann, J., Raeder, R., and Podbielski, A. (1995) Characterization of a gene coding for a type IIo bacterial IgG-binding protein. *Mol. Immunol.* **32**, 669–678

226. Glinton, K., Beck, J., Liang, Z., Qiu, C., Lee, S. W., Ploplis, V. A., and Castellino, F. J. (2017) Variable region in streptococcal M-proteins provides stable binding with host fibrinogen for plasminogen-mediated bacterial invasion. *J. Biol. Chem.* **292**, 6775–6785

227. Wistedt, A. C., Ringdahl, U., Müller-Esterl, W., and Sjöbring, U. (1995) Identification of a plasminogen-binding motif in PAM, a bacterial surface protein. *Mol. Microbiol.* **18**, 569–578

228. Morfeldt, E., Berggård, K., Persson, J., Drakenberg, T., Johnsson, E., Lindahl, E., Linse, S., and Lindahl, G. (2001) Isolated

hypervariable regions derived from streptococcal M proteins specifically bind human C4b-binding protein: implications for antigenic variation. *J. Immunol.* **167**, 3870–3877

229. Johnsson, E., Thern, A., Dahlbäck, B., Hedén, L. O., Wikström, M., and Lindahl, G. (1996) A highly variable region in members of the streptococcal M protein family binds the human complement regulator C4BP. *J. Immunol.* **157**, 3021–9

230. Jenkins, H. T., Mark, L., Ball, G., Persson, J., Lindahl, G., Uhrin, D., Blom, A. M., and Barlow, P. N. (2006) Human C4b-binding protein, structural basis for interaction with streptococcal M protein, a major bacterial virulence factor. *J. Biol. Chem.* **281**, 3690–3697

231. André, I., Persson, J., Blom, A. M., Nilsson, H., Drakenberg, T., Lindahl, G., and Linse, S. (2006) Streptococcal M protein: Structural studies of the hypervariable region, free and bound to human C4BP. *Biochemistry*. **45**, 4559–4568

232. Lars, S., Paul, O., Gunnar, L., Stenberg, L., O'Toole, P., and Lindahl, G. (1992) Many group A streptococcal strains express two different immunoglobulin-binding proteins, encoded by closely linked genes: characterization of the proteins expressed by four strains of different M-type. *Mol. Microbiol.* **6**, 1185–94

233. Johnsson, E., Andersson, G., Lindahl, G., and Hedén, L. O. (1994) Identification of the IgA-binding region in streptococcal protein Arp. *J. Immunol.* **153**, 3557–3564

234. Persson, J., Beall, B., Linse, S., and Lindahl, G. (2006) Extreme Sequence Divergence but Conserved Ligand-Binding Specificity in Streptococcus pyogenes M Protein. *PLoS Pathog.* **2**, e47

235. Berggard, K., Johnsson, E., Morfeldt, E., Persson, J., Stalhammar-Carlemalm, M., and Lindahl, G. (2001) Binding of human C4BP to the hypervariable region of M protein: a molecular mechanism of phagocytosis resistance in *Streptococcus pyogenes*. *Mol Microbiol*. **42**, 539–551

236. Frick, I. M., Åkesson, P., Cooney, J., Sjöbring, U., Schmidt, K. H., Gomi, H., Hattori, S., Tagawa, C., Kishimoto, F., and Björck, L. (1994) Protein H - A surface protein of *Streptococcus pyogenes* with separate binding sites for IgG and albumin. *Mol. Microbiol.* **12**, 143–151

237. Yung, D. L., and Hollingshead, S. K. (1996) DNA sequencing and gene expression of the *emm* gene cluster in an M50 group A Streptococcus strain virulent for mice. *Infect. Immun.* **64**, 2193–2200

238. Heden, L. O., and Lindahl, G. (1993) Conserved and variable regions in protein Arp, the IgA receptor of *Streptococcus pyogenes*. *J Gen Microbiol*. **139**, 2067–2074

239. Stenberg, L., O'Toole, P., and Lindahl, G. (1992) Many group A streptococcal strains express two different immunoglobulin-binding proteins, encoded by closely linked genes: characterization of the proteins expressed by four strains of different M-type. *Mol. Microbiol.* **6**, 1185–94

240. Frost, H. R., Sanderson-Smith, M., Walker, M., Botteaux, A., and Smeesters, P. R. (2018) Group A streptococcal M-like proteins: From pathogenesis to vaccine potential. *FEMS Microbiol. Rev.* **42**, 193–204

241. Ermert, D., Weckel, A., Agarwal, V., Frick, I.-M., Bjorck, L., Blom, A. M., and Björck, L. (2013) Binding of complement inhibitor C4b-binding protein to a highly virulent *Streptococcus pyogenes* M1 strain is mediated by protein H and enhances adhesion to and invasion of endothelial cells. *J. Biol. Chem.* **288**, 32172–83

242. Courtney, H. S., Hasty, D. L., and Dale, J. B. (2006) Anti-phagocytic mechanisms of *Streptococcus pyogenes*: binding of fibrinogen to M-related protein. *Mol. Microbiol.* **59**, 936–47

243. Perez-Caballero, D., Garcia-Laorden, I., Cortes, G., Wessels, M. R., de Cordoba, S. R., and Alberti, S. (2004) Interaction between complement regulators and *Streptococcus pyogenes*: binding of C4b-binding protein and factor H/factor H-like protein 1 to M18 strains involves two different cell surface molecules. *J Immunol*. **173**, 6899–6904

244. Podbielski, A., Schnitzler, N., Beyhs, P., and Boyle, M. D. (1996) M-related protein (Mrp) contributes to group A streptococcal resistance to phagocytosis by human granulocytes. *Mol. Microbiol.* **19**, 429–41

245. Li, Y., and Courtney, H. S. (2011) Promotion of phagocytosis of *Streptococcus pyogenes* in human blood by a fibrinogen-binding peptide. *Microbes Infect.* **13**, 413–418

246. Courtney, H. S., and Li, Y. (2013) Non-Immune Binding of Human IgG to M-Related Proteins Confers Resistance to Phagocytosis of Group A Streptococci in Blood. *PLoS One*. **8**, e78719

247. Krebs, B., Kaufhold, A., Boyle, M. D., and Podbielski, A. (1996) Different alleles of the fcrA/mrp gene of *Streptococcus pyogenes* encode M-related proteins exhibiting an identical immunoglobulin-binding pattern. *Med. Microbiol. Immunol.* **185**, 39–47

248. Thern, A., Wastfelt, M., and Lindahl, G. (1998) Expression of two different antiphagocytic M proteins by *Streptococcus pyogenes* of the OF+ lineage. *J Immunol*. **160**, 860–869

249. O'Toole, P. W., Stenberg, L., Rissler, M., and Lindahl, G. (1992) Two major classes in the M protein family in group A streptococci. *Proc. Natl. Acad. Sci. U. S. A.* **89**, 8661–5

250. Heath, D. G., and Cleary, P. P. (1989) Fc-receptor and M-protein genes of group A streptococci are products of gene duplication. *Proc. Natl. Acad. Sci. U. S. A.* **86**, 4741–5

251. Heath, D. G., Boyle, M. D. P., and Cleary, P. P. (1990) Isolated DNA repeat region from fcrA76, the Fc-binding protein gene from an M-type 76 strain of group A streptococci, encodes a protein with Fc-binding activity. *Mol. Microbiol.* **4**, 2071–2079

252. Boyle, M. D. P., Hawlitzky, J., Raeder, R., and Podbielski, A. (1994) Analysis of genes encoding two unique type IIa immunoglobulin G-binding proteins expressed by a single group A streptococcal isolate. *Infect. Immun.* **62**, 1336–1347

253. Pack, T. D., Podbielski, A., and Boyle, M. D. P. (1996) Identification of an amino acid signature sequence predictive of protein G-inhibitable IgG3-binding activity in group-A streptococcal IgG-binding proteins. *Gene*. **171**, 65–70

254. O'Connor, S. P., and Cleary, P. P. (1986) Localization of the streptococcal C5a peptidase to the surface of group A streptococci. *Infect. Immun.* **53**, 432–434

255. Cleary, P. P., Prahbu, U., Dale, J. B., Wexler, D. E., and Handley, J. (1992) Streptococcal C5a peptidase is a highly specific endopeptidase. *Infect. Immun.* **60**, 5219–5223

256. Chmouryguina, I., Suvorov, A., Ferrieri, P., Cleary, P. P., and Cleary, A. P. P. (1996) Conservation of the C5a peptidase genes in group A and B streptococci. *Infect. Immun.* **64**, 2387–2390

257. Ji, Y., Schnitzler, N., Demaster, E., and Cleary, P. (1998) Impact of M49, Mrp, Enn, and C5a peptidase proteins on colonization of the mouse oral mucosa by *Streptococcus pyogenes*. *Infect. Immun.* **66**, 5399–5405

258. Ji, Y., Mclandsborough, L., Kondagunta, A., and Cleary, P. P. (1996) C5a Peptidase Alters Clearance and Trafficking of Group A Streptococci by Infected Mice. *Infect. Immun.* **64**, 503–510

259. Ji, Y., Carlson, B., Kondagunta, A., and Cleary, P. P. (1997) Intranasal immunization with C5a peptidase prevents nasopharyngeal colonization of mice by the group A Streptococcus. *Infect. Immun.* **65**, 2080–2087

260. Tamura, G. S., Hull, J. R., Oberg, M. D., and Castner, D. G. (2006) High-affinity interaction between fibronectin and the group B streptococcal C5a peptidase is unaffected by a naturally occurring four-amino-acid deletion that eliminates peptidase activity. *Infect. Immun.* **74**, 5739–5746

261. Lynskey, N. N., Reglinski, M., Calay, D., Siggins, M. K., Mason, J. C., Botto, M., and Sriskandan, S. (2017) Multi-functional mechanisms of immune evasion by the streptococcal complement inhibitor C5a peptidase. *PLOS Pathog.* **13**, e1006493

262. Falugi, F., Zingaretti, C., Pinto, V., Mariani, M., Amodeo, L., Manetti, A. G. O., Capo, S., Musser, J. M., Orefici, G., Margarit, I., Telford, J. L., Grandi, G., and Mora, M. (2008) Sequence Variation in Group A *Streptococcus* Pili and Association of Pilus Backbone Types with Lancefield T Serotypes. *J. Infect. Dis.* **198**, 1834–1841

263. Margarit y Ros, I. (2016) *Streptococcus pyogenes Pili*

264. Manetti, A. G. O., Zingaretti, C., Falugi, F., Capo, S., Bombaci, M., Bagnoli, F., Gambellini, G., Bensi, G., Mora, M., Edwards, A. M., Musser, J. M., Graviss, E. A., Telford, J. L., Grandi, G., and Margarit, I. (2007) *Streptococcus pyogenes* pili promote pharyngeal cell adhesion and biofilm formation. *Mol. Microbiol.* **64**, 968–983

265. Abbot, E. L., Smith, W. D., Siou, G. P. S. S., Chiriboga, C., Smith, R. J., Wilson, J. A., Hirst, B. H., and Kehoe, M. A. (2007) Pili mediate specific adhesion of *Streptococcus pyogenes* to human tonsil and skin. *Cell. Microbiol.* **9**, 1822–1833

266. Smith, W. D., Pointon, J. A., Abbot, E., Kang, H. J., Baker, E. N., Hirst, B. H., Wilson, J. A., Banfield, M. J., and Kehoe, M. A. (2010) Roles of minor pilin subunits Spy0125 and Spy0130 in the serotype M1 *Streptococcus pyogenes* strain SF370. *J. Bacteriol.* **192**, 4651–4659

267. Linke-Winnebeck, C., Paterson, N. G., Young, P. G., Middleditch, M. J., Greenwood, D. R., Witte, G., and Baker, E. N. (2014) Structural model for covalent adhesion of the *Streptococcus pyogenes* pilus through a thioester bond. *J. Biol. Chem.* **289**, 177–189

268. Kreikemeyer, B., Nakata, M., Oehmcke, S., Gschwendtner, C., Normann, J., and Podbielski, A. (2005) *Streptococcus pyogenes* collagen type I-binding Cpa surface protein: Expression profile, binding characteristics, biological functions, and potential clinical impact. *J. Biol. Chem.* **280**, 33228–33239

269. Edwards, A. M., Manetti, A. G. O., Falugi, F., Zingaretti, C., Capo, S., Buccato, S., Bensi, G., Telford, J. L., Margarit, I., and Grandi, G. (2008) Scavenger receptor gp340 aggregates group A streptococci by binding pili. *Mol. Microbiol.* **68**, 1378–1394

270. Schwarz-Linek, U., Höök, M., and Potts, J. R. (2004) The molecular basis of fibronectin-mediated bacterial adherence to host cells. *Mol. Microbiol.* **52**, 631–641

271. Dinkla, K., Rohde, M., Jansen, W. T. M., Carapetis, J. R., Chhatwal, G. S., and Talay, S. R. (2003) *Streptococcus pyogenes* recruits collagen via surface-bound fibronectin: A novel colonization and immune evasion mechanism. *Mol. Microbiol.* **47**, 861–869

272. Medina, E., Schulze, K., Chhatwal, G. S., and Guzmán, C. A. (2000) Nonimmune interaction of the SfbI protein of *Streptococcus pyogenes* with the immunoglobulin G F(ab')2 fragment. *Infect. Immun.* **68**, 4786–4788

273. Talay, S. R., Zock, A., Rohde, M., Molinari, G., Oggioni, M., Pozzi, G., Guzman, C. A., and Chhatwal, G. S. (2000) Co-operative binding of human fibronectin to Sfbl protein triggers streptococcal invasion into respiratory epithelial cells. *Cell. Microbiol.* **2**, 521–535

274. Rohde, M., Müller, E., Chhatwal, G. S., and Talay, S. R. (2003) Host cell caveolae act as an entry-port for Group A streptococci. *Cell. Microbiol.* **5**, 323–342

275. Hyland, K. A., Wang, B., and Cleary, P. P. (2007) Protein F1 and *Streptococcus pyogenes* resistance to phagocytosis. *Infect. Immun.* **75**, 3188–3191

276. Walden, M., Edwards, J. M., Dziewulska, A. M., Bergmann, R., Saalbach, G., Kan, S. Y., Miller, O. K., Weckener, M., Jackson, R. J., Shirran, S. L., Botting, C. H., Florence, G. J., Rohde, M., Banfield, M. J., and Schwarz-Linek, U. (2015) An internal thioester in a pathogen surface protein mediates covalent host binding. *Elife*. **4**, 1–24

277. Ramachandran, V., McArthur, J. D., Behm, C. E., Gutzeit, C., Dowton, M., Fagan, P. K., Towers, R., Currie, B., Sriprakash, K. S., and Walker, M. J. (2004) Two distinct genotypes of prtF2, encoding a fibronectin binding protein, and evolution of the gene family in *Streptococcus pyogenes*. *J. Bacteriol.* **186**, 7601–7609

278. Amelung, S., Nerlich, A., Rohde, M., Spellerberg, B., Cole, J. N., Nizet, V., Chhatwal, G. S., and Talay, S. R. (2011) The FbaB-type fibronectin-binding protein of *Streptococcus pyogenes* promotes specific invasion into endothelial cells. *Cell. Microbiol.* **13**, 1200–11

279. Rocha, C. L., and Fischetti, V. A. (1999) Identification and characterization of a novel fibronectin-binding protein on the surface of

group A streptococci. *Infect. Immun.* **67**, 2720–8

280. Wästfelt, M., Stålhammar-Carlemalm, M., Delisse, A. M., Cabezon, T., and Lindahl, G. (1996) Identification of a family of Streptococcal surface proteins with extremely repetitive structure. *J. Biol. Chem.* **271**, 18892–18897

281. Lachenauer, C. S., Creti, R., Michel, J. L., and Madoff, L. C. (2000) Mosaicism in the alpha-like protein genes of group B streptococci. *Proc. Natl. Acad. Sci. U. S. A.* **97**, 9630–9635

282. Lindahl, G., Stalhammer-Carlemalm, M., and Areschoug, T. (2005) Surface Proteins of *Streptococcus agalactiae* and Related Proteins in Other Bacterial Pathogens. *Clin. Microbiol. Rev.* **18**, 102–127

283. Callebaut, I., Gilgès, D., Vigon, I., and Mornon, J. P. (2000) HYR, an extracellular module involved in cellular adhesion and related to the immunoglobulin-like fold. *Protein Sci.* **9**, 1382–90

284. Aupérin, T. C., Bolduc, G. R., Baron, M. J., Heroux, A., Filman, D. J., Madoff, L. C., and Hogle, J. M. (2005) Crystal structure of the N-terminal domain of the group B streptococcus alpha C protein. *J. Biol. Chem.* **280**, 18245–52

285. Baron, M. J., Bolduc, G. R., Goldberg, M. B., Aupérin, T. C., and Madoff, L. C. (2004) Alpha C protein of group B Streptococcus binds host cell surface glycosaminoglycan and enters cells by an actin-dependent mechanism. *J. Biol. Chem.* **279**, 24714–24723

286. Baron, M. J., Filman, D. J., Prophete, G. A., Hogle, J. M., and Madoff, L. C. (2007) Identification of a glycosaminoglycan binding region of the alpha C protein that mediates entry of group B Streptococci into host cells. *J. Biol. Chem.* **282**, 10526–10536

287. Bolduc, G. R., and Madoff, L. C. (2007) The group B streptococcal alpha C protein binds α1β1-integrin through a novel KTD motif that promotes internalization of GBS within human epithelial cells. *Microbiology*. **153**, 4039–4049

288. Bolduc, G. R., Baron, M. J., Gravekamp, C., Lachenauer, C. S., and Madoff, L. C. (2002) The alpha C protein mediates internalization of group B Streptococcus within human cervical epithelial cells. *Cell Microbiol*. **4**, 751–758

289. Linke, C., Siemens, N., Oehmcke, S., Radjainia, M., Law, R. H. P., Whisstock, J. C., Baker, E. N., and Kreikemeyer, B. (2012) The extracellular protein factor epf from *Streptococcus pyogenes* is a cell surface adhesin that binds to cells through an n-terminal domain containing a carbohydrate-binding module. *J. Biol. Chem.* **287**, 38178–38189

290. Linke, C., Siemens, N., Middleditch, M. J., Kreikemeyer, B., and Baker, E. N. (2012) Purification, crystallization and preliminary crystallographic analysis of the adhesion domain of Epf from *Streptococcus pyogenes*. *Acta Crystallogr. Sect. F Struct. Biol. Cryst. Commun.* **68**, 793–797

291. Zhang, S., Green, N. M., Sitkiewicz, I., LeFebvre, R. B., and Musser, J. M. (2006) Identification and characterization of an antigen I/II family protein produced by group A Streptococcus. *Infect. Immun.* **74**, 4200–4213

292. Maddocks, S. E., Wright, C. J., Nobbs, A. H., Brittan, J. L., Franklin, L., Strömberg, N., Kadioglu, A., Jepson, M. a, and Jenkinson, H. F. (2011) *Streptococcus pyogenes* antigen I/II-family polypeptide AspA shows differential ligand-binding properties and mediates biofilm formation. *Mol. Microbiol.* **81**, 1034–49

293. Franklin, L., Nobbs, A. H., Bricio-Moreno, L., Wright, C. J., Maddocks, S. E., Sahota, J. S., Ralph, J., O'Connor, M., Jenkinson, H. F., and Kadioglu, A. (2013) The AgI/II Family Adhesin AspA Is Required for Respiratory Infection by Streptococcus pyogenes. *PLoS One*. **8**, e62433

294. Chang, A., Khemlani, A., Kang, H., and Proft, T. (2011) Functional analysis of *Streptococcus pyogenes* nuclease A (SpnA), a novel group A streptococcal virulence factor. *Mol. Microbiol.* **79**, 1629–1642

295. O'Brien, K. L., Beall, B., Barrett, N. L., Cieslak, P. R., Reingold, A., Farley, M. M., Danila, R., Zell, E. R., Facklam, R., Schwartz, B., and Schuchat, A. (2002) Epidemiology of Invasive Group A *Streptococcus* Disease in the United States, 1995–1999. *Clin. Infect. Dis.* **35**, 268–276

296. Han, M., Gillard, B. K., Courtney, H. S., Ward, K., Rosales, C., Khant, H., Ludtke, S. J., and Pownall, H. J. (2009) Disruption of human plasma high-density lipoproteins by streptococcal serum opacity factor requires labile apolipoprotein A-I. *Biochemistry*. **48**, 1481–1487

297. Courtney, H. S., Hasty, D. L., Li, Y., Chiang, H. C., Thacker, J. L., and Dale, J. B. (1999) Serum opacity factor is a major fibronectin-binding protein and a virulence determinant of M type 2 *Streptococcus pyogenes*. *Mol. Microbiol.* **32**, 89–98

298. Rakonjac, J. V., Robbins, J. C., and Fischetti, V. A. (1995) DNA sequence of the serum opacity factor of group A streptococci: Identification of a fibronectin-binding repeat domain. *Infect. Immun.* **63**, 622–631

299. Katerov, V., Lindgren, P. E., Totolian, A. A., and Schalén, C. (2000) Streptococcal opacity factor: A family of bifunctional proteins with lipoproteinase and fibronectin-binding activities. *Curr. Microbiol.* **40**, 149–156

300. Zhu, L., Olsen, R. J., and Musser, J. M. (2017) Opacification Domain of Serum Opacity Factor Inhibits Beta-Hemolysis and Contributes to Virulence of *Streptococcus pyogenes*. *mSphere*. **2**, e00147-17

301. Biedzka-Sarek, M., Metso, J., Kateifides, A., Meri, T., Jokiranta, T. S., Muszyński, A., Radziejewska-Lebrecht, J., Zannis, V., Skurnik, M., and Jauhiainen, M. (2011) Apolipoprotein A-I exerts bactericidal activity against Yersinia enterocolitica serotype O:3. *J. Biol. Chem.* **286**, 38211–38219

302. Jeng, A., Sakota, V., Li, Z., Datta, V., Beall, B., and Nizet, V. (2003) Molecular genetic analysis of a group A Streptococcus operon encoding serum opacity factor and a novel fibronectin-binding protein, SfbX. *J. Bacteriol.* **185**, 1208–17

303. Wicken, A. J., and Knox, K. W. (1975) Lipoteichoic acids: a new class of bacterial antigen. *Science*. **187**, 1161–7

304. Ofek, I., Simpson, W. A., and Beachey, E. H. (1982) Formation of molecular complexes between a structurally defined M protein and acylated or deacylated lipoteichoic acid of *Streptococcus pyogenes*. *J. Bacteriol.* **149**, 426–433

305. Miorner, H., Johansson, G., and Kronvall, G. (1983) Lipoteichoic acid is the major cell wall component responsible for surface hydrophobicity of group A streptococci. *Infect. Immun.* **39**, 336–343

306. Beachey, E. H., Dale, J. B., Grebe, S., Ahmed, A., Simpson, W. A., and Ofek, I. (1979) Lymphocytes binding and T cell mitogenic properties of group A streptococcal lipoteichoic acid. *J Immunol*. **122**, 189–195

307. Ofek, I., and Beachey, E. H. (1979) Pathogenic streptococci : proceedings ..., Reedbooks, Chertsey [England]

308. Beachey, E. H., Simpson, W. A., Ofek, I., Hasty, D. L., Dale, J. B., and Whitnack, E. (1983) Attachment of *Streptococcus pyogenes* to mammalian cells. *Rev Infect Dis*. **5 Suppl 4**, S670-7

309. Courtney, H. S., Ofek, I., and Hasty, D. L. (1997) M protein mediated adhesion of M type 24 *Streptococcus pyogenes* stimulates release of interleukin-6 by HEp-2 tissue culture cells. *FEMS Microbiol. Lett.* **151**, 65–70

310. Courtney, H. S., Simpson, W. A., and Beachey, E. H. (1983) Binding of Streptococcal Lipoteichoic Acid to Fatty Acid- Binding Sites on Human Plasma Fibronectin. *J. Bacteriol.* **153**, 763–770

311. Kendall, E., and Dawson, H. (1937) A serologically inactive polysaccharide elaborated by mucoid strains of group A hemolytic streptococcus. *J. Biol. Chem.*

312. DeAngelis, P. L., Papaconstantinou, J., and Weigel, P. H. (1993) Isolation of a *Streptococcus pyogenes* gene locus that directs hyaluronan biosynthesis in acapsular mutants and in heterologous bacteria. *J. Biol. Chem.* **268**, 14568–14571

313. Willcocks, M. (1993) Identification and sequence determination of the capsid protein gene of human astrovirus serotype 1. *FEMS Microbiol. Lett.* **114**, 1–7

314. Dougherty, B. A., and Van de Rijn, I. (1993) Molecular characterization of hasB from an operon required for hyaluronic acid synthesis in group A streptococci. Demonstration of UDP-glucose dehydrogenase activity. *J. Biol. Chem.* **268**, 7118–7124

315. Dougherty, B. A., and van de Rijn, I. (1992) Molecular characterization of a locus required for hyaluronic acid capsule production in group A streptococci. *J. Exp. Med.* **175**, 1291–9

316. Flores, A. R., Jewell, B. E., Fittipaldi, N., Beres, S. B., and Musser, J. M. (2012) Human disease isolates of serotype M4 and M22 group A streptococcus lack genes required for hyaluronic acid capsule biosynthesis. *MBio*. **3**, 4–8

317. Flores, A. R., Chase McNeil, J., Shah, B., Van Beneden, C., and Shelburne, S. A. (2018) Capsule-Negative emm Types Are an Increasing Cause of Pediatric Group A Streptococcal Infections at a Large Pediatric Hospital in Texas. *J. Pediatric Infect. Dis. Soc.* 10.1093/jpids/piy053

318. Hollands, A., Pence, M. A. a, Timmer, A. M. M., Osvath, S. R. R., Turnbull, L., Whitchurch, C. B. B., Walker, M. J. J., and Nizet, V. (2010) Genetic Switch to Hypervirulence Reduces Colonization Phenotypes of the Globally Disseminated Group A *Streptococcus* M1T1 Clone. *J. Infect. Dis.* **202**, 11–19

319. Lancefield, R. C., and Todd, E. W. (1928) Antigenic Differences Between Matt Hemolytic Streptococci and Their Glossy Variants. *J. Exp. Med.* **48**, 769–90

320. Pancholi, V., and Fischetti, V. A. (1992) A major surface protein on group A streptococci is a glyceraldehyde-3-phosphate-dehydrogenase with multiple binding activity. *J. Exp. Med.* **176**, 415–26

321. Boël, G., Jin, H., and Pancholi, V. (2005) Inhibition of cell surface export of group A streptococcal anchorless surface dehydrogenase affects bacterial adherence and antiphagocytic properties. *Infect. Immun.* **73**, 6237–6248

322. Pancholi, V., and Fischetti, V. A. (1997) Regulation of the phosphorylation of human pharyngeal cell proteins by group A streptococcal surface dehydrogenase: signal transduction between streptococci and pharyngeal cells. *J. Exp. Med.* **186**, 1633–43

323. Terao, Y., Yamaguchi, M., Hamada, S., and Kawabata, S. (2006) Multifunctional glyceraldehyde-3-phosphate dehydrogenase of *Streptococcus pyogenes* is essential for evasion from neutrophils. *J. Biol. Chem.* **281**, 14215–14223

324. Jin, H., Agarwal, S., Agarwal, S., and Pancholi, V. (2011) Surface export of GAPDH/SDH, a glycolytic enzyme, is essential for Streptococcus pyogenes virulence. *MBio*. **2**, e00068-11

325. Terao, Y., Kawabata, S., Kunitomo, E., Nakagawa, I., and Hamada, S. (2002) Novel laminin-binding protein of *Streptococcus pyogenes*, Lbp, is involved in adhesion to epithelial cells. *Infect. Immun.* **70**, 993–997

326. Linke, C., Caradoc-Davies, T. T., Young, P. G., Proft, T., and Baker, E. N. (2009) The laminin-binding protein Lbp from *Streptococcus pyogenes* is a zinc receptor. *J. Bacteriol.* **191**, 5814–5823

327. Lukomski, S., Nakashima, K., Abdi, I., Cipriano, V. J., Ireland, R. M., Reid, S. D., Adams, G. G., and Musser, J. M. (2000) Identification and characterization of the scl gene encoding a group A Streptococcus extracellular protein virulence factor with similarity to human collagen. *Infect. Immun.* **68**, 6542–6553

328. Lukomski, S., Nakashima, K., Abdi, I., Cipriano, V. J., Shelvin, B. J., Graviss, E. A., and Musser, J. M. (2001) Identification and characterization of a second extracellular collagen-like protein made by group A Streptococcus: Control of production at the level of translation. *Infect. Immun.* **69**, 1729–1738

329. Humtsoe, J. O., Kim, J. K., Xu, Y., Keene, D. R., Höök, M., Lukomski, S., and Wary, K. K. (2005) A streptococcal collagen-like protein interacts with the α2β1 integrin and induces intracellular signaling. *J. Biol. Chem.* **280**, 13848–13857

330. Caswell, C. C., Lukomska, E., Seo, N. S., Höök, M., and Lukomski, S. (2007) Scl1-dependent internalization of group A Streptococcus via direct interactions with the α2β1 integrin enhances pathogen survival and re-emergence. *Mol. Microbiol.* **64**, 1319–1331

331. Caswell, C. C., Barczyk, M., Keene, D. R., Lukomska, E., Gullberg, D. E., and Lukomski, S. (2008) Identification of the first prokaryotic collagen sequence motif that mediates binding to human collagen receptors, integrins α 2β1 and α11β1. *J. Biol. Chem.* **283**, 36168–36175

332. Caswell, C. C., Han, R., Hovis, K. M., Ciborowski, P., Keene, D. R., Marconi, R. T., and Lukomski, S. (2008) The Scl1 protein of M6-type group A Streptococcus binds the human complement regulatory protein, factor H, and inhibits the alternative pathway of

complement. *Mol. Microbiol.* **67**, 584–596

333. Caswell, C. C., Oliver-Kozup, H., Han, R., Lukomska, E., and Lukomski, S. (2010) Scl1, the multifunctional adhesin of group A Streptococcus, selectively binds cellular fibronectin and laminin, and mediates pathogen internalization by human cells. *FEMS Microbiol. Lett.* **303**, 61–68

334. Reuter, M., Caswell, C. C., Lukomski, S., and Zipfel, P. F. (2010) Binding of the human complement regulators CFHR1 and factor H by streptococcal collagen-like protein 1 (Scl1) via their conserved C termini allows control of the complement cascade at multiple levels. *J. Biol. Chem.* **285**, 38473–38485

335. Han, R., Caswell, C. C., Lukomska, E., Keene, D. R., Pawlowski, M., Bujnicki, J. M., Kim, J. K., and Lukomski, S. (2006) Binding of the low-density lipoprotein by streptococcal collagen-like protein Scl1 of *Streptococcus pyogenes*. *Mol. Microbiol.* **61**, 351–367

336. Gao, Y., Liang, C., Zhao, R., Lukomski, S., and Han, R. (2010) The Scl1 of M41-type group A Streptococcus binds the high-density lipoprotein. *FEMS Microbiol. Lett.* **309**, 55–61

337. Ouattara, M., Bentley Cunha, E., Li, X., Huang, Y. S., Dixon, D., and Eichenbaum, Z. (2010) Shr of group A streptococcus is a new type of composite NEAT protein involved in sequestering haem from methaemoglobin. *Mol. Microbiol.* **78**, 739–756

338. Fisher, M., Huang, Y. S., Li, X., McIver, K. S., Toukoki, C., and Eichenbaum, Z. (2008) Shr is a broad-spectrum surface receptor that contributes to adherence and virulence in group A streptococcus. *Infect. Immun.* **76**, 5006–5015

339. Dahesh, S., Nizet, V., and Cole, J. N. (2012) Study of streptococcal hemoprotein receptor (Shr) in iron acquisition and virulence of M1T1 group A streptococcus. *Virulence*. **3**, 566–575

340. Hoshino, M., Nakakido, M., Nagatoishi, S., Aikawa, C., Nakagawa, I., and Tsumoto, K. (2017) Biophysical characterization of the interaction between heme and proteins responsible for heme transfer in *Streptococcus pyogenes*. *Biochem. Biophys. Res. Commun.* **493**, 1109–1114

341. Gase, K., Ferretti, J. J., Primeaux, C., and Mcshan, W. M. (1999) Identification, cloning, and expression of the CAMP factor gene (cfa) of group A streptococci. *Infect. Immun.* **67**, 4725–4731

342. Kurosawa, M., Oda, M., Domon, H., Isono, T., Nakamura, Y., Saitoh, I., Hayasaki, H., Yamaguchi, M., Kawabata, S., and Terao, Y. (2017) *Streptococcus pyogenes* CAMP factor promotes bacterial adhesion and invasion in pharyngeal epithelial cells without serum via PI3K/Akt signaling pathway. *Microbes Infect.* 10.1016/j.micinf.2017.09.007

343. Pancholi, V., and Fischetti, V. A. (1998) alpha-Enolase, a Novel Strong Plasmin(ogen) Binding Protein on the Surface of Pathogenic Streptococci. *J. Biol. Chem.* **273**, 14503–15

344. Derbise, A., Song, Y. P., Parikh, S., Fischetti, V. A., and Pancholi, V. (2004) Role of the C-Terminal Lysine Residues of Streptococcal Surface Enolase in Glu- and Lys-Plasminogen-Binding Activities of Group A Streptococci. *Infect. Immun.* **72**, 94–105

345. Cork, A. J., Ericsson, D. J., Law, R. H. P., Casey, L. W., Valkov, E., Bertozzi, C., Stamp, A., Jovcevski, B., Aquilina, J. A., Whisstock, J. C., Walker, M. J., and Kobe, B. (2015) Stability of the Octameric Structure Affects Plasminogen-Binding Capacity of Streptococcal Enolase. *PLoS One*. **10**, e0121764

346. Pandiripally, V., Wei, L., Skerka, C., Zipfel, P. F., and Cue, D. (2003) Recruitment of complement factor H-like protein 1 promotes intracellular invasion by group A streptococci. *Infect. Immun.* **71**, 7119–28

347. Agrahari, G., Liang, Z., Mayfield, J. A., Balsara, R. D., Ploplis, V. A., and Castellino, F. J. (2013) Complement-mediated opsonization of invasive group A *Streptococcus pyogenes* strain AP53 is regulated by the bacterial two-component cluster of virulence responder/sensor (covRS) system. *J. Biol. Chem.* **288**, 27494–27504

348. Pandiripally, V., Gregory, E., and Cue, D. (2002) Acquisition of Regulators of Complement Activation by. *Society*. **70**, 6206–6214

349. Terao, Y., Kawabata, S., Kunitomo, E., Murakami, J., Nakagawa, I., and Hamada, S. (2001) Fba, a novel fibronectin-binding protein from *Streptococcus pyogenes*, promotes bacterial entry into epithelial cells, and the fba gene is positively transcribed under the Mga regulator. *Mol. Microbiol.* **42**, 75–86

350. Wei, L., Pandiripally, V., Gregory, E., Clymer, M., and Cue, D. (2005) Impact of the SpeB protease on binding of the complement regulatory proteins factor H and factor H-like protein 1 by *Streptococcus pyogenes*. *Infect. Immun.* **73**, 2040–2050

351. Gallotta, M., Gancitano, G., Pietrocola, G., Mora, M., Pezzicoli, A., Tuscano, G., Chiarot, E., Nardi-Dei, V., Taddei, A. R., Rindi, S., Speziale, P., Soriani, M., Grandi, G., Margarit, I., and Bensi, G. (2014) SpyAD, a moonlighting protein of group A Streptococcus contributing to bacterial division and host cell adhesion. *Infect. Immun.* **82**, 2890–2901

352. Price, M. N., and Arkin, A. P. (2016) A Theoretical Lower Bound for Selection on the Expression Levels of Proteins. *Genome Biol. Evol.* **8**, 1917–1928

353. Price, M. N., Wetmore, K. M., Deutschbauer, A. M., and Arkin, A. P. (2016) A comparison of the costs and benefits of bacterial gene expression. *PLoS One*. **11**, 1–22

354. Somerville, G. A., and Proctor, R. A. (2009) At the Crossroads of Bacterial Metabolism and Virulence Factor Synthesis in Staphylococci. *Microbiol. Mol. Biol. Rev.* **73**, 233–248

355. Graham, M. R., Smoot, L. M., Migliaccio, C. A. L., Virtaneva, K., Sturdevant, D. E., Porcella, S. F., Federle, M. J., Adams, G. J., Scott, J. R., and Musser, J. M. (2002) Virulence control in group A Streptococcus by a two-component gene regulatory system: Global expression profiling and *in vivo* infection modeling. *Proc. Natl. Acad. Sci.* **99**, 13855–13860

356. Federle, M. J., Mciver, K. S., Scott, J. R., and Iver, K. S. M. C. (1999) A Response Regulator That Represses Transcription of Several Virulence Operons in the Group A Streptococcus. **181**, 3649–3657

357. Sumby, P., Whitney, A. R., Graviss, E. A., DeLeo, F. R., and Musser, J. M. (2006) Genome-wide analysis of group A streptococci reveals a mutation that modulates global phenotype and disease specificity. *PLoS Pathog.* **2**, 0041–0049

358. Levin, B. R., and Bull, J. J. (1994) Short-sighted evolution and the virulence of pathogenic microorganisms. *Trends Microbiol.* **2**, 76–81

359. Gryllos, I., Tran-Winkler, H. J., Cheng, M.-F., Chung, H., Bolcome, R., Lu, W., Lehrer, R. I., and Wessels, M. R. (2008) Induction of group A Streptococcus virulence by a human antimicrobial peptide. *Proc. Natl. Acad. Sci. U. S. A.* **105**, 16755–60

360. Roberts, S. A., Churchward, G. G., and Scott, J. R. (2007) Unraveling the regulatory network in *Streptococcus pyogenes*: The global response regulator CovR represses rivR directly. *J. Bacteriol.* **189**, 1459–1463

361. McIver, K. S. (2009) Stand-alone response regulators controlling global virulence networks in *Streptococcus pyogenes*. *Contrib. Microbiol.* **16**, 103–119

362. Scott, J. R., Cleary, P., Caparon, M. G., Kehoe, M., Heden, L., Musser, J. M., Hollingshead, S., and Podbielski, A. (1995) New name for the positive regulator of the M protein of group A streptococcus. *Mol. Microbiol.* **17**, 799

363. Hondorp, E. R., and McIver, K. S. (2007) The Mga virulence regulon: Infection where the grass is greener. *Mol. Microbiol.* **66**, 1056–1065

364. Chaussee, M. S., Sylva, G. L., Sturdevant, D. E., Smoot, L. M., Graham, M. R., Watson, R. O., and Musser, J. M. (2002) Rgg Influences the Expression of Multiple Regulatory Loci To Coregulate Virulence Factor Expression in *Streptococcus pyogenes* . *Infect. Immun.* **70**, 762–770

365. Beckert, S., Kreikemeyer, B., and Podbielski, A. (2001) Group A Streptococcal rofA Gene Is Involved in the Control of Several Virulence Genes and Eukaryotic Cell Attachment and Internalization. *Society*. **69**, 534–537

366. Deutscher, J., Francke, C., and Postma, P. W. (2006) How Phosphotransferase System-Related Protein Phosphorylation Regulates Carbohydrate Metabolism in Bacteria. *Microbiol. Mol. Biol. Rev.* **70**, 939–1031

367. Ribardo, D. A., and McIver, K. S. (2003) amrA encodes a putative membrane protein necessary for maximal exponential phase expression of the Mga virulence regulon in *Streptococcus pyogenes*. *Mol. Microbiol.* **50**, 673–685

368. Almengor, A. C., Kinkel, T. L., Day, S. J., and McIver, K. S. (2007) The catabolite control protein CcpA binds to Pmga and influences expression of the virulence regulator Mga in the group A streptococcus. *J. Bacteriol.* **189**, 8405–8416

369. Hondorp, E. R., Hou, S. C., Hause, L. L., Gera, K., Lee, C.-E., and McIver, K. S. (2013) PTS phosphorylation of Mga modulates regulon expression and virulence in the group A streptococcus. *Mol. Microbiol.* **88**, 1176–1193

370. Ribardo, D. A., and McIver, K. S. (2006) Defining the Mga regulon: Comparative transcriptome analysis reveals both direct and indirect regulation by Mga in the group A streptococcus. *Mol. Microbiol.* **62**, 491–508

371. Granok, A. B., Parsonage, D., Ross, R. P., and Caparon, M. G. (2000) The RofA binding site in *Streptococcus pyogenes* is utilized in multiple transcriptional pathways. *J. Bacteriol.* **182**, 1529–1540

372. Fogg, G. C., and Caparon, M. G. (1997) Constitutive expression of fibronectin binding in Streptococcus pyogenes as a result of anaerobic activation of rofA . **179**, 6172–6180

373. Kreikemeyer, B., Beckert, S., Braun-Kiewnick, A., and Podbielski, A. (2002) Group A streptococcal rofA-type global regulators exhibit a strain-specific genomic presence and regulation pattern. *Microbiology*. **148**, 1501–1511

374. Kratovac, Z., Manoharan, A., Luo, F., Lizano, S., and Bessen, D. E. (2007) Population genetics and linkage analysis of loci within the FCT region of *Streptococcus pyogenes*. *J. Bacteriol.* **189**, 1299–1310

375. Kreikemeyer, B., Nakata, M., Köller, T., Hildisch, H., Kourakos, V., Standar, K., Kawabata, S., Glocker, M. O., and Podbielski, A. (2007) The *Streptococcus pyogenes* serotype M49 Nra-Ralp3 transcriptional regulatory network and its control of virulence factor expression from the novel eno ralp3 epf sagA pathogenicity region. *Infect. Immun.* **75**, 5698–5710

376. Podbielski, A., Woischnik, M., Leonard, B. A. B., and Schmidt, K. H. (1999) Characterization of nra, a global negative regulator gene in group A streptococci. *Mol. Microbiol.* **31**, 1051–1064

377. Kwinn, L. A., Khosravi, A., Aziz, R. K., Timmer, A. M., Doran, K. S., Kotb, M., and Nizet, V. (2007) Genetic characterization and virulence role of the RALP3/LSA locus upstream of the streptolysin S operon in invasive M1T1 group A Streptococcus. *J. Bacteriol.* **189**, 1322–1329

378. Treviño, J., Liu, Z., Cao, T. N., Ramirez-Peña, E., and Sumby, P. (2013) RivR is a negative regulator of virulence factor expression in group a Streptococcus. *Infect. Immun.* **81**, 364–372

379. Dmitriev, A. V., McDowell, E. J., and Chaussee, M. S. (2008) Inter- and intraserotypic variation in the *Streptococcus pyogenes* Rgg regulon. *FEMS Microbiol. Lett.* **284**, 43–51

380. Dmitriev, A. V., McDowell, E. J., Kappeler, K. V., Chaussee, M. A., Rieck, L. D., and Chaussee, M. S. (2006) The Rgg regulator of *Streptococcus pyogenes* influences utilization of nonglucose carbohydrates, prophage induction, and expression of the NAD-glycohydrolase virulence operont. *J. Bacteriol.* **188**, 7230–7241

381. Sonenshein, A. L. (2005) CodY, a global regulator of stationary phase and virulence in Gram-positive bacteria. *Curr. Opin. Microbiol.* **8**, 203–207

382. Reid, S. D., Chaussee, M. S., Doern, C. D., Chaussee, Michelle A. Montgomery, A. G., Sturdevant, D. E., and Musser, J. M. (2006) Inactivation of the group A Streptococcus regulator srv results in chromosome wide reduction of transcript levels, and changes in extracellular levels of Sic and SpeB. *FEMS Immunol. Med. Microbiol.* **48**, 283–292

383. Rosey, E. L., Oskouian, B., and Stewart, G. C. (1991) Lactose metabolism by *Staphylococcus aureus*: Characterization of lacABCD, the structural genes of the tagatose 6-phosphate pathway. *J. Bacteriol.* **173**, 5992–5998

384. Cusumano, Z., and Caparon, M. (2013) Adaptive evolution of the *Streptococcus pyogenes* regulatory aldolase lacD.1. *J. Bacteriol.* **195**, 1294–1304

385. Loughman, J. A., and Caparon, M. (2006) Regulation of SpeB in Streptococcus pyogenes by pH and NaCl: A model for *in vivo* gene expression. *J. Bacteriol.* **188**, 399–408

386. Reid, S. D., Montgomery, A. G., and Musser, J. M. (2004) Identification of srv, A PrfA-Like Regulator of Group A Streptococcus That Influences Virulence. *Infect. Immun.* **72**, 1799–1803

387. Dutta, T., and Srivastava, S. (2018) Small RNA-mediated regulation in bacteria: A growing palette of diverse mechanisms. *Gene*. **656**, 60–72

388. Liu, Z., Treviño, J., Ramirez-Peña, E., and Sumby, P. (2012) The small regulatory RNA FasX controls pilus expression and adherence in the human bacterial pathogen group A Streptococcus. *Mol. Microbiol.* **86**, 140–154

389. Ramirez-Peña, E., Treviño, J., Liu, Z., Perez, N., and Sumby, P. (2010) The group A Streptococcus small regulatory RNA FasX enhances streptokinase activity by increasing the stability of the ska mRNA transcript. *Mol. Microbiol.* **78**, 1332–1347

390. Pappesch, R., Warnke, P., Mikkat, S., Normann, J., Wisniewska-Kucper, A., Huschka, F., Wittmann, M., Khani, A., Schwengers, O., Oehmcke-Hecht, S., Hain, T., Kreikemeyer, B., and Patenge, N. (2017) The Regulatory Small RNA MarS Supports Virulence of *Streptococcus pyogenes*. *Sci. Rep.* **7**, 1–15

391. Mangold, M., Siller, M., Roppenser, B., Vlaminckx, B. J. M., Penfound, T. A., Klein, R., Novak, R., Novick, R. P., and Charpentier, E. (2004) Synthesis of group A streptococcal virulence factors is controlled by a regulatory RNA molecule. *Mol. Microbiol.* **53**, 1515–1527

392. Le Rhun, A., Beer, Y. Y., Reimegård, J., Chylinski, K., and Charpentier, E. (2016) RNA sequencing uncovers antisense RNAs and novel small RNAs in *Streptococcus pyogenes*. *RNA Biol.* **13**, 177–195

393. Lewontin, R. C. (1970) The Units of Selection. *Annu. Rev. Ecol. Syst.* **1**, 1–18

394. Darwin, C. (1859) *On the Origin of Species by Means of Natural Selection*, Murray, London

395. Rumbaugh, K. P., Diggle, S. P., Watters, C. M., Ross-Gillespie, A., Griffin, A. S., and West, S. A. (2009) Quorum Sensing and the Social Evolution of Bacterial Virulence. *Curr. Biol.* **19**, 341–345

396. Swift, S., Downie, J. A., Whitehead, N. A., Barnard, A. M. L., Salmond, G. P. C., and Williams, P. D. (2001) Quorum sensing as a population-density-dependent determinant of bacterial physiology. *Adv. Microb. Physiol.* **45**, 199–270

397. Schluter, J., Schoech, A. P., Foster, K. R., and Mitri, S. (2016) The Evolution of Quorum Sensing as a Mechanism to Infer Kinship. *PLoS Comput. Biol.* **12**, 1–18

398. Jimenez, J. C., and Federle, M. J. (2014) Quorum sensing in group A Streptococcus. *Front. Cell. Infect. Microbiol.* **4**, 1–17

399. Plainvert, C., Dinis, M., Ravins, M., Hanski, E., Touak, G., Dmytruk, N., Fouet, A., and Poyarta, C. (2014) Molecular epidemiology of sil locus in clinical *Streptococcus pyogenes* strains. *J. Clin. Microbiol.* **52**, 2003–2010

400. Chatterjee, C., Paul, M., Xie, L., and van der Donk, W. A. (2005) Biosynthesis and Mode of Action of Lantibiotics. *Chem. Rev.* **105**, 633–684

401. Nyberg, P., Rasmussen, M., von Pawel-Rammingen, U., and Björck, L. (2004) SpeB modulates fibronectin-dependent internalization of *Streptococcus pyogenes* by efficient proteolysis of cell-wall-anchored protein F1. *Microbiology*. **150**, 1559–1569

402. Kansal, R. G., McGeer, A., Low, D. E., Norrby-Teglund, A., and Kotb, M. (2000) Inverse relation between disease severity and expression of the streptococcal cysteine protease, SpeB, among clonal M1T1 isolates recovered from invasive group A streptococcal infection cases. *Infect. Immun.* **68**, 6362–6369

403. Simpson, W. a, Ofek, I., and Beachey, E. H. (1980) Binding of streptococcal lipoteichoic acid to the fatty acid binding sites on serum albumin. *J. Biol. Chem.* **255**, 6092–6097

404. Schmidt, K. H., Mann, K., Cooney, J., and Köhler, W. (1993) Multiple binding of type 3 streptococcal M protein to human fibrinogen, albumin and fibronectin. *FEMS Immunol. Med. Microbiol.* **7**, 135–143

405. Doern, C. D., Roberts, A. L., Hong, W., Nelson, J., Lukomski, S., Swords, W. E., and Reid, S. D. (2009) Biofilm formation by group A Streptococcus: A role for the streptococcal regulator of virulence (Srv) and streptococcal cysteine protease (SpeB). *Microbiology*. **155**, 46–52

406. Kania, R. E., Lamers, G. E. M., Vonk, M. J., Huy, P. T. B., Hiemstra, P. S., Bloemberg, G. V., and Grote, J. J. (2007) Demonstration of bacterial cells and glycocalyx in biofilms on human tonsils. *Arch. Otolaryngol. - Head Neck Surg.* **133**, 115–121

407. Betts, C., Shinde, A. V, Water, L. Van De, and Lukomski, S. (2014) The group A streptococcal collagen-like protein 1, Scl1, mediates biofilm formation by targeting the EDA-containing variant of cellular fibronectin expressed in wounded tissue Heaven. **87**, 672–689

408. Lembke, C., Podbielski, A., Hidalgo-grass, C., Jonas, L., Hanski, E., Kreikemeyer, B., Hidalgo-grass, C., and Kreikemeyer, B. (2006) Characterization of Biofilm Formation by Clinically Relevant Serotypes of Group A Streptococci. *Appl. Environ. Microbiol.* **72**, 2864–2875

409. Köller, T., Manetti, A. G. O., Kreikemeyer, B., Lembke, C., Margarit, I., Grandi, G., and Podbielski, A. (2010) Typing of the pilus-protein-encoding FCT region and biofilm formation as novel parameters in epidemiological investigations of *Streptococcus pyogenes* isolates from various infection sites. *J. Med. Microbiol.* **59**, 442–52

410. Manetti, A. G. O., Köller, T., Becherelli, M., Buccato, S., Kreikemeyer, B., Podbielski, A., Grandi, G., and Margarit, I. (2010) Environmental Acidification Drives S. pyogenes Pilus Expression and Microcolony Formation on Epithelial Cells in a FCT-Dependent Manner. *PLoS One*. **5**, e13864

411. Fiedler, T., Koller, T., and Kreikemeyer, B. (2015) *Streptococcus pyogenes* biofilms formation, biology, and clinical relevance. *Front. Cell. Infect. Microbiol.* **5**, 1–11

412. Chang, J. C., LaSarre, B., Jimenez, J. C., Aggarwal, C., and Federle, M. J. (2011) Two Group A Streptococcal Peptide Pheromones Act through Opposing Rgg Regulators to Control Biofilm Development. *PLoS Pathog.* **7**, e1002190

413. Siemens, N., Chakrakodi, B., Shambat, S. M. M., Morgan, M. M., Bergsten, H., Hyldegaard, O., Skrede, S., Arnell, P., Madsen, M. B. B., Johansson, L., Group, I. S., Juarez, J., Bosnjak, L., Mörgelin, M., Svensson, M., and Norrby-Teglund, A. (2016) Biofilm in group A streptococcal necrotizing soft tissue infections. *JCI Insight*. **1**, 151–157

414. Marks, L. R., Mashburn-Warren, L., Federle, M. J., and Hakansson, A. P. (2014) Streptococcus pyogenes Biofilm Growth *In Vitro* and *In Vivo* and Its Role in Colonization, Virulence, and Genetic Exchange. *J. Infect. Dis.* **210**, 25–34

415. Ogawa, T., Terao, Y., Sakata, H., Okuni, H., Ninomiya, K., Ikebe, K., Maeda, Y., and Kawabata, S. (2011) Epidemiological characterization of *Streptococcus pyogenes* isolated from patients with multiple onsets of pharyngitis. *FEMS Microbiol. Lett.* **318**, 143–51

416. Podbielski, A., and Kreikemeyer, B. (2001) Persistence of group A streptococci in eukaryotic cells—a safe place? *Lancet*. **358**, 5–6

417. Hasty, D. L., Ofek, I., Courtney, H. S., and Doyle, R. J. (1992) Multiple adhesins of streptococci. *Infect. Immun.* **60**, 2147–2152

418. Molinari, G., Talay, S. R., Valentin-Weigand, P., Rohde, M., and Chhatwal, G. S. (1997) The fibronectin-binding protein of *Streptococcus pyogenes*, SfbI, is involved in the internalization of group A streptococci by epithelial cells. *Infect. Immun.* **65**, 1357–63

419. Hanski, E., and Caparon, M. (1992) Protein F, a fibronectin-binding protein, is an adhesin of the group A streptococcus. *Proc. Natl. Acad. Sci. U. S. A.* **89**, 6172–6176

420. Talay, S. R., Valentin-Weigand, P., Jerlstrom, P. G., Timmis, K. N., and Chhatwal, G. S. (1992) Fibronectin-binding protein of *Streptococcus pyogenes*: Sequence of the binding domain involved in adherence of streptococci to epithelial cells. *Infect. Immun.* **60**, 3837–3844

421. Sumitomo, T., Nakata, M., Higashino, M., Yamaguchi, M., and Kawabata, S. (2016) Group A Streptococcus exploits human plasminogen for bacterial translocation across epithelial barrier via tricellular tight junctions. *Sci. Rep.* **7**, 1–8

422. Mulay, S. R., Desai, J., Kumar, S. V., Eberhard, J. N., Thomasova, D., Romoli, S., Grigorescu, M., Kulkarni, O. P., Popper, B., Vielhauer, V., Zuchtriegel, G., Reichel, C., Bräsen, J. H., Romagnani, P., Bilyy, R., Munoz, L. E., Herrmann, M., Liapis, H., Krautwald, S., Linkermann, A., and Anders, H.-J. (2016) Re-evaluation of HeLa, HeLa S3, and HEp-2 karyotypes. *Nat. Commun.* **7**, 10274

423. Masters, J. R. (2002) HeLa cells 50 years on: the good, the bad and the ugly. *Nat. Rev. Cancer*. **2**, 315–319

424. Darmstadt, G. L., Mentele, L., Fleckman, P., and Rubens, C. E. (1999) Role of keratinocyte injury in adherence of *Streptococcus pyogenes*. *Infect. Immun.* **67**, 6707–6709

425. Kreikemeyer, B., Klenk, M., and Podbielski, A. (2004) The intracellular status of *Streptococcus pyogenes*: Role of extracellular matrix-binding proteins and their regulation. *Int. J. Med. Microbiol.* **294**, 177–188

426. LaPenta, D., Rubens, C., Chi, E., and Cleary, P. P. (1994) Group A streptococci efficiently invade human respiratory epithelial cells. *Proc. Natl. Acad. Sci. U. S. A.* **91**, 12115–9

427. Fraunholz, M., and Sinha, B. (2012) Intracellular *Staphylococcus aureus*: Live-in and let die. *Front. Cell. Infect. Microbiol.* **2**, 1–10

428. Dombek, P. E., Cue, D., Sedgewick, J., Lam, H., Ruschkowski, S., Finlay, B. B., and Cleary, P. P. (1999) High-frequency intracellular invasion of epithelial cells by serotype M1 group A streptococci: M1 protein-mediated invasion and cytoskeletal rearrangements. *Mol. Microbiol.* **31**, 859–870

429. Purushothaman, S. S. S. S. S., Wang, B., and Cleary, P. P. (2003) M1 protein triggers a phosphoinositide cascade for group A Streptococcus invasion of epithelial cells. *Infect. Immun.* **71**, 5823–5830

430. Purushothaman, S. S., Park, H. S., and Cleary, P. P. (2004) Promotion of fibronectin independent invasion by C5a peptidase into epithelial cells in group A Streptococcus. *Indian J. Med. Res. Suppl.* **119**, 44–47

431. Cywes, C., Stamenkovic, I., and Wessels, M. R. (2000) CD44 as a receptor for colonization of the pharynx by group A Streptococcus. *J. Clin. Invest.* **106**, 995–1002

432. Schrager, H. M., Albertí, S., Cywes, C., Dougherty, G. J., and Wessels, M. R. (1998) Hyaluronic acid capsule modulates M protein-mediated adherence and acts as a ligand for attachment of group A streptococcus to CD44 on human keratinocytes. *J. Clin. Invest.* **101**, 1708–1716

433. Cywes, C., and Wessels, M. R. (2001) Group A Streptococcus tissue invasion by CD44-mediated cell signalling. *Nature*. **414**, 648–52

434. Chen, S.-M., Tsai, Y.-S., Wu, C.-M., Liao, S.-K., Wu, L.-C., Chang, C.-S., Liu, Y.-H., and Tsai, P.-J. (2010) Streptococcal collagen-like surface protein 1 promotes adhesion to the respiratory epithelial cell. *BMC Microbiol.* **10**, 320

435. Kreikemeyer, B., Oehmcke, S., Nakata, M., Hoffrogge, R., and Podbielski, A. (2004) Streptococcus pyogenes fibronectin-binding protein F2: Expression profile, binding characteristics, and impact on eukaryotic cell interactions. *J. Biol. Chem.* **279**, 15850–15859

436. Pandiripally, V., Wei, L., Skerka, C., Zipfel, P. F., and Cue, D. (2003) Recruitment of Complement Factor H-Like Protein 1 Promotes Intracellular Invasion by Group A Streptococci Recruitment of Complement Factor H-Like Protein 1 Promotes Intracellular Invasion by Group A Streptococci. *Infect. Immun.* **71**, 7119–7128

437. Timmer, A. M., Kristian, S. A., Datta, V., Jeng, A., Gillen, C. M., Walker, M. J., Beall, B., and Nizet, V. (2006) Serum opacity

factor promotes group A streptococcal epithelial cell invasion and virulence. *Mol. Microbiol.* **62**, 15–25

438. Courtney, H. S., Zhang, Y. M., Frank, M. W., and Rock, C. O. (2006) Serum opacity factor, a streptococcal virulence factor that binds to apolipoproteins A-I and A-II and disrupts high density lipoprotein structure. *J. Biol. Chem.* **281**, 5515–5521

439. Österlund, A., and Engstrand, L. (1995) Intracellular penetration and survival of *Streptococcus pyogenes* in respiratory epithelial cells in vitro. *Acta Otolaryngol.* **115**, 685–8

440. Österlund, A., Popa, R., and Nikkilä, T. (1997) Intracellular reservoir of Streptococcus pyogenes in vivo: a possible explanation for recurrent pharyngotonsillitis. *Laryngoscope*. **107**, 640–647

441. Kaplan, E. L., Chhatwal, G. S., and Rohde, M. (2006) Reduced ability of penicillin to eradicate ingested group A streptococci from epithelial cells: clinical and pathogenetic implications. *Clin. Infect. Dis.* **43**, 1398–1406

442. Marouni, M. J., Barzilai, A., Keller, N., Rubinstein, E., and Sela, S. (2004) Intracellular survival of persistent group A Streptococci in cultured epithelial cells. *Int. J. Med. Microbiol.* **294**, 27–33

443. Sela, S., Marouni, M. J., Perry, R., and Barzilai, A. (2000) Effect of lipoteichoic acid on the uptake of *Streptococcus pyogenes* HEp-2 cells. *FEMS Microbiol. Lett.* **193**, 187–93

444. Facinelli, B., Spinaci, C., Magi, G., Giovanetti, E., and Varaldo, P. E. (2001) Association between erythromycin resistance and ability to enter human respiratory cells in group A streptococci. *Lancet*. **358**, 30–33

445. Jadoun, J., Ozeri, V., Burstein, E., Skutelsky, E., Hanski, E., and Sela, S. (1998) Protein F1 is required for efficient entry of *Streptococcus pyogenes* into epithelial cells. *J. Infect. Dis.* **178**, 147–58

446. Jadoun, J., Burstein, E., Hanski, E., and Sela, S. (1997) Proteins M6 and F1 are required for efficient invasion of group A streptococci into cultured epithelial cells. *Adv Exp Med Biol*. **418**, 511–515

447. Haller, M., Fluegge, K., Arri, S. J., Adams, B., and Berner, R. (2005) Association between resistance to erythromycin and the presence of the fibronectin binding protein F1 gene, prtF1, in *Streptococcus pyogenes* isolates from German pediatric patients. *Antimicrob. Agents Chemother.* **49**, 2990–2993

448. Molinari, G., and Chhatwal, G. S. (1999) Role played by the fibronectin-binding protein SfbI (Protein F1) of *Streptococcus pyogenes* in bacterial internalization by epithelial cells. *J Infect Dis*. **179**, 1049–1050

449. Ozeri, V., Rosenshine, I., Mosher, D. F., Fässler, R., and Hanski, E. (1998) Roles of integrins and fibronectin in the entry of *Streptococcus pyogenes* into cells via protein F1. *Mol. Microbiol.* **30**, 625–37

450. Shi, F., and Sottile, J. (2008) Caveolin-1-dependent 1 integrin endocytosis is a critical regulator of fibronectin turnover. *J. Cell Sci.* **121**, 2360–2371

451. Odrljin, T. M., Haidaris, C. G., Lerner, N. B., and Simpson-Haidaris, P. J. (2001) Integrin alphavbeta3-mediated endocytosis of immobilized fibrinogen by A549 lung alveolar epithelial cells. *Am. J. Respir. Cell Mol. Biol.* **24**, 12–21

452. Panetti, T. S., Wilcox, S. A., Horzempa, C., and McKeown-Longo, P. J. (1995) αvβ5 Integrin Receptor-mediated Endocytosis of Vitronectin Is Protein Kinase C-dependent. *J. Biol. Chem.* **270**, 18593–18597

453. Nakagawa, S., Matsumoto, M., Katayama, Y., Oguma, R., Wakabayashi, S., Nygaard, T., Saijo, S., Inohara, N., Otto, M., Matsue, H., Núñez, G., and Nakamura, Y. (2017) *Staphylococcus aureus* Virulent PSMα Peptides Induce Keratinocyte Alarmin Release to Orchestrate IL-17-Dependent Skin Inflammation. *Cell Host Microbe*. **22**, 667–677.e5

454. O'Seaghdha, M., and Wessels, M. R. (2013) Streptolysin O and its Co-Toxin NAD-glycohydrolase Protect Group A Streptococcus from Xenophagic Killing. *PLoS Pathog.* **9**, e1003394

455. Joubert, P. E., Meiffren, G., Grégoire, I. P., Pontini, G., Richetta, C., Flacher, M., Azocar, O., Vidalain, P. O., Vidal, M., Lotteau, V., Codogno, P., Rabourdin-Combe, C., and Faure, M. (2009) Autophagy Induction by the Pathogen Receptor CD46. *Cell Host Microbe*. **6**, 354–366

456. Thurston, T. L. M. (2009) The tbk1 adaptor and autophagy receptor ndp52 restricts the proliferation of ubiquitin-coated bacteria. *Nat. Immunol.* **10**, 1215–1222

457. Nakagawa, I., Amano, A., Mizushima, N., Yamamoto, A., Yamaguchi, H., Kamimoto, T., Nara, A., Funao, J., Nakata, M., Tsuda, K., Hamada, S., and Yoshimori, T. (2004) Autophagy defends cells against invading group A Streptococcus. *Science*. **306**, 1037–40

458. Barnett, T. C., Liebl, D., Seymour, L. M., Gillen, C. M., Lim, J. Y., Larock, C. N., Davies, M. R., Schulz, B. L., Nizet, V., Teasdale, R. D., and Walker, M. J. (2013) The globally disseminated M1T1 clone of group A Streptococcus evades autophagy for intracellular replication. *Cell Host Microbe*. **14**, 675–82

459. Bricker, A. L., Cywes, C., Ashbaugh, C. D., and Wessels, M. R. (2002) NAD+-glycohydrolase acts as an intracellular toxin to enhance the extracellular survival of group A streptococci. *Mol. Microbiol.* **44**, 257–269

460. Logsdon, L. K., Håkansson, A. P., Cortés, G., and Wessels, M. R. (2011) Streptolysin o inhibits clathrin-dependent internalization of group a streptococcus. *MBio*. 10.1128/mBio.00332-10

461. Abu Kwaik, Y., and Bumann, D. (2013) Microbial quest for food *in vivo*: "Nutritional virulence" as an emerging paradigm. *Cell. Microbiol.* **15**, 882–890

462. Rohmer, L., Hocquet, D., and Miller, S. I. (2011) Are pathogenic bacteria just looking for food? Metabolism and microbial pathogenesis. *Trends Microbiol.* **19**, 341–348

463. Carroll, R. K., and Musser, J. M. (2011) From transcription to activation: How group A streptococcus, the flesh-eating pathogen, regulates SpeB cysteine protease production. *Mol. Microbiol.* **81**, 588–601

464. Podbielski, A., Pohl, B., Woischnik, M., Körner, C., Schmidt, K. H., Rozdzlnski, E., and Leonard, B. A. B. (1996) Molecular characterization of group A streptococcal (GAS) oligopeptide permease (Opp) and its effect on cysteine protease production. *Mol. Microbiol.* **21**, 1087–1099

465. Kunji, E. R. S., Hagting, A., De Vries, C. J., Juillard, V., Haandrikman, A. J., Poolman, B., and Konings, W. N. (1995) Transport of β-casein-derived peptides by the oligopeptide transport system is a crucial step in the proteolytic pathway of Lactococcus lactis. *J. Biol. Chem.* **270**, 1569–1574

466. Finkel, S., and Kolter, R. (2001) DNA as a nutrient: novel role for bacterial competance gene homologs. *J. Bacteriol.* **183**, 6288–6293

467. Remmington, A., and Turner, C. E. (2018) The DNases of pathogenic lancefield streptococci. *Microbiol. (United Kingdom)*. **164**, 242–250

468. Starr, C. R., and Engleberg, N. C. (2006) Role of hyaluronidase in subcutaneous spread and growth of group A streptococcus. *Infect. Immun.* **74**, 40–48

469. Los, F. C. O., Randis, T. M., Aroian, R. V., and Ratner, A. J. (2013) Role of Pore-Forming Toxins in Bacterial Infectious Diseases. *Microbiol. Mol. Biol. Rev.* **77**, 173–207

470. Baruch, M., Hertzog, B. B., Ravins, M., Anand, A., Cheng, C. Y., Biswas, D., Tirosh, B., and Hanski, E. (2014) Induction of endoplasmic reticulum stress and unfolded protein response constitutes a pathogenic strategy of group A streptococcus. *Front. Cell. Infect. Microbiol.* **4**, 105

471. Sumitomo, T., Nakata, M., Higashino, M., Jin, Y., Terao, Y., Fujinaga, Y., and Kawabata, S. (2011) Streptolysin S contributes to group A streptococcal translocation across an epithelial barrier. *J. Biol. Chem.* **286**, 2750–2761

472. Sumitomo, T., Nakata, M., Higashino, M., Terao, Y., and Kawabata, S. (2013) Group A streptococcal cysteine protease cleaves epithelial junctions and contributes to bacterial translocation. *J. Biol. Chem.* **288**, 13317–24

473. Pancholi, V., Fontan, P., and Jin, H. (2003) Plasminogen-mediated group A streptococcal adherence to and pericellular invasion of human pharyngeal cells. *Microb. Pathog.* **35**, 293–303

474. Sumitomo, T., Mori, Y., Nakamura, Y., Honda-Ogawa, M., Nakagawa, S., Yamaguchi, M., Matsue, H., Terao, Y., Nakata, M., and Kawabata, S. (2018) Streptococcal cysteine protease-mediated cleavage of desmogleins is involved in the pathogenesis of cutaneous infection. *Front. Cell. Infect. Microbiol.* **8**, 3389–10

475. Lähteenmäki, K., Virkola, R., Pouttu, R., Kuusela, P., and Kukkonen, M. (1995) Bacterial plasminogen receptors : in vitro evidence for a role in degradation of the mammalian extracellular matrix . *Infect. Immun.* **63**, 3659–3664

476. Sun, H., Ringdahl, U., Momeister, J. W., Fay, W. P., Engleberg, N. C., Yang, A. Y., Rozek, L. S., Wang, X., Sjöbring, U., and Ginsburg, D. (2004) Plasminogen is a critical host pathogenicity factor for group A streptococcal infection. *Science (80-.).* **305**, 1283–1286

477. Sun, H., Wang, X., Degen, J. L., and Ginsburg, D. (2009) Reduced thrombin generation increases host susceptibility to group A streptococcal infection. *Blood*. **113**, 1358–1364

478. Kotarsky, H., Hellwage, J., Johnsson, E., Skerka, C., Svensson, H. G., Lindahl, G., Sjöbring, U., and Zipfel, P. F. (1998) Identification of a domain in human factor H and factor H-like protein-1 required for the interaction with streptococcal M proteins. *J. Immunol.* **160**, 3349–54

479. Courtney, H. S., Hasty, D. L., and Dale, J. B. (2002) Molecular mechanisms of adhesion, colonization, and invasion of group A streptococci. *Ann. Med.* **34**, 77–87

480. Hollands, A., Gonzalez, D., Leire, E., Donald, C., Gallo, R. L., Sanderson-Smith, M., Dorrestein, P. C., and Nizet, V. (2012) A bacterial pathogen co-opts host plasmin to resist killing by cathelicidin antimicrobial peptides. *J. Biol. Chem.* **287**, 40891–40897

481. LaRock, C. N., Döhrmann, S., Todd, J., Corriden, R., Olson, J., Johannssen, T., Lepenies, B., Gallo, R. L., Ghosh, P., and Nizet, V. (2015) Group A Streptococcal M1 Protein Sequesters Cathelicidin to Evade Innate Immune Killing. *Cell Host Microbe*. **18**, 471–477

482. Egesten, A., Frick, I. M., Mörgelin, M., Olin, A. I., and Björck, L. (2011) Binding of albumin promotes bacterial survival at the epithelial surface. *J. Biol. Chem.* **286**, 2469–2476

483. Timmer, A. M., Timmer, J. C., Pence, M. A., Hsu, L. C., Ghochani, M., Frey, T. G., Karin, M., Salvesen, G. S., and Nizet, V. (2009) Streptolysin O promotes group A streptococcus immune evasion by accelerated macrophage apoptosis. *J. Biol. Chem.* **284**, 862–871

484. Valderrama, J. A., Riestra, A. M., Gao, N. J., LaRock, C. N., Gupta, N., Ali, S. R., Hoffman, H. M., Ghosh, P., and Nizet, V. (2017) Group A streptococcal M protein activates the NLRP3 inflammasome. *Nat. Microbiol.* **2**, 1425–1434

485. Kuo, C. F., Wu, J. J., Tsai, P. J., Kao, F. J., Lei, H. Y., Lin, M. T., and Lin, Y. S. (1999) Streptococcal pyrogenic exotoxin B induces apoptosis and reduces phagocytic activity in U937 cells. *Infect. Immun.* **67**, 126–130

486. Miyoshi-Akiyama, T., Takamatsu, D., Koyanagi, M., Zhao, J., Imanishi, K., and Uchiyama, T. (2005) Cytocidal effect of Streptococcus pyogenes on mouse neutrophils *in vivo* and the critical role of streptolysin S. *J. Infect. Dis.* **192**, 107–116

487. Goldmann, O., Sastalla, I., Wos-oxley, M., Rohde, M., and Medina, E. (2009) *Streptococcus pyogenes* induces oncosis in macrophages through the activation of an inflammatory programmed cell death pathway. *Cell. Microbiol.* **11**, 138–155

488. Hryniewicz, W., and Pryjma, J. (1977) Effect of streptolysin S on human and mouse T and B lymphocytes. *Infect. Immun.* **16**, 730–733

489. Sharma, O., O'Seaghdha, M., Velarde, J. J., and Wessels, M. R. (2016) NAD+-Glycohydrolase Promotes Intracellular Survival of

Group A Streptococcus. *PLOS Pathog.* **12**, e1005468

490. Tsai, P., Kuo, C., Lin, K., and Lin, Y. (1998) Effect of group A streptococcal cysteine protease on invasion of epithelial cells. *Infect. ....* [online] http://iai.asm.org/content/66/4/1460.short (Accessed September 1, 2014)

491. Janeway, C., Travers, P., Walport, M., and Shlomchik, M. (2005) The immune system in health and disease. *Immunobiology*

492. Medina, E., Molinari, G., Rohde, M., Haase, B., Chhatwal, G. S., and Guzmán, C. A. (1999) Fc-mediated nonspecific binding between fibronectin-binding protein I of *Streptococcus pyogenes* and human immunoglobulins. *J. Immunol.* **163**, 3396–3402

493. Su, Y. F., Chuang, W. J., Wang, S. M., Chen, W. Y., Chiang-Ni, C., Lin, Y. S., Wu, J. J., and Liu, C. C. (2011) The deficient cleavage of M protein-bound IgG by IdeS: Insight into the escape of *Streptococcus pyogenes* from antibody-mediated immunity. *Mol. Immunol.* **49**, 134–142

494. Agrahari, G., Liang, Z., Glinton, K., Lee, S. W., Ploplis, V. A., and Castellino, F. J. (2016) *Streptococcus pyogenes* employs strain-dependent mechanisms of C3B inactivation to inhibit phagocytosis and killing of bacteria. *J. Biol. Chem.* **291**, 9181–9189

495. Barthel, D., Schindler, S., and Zipfel, P. F. (2012) Plasminogen is a complement inhibitor. *J. Biol. Chem.* **287**, 18831–18842

496. Honda-Ogawa, M., Sumitomo, T., Mori, Y., Hamd, D. T., Ogawa, T., Yamaguchi, M., Nakata, M., and Kawabata, S. (2017) *Streptococcus pyogenes* endopeptidase O contributes to evasion from complement-mediated bacteriolysis via binding to human complement factor C1q. *J. Biol. Chem.* **292**, 4244–4254

497. Carlsson, F., Sandin, C., and Lindahl, G. (2005) Human fibrinogen bound to *Streptococcus pyogenes* M protein inhibits complement deposition via the classical pathway. *Mol. Microbiol.* **56**, 28–39

498. Moses, A. E., Wessels, M. R., Zalcman, K., and Albertí, S. (1997) Relative contributions of hyaluronic acid capsule and M protein to virulence in a mucoid strain of the group A Streptococcus . **65**, 64–71

499. Dale, J. B., Washburn, R. G., Marques, M. B., and Wessels, M. R. (1996) Hyaluronate capsule and surface M protein in resistance to opsonization of group A streptococci. *Infect. Immun.* **64**, 1495–1501

500. Hoe, N. P., Ireland, R. M., DeLeo, F. R., Gowen, B. B., Dorward, D. W., Voyich, J. M., Liu, M., Burns, E. H., Culnan, D. M., Bretscher, A., and Musser, J. M. (2002) Insight into the molecular basis of pathogen abundance: group A Streptococcus inhibitor of complement inhibits bacterial adherence and internalization into human cells. *Proc. Natl. Acad. Sci. U. S. A.* **99**, 7646–51

501. Thulin, P., Johansson, L., Low, D. E., Gan, B. S., Kotb, M., McGeer, A., and Norrby-Teglund, A. (2006) Viable group A streptococci in macrophages during acute soft tissue infection. *PLoS Med.* **3**, e53

502. Hertzén, E., Johansson, L., Wallin, R., Schmidt, H., Kroll, M., Rehn, A. P., Kotb, M., Mörgelin, M., and Norrby-Teglund, A. (2010) M1 protein-dependent intracellular trafficking promotes persistence and replication of *Streptococcus pyogenes* in macrophages. *J. Innate Immun.* **2**, 534–45

503. Staali, L., Mörgelin, M., Björck, L., and Tapper, H. (2003) *Streptococcus pyogenes* expressing M and M-like surface proteins are phagocytosed but survive inside human neutrophils. *Cell. Microbiol.* **5**, 253–265

504. Medina, E., Goldmann, O., Toppel, A. W., and Chhatwal, G. S. (2003) Survival of *Streptococcus pyogenes* within host phagocytic cells: a pathogenic mechanism for persistence and systemic invasion. *J. Infect. Dis.* **187**, 597–603

505. Bastiat-Sempe, B., Love, J. F., Lomayesva, N., and Wessels, M. R. (2014) Streptolysin O and NAD-glycohydrolase prevent phagolysosome acidification and promote group A Streptococcus survival in macrophages. *MBio*. **5**, e01690-14

506. O'Neill, A. M., Thurston, T. L. M. M., and Holden, D. W. (2016) Cytosolic Replication of Group A Streptococcus in Human Macrophages. *MBio*. **7**, e00020-16

507. Fischetti, V. A., and Dale, J. B. (2016) One More Disguise in the Stealth Behavior of Streptococcus pyogenes. *MBio*. **7**, 1–2

508. Döhrmann, S., Anik, S., Olson, J., Anderson, E. L., Etesami, N., No, H., Snipper, J., Nizet, V., and Okumura, C. Y. M. (2014) Role for streptococcal collagen-like protein 1 in M1T1 group A Streptococcus resistance to neutrophil extracellular traps. *Infect. Immun.* **82**, 4011–4020

509. LaRock, C. N., Todd, J., LaRock, D. L., Olson, J., O'Donoghue, A. J., Robertson, A. A. B., Cooper, M. A., Hoffman, H. M., and Nizet, V. (2016) IL-1β is an innate immune sensor of microbial proteolysis. *Sci. Immunol.* **1**, eaah3539-eaah3539

510. Harder, J., Franchi, L., Muñoz-Planillo, R., Park, J.-H., Reimer, T., and Núñez, G. (2009) Activation of the Nlrp3 Inflammasome by Streptococcus pyogenes Requires Streptolysin O and NF- B Activation but Proceeds Independently of TLR Signaling and P2X7 Receptor. *J. Immunol.* **183**, 5823–5829

511. Blaschke, U., Beineke, A., Klemens, J., Medina, E., and Goldmann, O. (2017) Induction of Cyclooxygenase 2 by *Streptococcus pyogenes* Is Mediated by Cytolysins. *J. Innate Immun.* **9**, 587–597

512. Latvala, S., M??kel??, S. M., Miettinen, M., Charpentier, E., and Julkunen, I. (2014) Dynamin inhibition interferes with inflammasome activation and cytokine gene expression in *Streptococcus pyogenes*-infected human macrophages. *Clin. Exp. Immunol.* **178**, 320–333

513. Nilsson, M., Sørensen, O., Mörgelin, M., Weineisen, M., Sjöbring, U., and Herwald, H. (2006) Activation of human polymorphonuclear neutrophils by streptolysin O from *Streptococcus pyogenes* leads to the release of proinflammatory mediators. *Thromb. Haemost.* **95**, 982–990

514. Schneemann, M., and Schoeden, G. (2006) Macrophage biology and immunology: man is not a mouse. *J. Leukoc. Biol.* **81**, 579–579

515. Nahary, L., Tamarkin, A., Kayam, N., Sela, S., Fry, L., Baker, B., Powles, A., Rogers, S., and Benhar, I. (2008) An investigation of antistreptococcal antibody responses in guttate psoriasis. *Arch. Dermatol. Res.* **300**, 441–449

516. Norrby-Teglund, a, Thulin, P., Gan, B. S., Kotb, M., McGeer, a, Andersson, J., and Low, D. E. (2001) Evidence for superantigen involvement in severe group a streptococcal tissue infections. *J. Infect. Dis.* **184**, 853–860

517. Reglinski, M., and Sriskandan, S. (2014) The contribution of group A streptococcal virulence determinants to the pathogenesis of sepsis. *Virulence*. **5**, 127–136

518. Commons, R. J., Smeesters, P. R., Proft, T., Fraser, J. D., Robins-Browne, R., and Curtis, N. (2014) Streptococcal superantigens: Categorization and clinical associations. *Trends Mol. Med.* **20**, 48–62

519. Sriskandan, S., Faulkner, L., and Hopkins, P. (2007) *Streptococcus pyogenes*: Insight into the function of the streptococcal superantigens. *Int. J. Biochem. Cell Biol.* **39**, 12–19

520. MacDonald, H. R., Lees, R. K., Baschieri, S., Herrmann, T., and Lussow, A. R. (1993) Peripheral T-Cell Reactivity to Bacterial Superantigens *in vivo*: The Response/Anergy Paradox. *Immunol. Rev.* **133**, 105–117

521. Taylor, A. L., and Llewelyn, M. J. (2010) Superantigen-Induced Proliferation of Human CD4+CD25- T Cells Is Followed by a Switch to a Functional Regulatory Phenotype. *J. Immunol.* **185**, 6591–6598

522. Taylor, A. L., Cross, E. L. A., and Llewelyn, M. J. (2012) Induction of contact-dependent CD8+regulatory T cells through stimulation with staphylococcal and streptococcal superantigens. *Immunology*. **135**, 158–167

523. Kasper, K. J., Zeppa, J. J., Wakabayashi, A. T., Xu, S. X., Mazzuca, D. M., Welch, I., Baroja, M. L., Kotb, M., Cairns, E., Cleary, P. P., Haeryfar, S. M. M., and McCormick, J. K. (2014) Bacterial Superantigens Promote Acute Nasopharyngeal Infection by Streptococcus pyogenes in a Human MHC Class II-Dependent Manner. *PLoS Pathog.* **10**, e1004155

524. Zeppa, J. J., Kasper, K. J., Mohorovic, I., Mazzuca, D. M., Haeryfar, S. M. M., and McCormick, J. K. (2017) Nasopharyngeal infection by Streptococcus pyogenes requires superantigen-responsive Vβ-specific T cells. *Proc. Natl. Acad. Sci.* **114**, 10226–10231

525. Sähr, A., Förmer, S., Hildebrand, D., Heeg, K., Sastalla, I., Parker, D., Karauzum, H., Heeg, K., Sähr, A., Förmer, S., Hildebrand, D., Heeg, K., Sastalla, I., Parker, D., Karauzum, H., and Heeg, K. (2015) T-cell activation or tolerization: The Yin and Yang of bacterial superantigens. *Front. Microbiol.* **6**, 1–12

526. Bradford Kline, J., and Collins, C. M. (1996) Analysis of the superantigenic activity of mutant and allelic forms of streptococcal pyrogenic exotoxin A. *Infect. Immun.* **64**, 861–869

527. Ali, N., and Rosenblum, M. D. (2017) Regulatory T cells in skin. *Immunology*. **152**, 372–381

528. Kotb, M., Norrby-Teglund, A., McGeer, A., El-Sherbini, H., Dorak, M. T., Khurshid, A., Green, K., Peeples, J., Wade, J., Thomson, G., Schwartz, B., and Low, D. E. (2002) An immunogenetic and molecular basis for differences in outcomes of invasive group A streptococcal infections. *Nat. Med.* **8**, 1398–1404

529. Roberts, A. L., Connolly, K. L., Kirse, D. J., Evans, A. K., Poehling, K. A., Peters, T. R., and Reid, S. D. (2012) Detection of group A Streptococcus in tonsils from pediatric patients reveals high rate of asymptomatic streptococcal carriage. *BMC Pediatr.* **12**, 3

530. Medina, E., Goldmann, O., Rohde, M., Lengeling, A., and Chhatwals, G. S. (2001) Genetic Control of Susceptibility to Group A Streptococcal Infection in Mice. *J. Infect. Dis.* . **184**, 846–852

531. Goldmann, O., Chhatwal, G. S., and Medina, E. (2004) Role of host genetic factors in susceptibility to group A streptococcal infections. *Indian J Med Res*. **119 Suppl**, 141–143

532. Mishalian, I., Ordan, M., Peled, A., Maly, A., Eichenbaum, M. B., Ravins, M., Aychek, T., Jung, S., and Hanski, E. (2011) Recruited Macrophages Control Dissemination of Group A Streptococcus from Infected Soft Tissues. *J. Immunol.* **187**, 6022–6031

533. Rodriguez, R. S., Pauli, M., Neuhaus, I., and Al, E. (2014) Memory regulatory T cells reside in human skin. *J. Clin. Invest.* **124**, 1027–36

534. Watson, M. E., Neely, M. N., and Caparon, M. G. (2016) Animal Models of *Streptococcus pyogenes* Infection. *Streptococcus pyogenes Basic Biol. to Clin. Manifestations*

535. Roberts, S., Scott, J. R., Husmann, L. K., and Zurawski, C. a (2006) Murine models of *Streptococcus pyogenes* infection. *Curr Protoc Microbiol*. **Chapter 9**, Unit 9D 5

536. Lancefield, R. C. (1962) Current knowledge of type-specific M antigens of group A streptococci. *J. Immunol.* **89**, 307–313

537. Hook, E. W., Wagner, R. R., and Lancefield, R. C. (1960) An epizootic in swiss mice caused by a group a streptococcus, newly designated type 50. *Am. J. Epidemiol.* **72**, 111–119

538. Watson, M. E., Nielsen, H. V, Hultgren, S. J., and Caparon, M. G. (2013) Murine vaginal colonization model for investigating asymptomatic mucosal carriage of *Streptococcus pyogenes*. *Infect. Immun.* **81**, 1606–17

539. Mead, P. B., and Winn, W. C. (2000) Vaginal-rectal colonization with group A streptococci in late pregnancy. *Infect. Dis. Obstet. Gynecol.* **8**, 217–219

540. Gorton, D., Govan, B., Olive, C., and Ketheesan, N. (2006) A role for an animal model in determining the immune mechanisms involved in the pathogenesis of rheumatic heart disease. *Int. Congr. Ser.* **1289**, 289–292

541. Segal, N., Givon-Lavi, N., Leibovitz, E., Yagupsky, P., Leiberman, A., and Dagan, R. (2005) Acute Otitis Media Caused by *Streptococcus pyogenes* in Children. *Clin. Infect. Dis.* **41**, 35–41

542. Roberts, A. L., Connolly, K. L., Doern, C. D., Holder, R. C., and Reid, S. D. (2010) Loss of the group A Streptococcus regulator Srv decreases biofilm formation *in vivo* in an otitis media model of infection. *Infect. Immun.* **78**, 4800–4808

543. Parker, D. (2017) Humanized mouse models of *Staphylococcus aureus* infection. *Front. Immunol.* **8**, 1–6

544. Davis, P. H., and Stanley, S. L. (2003) Breaking the species barrier: Use of SCID mouse-human chimeras for the study of human infectious diseases. *Cell. Microbiol.* **5**, 849–860

545. Ly, D., Taylor, J. M., Tsatsaronis, J. A., Monteleone, M. M., Skora, A. S., Donald, C. A., Maddocks, T., Nizet, V., West, N. P., Ranson, M., Walker, M. J., McArthur, J. D., and Sanderson-Smith, M. L. (2014) Plasmin(ogen) Acquisition by Group A Streptococcus Protects against C3b-Mediated Neutrophil Killing. *J. Innate Immun.* **6**, 240–250

546. Ermert, D., Shaughnessy, J., Joeris, T., Kaplan, J., Pang, C. J., Kurt-Jones, E. A., Rice, P. A., Ram, S., and Blom, A. M. (2015) Virulence of Group A Streptococci Is Enhanced by Human Complement Inhibitors. *PLoS Pathog.* **11**, 1–20

547. Gustafsson, M. C. U., Lannergård, J., Nilsson, O. R., Kristensen, B. M., Olsen, J. E., Harris, C. L., Ufret-Vincenty, R. L., Stålhammar-Carlemalm, M., and Lindahl, G. (2013) Factor H Binds to the Hypervariable Region of Many *Streptococcus pyogenes* M Proteins but Does Not Promote Phagocytosis Resistance or Acute Virulence. *PLoS Pathog.* **9**, e1003323

548. Sriskandan, S., Unnikrishnan, M., Krausz, T., Dewchand, H., Van Noorden, S., Cohen, J., and Altmann, D. M. (2001) Enhanced susceptibility to superantigen-associated streptococcal sepsis in human leukocyte antigen-DQ transgenic mice. *J Infect Dis*. **184**, 166–173

549. Scaramuzzino, D. A., McNiff, J. M., and Bessen, D. E. (2000) Humanized *in vivo* model for streptococcal impetigo. *Infect. Immun.* **68**, 2880–2887

550. Lizano, S., Luo, F., and Bessen, D. E. (2007) Role of streptococcal T antigens in superficial skin infection. *J. Bacteriol.* **189**, 1426–1434

551. Taranta, A., Spagnuolo, M., Davidson, M., Goldstein, G., and Uhr, J. W. (1969) Experimental streptococcal infections in baboons. . *Transplant. Proc.* . **1**, 992–993

552. Virtaneva, K., Graham, M. R., Porcella, S. F., Hoe, N. P., Su, H., Graviss, E. A., Tracie, J., Allison, J. E., Lemon, W. J., John, R., Parnell, M. J., Musser, J. M., Gardner, T. J., and Bailey, J. R. (2003) Group A Streptococcus Gene Expression in Humans and Cynomolgus Macaques with Acute Pharyngitis Group A Streptococcus Gene Expression in Humans and Cynomolgus Macaques with Acute Pharyngitis. *Society*. **71**, 2199–2207

553. Gryllos, I., Cywes, C., Shearer, M. H., Cary, M., Kennedy, R. C., and Wessels, M. R. (2001) Regulation of capsule gene expression by group A Streptococcus during pharyngeal colonization and invasive infection. *Mol. Microbiol.* **42**, 61–74

554. Ashbaugh, C. D., Moser, T. J., Shearer, M. H., White, G. L., Kennedy, R. C., and Wessels, M. R. (2000) Bacterial determinants of persistent throat colonization and the associated immune response in a primate model of human group a streptococcal pharyngeal infection. *Cell. Microbiol.* **2**, 283–292

555. Stevens, D., Bryant, A., Hackett, S., Chang, A., Peer, G., Kosanke, S., Emerson, T., and Hinshaw, L. (1996) Group A streptococcal bacteremia: the role of tumor necrosis factor in shock and organ failure. *J. Infect. Dis.* **173**, 619–26.

556. Akter, F. (2016) Principles of Tissue Engineering. in *Tissue Engineering Made Easy*, pp. 3–16, 10.1016/B978-0-12-805361-4.00002-3

557. Siemens, N., Kittang, B. R., Chakrakodi, B., Oppegaard, O., Johansson, L., Bruun, T., Mylvaganam, H., Arnell, P., Hyldegaard, O., Nekludov, M., Karlsson, Y., Svensson, M., Skrede, S., and Norrby-Teglund, A. (2015) Increased cytotoxicity and streptolysin O activity in group G streptococcal strains causing invasive tissue infections. *Sci. Rep.* **5**, 16945

558. Hill, D. S., Robinson, N. D. P., Caley, M. P., Chen, M., O'Toole, E. A., Armstrong, J. L., Przyborski, S., and Lovat, P. E. (2015) A Novel Fully Humanized 3D Skin Equivalent to Model Early Melanoma Invasion. *Mol. Cancer Ther.* **14**, 2665–2673

559. Li, L., Fukunaga-Kalabis, M., and Herlyn, M. (2011) The Three-Dimensional Human Skin Reconstruct Model: a Tool to Study Normal Skin and Melanoma Progression. *J. Vis. Exp.* 10.3791/2937

560. Lee, V., Singh, G., Trasatti, J. P., Bjornsson, C., Xu, X., Tran, T. N., Yoo, S.-S., Dai, G., and Karande, P. (2014) Design and Fabrication of Human Skin by Three-Dimensional Bioprinting. *Tissue Eng. Part C Methods*. **20**, 473–484

561. Ramadan, Q., and Ting, F. C. W. (2016) In vitro micro-physiological immune-competent model of the human skin. *Lab Chip*. **16**, 1899–1908

562. Kim, M. S., Lee, B., Kim, H. N., Bang, S., Yang, H. S., Kang, S. M., Suh, K.-Y., Park, S.-H., and Jeon, N. L. (2017) 3D tissue formation by stacking detachable cell sheets formed on nanofiber mesh. *Biofabrication*. **9**, 015029

563. Schaudinn, C., Dittmann, C., Jurisch, J., Laue, M., Günday-Türeli, N., Blume-Peytavi, U., Vogt, A., and Rancan, F. (2017) Development, standardization and testing of a bacterial wound infection model based on *ex vivo* human skin. *PLoS One*. **12**, 1–13

564. Rubinchik, E., and Pasetka, C. (2010) *Ex Vivo* Skin Infection Model (Giuliani, A., and Rinaldi, A. C. eds), pp. 359–369, Methods in Molecular Biology, Humana Press, Totowa, NJ, **618**, 359–369

565. Bell, S., Howard, A., Wilson, J. A., Abbot, E. L., Smith, W. D., Townes, C. L., Hirst, B. H., and Hall, J. (2012) *Streptococcus pyogenes* infection of tonsil explants is associated with a human β-defensin 1 response from control but not recurrent acute tonsillitis patients. *Mol. Oral Microbiol.* **27**, 160–171

566. Ashrafi, M., Novak-Frazer, L., Bates, M., Baguneid, M., Alonso-Rasgado, T., Xia, G., Rautemaa-Richardson, R., and Bayat, A. (2018) Validation of biofilm formation on human skin wound models and demonstration of clinically translatable bacteria-specific volatile signatures. *Sci. Rep.* **8**, 9431

567. De Wever, B., Kurdykowski, S., and Descargues, P. (2015) Human Skin Models for Research Applications in Pharmacology and Toxicology: Introducing NativeSkin ® , the "Missing Link" Bridging Cell Culture and/or Reconstructed Skin Models and Human Clinical Testing. *Appl. Vitr. Toxicol.* **1**, 26–32

568. Gellersen, B., and Brosens, J. J. (2014) Cyclic decidualization of the human endometrium in reproductive health and failure. *Endocr. Rev.* **35**, 851–905

569. Iwahashi, M., Muragaki, Y., Ooshima, a, Yamoto, M., and Nakano, R. (1996) Alterations in distribution and composition of the extracellular matrix during decidualization of the human endometrium. *J. Reprod. Fertil.* **108**, 147–155

570. Trundley, A., Gardner, L., Northfield, J., Chang, C., and Moffett, A. (2006) Methods for isolation of cells from the human fetal-maternal interface. *Methods Mol. Med.* **122**, 109–22

571. Marcellin, L., Schmitz, T., Messaoudene, M., Chader, D., Parizot, C., Jacques, S., Delaire, J., Gogusev, J., Schmitt, A., Lesaffre, C., Breuiller-Fouché, M., Caignard, A., Vaiman, D., Goffinet, F., Cabrol, D., Gorochov, G., and Méhats, C. (2017) Immune Modifications in Fetal Membranes Overlying the Cervix Precede Parturition in Humans. *J. Immunol.* **198**, 1345–1356

572. Mori, M., Bogdan, A., Balassa, T., Csabai, T., and Szekeres-Bartho, J. (2016) The decidua-the maternal bed embracing the embryo-maintains the pregnancy. *Semin. Immunopathol.* **38**, 635–649

573. Flores-Herrera, H., García-López, G., Díaz, N. F., Molina-Hernández, A., Osorio-Caballero, M., Soriano-Becerril, D., and Zaga-Clavellina, V. (2012) An experimental mixed bacterial infection induced differential secretion of proinflammatory cytokines (IL-1β, TNFα) and proMMP-9 in human fetal membranes. *Placenta*. **33**, 271–277

574. Zaga-Clavellina, V., Flores-Espinosa, P., Pineda-Torres, M., Sosa-González, I., Vega-Sánchez, R., Estrada-Gutierrez, G., Espejel-Núñez, A., Flores-Pliego, A., Maida-Claros, R., Estrada-Juárez, H., and Chávez-Mendoza, A. (2014) Tissue-specific IL-10 secretion profile from term human fetal membranes stimulated with pathogenic microorganisms associated with preterm labor in a two-compartment tissue culture system. *J. Matern. Neonatal Med.* **27**, 1320–1327

575. Zaga-Clavellina, V., Garcia-Lopez, G., Flores-Herrera, H., Espejel-Nuñez, A., Flores-Pliego, A., Soriano-Becerril, D., Maida-Claros, R., Merchant-Larios, H., and Vadillo-Ortega, F. (2007) In vitro secretion profiles of interleukin (IL)-1beta, IL-6, IL-8, IL-10, and TNF alpha after selective infection with Escherichia coli in human fetal membranes. *Reprod. Biol. Endocrinol.* **5**, 1–7

576. Zaga-Clavellina, V., Martha, R. V. M., and Flores-Espinosa, P. (2012) In vitro secretion profile of pro-inflammatory cytokines IL-1β, TNF-α, IL-6, and of Human Beta-Defensins (HBD)-1, HBD-2, and HBD-3 from human chorioamniotic membranes after selective stimulation with gardnerella vaginalis. *Am. J. Reprod. Immunol.* **67**, 34–43

577. Canavan, T. P., and Simhan, H. N. (2007) Innate immune function of the human decidual cell at the maternal-fetal interface. *J. Reprod. Immunol.* **74**, 46–52

578. Keelan, J. A., Wong, P. M., Bird, P. S., and Mitchell, M. D. (2010) Innate inflammatory responses of human decidual cells to periodontopathic bacteria. *Am. J. Obstet. Gynecol.* **202**, 471.e1-471.e11

579. Dudley, D. J., Edwin, S. S., Dangerfield, A., Jackson, K., and Trautman, M. S. (1997) Regulation of decidual cell and chorion cell production of interleukin-10 by purified bacterial products. *Am. J. Reprod. Immunol.* **38**, 246–251

580. Barnett, T. C., Bowen, A. C., and Carapetis, J. R. (2018) The fall and rise of Group A Streptococcus diseases. *Epidemiol. Infect.* 10.1017/S0950268818002285

581. Kaplan, E. L. (1991) The resurgence of group A streptococcal infections and their sequelae. *Eur. J. Clin. Microbiol. Infect. Dis.* **10**, 55–57

582. Lev-Sagie, A., Hochner-Celnikier, D., Stroumsa, D., Khalaileh, A., Daum, H., and Moses, A. E. (2017) Group A streptococcus: is there a genital carrier state in women following infection? *Eur. J. Clin. Microbiol. Infect. Dis.* **36**, 91–93

583. Mason, K. L., and Aronoff, D. M. (2012) Postpartum Group A Streptococcus Sepsis and Maternal Immunology. *Am. J. Reprod. Immunol.* **67**, 91–100

584. Hynes, R. O. (2002) Integrins: Bidirectional, allosteric signaling machines. *Cell*. **110**, 673–687

585. Alberts, B., Johnson, A., Lewis, J., Raff, M., Roberts, K., and Walter, P. (2008) Cell junctions, cell adhesion, and the extracellular matrix. in *Molecular biology of the cell*

586. Belkin, A. M., and Stepp, M. A. (2000) Integrins as receptors for laminins. *Microsc. Res. Tech.* **51**, 280–301

587. Lafoya, B., Munroe, J. A., Miyamoto, A., Detweiler, M. A., Crow, J. J., Gazdik, T., and Albig, A. R. (2018) Beyond the matrix: The many non-ECM ligands for integrins. *Int. J. Mol. Sci.* **19**, 1–33

588. Behera, A. K., Durand, E., Cugini, C., Antonara, S., Bourassa, L., Hildebrand, E., Hu, L. T., and Coburn, J. (2008) *Borrelia burgdorferi* BBB07 interaction with integrin alpha3beta1 stimulates production of pro-inflammatory mediators in primary human chondrocytes. *Cell Microbiol.* **10**, 320–331

589. Wood, E., Tamborero, S., Mingarro, I., and Esteve-Gassent, M. D. (2013) BB0172, a *Borrelia burgdorferi* outer membrane protein that binds integrin alpha3beta1. *J. Bacteriol.* **195**, 3320–3330

590. Feire, A. L., Koss, H., and Compton, T. (2004) Cellular integrins function as entry receptors for human cytomegalovirus via a highly conserved disintegrin-like domain. *Proc. Natl. Acad. Sci. U. S. A.* **101**, 15470–5

591. Akula, S. M., Pramod, N. P., Wang, F. Z., and Chandran, B. (2002) Integrin α3β1 (CD 49c/29) is a cellular receptor for Kaposi's sarcoma-associated herpesvirus (KSHV/HHV-8) entry into the target cells. *Cell*. **108**, 407–419

592. Di Giovine, M., Salone, B., Martina, Y., Amati, V., Zambruno, G., Cundari, E., Failla, C. M., and Saggio, I. (2001) Binding properties, cell delivery, and gene transfer of adenoviral penton base displaying bacteriophage. *Virology*. **282**, 102–112

593. Fothergill, T., and McMillan, N. A. J. (2006) Papillomavirus virus-like particles activate the PI3-kinase pathway via alpha-6 beta-4 integrin upon binding. *Virology*. **352**, 319–328

594. Ramathal, C., Bagchi, I., Taylor, R., and Bagchi, M. (2010) Endometrial Decidualization: Of Mice and Men. *Semin. Reprod. Med.* **28**, 017–026

595. Aluvihare, V. R., Kallikourdis, M., and Betz, A. G. (2004) Regulatory T cells mediate maternal tolerance to the fetus. *Nat. Immunol.* **5**, 266–271

596. Samstein, R. M., Josefowicz, S. Z., Arvey, A., Treuting, P. M., and Rudensky, A. Y. (2012) Extrathymic generation of regulatory T cells in placental mammals mitigates maternal-fetal conflict. *Cell*. **150**, 29–38

597. Lissauer, D., Kilby, M. D., and Moss, P. (2017) Maternal effector T cells within decidua: The adaptive immune response to pregnancy? *Placenta*. **60**, 140–144

598. Erlebacher, A. (2013) Immunology of the Maternal-Fetal Interface. *Annu. Rev. Immunol.* **31**, 387–411

599. Torgerson, R. R., and McNiven, M. a (1998) The actin-myosin cytoskeleton mediates reversible agonist-induced membrane blebbing. *J. Cell Sci.* **111 (Pt 1**, 2911–22

600. Atkin-Smith, G. K., and Poon, I. K. H. (2017) Disassembly of the Dying: Mechanisms and Functions. *Trends Cell Biol.* **27**, 151–162

601. Carey, A. J., Weinberg, J. B., Dawid, S. R., Venturini, C., Lam, A. K., Nizet, V., Caparon, M. G., Walker, M. J., Watson, M. E., and Ulett, G. C. (2016) Interleukin-17A Contributes to the Control of *Streptococcus pyogenes* Colonization and Inflammation of the Female Genital Tract. *Sci. Rep.* **6**, 26836

602. Park, H.-R., Harris, S. M., Boldenow, E., McEachin, R. C., Sartor, M., Chames, M., and Loch-Caruso, R. (2017) Group B Streptococcus Activates Transcriptomic Pathways Related to Premature Birth in Human Extraplacental Membranes In Vitro. *Biol. Reprod.* **98**, 396–407

603. Schweitzer, A. N., Borriello, F., Wong, R. C., Abbas, A. K., and Sharpe, A. H. (1997) Role of costimulators in T cell differentiation: studies using antigen-presenting cells lacking expression of CD80 or CD86. *J Immunol.* **158**, 2713–22

604. Hargrave, M., Bowles, J., and Koopman, P. (2006) *In situ* hybridization of whole-mount embryos. *Methods Mol Biol*. **326**, 103–113

605. Tsatsaronis, J. A., Walker, M. J., and Sanderson-Smith, M. L. (2014) Host Responses to Group A Streptococcus: Cell Death and Inflammation. *PLoS Pathog.* **10**, e1004266

Résumé

Streptococcus pyogenes, également appelé Streptocoque du Goupe A (SGA), est un pathogène à l'origine d'une grande diversité d'infections, allant d'infections superficielles comme l'angine aux infections invasives, comme la fasciite nécrosante et les endométrites. Au 19ème siècle, une femme sur dix mourait après l'accouchement de fièvre puerpérale, notamment d'endométrite. En France, les infections gynéco-obstétricales correspondent encore de nos jours à 27 % des infections invasives à SGA chez les femmes. Les souches de SGA présentent une forte diversité génétique et de répertoire de facteurs de virulence. Le génotype *emm28* est le troisième génotype le plus prévalent en France et il est associé aux endométrites. Nous avons analysé par deux axes complémentaires les facteurs et mécanismes impliqués dans les endométrites à SGA.

Par des approches de biochimie et de biologie cellulaire, nous avons caractérisé l'interaction entre les cellules de l'hôte et R28, une protéine de surface spécifique du génotype *emm28*. Le domaine N-terminal de R28 ($R28_{Nt}$) et ses deux sous-domaines favorisent la fixation des bactéries à des cellules endométriales, cervicales et déciduales. Ils fixent de manière directe les intégrines α3β1, α6β1 et α6β4. Par ailleurs, $R28_{Nt}$ promeut aussi l'adhésion à des cellules épithéliales de la peau et des poumons. Ces résultats suggèrent que la fixation des intégrines par $R28_{Nt}$ concourt, non seulement, aux endométrites dues au génotype *emm28*, mais aussi, et de manière plus générale, à la prévalence de ce génotype.

Afin de mieux caractériser les étapes précoces essentielles au développement des endométrites à SGA, nous avons développé un modèle original d'infection : nous infectons *ex vivo* la décidue humaine, qui correspond à la membrane utérine durant la grossesse. Nous avons analysé les effets de l'infection de la décidue par des techniques de microscopie et d'analyse d'image de pointes. SGA adhère au tissu et se multiplie au contact de celui-ci grâce à des éléments sécrétés par le tissu. Sur ce tissu, SGA forme des biofilms composés d'ultrastructures ressemblant, pour certains, à des fils reliant deux coques d'une même chaine et, pour d'autres, à des filaments reliant plusieurs chaînettes ; certains s'organisent en réseau. GAS envahit en profondeur le tissu, ce qui dépend de l'expression de la cystéine protéase SpeB. SGA induit la mort de la moitié des cellules en moins de 4 h à travers la sécrétion de différents facteurs, dont la Streptolysine O (SLO). Enfin, GAS est capable de restreindre la réponse immunitaire du tissu à l'échelle transcriptomique et protéique, le contrôle protéique dépendant de l'expression de SLO et de SpeB.

Abstract

Streptococcus pyogenes (Group A Streptococcus, GAS), is a Gram-positive pathogen responsible for a wide range of diseases, from superficial infections such as pharyngitis to invasive infections such as necrotizing fasciitis and puerperal fever that includes endometritis. Puerperal fever was a huge social burden in the 19th century, killing one woman out of ten after delivery, and gyneco-obstetrical infections still correspond to 27% of woman GAS invasive infections in France. GAS strains are genetically diverse and harbor specific virulence factors repertoires. *emm28* is the third most prevalent genotype in France and it is associated with endometritis. By two complementary axes, we analyzed factors and mechanisms involved in GAS endometritis.

Using biochemical and cellular approaches, we characterized the interaction between *emm28*-specific surface protein, R28, and host cells. R28 N-terminal domain, $R28_{Nt}$, and its two subdomains promote the binding to endometrial, cervical and decidual cells. They directly interact with the integrins α3β1, α6β1 and α6β4. $R28_{Nt}$ also promotes adhesion to pulmonary and skin epithelial cells. Our results suggest that $R28_{Nt}$-integrin interactions contribute not only to *emm28*-elicited endometritis, but also to the overall prevalence of the *emm28* strains.

To further characterize the initial events involved in the establishment of GAS endometritis, we developed a novel infection model: we infected *ex vivo* the human decidua, the mucosal uterine lining during pregnancy. We analyzed the outcome of the infection using state-of-the-art imaging set-up, image processing and analysis. GAS adheres to the tissue and grows at its surface; secreted host factors promote this growth. GAS readily forms biofilm at the tissue surface; thread-like and inter-chains filaments ultra-structures compose these biofilms. GAS invades the tissue and this depends on the expression of the cysteine protease SpeB. GAS induces the cell death of half of the cells within 4 h and this cytotoxicity depends on secreted factors, including the Streptolysin O (SLO). Finally, GAS restrains the tissue immune response at the transcriptional and protein levels, the latter depending on the expression of SLO and SpeB.

PhD dissertation by Mr Antonin WECKEL

"Molecular mechanisms of *Streptococcus pyogenes* tissue colonization and invasion"

INSERM, Institut Cochin, Team « Barriers and Pathogens ». 22 rue Méchain, 75014 Paris.